

Lecture on Grain Boundary & Interface Engineering

at Department of Materials Engineering, IISc, (No.1)

(16, November, 2015, Bangalore, India)

Grain Boundary and Interface Engineering for Structural and Functional Materials (Basic Knowledge of GBE)

Tadao Watanabe

Lab. of Materials Design and Interface Engineering, Dept. of Nanomechanics,
Graduate School of Engineering, Tohoku University, Sendai, Japan
Guest Scientist, Key Laboratory of Anisotropy and Texture of Materials,
Northeastern University (NEU) , Shenyang, China.

Acknowledgements

Coworkers at Tohoku Univ.:

H. Kokawa, S. Tsunekawa, T. Matsuzaki, K. Kawahara
S. Yamaura, S. Kobayashi, H. Fujii (S. V. R. Murthy+)

Coworkers : L. Zuo, X. Zhao, at NEU and Claude Esling at Univ. Metz

Outline

1. Historical Background of Grain Boundary Engineering

Basic Studies of

- (1). “Structure-dependent Grain Boundary (GB) Properties” in Bicrystals for Design and Control of GB-Related Bulk Properties in Polycrystals:
- (2). “New Microstructural Parameters” to characterize “GB Microstructure” and to bridge a Gap between Individual Grain Boundaries and Bulk Properties in a Polycrystal:
“GB Character Distribution (GBCD)”, “GB Connectivity” & etc.

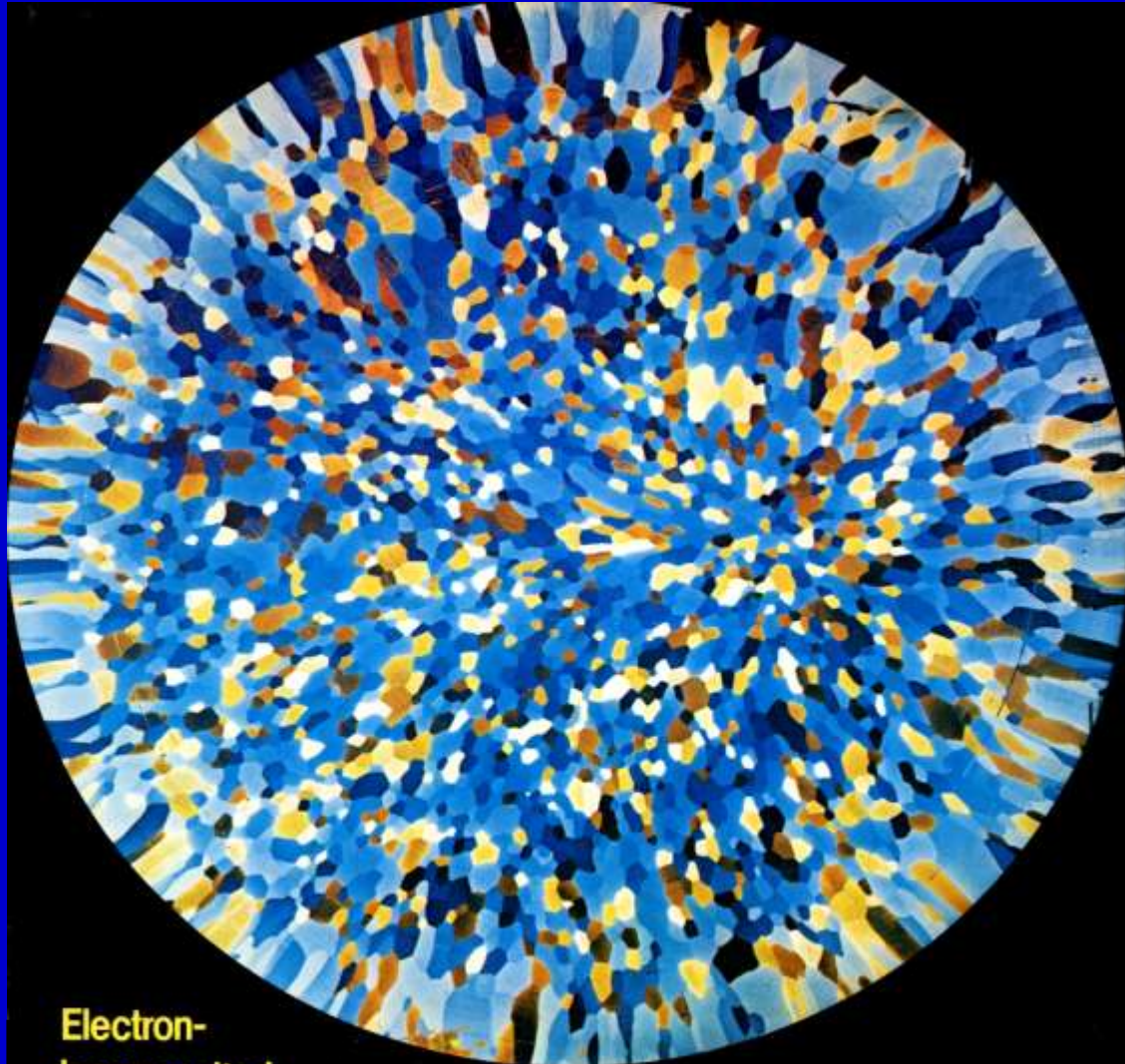
2. Control of Texture and Grain Boundary Microstructures

How to relate “Texture” to “GB Microstructure” in Polycrystals.
How to manipulate Microscale Texture and GB Microstructure.

3. Grain Boundary Engineering for GB-controlled Bulk Properties in “Structural” and “Functional” Materials

4. Future Perspective of Interface Engineering for Biological Materials.

A Polycrystal System of Grains and Grain Boundaries (Mo ingot solidified from the melt)



Electron-
beam melted
molybdenum ingot starts processing route to 0.9mm wire

TABLE

Year				
1940's	1970's	<p><u>O-Lattice/DSC Lattice Theory (Bollmann, 1970)</u></p> <p><u>Computer Simulations of Grain Boundary Structure (Weins, 1970, Hasson-Goux-Biscondi, 1971, Dahl-Beeler-Bourquin, 1971)</u></p> <p>Plane Matching Model (Pumphrey, 1972)</p> <p>Near CSL Model in HCP (Bruggeman-Bishop-Hartt, 1972)</p>	<p><u>Structure Property Relationship in Bicrystals (Biscondi et al, 1970)</u></p> <p><u>TEM of Boundary Structure in Bicrystals (Schober-Balluffi, 1970; Sass-Tan-Balluffi, 1975)</u></p> <p>TEM of Grain/Interphase Boundaries (Smith-Pond-Clarke-King, 1977-79) Ralph-Howell-Jones, 197 ; Aaronson-Kinsmann-Laird, 1970, Nemoto, 1974)</p> <p>Boundary Chemistry Analysis by AES (Joshi-Stein-White, 1976; Seah-Hondros, 1973)</p>	le
1950's	1980's	<p>Grain Boundary Structure and Property Simulation (Vitek-Sutton-Srolovitz, 1983, Wolf, 1985; Paidar, 1987; Kohyama et al., 1988) Polycrystalline</p> <p>Triple Junction (Bollmann 1984)</p> <p><u>The Concept of Grain Boundary Design and Control through GBCD Control in Polycrystals (Watanabe, 1984)</u></p> <p><u>Nanocrystalline Materials (Gleiter, 1986)</u></p>	<p>Statistical Analysis of Grain Boundaries by SEM-ECP (GBCD) (Ishida 1981; Watanabe, 1981)</p> <p>HREM Studies of Grain Boundary and Interfaces (Ishida-Ichinose, 1981; Ruhle et al, 1982; Bourret, 1985, Structure Property in Bicrystals (Miura et al. 198 ; Yoshinaga et al 1983 ; Watanabe et al. 1984)</p> <p>Structure Property in Electronic Ceramics and Superconductors (Smith et al. 1988, Dimos et al. 1988)</p>	ry 2,
1960's	1990's	<p>Electronic Structure of Grain Boundaries and Interfaces (Sutton, 1991)</p> <p>Texture GBCD Relationship (Garbacz-Grabski, 1993)</p>	<p><u>Development of OIM (Dingley-Adams-Field-Wright, 1993)</u></p> <p>Grain Boundary Engineering for Advanced Materials (Palumbo-Aust, 1993, Babcock, 1993)</p> <p>Boundary Plane Analysis (Randle, 1994)</p>	n, ies wn, 70)

A Brief History of Studies of Grain Boundary Structure and Properties leading to Grain Boundary Engineering

1900s-1940s

Amorphous Cement Theory (**Rosenhain-Ewen: 1912**)

Transition-Lattice Theory (**Hargreaves-Hill: 1929**)

GB Structure : CSL Model (**Kronberg-Wilson: 1949**)

Geometrical and Topological Approach to GB microstructure (**C. S. Smith: 1948**)

1950s-1960s

Dislocation Theory of Low-angle GBs (**Read-Schokley: 1952, Amelincks: 1957**)

Boundary Structure and Properties in Bicrystals (**Chalmers-Aust, R. W. Cahn: 1953**)

Thermodynamics of GBs (**J. W. Cahn,1956**), First Book on GBs (**D. McLean: 1957**)

Geometrical and Mathematical Approach to CSL (**Brandon, Ranganathan :1966**)

FIM, TEM Observations (**Ryan-Suiter, Ralph-Jones, Gleiter**)

1970s- 1980s

HREM of GB (**Schober-Balluffi, Sass, Pond-Smith, Ishida-Ichinose, Thibault, Bourret-Bacman, Rühle**)

Bicrystal Work in Metals (**France, Russia, Japan**), O-Lattice Theory (**Bollmann: 1968**)

Computer Calculations (**Biscondi, Vitel-Sutton, Wolf, Kohyama**)

Microscale Texture (**Gottstein-Lücke: 1978, Bunge-Esling,: 1986**)

Nanocrystalline Materials (**Gleiter : 1986**),

Grain Boundary Engineering (**Watanabe: 1983-1984, Aust –Palumbo: 1989**)

1990s-2000s

SEM-EBSD/OIM (**Adams, Wright, Kunze: 1994**),

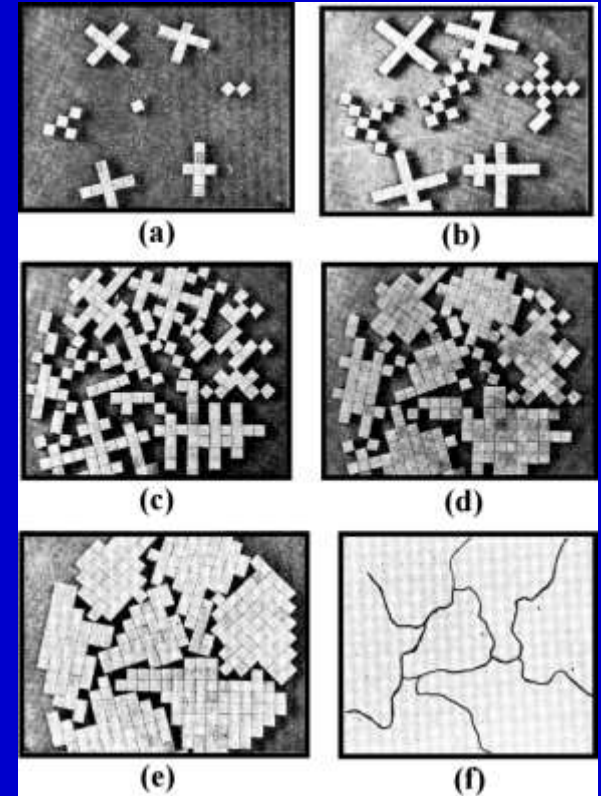
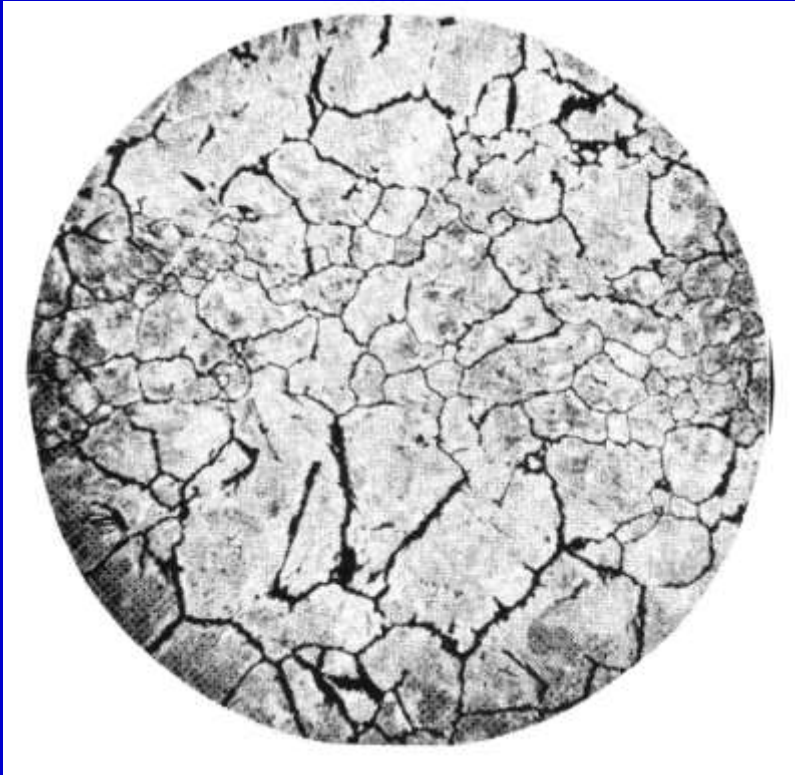
Bicrystals (Metals: **Gottstein-Shvindlerman-Molodov,**

Ceramics :**Sakuma-Ikuhara- Yamomoto-Shibata**)

Observations of Grain Boundaries.

(a) First Observation of Grain Boundaries By Sorby with a Optical Microscope ($\times 9$).

H. C. Sorby, J. Iron and Steel Inst., 1 (1887), 225.

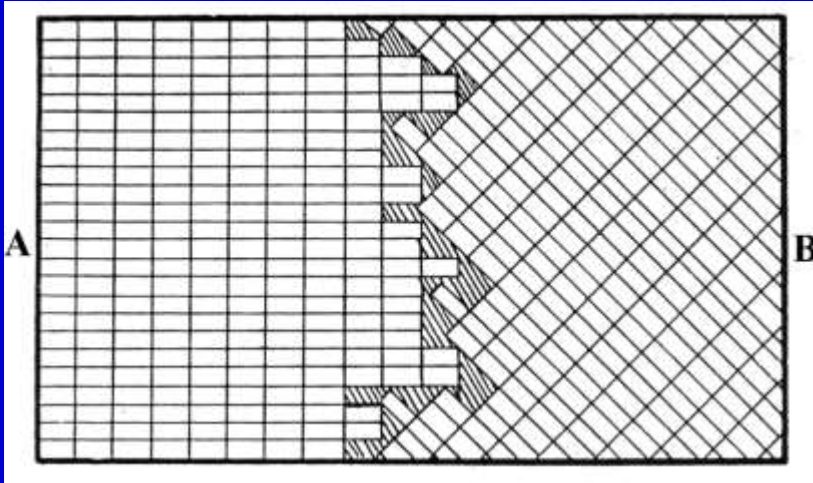


Early Photomicrograph of Blister Steel made by Sorby (magnification $\times 9$) and Described 'A Mass of Grains ("System"), which Cohere less strongly than Separate Parts of Individual Crystals'.

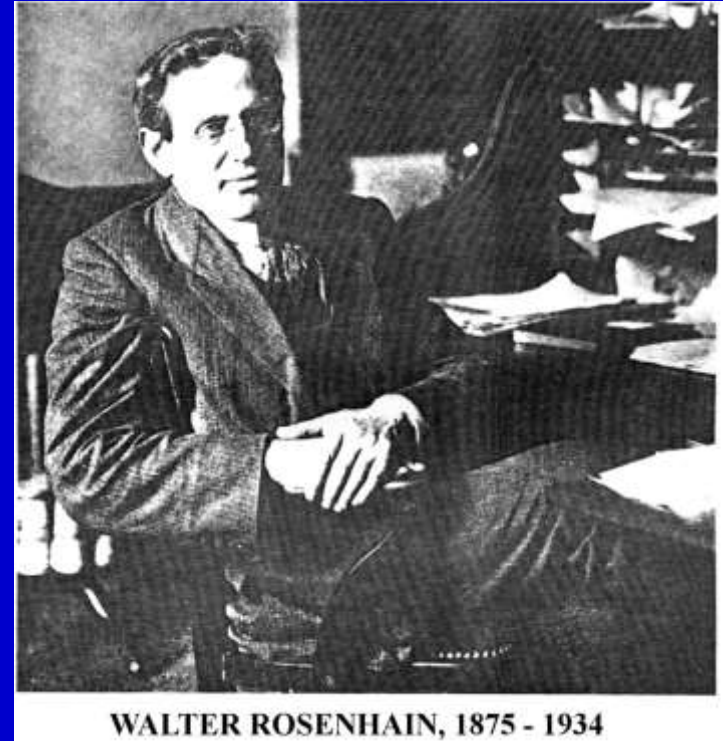
Rosenhain's Visual Representation of the Evolution of the 'Inter-crystalline Junction' as the 'Accidental' Meeting Line of Adjacent Growing Crystals of Different Orientation, Stuck together by the Residue Amorphous Glue.

Early Theories of Grain Boundary Structure in 1900s-1920s

Amorphous Cement Theory



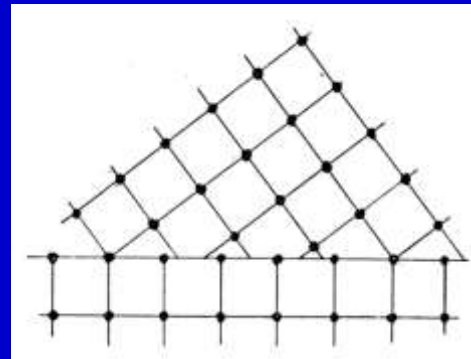
It is proposed that a thin layer of amorphous metal may be formed and may persist in the intercrystalline boundaries, even in the absence of strain. (W. Rosenhain, D. Ewen: J. Inst. Metals, 8 ([1912](#)), 149~185.)



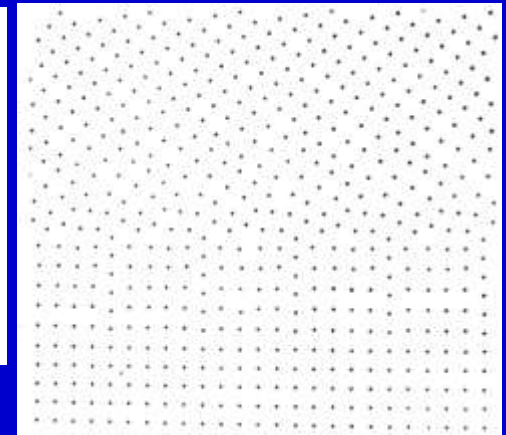
WALTER ROSENHAIN, 1875 - 1934

Transition-Lattice Theory

Formation of Transition Zone Patterns. To illustrate the conception and not to give the actual positions of the atoms (F. Hargreaves, R. J. Hills: J. Inst. Metal, 41 ([1929](#)), 257~288)



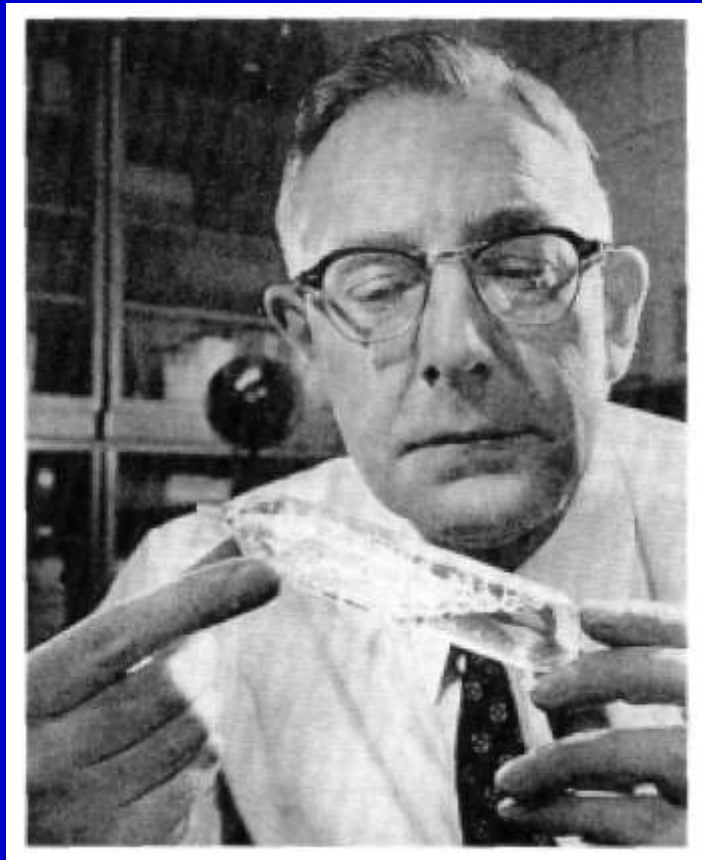
$36.5^\circ \langle 001 \rangle / \Sigma 5$



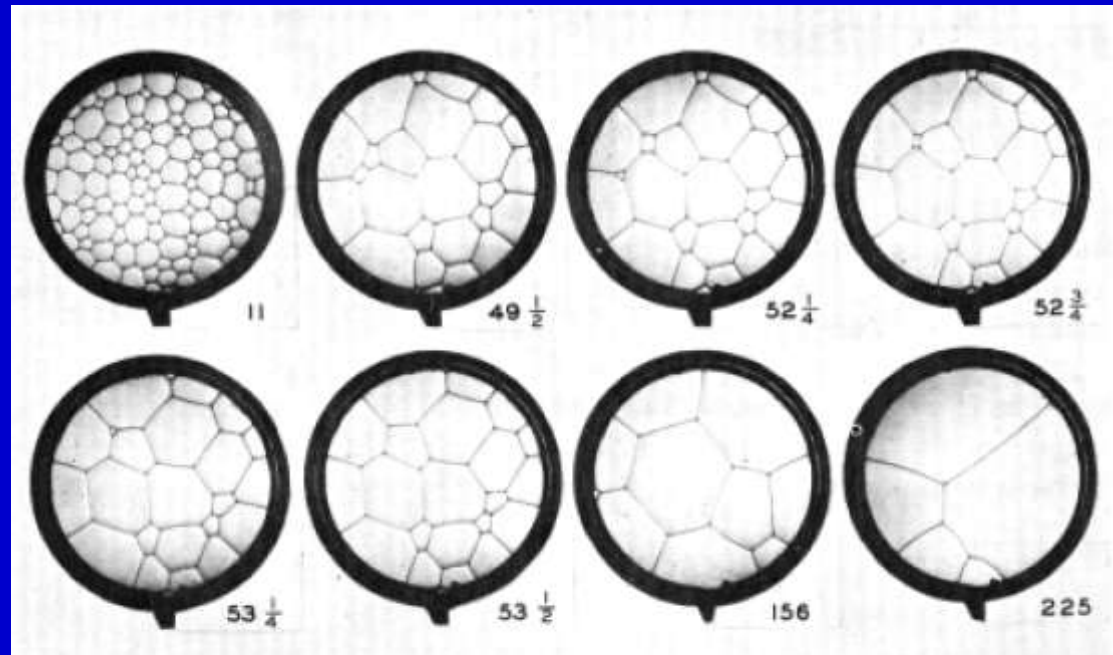
Background of Grain Boundary & Interface Engineering

Geometrical and Topological Approach to Microstructure
in Polycrystal (1940s-1950s)

“Soap Bubble Model” of Grain Growth
and Microstructural Evolution.



Cyril Stanley Smith
(1903 ~ 1992)



Growth of soap cells in a flat container. (From Smith, C. S., ASM Seminar, Metal Interfaces, 1952, p. 65)

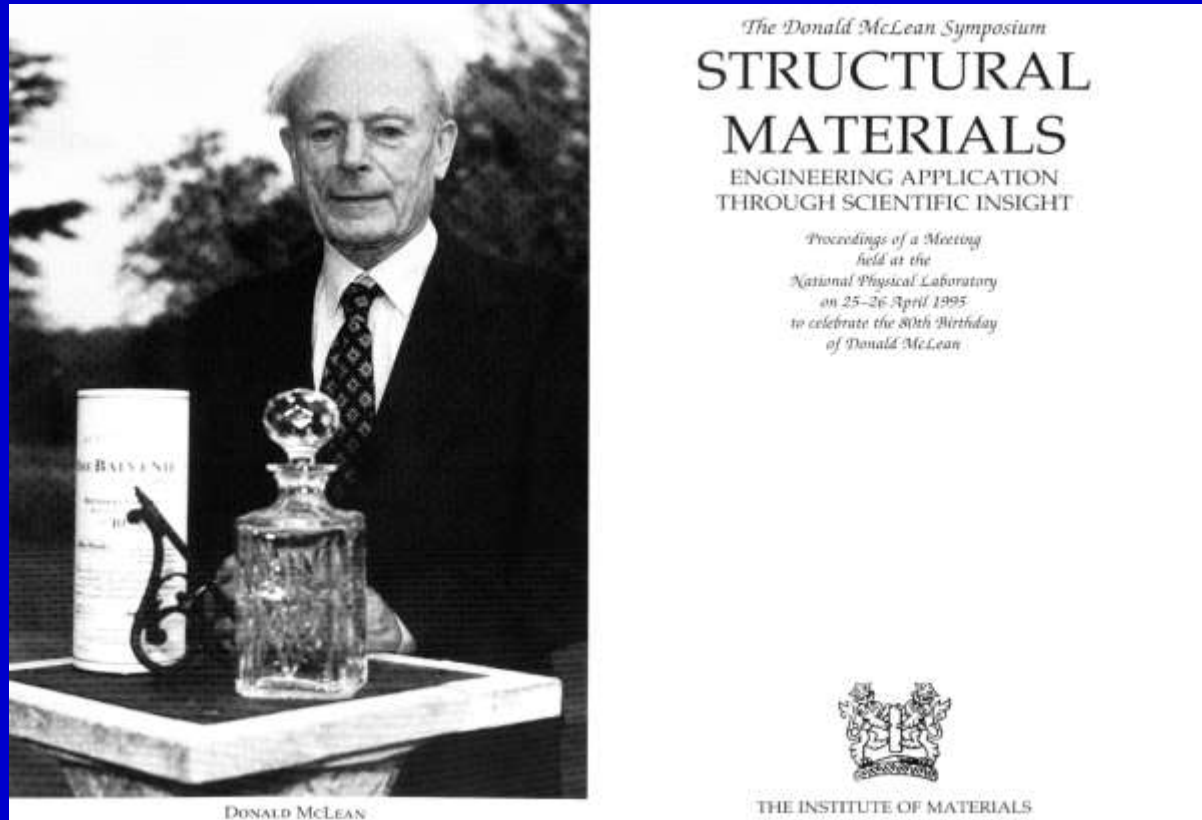
First Book on “Grain Boundary Structure and Properties”

D. Mclean, “Grain Boundaries in Metals”,

Clarendon Press, Oxford (1957).

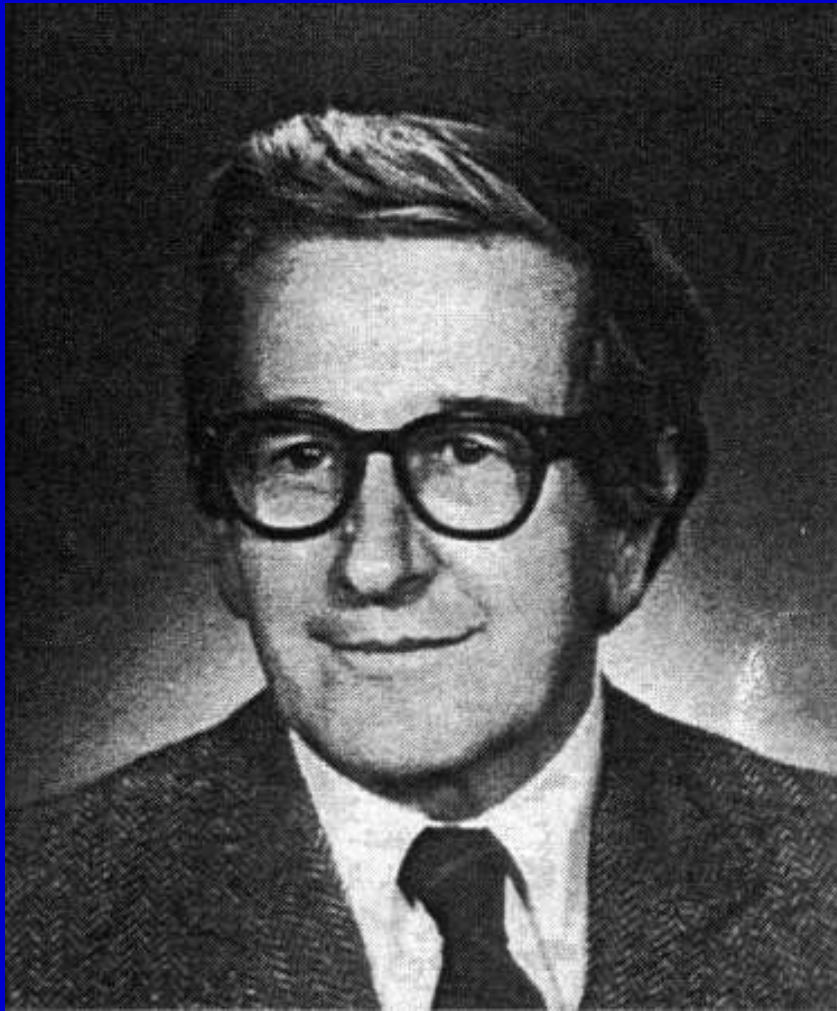
The Donald McLean Symposium on Structural Materials

Proc. Book: The Inst. Materials, (1996), ed. by E. D. Hondros, M. McLean

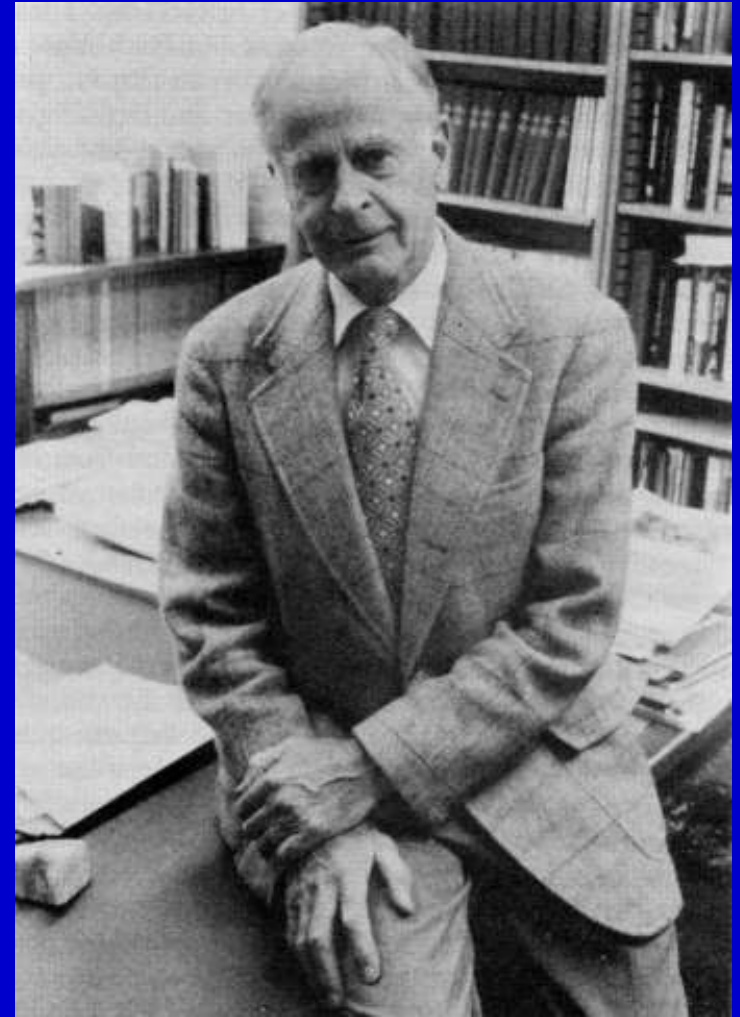


Importance of Grain Boundary Structure

K.T. Aust and B. Chalmers : “Energies and Structure of Grain Boundaries”,
Metal Interfaces, ASM, (1952), 153-178.

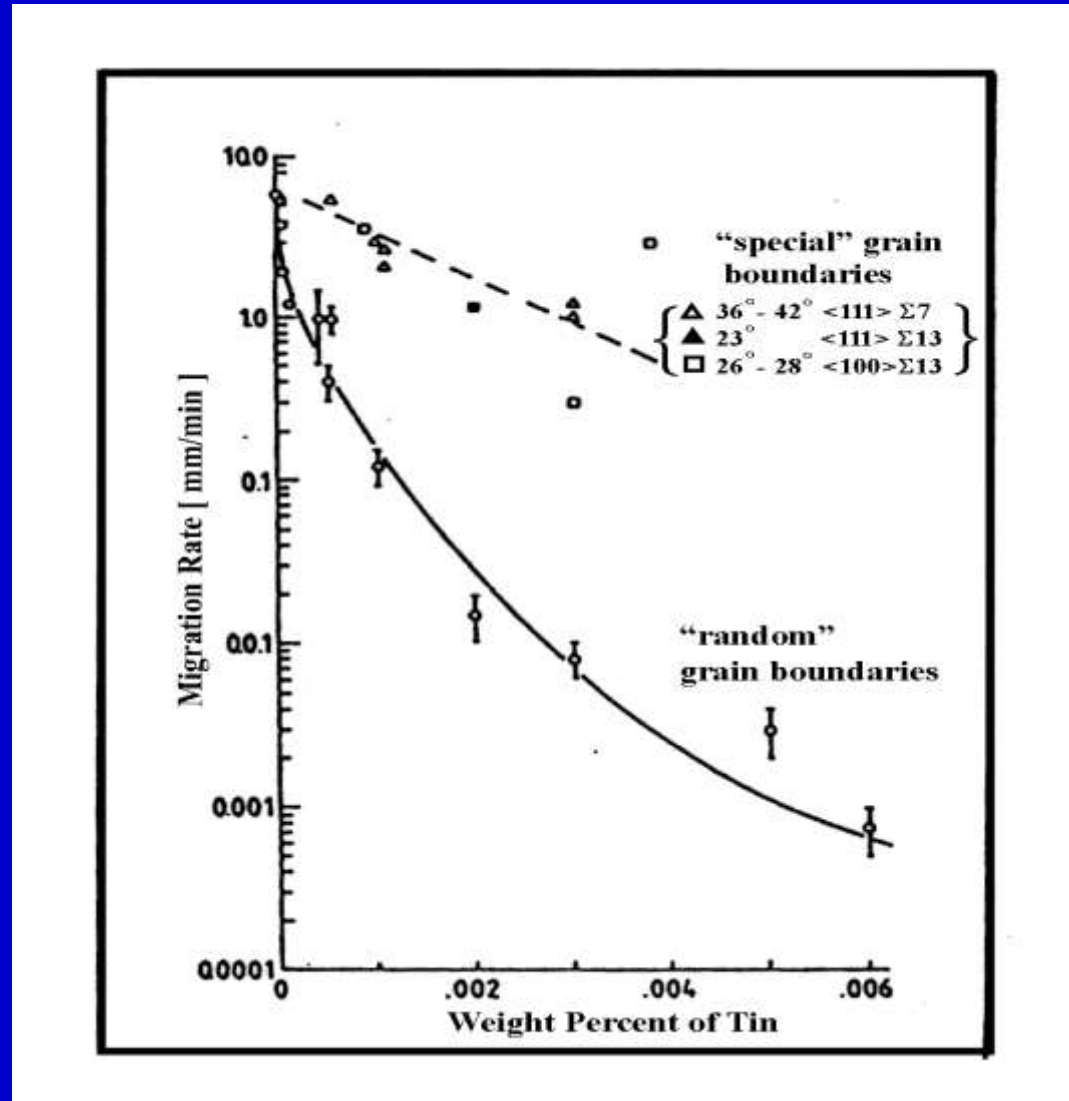


K. T. Aust



B. Chalmers

Effects of Grain Boundary Structure on Grain Boundary Migration (Pb-Sn Alloy bicrystals)



K. T. Aust and J. W. Rutter, *Trans. Met. Soc. AIME.*, 215 (1959), 119-127.

Structure-dependent Grain Boundary Migration in Metals of Different Purity.

G. Gottstein, L. S. Shvindlerman: Scripta Met., 27 (1992), 1515-1520.

Scripta METALLURGICA
et MATERIALIA

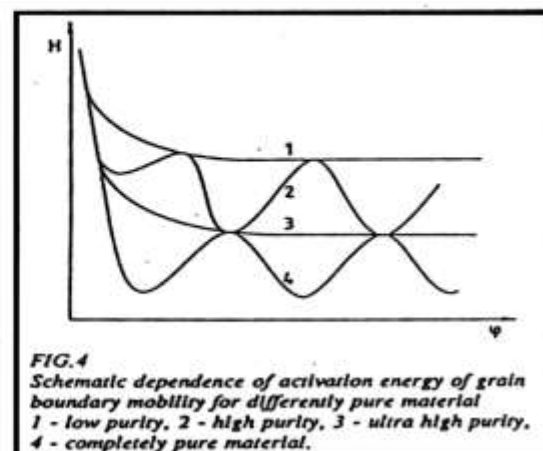
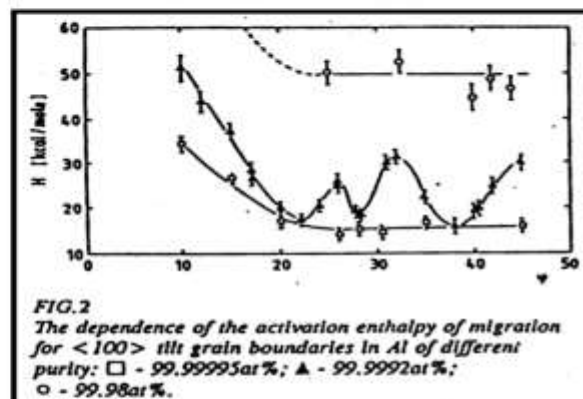
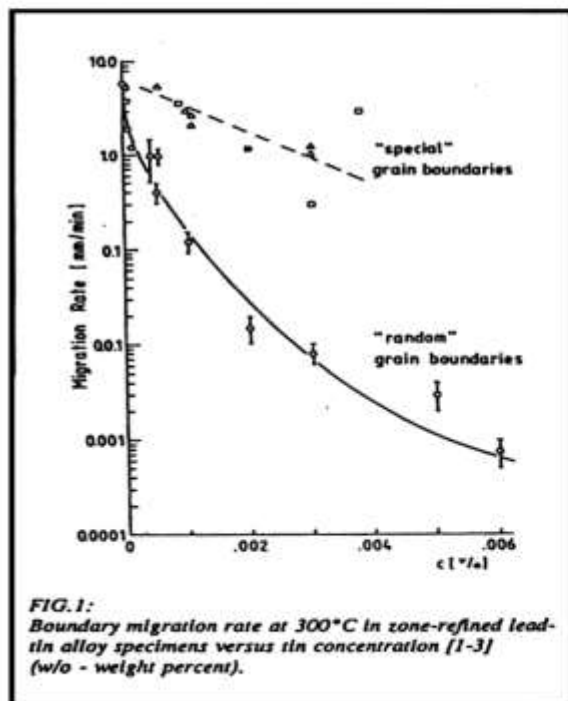
Vol. 27, pp. 1515-1520, 1992
Printed in the U.S.A.

Pergamon Press Ltd.
All rights reserved

CONFERENCE SET No. 1

ON THE ORIENTATION DEPENDENCE OF GRAIN BOUNDARY MIGRATION

G. Gottstein and L.S. Shvindlerman[?]
Institut für Metallkunde und Metallphysik, RWTH Aachen,
Kopernikusstr. 14, W-5100 Aachen, FRG
[?] Institute of Solid State Physics, Russian Academy of Sciences,
Chernogolovka, Russia



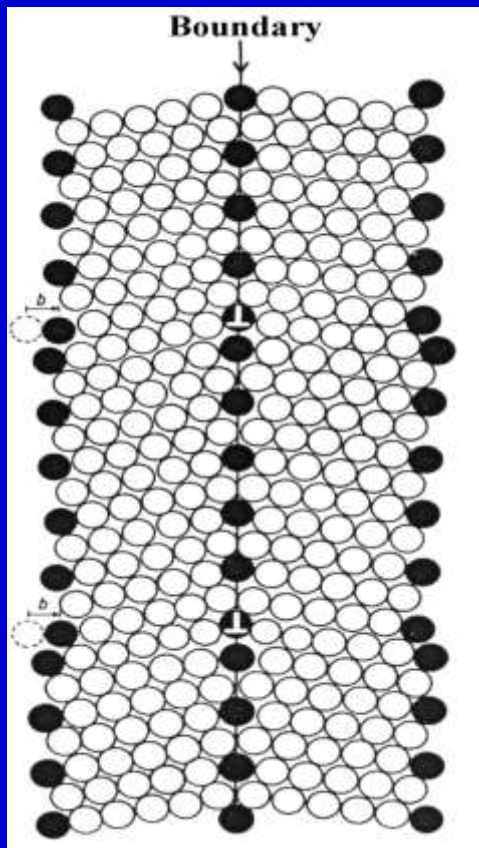
Pioneers in Grain Boundary Research Field



**Mrs. Brandon, Prof. S. Ranganathan (IISc.), Prof. D. Brandon
(Technion)**

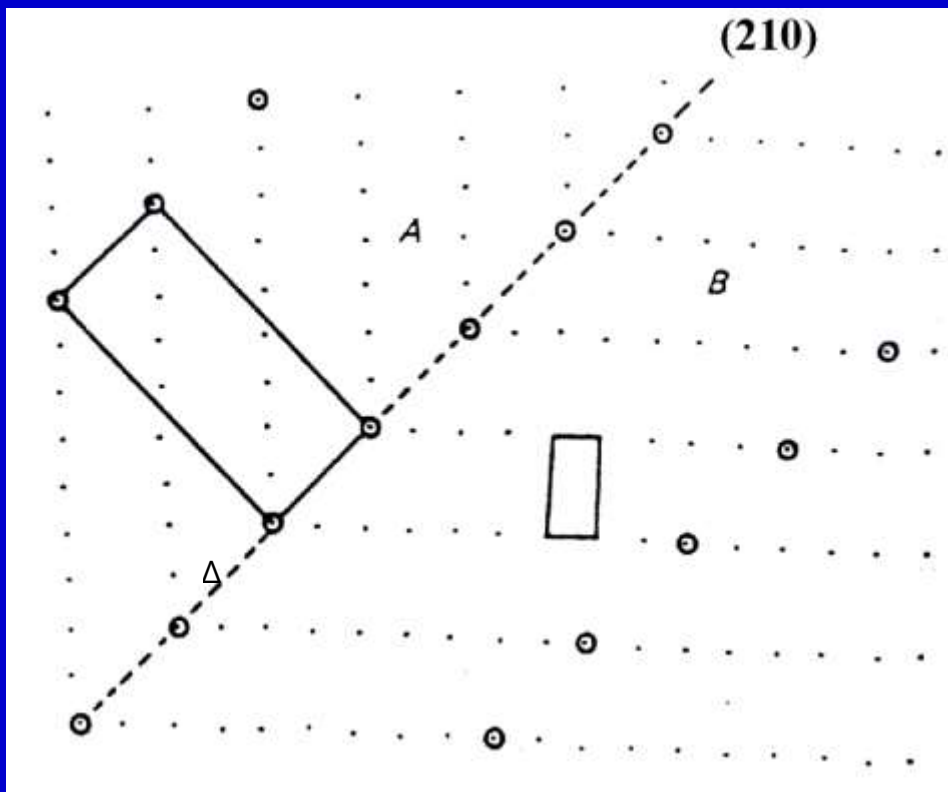
Mathematical Prediction of Coincidence-Site-Lattice Boundaries

$\Sigma = 11$ Boundary.



**Brandon's
Criterion**

$$\Delta\theta = \frac{15^\circ}{\sqrt{\Sigma}}$$



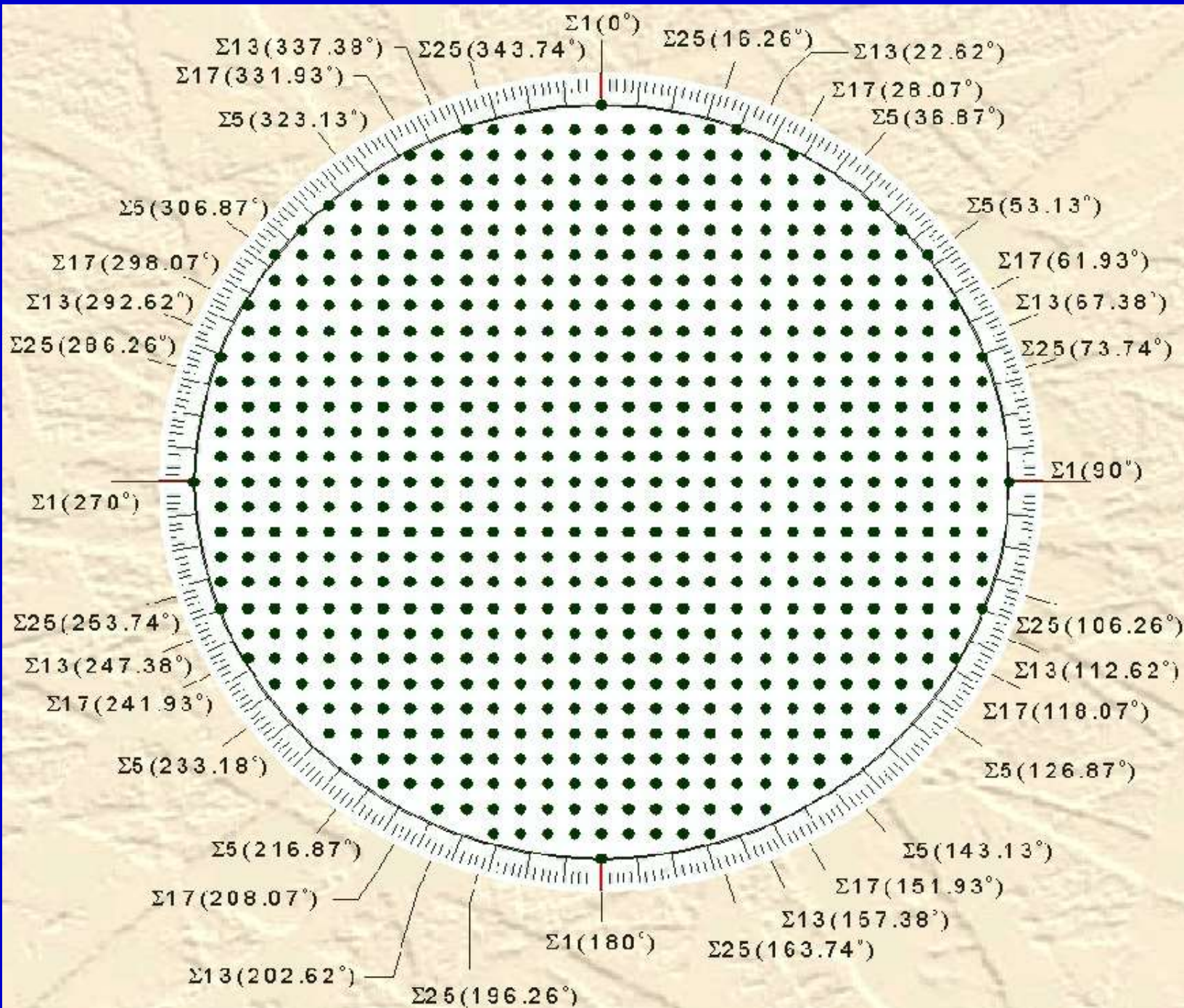
Ranganathan's equation

$$\Sigma = x^2 + R y^2$$

$$R = \sqrt{h^2 + k^2 + l^2}$$

Coincidence-Site Lattice (with $\Sigma=9$) based on [210].
(S. Ranganathan: Acta Cryst., 21 (1966), 197.)

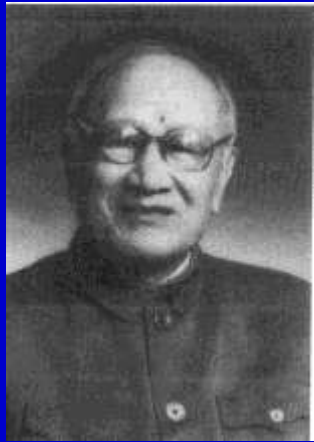
(D. Brandon, Acta Met., 14 (1966), 1479)



General Form of the Complete Set of 24 Angle-Axis Pairs for Each Cubic C. S. L. Orientation Relation

$\Sigma 1$	0° on any axis	6 of 90° on <100> 8 of 120° on <111>	3 of 180° on <100> 6 of 180° on <110>	$\Sigma 19b$	46.83° on 73.17° same 166.83° <111>	3 of 71.59° on <320> 3 of 110.01° on <551> 3 of 121.76° on <520>	3 of 139.74° on <733> 3 of 142.14° on <530> 3 of 153.47° on <411> 3 of 180° on <532>
$\Sigma 3$	2 of 60° on 180° same <111>	3 of 70.53° on 3 of 109.47° same <110>	6 of 131.81° on <210> 6 of 146.44° on <311> 3 of 180° on <211>	$\Sigma 21a$	21.79° on 98.21° same 141.79° <111>	3 of 79.02° on <410> 3 of 103.77° on <510> 3 of 113.87° on <553>	3 of 128.25° on <322> 3 of 162.25° on <540> 3 of 167.48° on <911> 3 of 180° on <541>
$\Sigma 5$	36.87° on 53.13° same 126.87° same 143.13° <100>	4 of 95.74° on <311> 4 of 101.54° on <211> 4 of 143.13° on <221>	4 of 154.16° on <331> 2 of 180° on <210> 2 of 180° on <310>	$\Sigma 21b$	44.40° on <211> 58.40° on <210> 79.02° on <322> 80.41° on <531> 103.77° on <431> 113.87° on <731>	124.84° on <441> 124.84° on <522> 128.25° on <410> 141.79° on <751> 144.05° on <532> 144.05° on <611>	154.80° on <210> 162.25° on <443> 2 of 162.25° on <621> 2 of 167.48° on <753> 180° on <421>
$\Sigma 7$	38.21° on 81.79° same 158.21° <111>	3 of 73.40° on <210> 3 of 110.92° on <331> 3 of 115.38° on <310>	3 of 135.58° on <211> 3 of 149.00° on <320> 3 of 158.21° on <511> 3 of 180° on <321>	$\Sigma 23$	40.45° on <311> 55.56° on <310> 85.01° on <421> 86.25° on <533> 102.55° on <321> 107.72° on <521>	117.16° on <733> 127.49° on <610> 130.71° on <331> 143.56° on <911> 143.56° on <753> 145.70° on <541>	155.94° on <332> 163.04° on <210> 2 of 163.04° on <542> 2 of 168.04° on <931> 180° on <631>
$\Sigma 9$	38.94° on 141.06° same <110>	2 of 67.11° on <311> 2 of 90° on <221> 2 of 96.38° on <210> 2 of 120° on <511> 4 of 123.75° on <321>	2 of 152.73° on <410> 2 of 152.73° on <322> 4 of 160.81° on <531> 1 of 180° on <221> 1 of 180° on <411>	$\Sigma 25a$	16.25° on 73.75° same 106.25° same 163.75° <100>	4 of 91.13° on <711> 4 of 111.10° on <433> 4 of 129.80° on <443>	4 of 168.53° on <771> 2 of 180° on <430> 2 of 180° on <710>
$\Sigma 11$	50.48° on and 129.52° same <110>	2 of 62.96° on <211> 2 of 82.16° on <331> 2 of 100.48° on <320> 4 of 126.22° on <531> 2 of 129.52° on <411>	2 of 144.90° on <310> 4 of 155.38° on <421> 2 of 162.66° on <533> 1 of 180° on <311> 1 of 180° on <332>	$\Sigma 25b$	51.68° on <331> 63.88° on <321> 73.75° on <221> 90° on <430> 91.13° on <551> 111.10° on <530>	2 of 120° on <751> 129.80° on <540> 2 of 129.80° on <621> 2 of 132.86° on <421> 2 of 145.09° on <931> 2 of 147.15° on <631>	156.93° on <211> 2 of 163.75° on <632> 168.53° on <311> 168.53° on <755> 180° on <543>
$\Sigma 13a$	22.62° on 67.38° same 112.62° same 157.38° <100>	4 of 92.20° on <511> 4 of 107.92° on <322> 4 of 133.81° on <332>	4 of 164.06° on <551> 2 of 180° on <320> 2 of 180° on <510>	$\Sigma 27a$	31.58° on 148.42° same <110>	2 of 70.51° on <411> 2 of 94.25° on <520> 2 of 95.30° on <553> 2 of 114.05° on <611> 4 of 122.50° on <753>	2 of 146.44° on <755> 2 of 157.82° on <510> 4 of 164.36° on <641> 180° on <511> 180° on <552>
$\Sigma 13b$	27.80° on 92.20° same 147.80° <111>	3 of 76.66° on <310> 3 of 107.92° on <410> 3 of 112.62° on <221>	3 of 130.83° on <533> 3 of 157.38° on <430> 3 of 164.06° on <711> 3 of 180° on <431>	$\Sigma 27b$	35.42° on <210> 60° on <511> 79.32° on <311> 94.25° on <432> 95.30° on <731> 109.47° on <411>	2 of 114.05° on <532> 2 of 122.50° on <911> 2 of 131.81° on <542> 146.44° on <771> 148.42° on <710> 2 of 148.42° on <543>	2 of 157.82° on <431> 164.36° on <720> 2 of 168.97° on <951> 168.97° on <773> 180° on <721>
$\Sigma 15$	48.19° on <210> 50.70° on <311> 78.46° on <211> 2 of 86.18° on <321> 2 of 99.59° on <531> 2 of 113.58° on <421>	117.82° on <311> 134.43° on <551> 134.43° on <711> 2 of 137.17° on <431> 137.17° on <510> 2 of 150.07° on <321>	2 of 158.96° on <432> 158.96° on <520> 165.16° on <553> 2 of 165.16° on <731> 180° on <521>	$\Sigma 29a$	43.61° on 46.39° same 133.61° same 136.39° <100>	4 of 97.93° on <522> 4 of 98.92° on <733> 4 of 147.65° on <773>	4 of 149.55° on <552> 2 of 180° on <520> 2 of 180° on <730>
$\Sigma 17a$	28.07° on 61.93° same 118.07° same 151.93° <100>	4 of 93.37° on <411> 4 of 105.35° on <533> 4 of 137.33° on <553>	4 of 160.25° on <441> 2 of 180° on <410> 2 of 180° on <530>	$\Sigma 29b$	46.39° on <221> 66.63° on <531> 76.02° on <332> 84.07° on <320> 97.93° on <441> 112.29° on <210>	2 of 116.62° on <541> 2 of 124.68° on <931> 2 of 133.61° on <632> 136.40° on <430> 2 of 147.65° on <951> 149.55° on <211>	2 of 149.55° on <721> 164.92° on <722> 164.92° on <544> 2 of 169.36° on <953> 180° on <432>
$\Sigma 17b$	2 of 61.93° on <221> 2 of 63.82° on <331> 86.63° on 93.37° same <110>	2 of 118.07° on <430> 2 of 121.97° on <320> 4 of 137.33° on <731> 4 of 139.88° on <521>	2 of 160.25° on <522> 2 of 166.07° on <733> 180° on <322> 180° on <433>	$\Sigma 19a$	26.53° on 153.47° same <110>	2 of 73.17° on <511> 2 of 93.02° on <310> 2 of 99.08° on <332> 2 of 110.01° on <711> 4 of 121.76° on <432>	2 of 142.14° on <433> 2 of 161.33° on <610> 4 of 166.83° on <751> 180° on <331> 180° on <611>

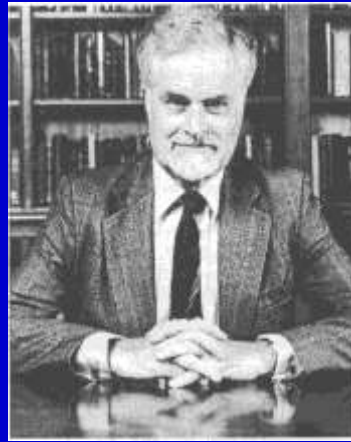
**Our Pioneers who have led us for many years in
research field of Grain Boundary and Interfaces**



T. S. Ke



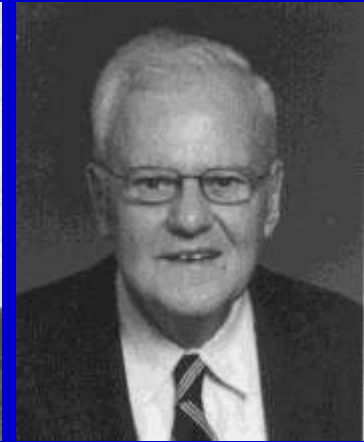
D. McLean



R. W. Cahn



J. W. Christian



H. I. Aaronson



R. C. Gifkins

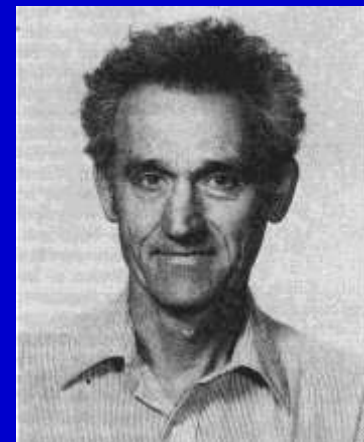


P. Haasen



D. A. Smith

Y. Ishida



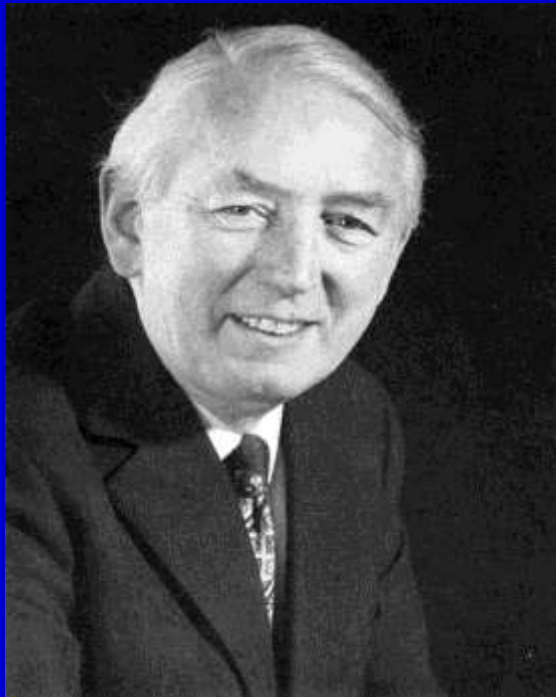
R. W. Balluffi

Effects of Grain Boundaries on “Bulk Properties”

Two-fold Effects: “Beneficial” or “Detrimental”

Early Work on “Grain Size Effects” on Deformation and Fracture.

“Hall-Petch Relationship”

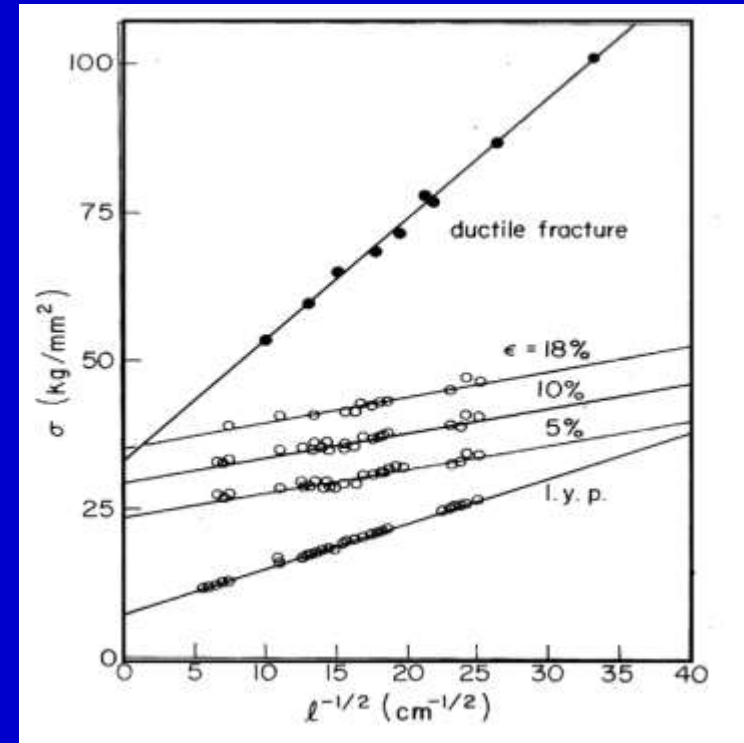


N. J. Petch

**Flow Stress, σ
or
Fracture Stress,**

$$\sigma = \sigma_0 + k d^{-\frac{1}{2}}$$

d : Grain Size



E.O.Hall; Proc. Phys. Soc., Lond. B, 64 (1951), 747.

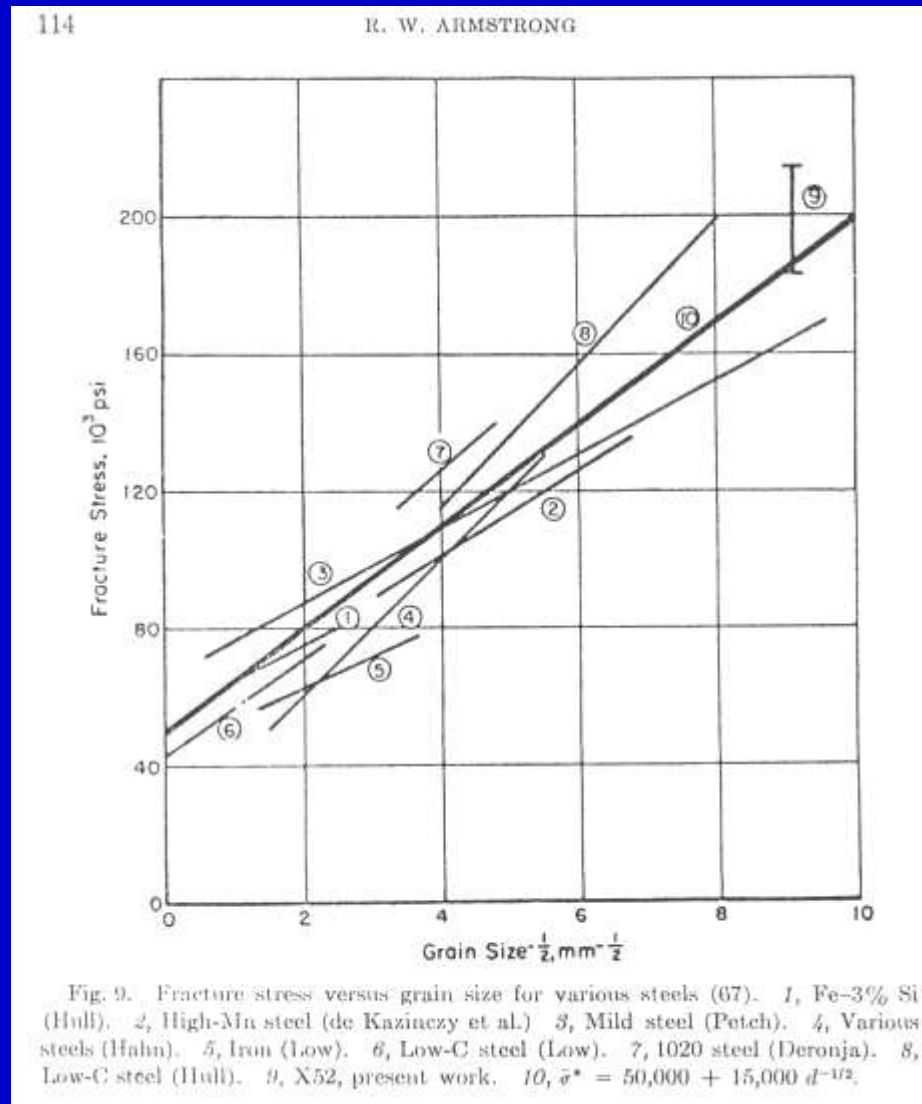
N. J. Petch, ;J. Iron St. Inst., 174 (1953), 25.

Hall-Petch Plots for Lower Yield Stress, Flow Stress and Fracture Stress for Mild Steel.

“Grain Size Effect” = “G.B. Density Effect” ignores “Structural Effect”.

Grain Size Dependence of Fracture Stress in Various Steels

A.R. Rosenfield & G.T. Hahn: Trans. ASM., 59 (1966), 962



Roles of Grain Boundaries in Plastic Deformation

Grain Boundaries as Preferential Sites for

“Dislocation Nucleation”

Journal of the Less-Common Metals 28(1972) 357-385, 357
Elsevier Sequoia S.A., Lausanne - Printed in The Netherlands

SOME REFLECTIONS AND DIRECT OBSERVATIONS OF IMPERFECTIONS IN METALS*

A. BERGHEZAN and A. FOURDEUX
U.C.L. University, Louvain-la-Neuve (Belgium)
(Received February 11th, 1972)

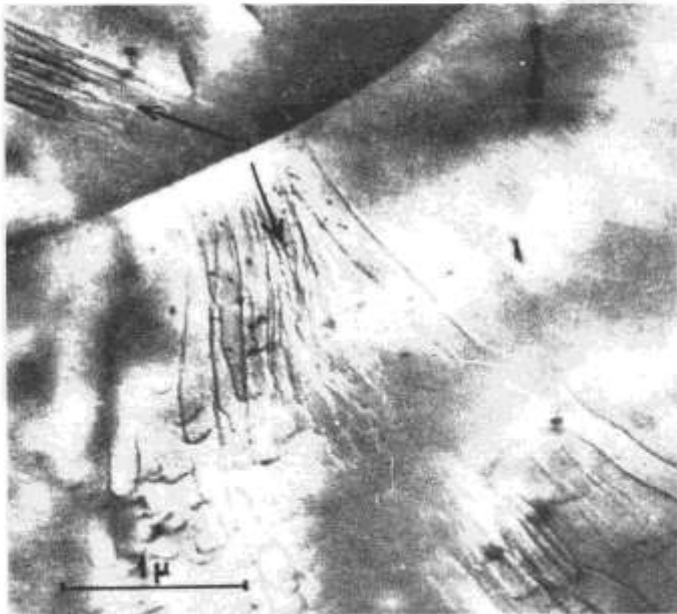
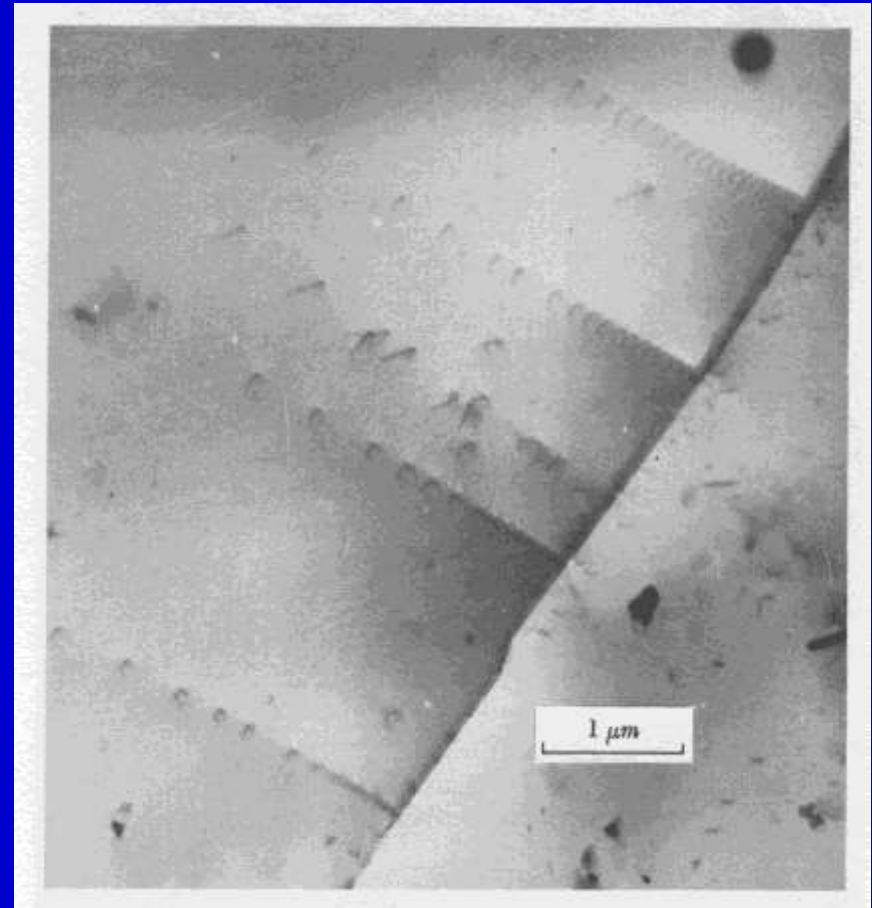


Fig. 8. A great deal of evidence has been found concerning the important role of grain boundaries in the mechanism (generation) of dislocations. The Figure clearly shows that grain-boundaries act as dislocation sources (Nobrium sample strained inside the microscope)

“Dislocation Pile-up”

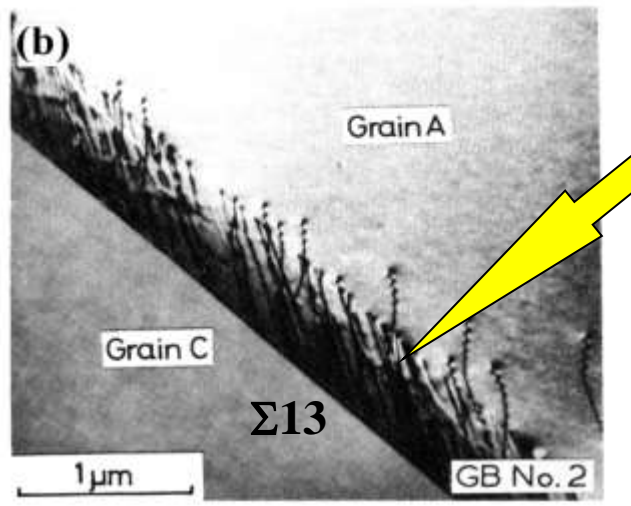
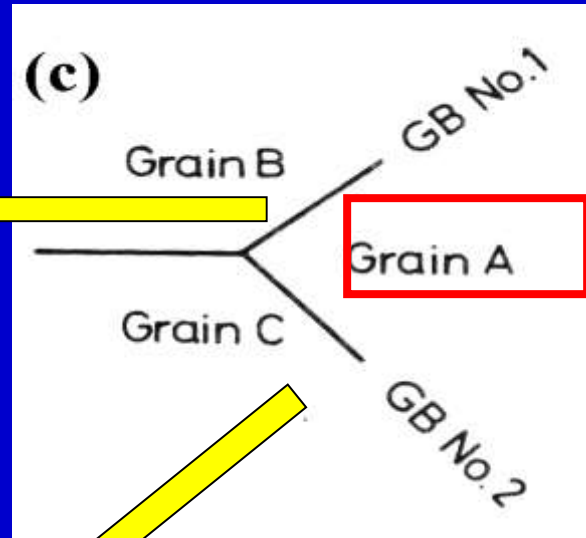
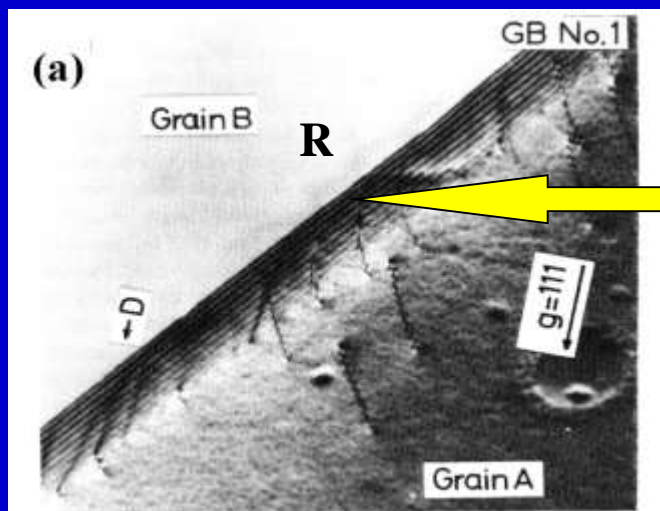


Nb: A. Berghezan & A. Fourdeux:
J. Less Common Metals, 28(1972), 357

Stainless Steel; M. J. Whelan, & P. B. Hirsch;
Phil. Mag., 2(1957), 1121

Interactions of Lattice Dislocations with Grain Boundaries

Aluminium Polycrystal Specimen Crept up to 1.3% Elongation
at Tensile Stress of 5 MPa and 600K.



Type of grain boundary ;

- (a) G.B. No. 1: Random Boundary,
- (b) G.B. No.2: slightly off- $\Sigma 13b$ Coincidence Boundary:

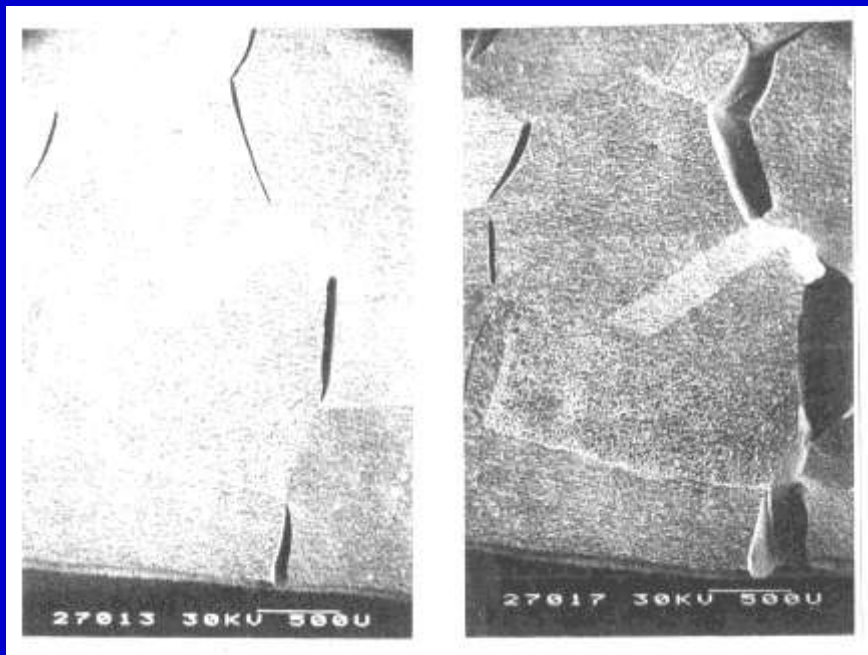
H. Kokawa, T. Watanabe and S. Karashima;
J. Mater. Sci., 18 (1983), 1183-1194.

Heterogeneity of Grain Boundary Phenomena in Polycrystalline Materials

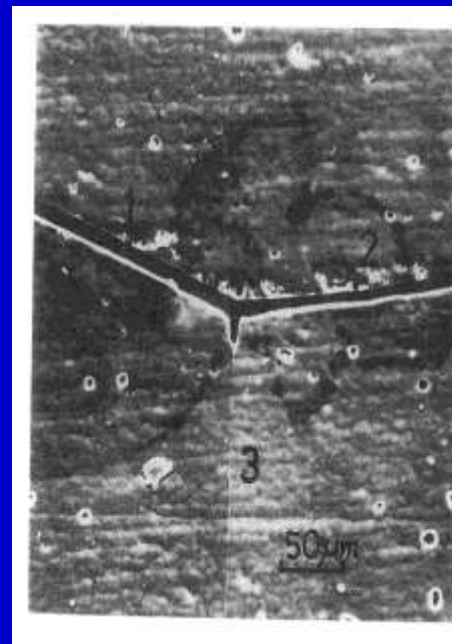
“The extent of occurrence” of grain boundary phenomenon are quite different from boundary to boundary, demonstrating “the difference in effectiveness of GB” as preferential sites for metallurgical phenomena controlling bulk properties.

This suggests Possible Effects of “GB Type and Structure” on “GB Properties”.

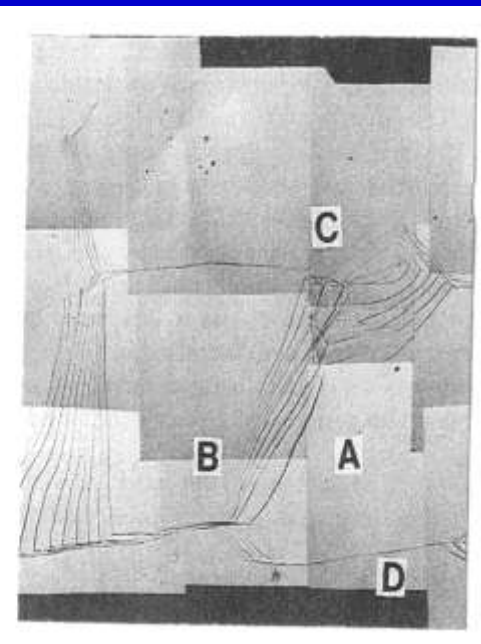
Grain Boundary Fracture



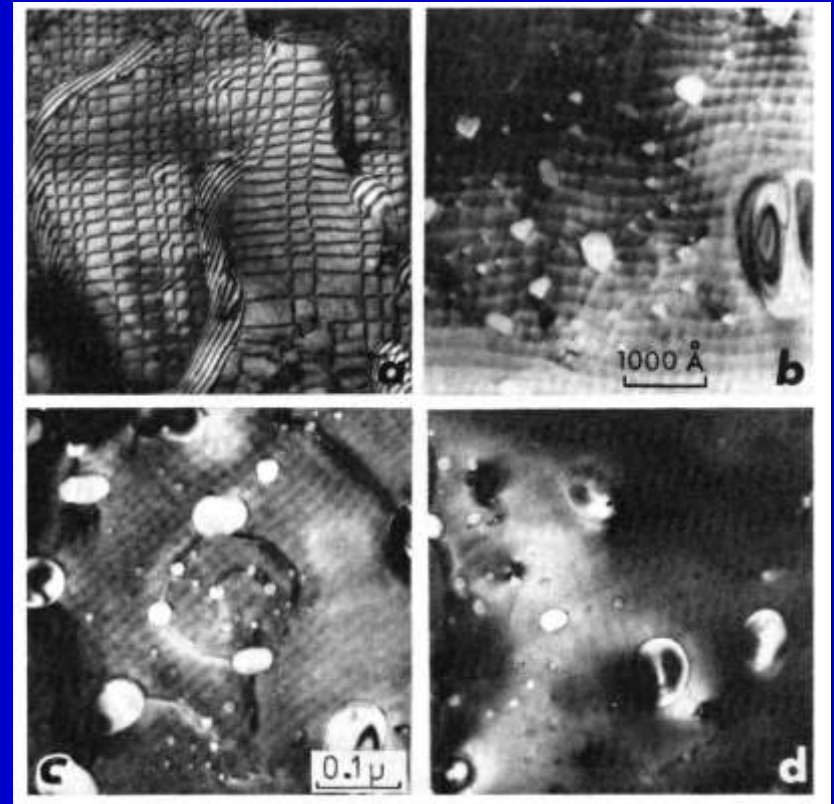
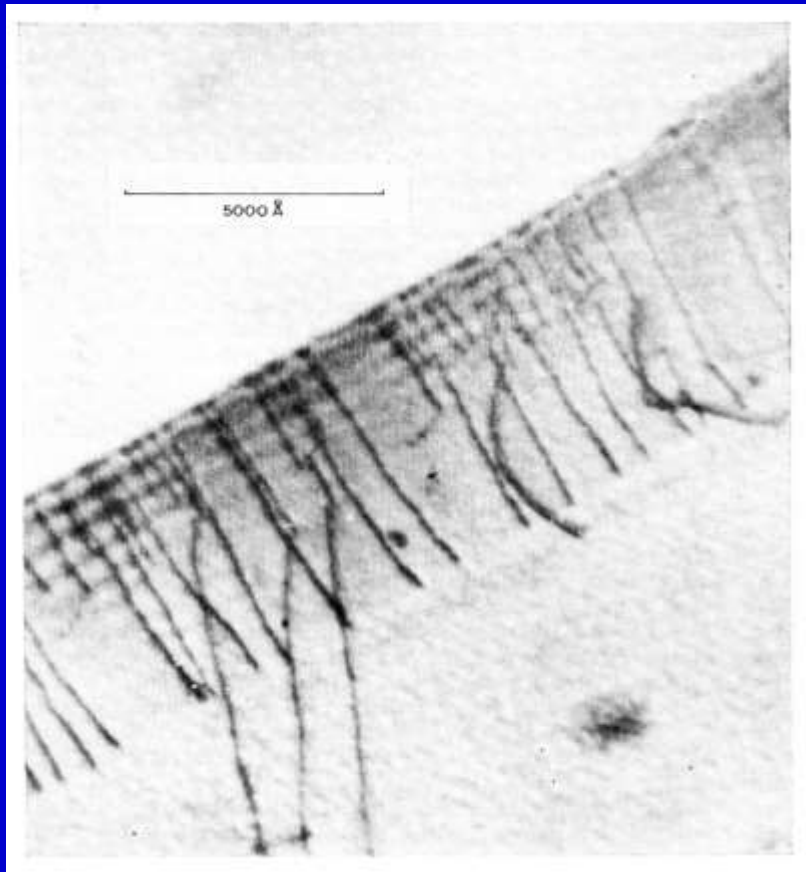
Corrosion



Migration



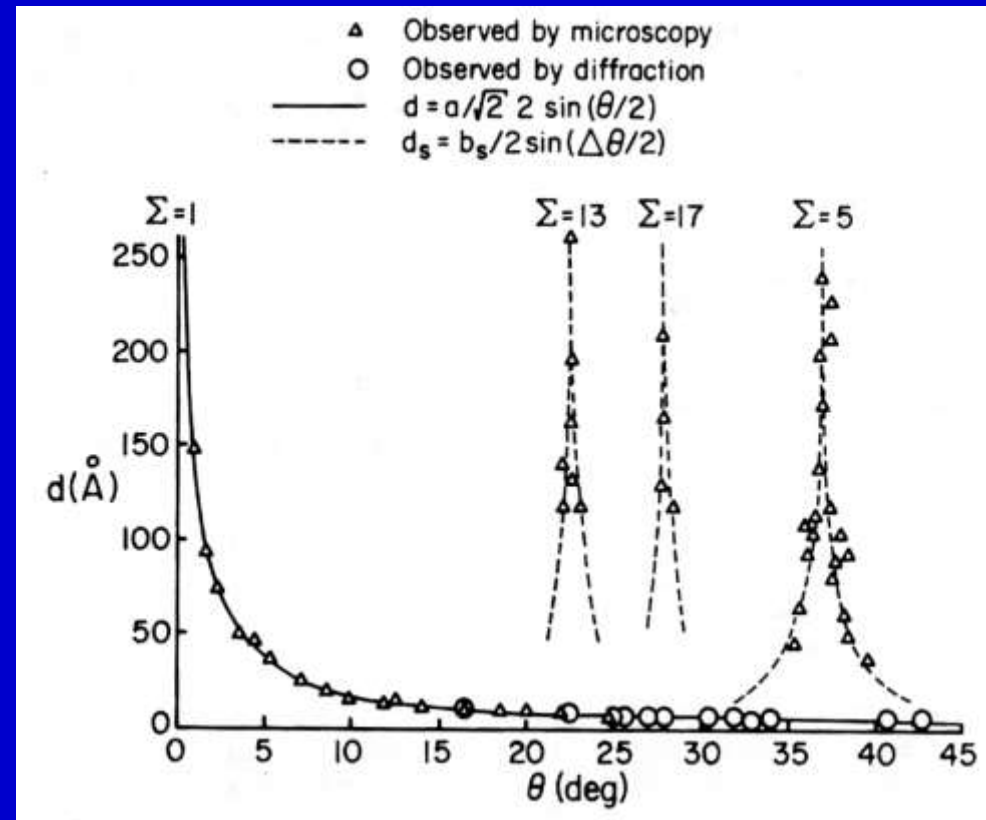
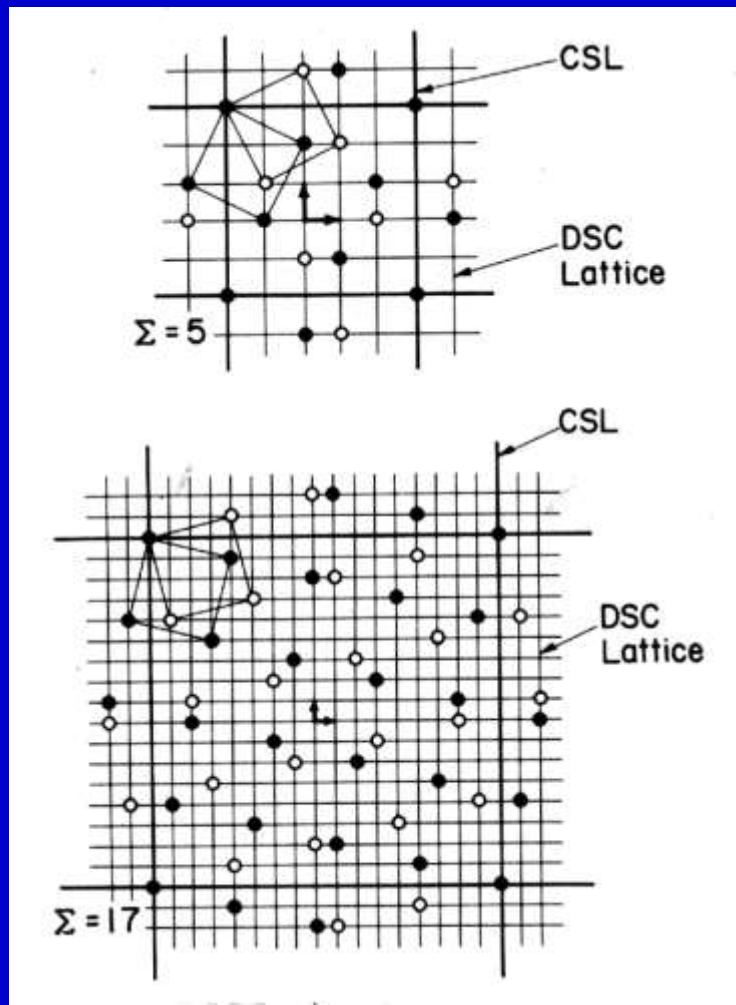
TEM Observations of GB Intrinsic and Extrinsic Dislocations



Absorbed Lattice Dislocations in a Grain Boundary in an Fe-0.75%Mn-0.01%N Alloy, Creep Tested at 773K to 0.94% Strain. (Y. Ishida and M. Henderson Brown, Acta Metall., 15 (1967), 857-860.)

Square Networks of Screw GBD's Observed in Vicinities of CSL Misorientations : (a) near $\theta = 0^\circ$, $\Sigma = 1$; (b) near $\theta = 36.9^\circ$, $\Sigma = 5$; (c) near $\theta = 22.6^\circ$, $\Sigma = 13$; (d) near $\theta = 28.1^\circ$, $\Sigma = 17$. Note that the GBD Contrast Decreases as Σ Increases. (R.W. Balluffi, Y. Komen and T. Schober, Suf. Sci., 31 (1972), 68-103.)

Displacement Shift Complete (DSC) Lattice Model

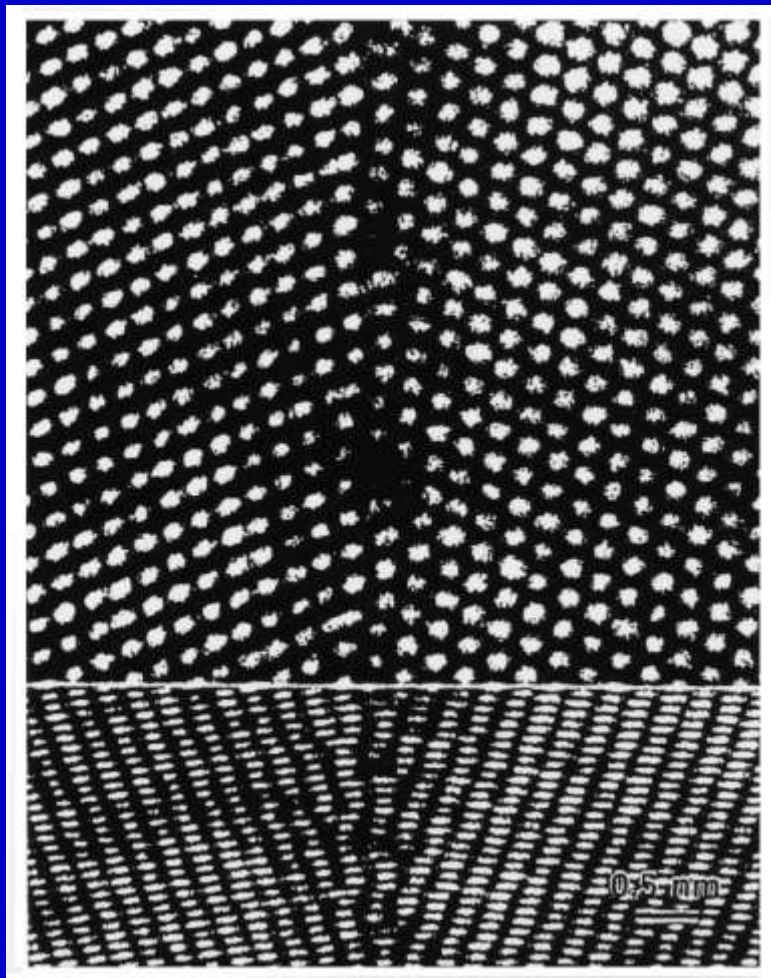


DSC-Lattices formed by interpenetrating (001) planes of simple Cubic Lattices rotated with respect to one another by Angle θ around [001]. Top: $\theta = 36.9$ ($\Sigma = 5$). Bottom: $\theta = 28.1$ ($\Sigma = 17$). The Burgers vectors of the DSC-intrinsic dislocations are shown at the center of each diagram.

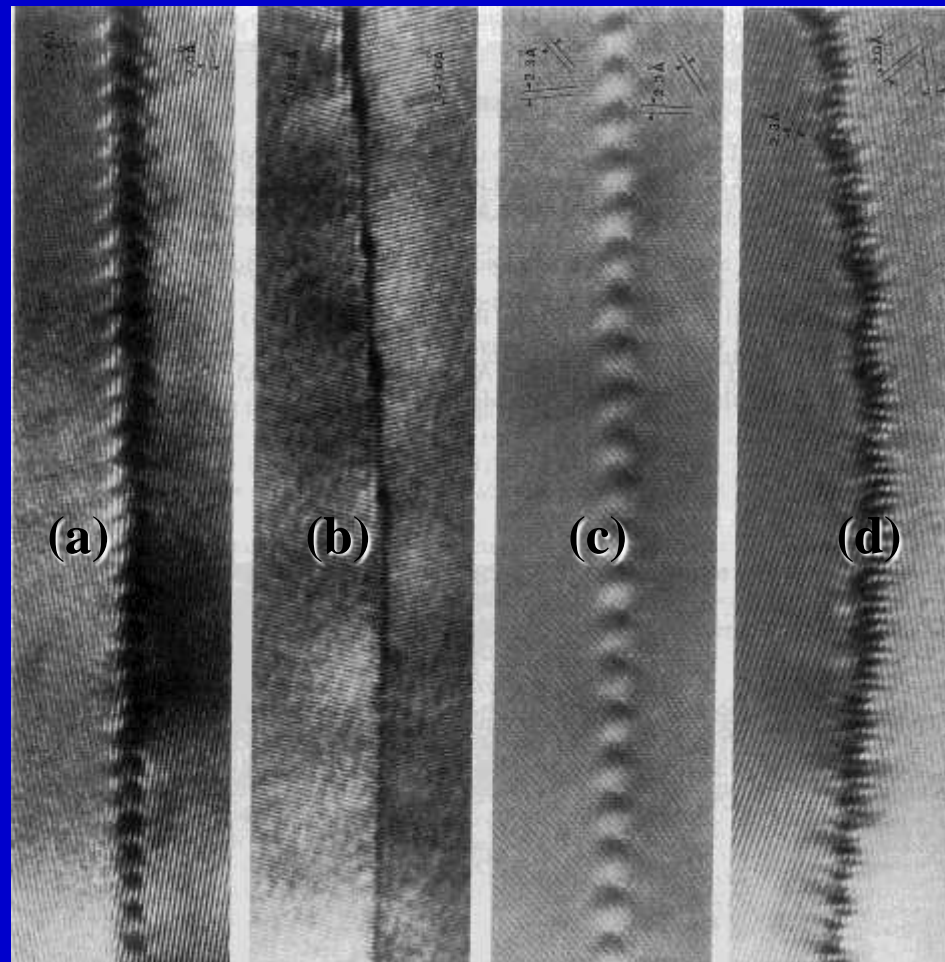
Observed Primary Relaxation Spacing, d , and Secondary Relaxation Spacing, d_s , in [001] Twist Boundaries in Gold as a Function of Twist Angle θ .

R. W. Balluffi: "Grain Boundary Structure and Segregation", Interfacial Segregation, ASM., (1979), 193-237.

High Resolution TEM Observations of Grain Boundaries in Gold



HREM Image of the (443) Symmetric Tilt GB (tilt angle $\psi = 55$, $\Sigma = 41$).



(a) $18^\circ[001] / (610)$ (b) $28^\circ[001] / (410)$
(c) $10^\circ[110] / (881)$ (d) $28^\circ[110] / (331)$

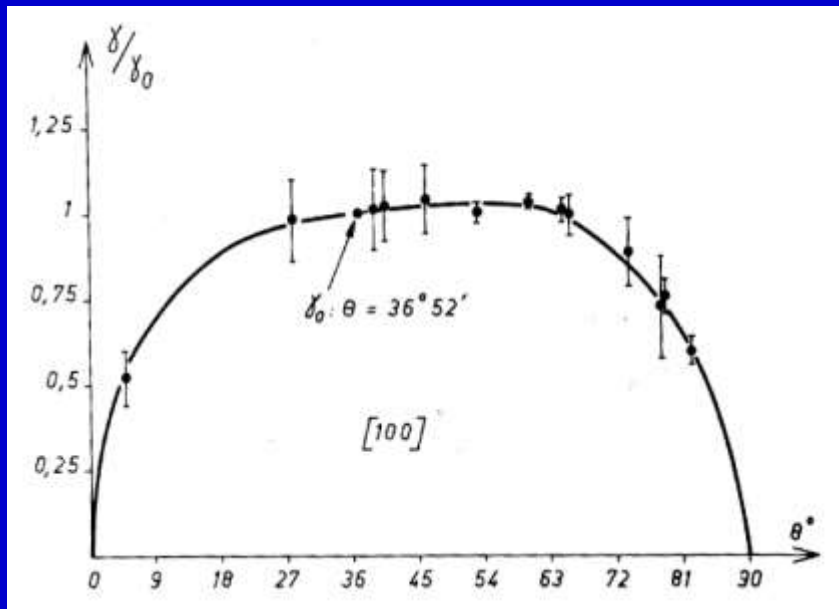
High Resolution Micrographs Various Tilt Grain Boundary Structures Exhibiting Dislocation Strain Field and Lattice Fringe Contrasts in Gold.

(W. Krakow and D. A. Smith, Trans. JIM Suppl. 27 ([1986](#)), 277-284)

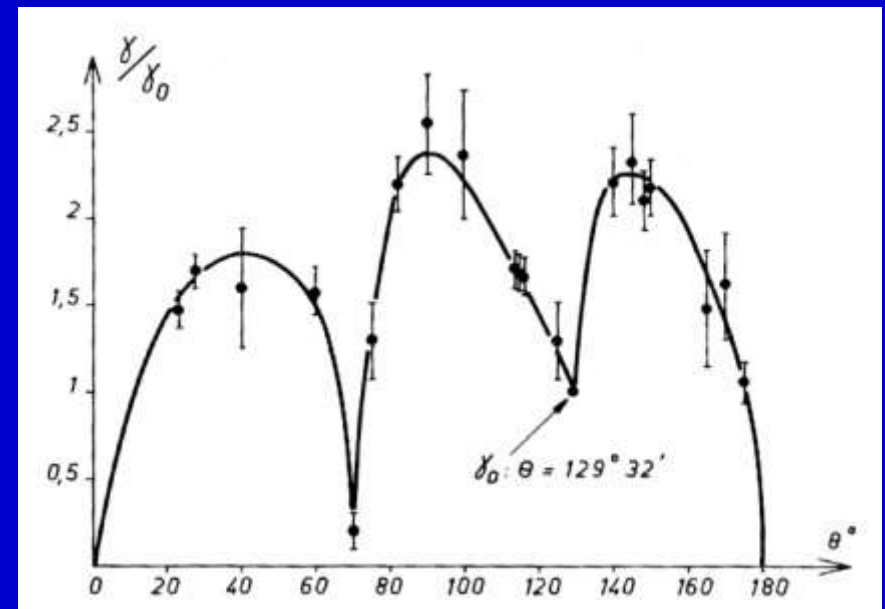
Misorientation-dependent Grain Boundary Energy

in [100] and [110 tilt] Al Bicrystals

(a) [100] tilt



(b) [110] tilt

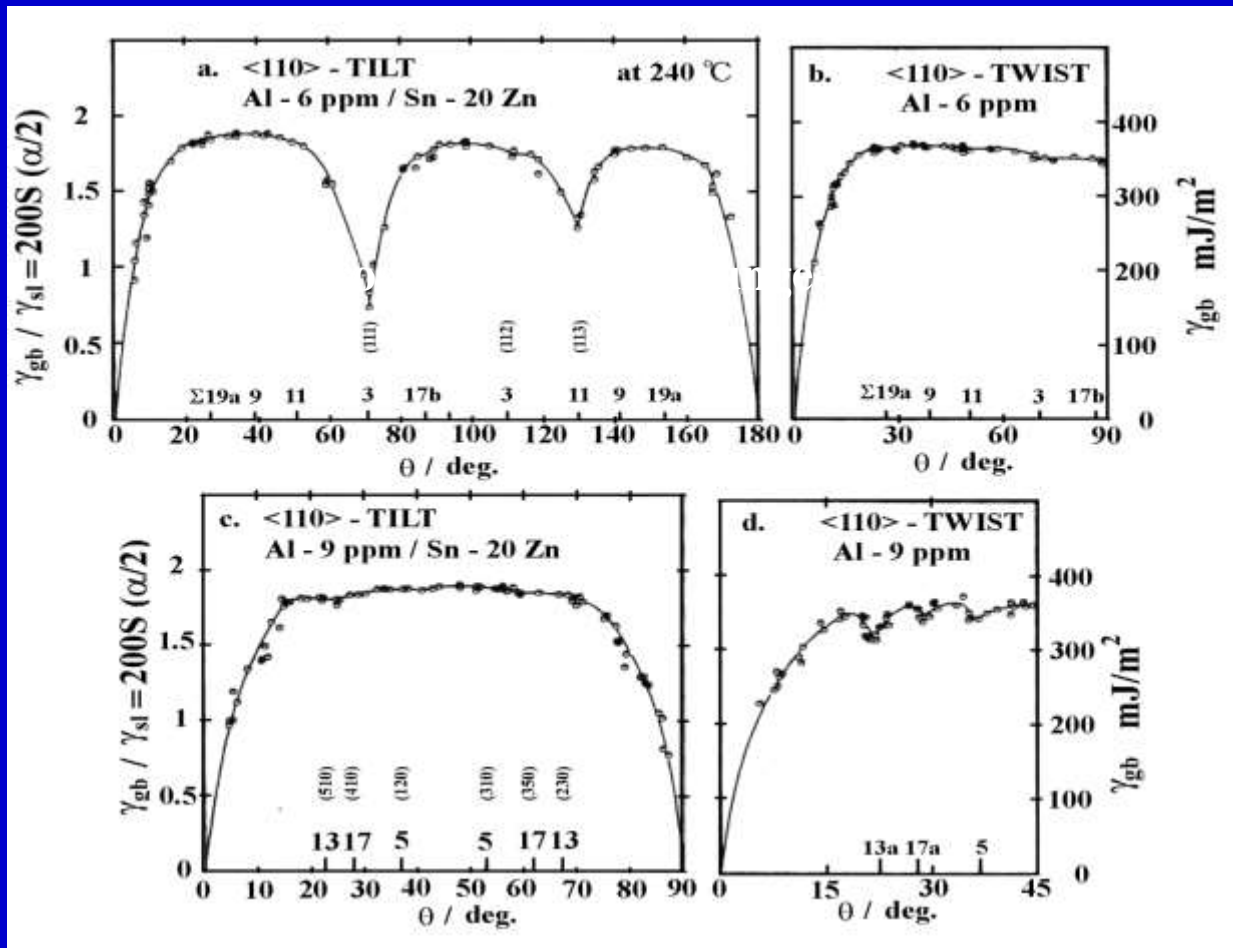


Variations in Grain Boundary Energy for Symmetric Tilt Grain Boundaries in Al Bicrystal. (G. Hasson, J. -Y. Boos, I. Herbeuval, M. Biscondi and C. Goux : Surface Science, 31 (1972), 115-137.)

Basic Study of Grain Boundary Properties in Bicrystals

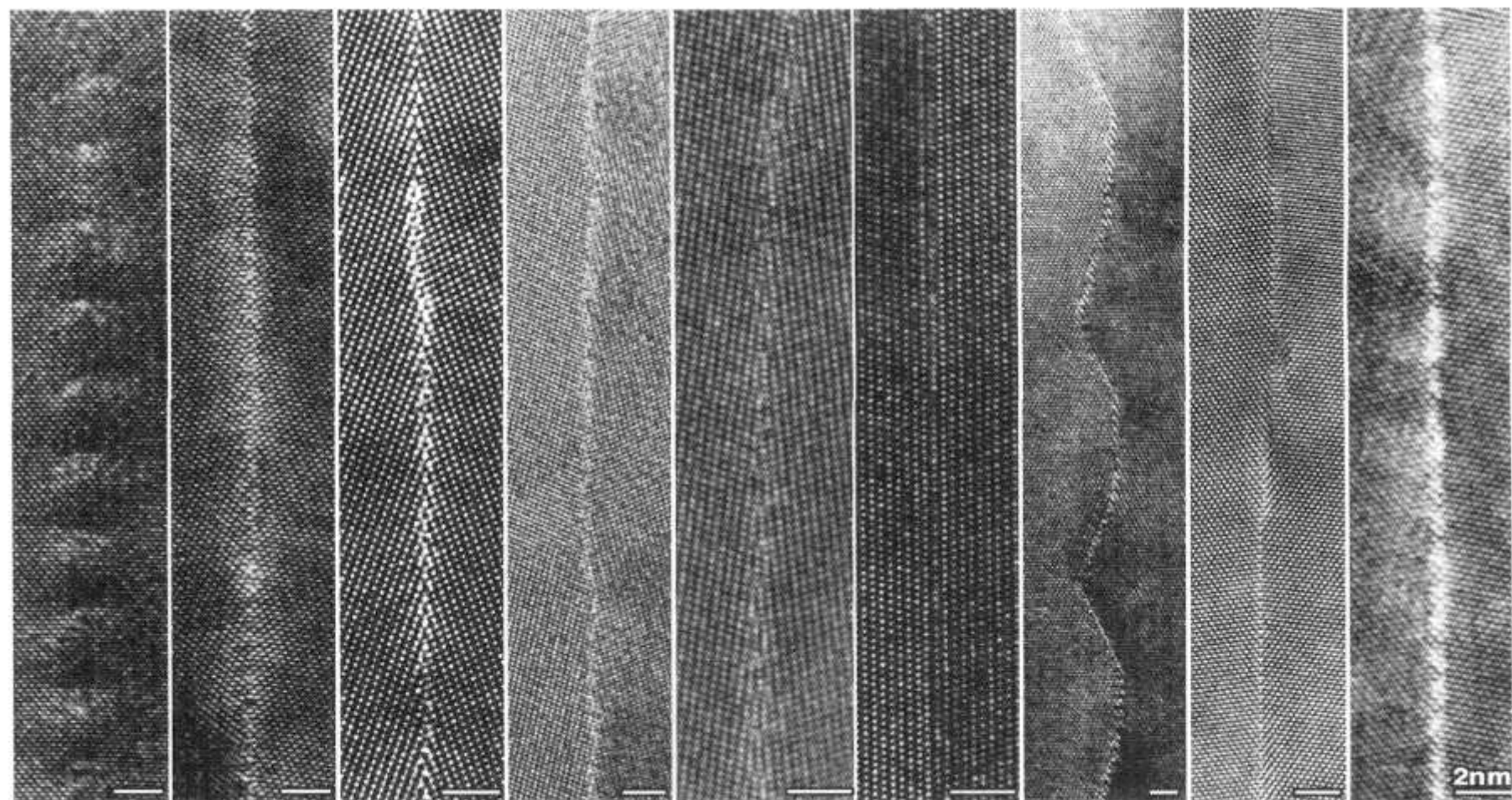
Example: Structure-dependent Grain Boundary Energy

A. Otsuki: Al bicrystals: Trans. JIM., 27 (1986), 789, J. de. Phys., 49 (1988), C5-563,
Si bicrystals: Acta Mater., 49 (2001), 1737-1745.



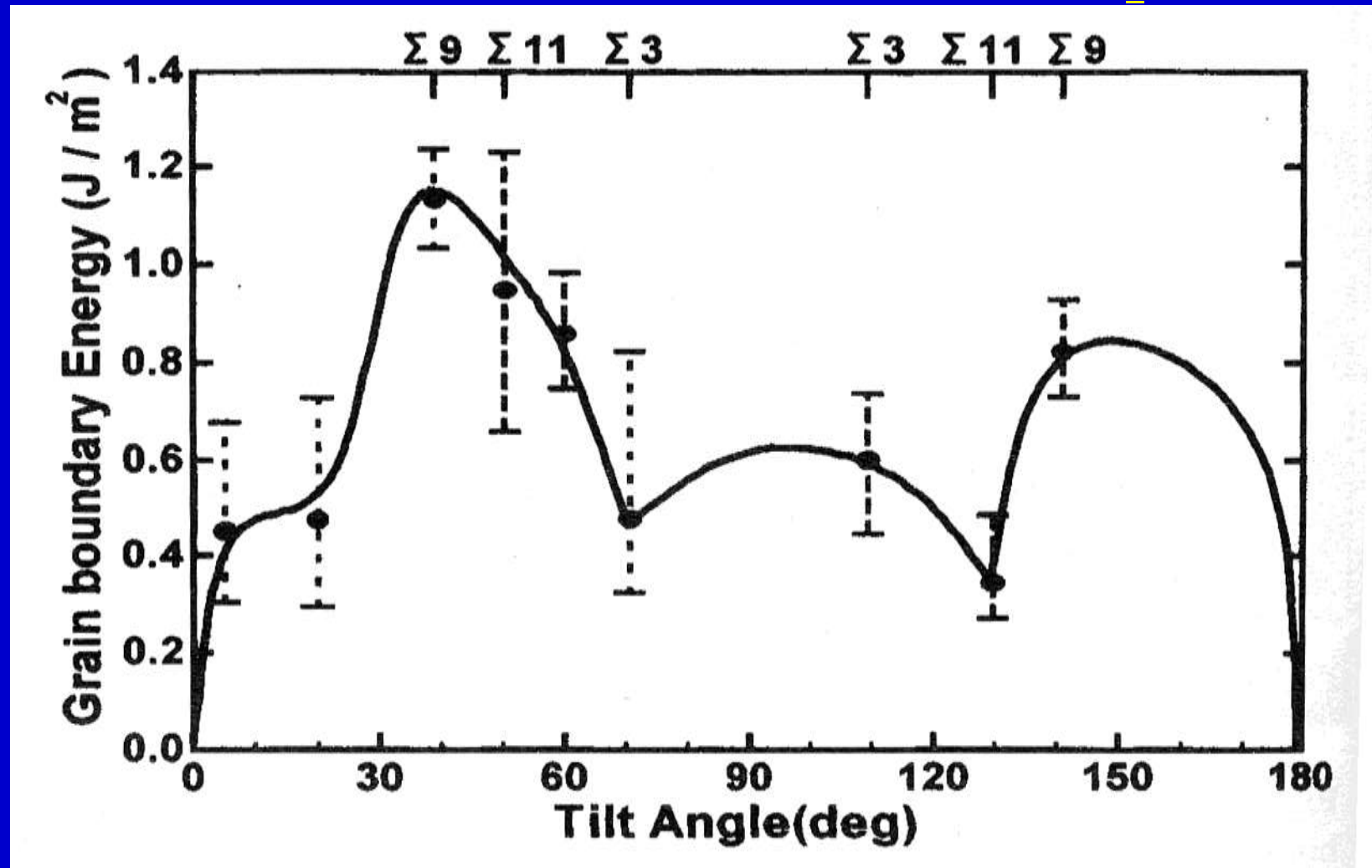
HREM Images for Grain Boundary Atomic Structures depending on Misorientation in ZrO₂ Bicrystals

Y. Ikuhara, N. Shibata, T. Watanabe, F. Oba, T. Yamamoto and T. Sakuma,
Ann. Chim. Sci. Mat.: 27 (2002) Suppl 1, S21-30.



5.0° 20.0° 39.0° Σ 9 50.5° Σ 11 60.0° 70.5° Σ 3 109.5° Σ 9 129.5° Σ 11 141.0° Σ 9

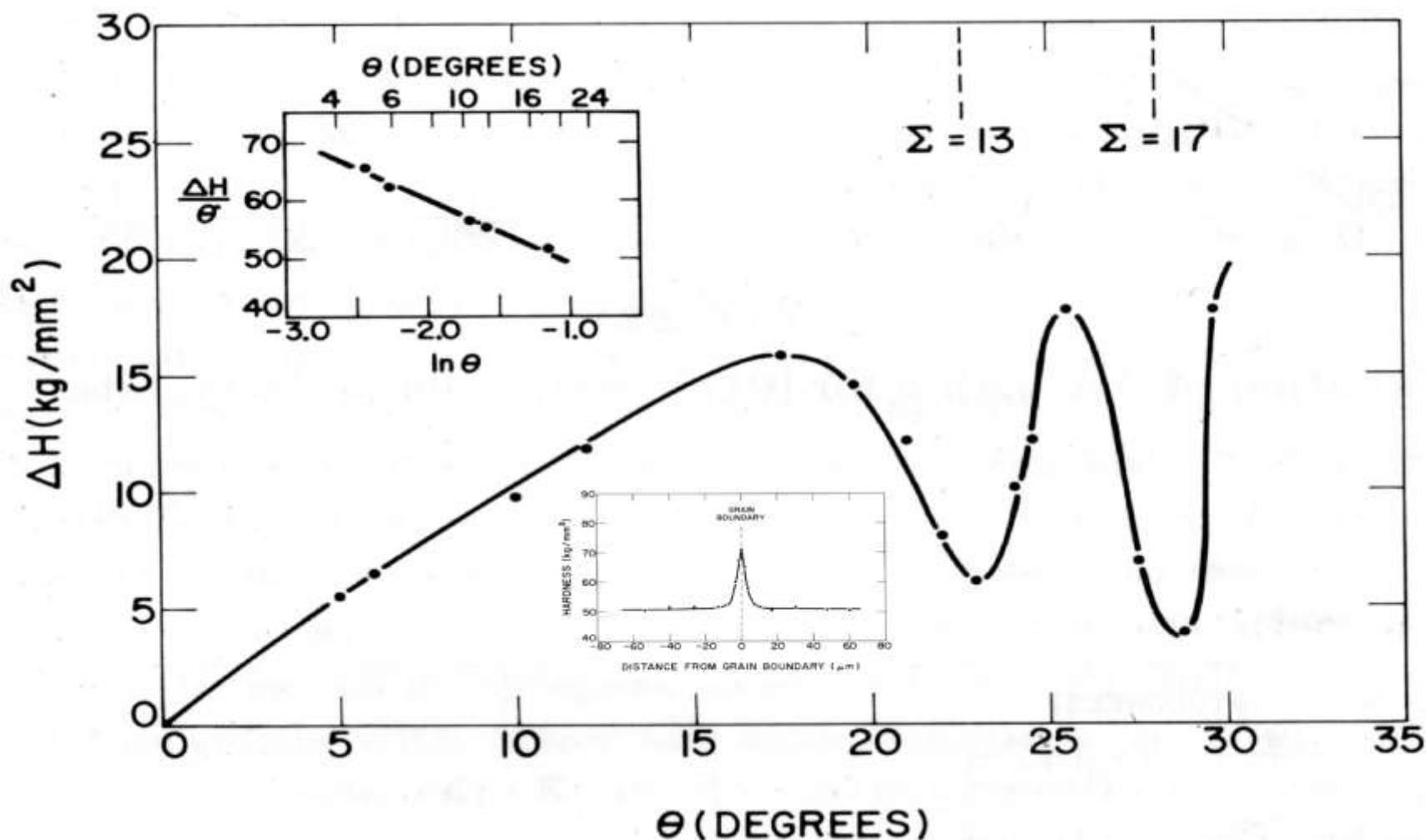
Misorientation Dependence of Grain Boundary Energy <110> Symmetric Tilt Boundaries in ZrO₂



Y. Ikuhara, N. Shibata, T. Watanabe, F. Oba, T. Yamamoto and T. Sakuma;
Proc. Japan-France Joint Symp., Ann Chim Sci. Mat., 27(2002), Suppl 1:
S21-30 , or H. Yoshida et al; Acta Mater., 52 (2004), 2349.

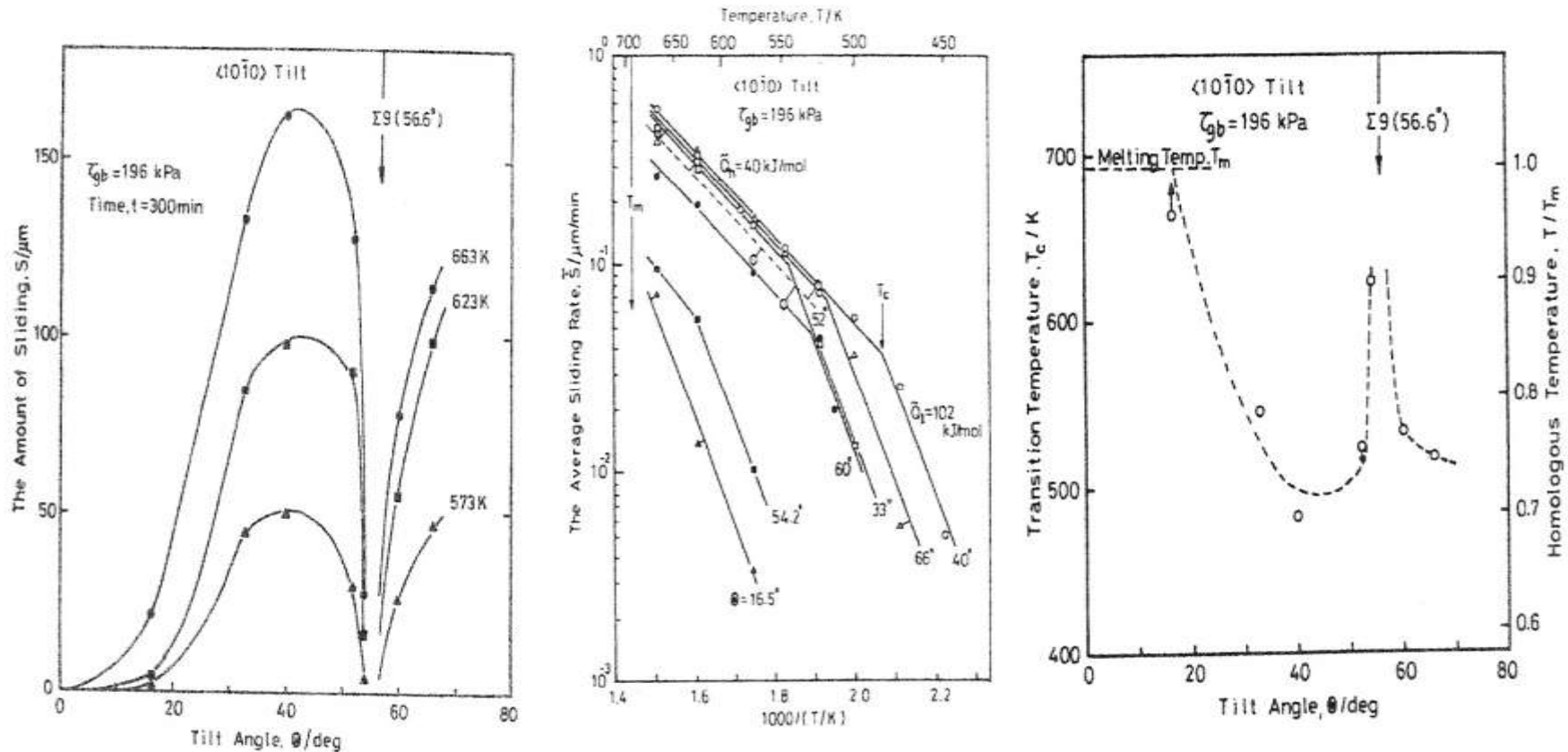
Structure-Dependent Grain Boundary Hardness in $\langle 100 \rangle$ Tilt Niobium Bicrystals.

Y. T. Chou, B. C. Cai, A. D. Romig, Jr., L. S. Lin; *Phil. Mag. A*, 47 (1983), 363-368.



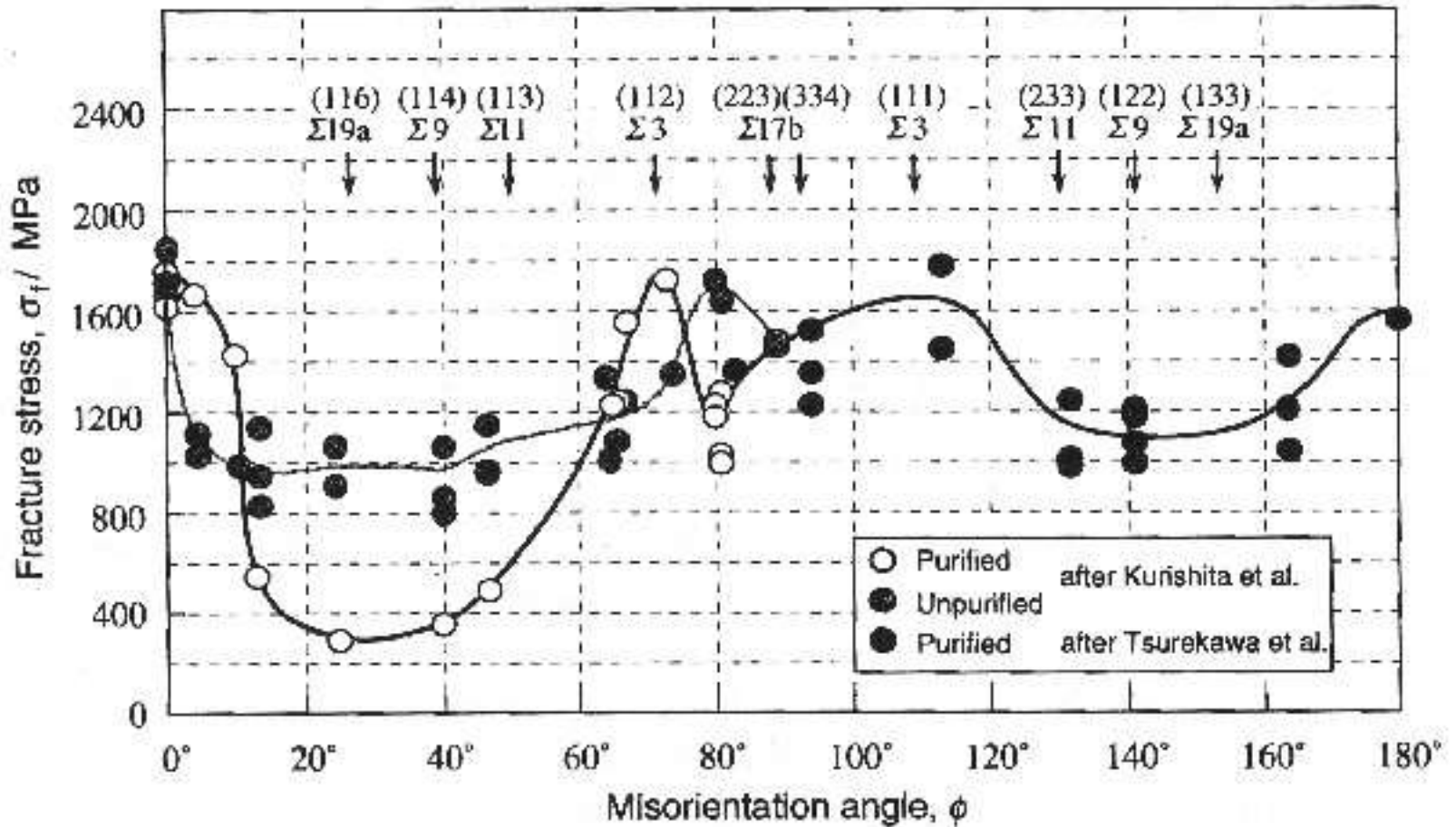
Structure-dependent Grain Boundary Sliding and Structural Transformation in $\langle 10\bar{1}0 \rangle$ Symmetric Tilt Zinc Bicrystals.

T. Watanabe, S. Kimura, S. Karashima: *Phil. Mag.*, 49 (1984), 845-864.
“The Effect of a grain boundary structural transformation on Sliding in $\langle 10\bar{1}0 \rangle$ tilt zinc bicrystals”.



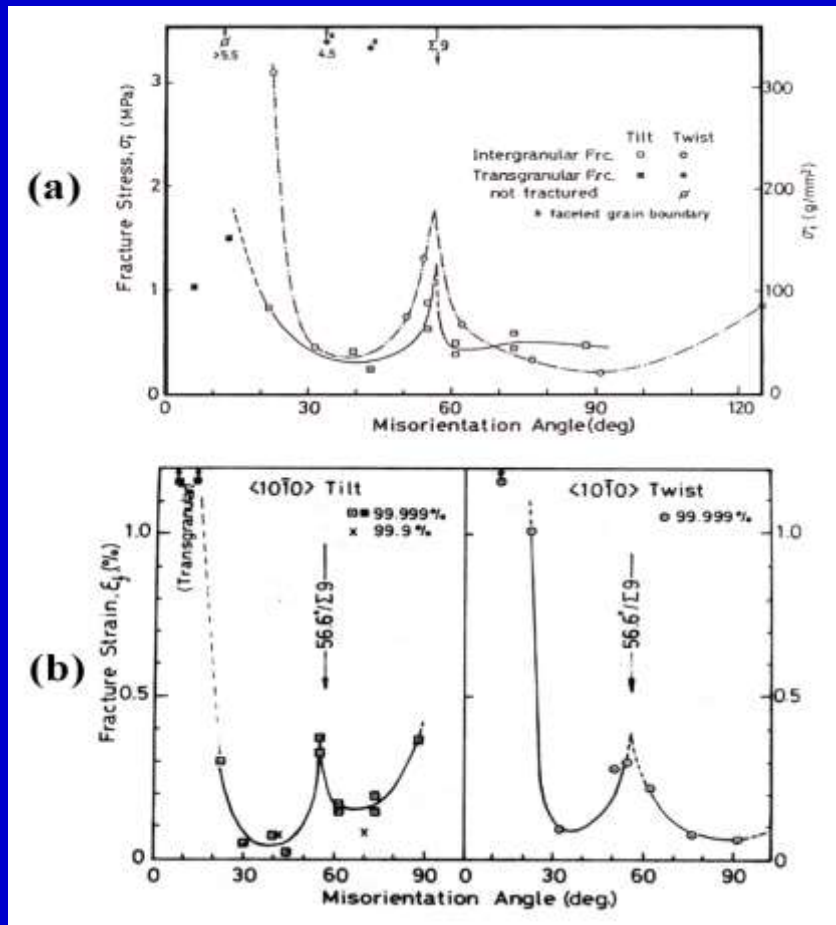
Structure-Dependent Fracture Stress in Mo Bicrystals with $\langle 110 \rangle$ Symmetric Tilt Boundaries

S. Tsurekawa, Tanaka and H. Yoshinaga: Mater. Sci. Eng., A 176 (1994), 341.



Structure-Dependent Fracture Stress and Strain

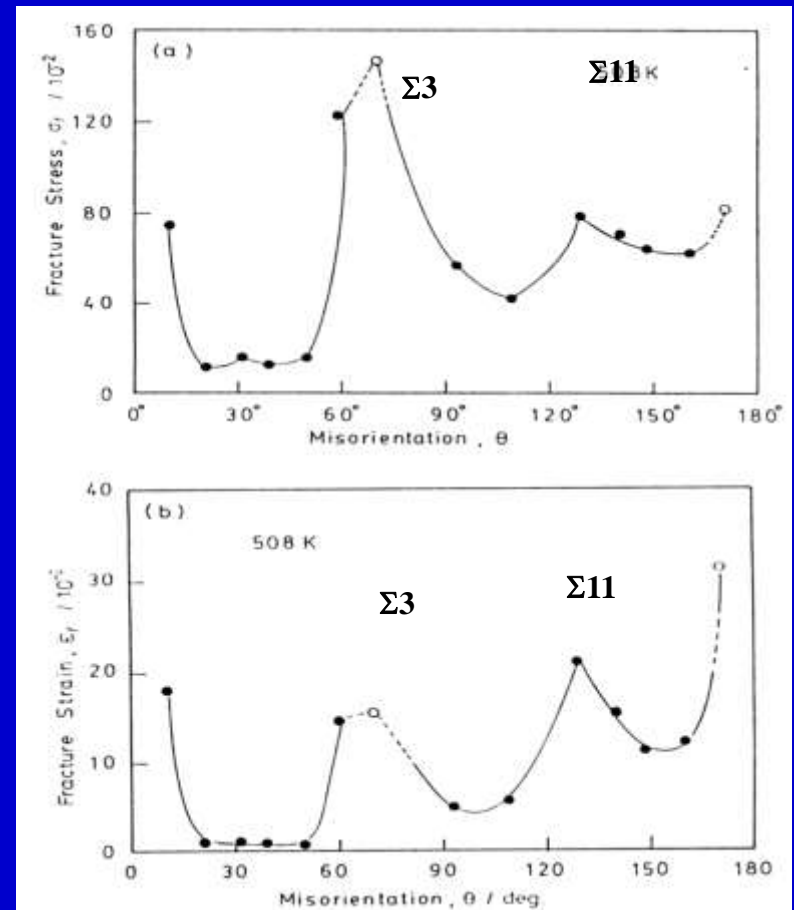
Liquid Hg-induced Fracture in Zn



Structure-Dependent Fracture Stress and Strain in <1010> Tilt and <10 $\bar{1}$ 0> Twist Zinc Bicrystals.

(T. Watanabe, S. Shima and S. Karashima: Embrittlement by liquid and solid metals, Met. Soc. AIME, (1984), 161-172)

Bismuth-induced Fracture in Cu



Structure-Dependent Fracture Stress and Strain in Cu-Bi <110> Tilt Bicrystals.

(H. Miura, T. Yoshida, T. Sakai, M. Kato and T. Mori, J. Jpn. Inst. Metals, 57 (1993), 479-485)

Fracture Stress Data for Different Types of Grain Boundaries

L. C. Lim and T. Watanabe; Acta Metall. Mater., 38 (1990), No.12, 2507-2516.

Table 1. Fracture stress of coincidence boundaries

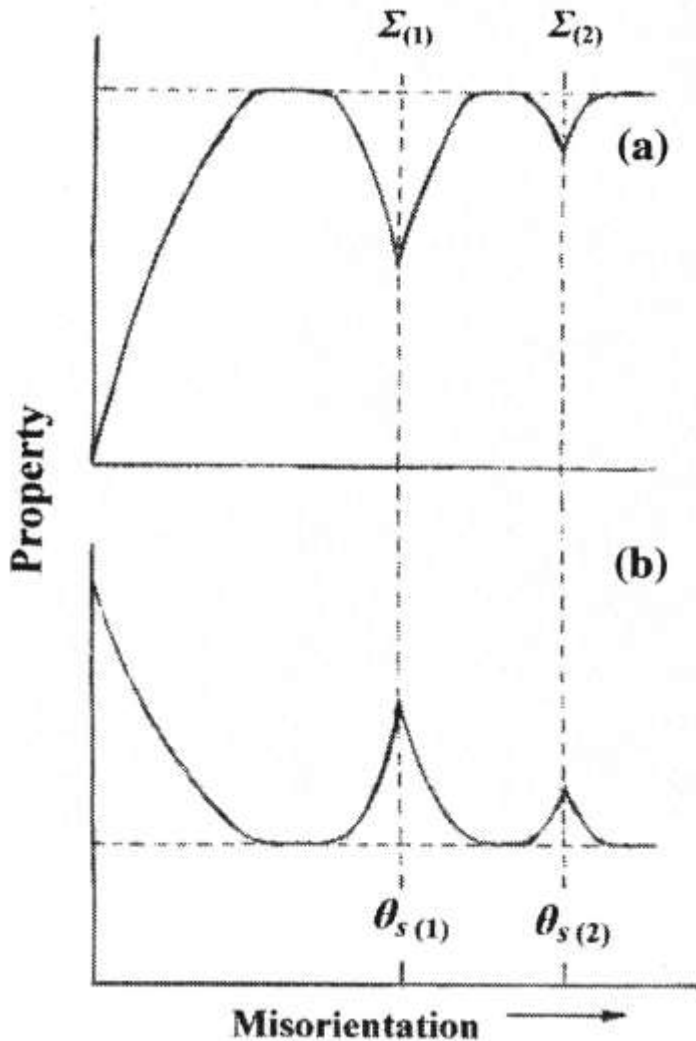
Material	Type of boundary	Test condition	Fracture stress			Reference
			Coincidence σ_{Σ}	Random σ_R	σ_{Σ}/σ_R	
Mo	$\langle 100 \rangle$ Sym. tilt	R.T. ^a	1340 MPa (5°/Σ 1)	75 MPa	17.8	[13]
			1150 MPa (8°/Σ 1)		15.3	
	$\langle 110 \rangle$ Sym. tilt	R.T.	800 MPa (109°/Σ 3)	88 MPa	9.1	[13]
			570 MPa (50°/Σ 11)		6.5	
Mo	$\langle 100 \rangle$ Sym. tilt	R.T.	533 MPa (9.3°/Σ 1)	106–120 MPa	4.4–5.0	[14]
	$\langle 110 \rangle$ Sym. tilt	R.T.	293 MPa (10°/Σ 1)		67 MPa	
			400 MPa (110°/Σ 3)		6.0	
			400 MPa (50°/Σ 11)		6.0	
Mo	$\langle 110 \rangle$ Sym. tilt	77 K	1720 MPa (70°/Σ 3)	280 MPa	6.1	[15]
Mo	$\langle 110 \rangle$ Twist	77 K	1440 MPa (73°/Σ 3)	623 MPa	2.3	[16]
Si	$\langle 111 \rangle$ Twist	R.T.	300 MPa (25°/Σ 7)	140 MPa	2.1	[17]
Zn	$\langle 10\bar{1}0 \rangle$ Sym. tilt	Liquid Ga 303 K	0.86 MPa (55°/Σ 9)	0.24 MPa	3.6	[18]
	$\langle 10\bar{1}0 \rangle$ Twist	Liquid Ga 303 K	1.3 MPa (54°/Σ 9)		0.20–0.33 MPa	
Al	$\langle 110 \rangle$ Tilt	Liquid Sn–Zn 513 K	25 MPa (5°/Σ 1)	4.9 MPa	5.1	[19]
			39 MPa (70°/Σ 3)		8.0	
			23 MPa (120°/Σ 11)		4.7	
			3 kN/m ^b (70°/Σ 3)			
Al	$\langle 110 \rangle$ Sym. tilt	Liquid Hg–Ga	2.4 kN/m ^b (130°/Σ 11)	0.3–0.4 kN/m ^b	7.5–10.0	[20]
					6.0–8.0	

^aR.T. = room temperature.

^bCrack extension force at 3.5 μm/s.

Schematic Diagram of Two Types of Structure-dependent Grain Boundary Properties in Bicrystals

T. Watanabe: “Grain boundary engineering: historical perspective and future prospects”,
J. Mater. Sci., 46 (2011), 4095-4115



I. Type-A Boundary Properties: Curve (a)

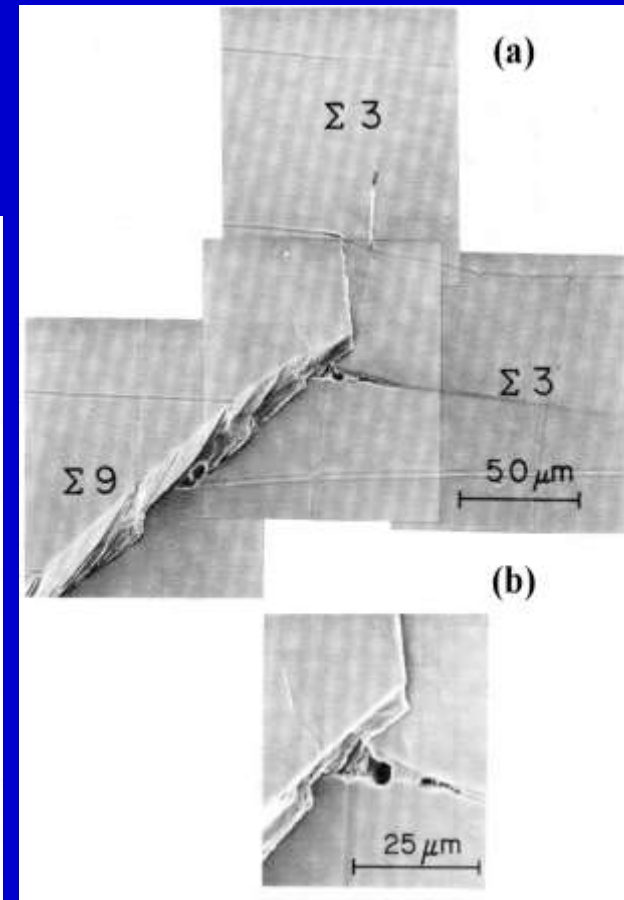
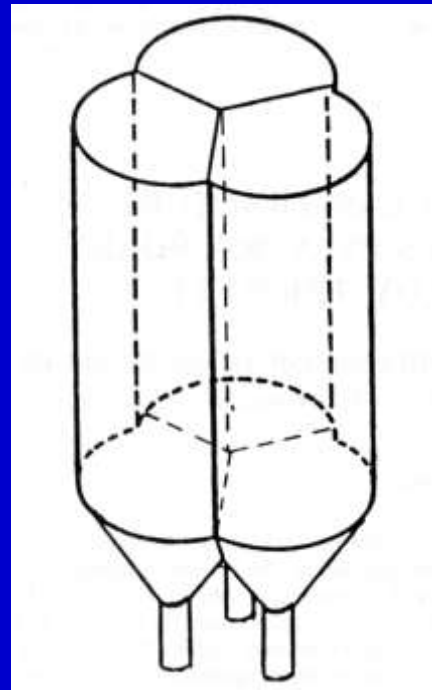
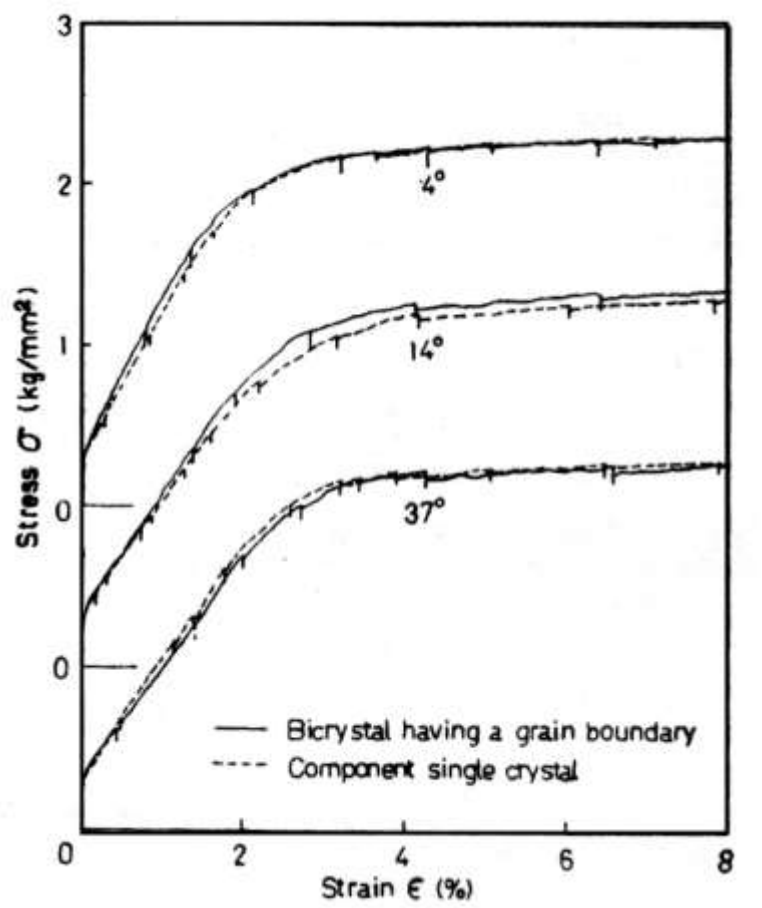
- Grain Boundary Energy (level),
- Corrosion (width / depth),
- Segregation (amount / width, activation energy)
- Diffusion, • Migration, • Sliding (rate / activation energy)
- Hardness (level / width)
- Electrical Resistivity (level)

II. Type-B Boundary Properties: Curve (b)

- Migration (activation energy for middle level purity)
- Fracture (Stress/ Strain level)
- Precipitation (nuclei density)
- Critical temperature T_c for GB phase transformation
- Critical current J_c for superconductivity.

Basic Study of Deformation in Bicrystals and Tricrystal

(S. Miura, S. Hashimoto, et al.)



Stress-strain Curves of $\langle 100 \rangle$ Bicrystals having 4°, 14° and 37° Boundaries and Component Single Crystals.

(S. Miura and Y. Saeki: Acta Met.. 26 (1978), 93-101.)

SEM Micrographs Showing (a) the Surface of Tricrystal Specimen Deformed at 1073K under 6 MPa for 200h and (b) the Enlarged View of Triple Junction. (S. Miura, T. Okada, S. Onaka and S. Hashimoto: Colloq. de Phys., C1, 51 (1990), C1-587-592.)

From “GB Science” to “GB Engineering”

(Started in 1980s and being attempted increasingly up to now)

Progressing Steps to “Grain Boundary and Interface Engineering”.

1. Recognition of Basic knowledge of “Structure-dependent Properties” “Effectiveness” of grain boundaries and interfaces.
2. Quantitative and Statistical analysis of “Grain Boundary Microstructure (GBM)” in Polycrystalline Materials.
3. Need of “New Microstructural Parameters” to describe GBM.
4. Importance of “Grain Boundary Character Distribution (GBCD)” and “Grain Boundary Connectivity.” –OIM Analysis.
5. “Design and Control of Grain Boundary Microstructures” based on the Understanding of “Percolation Processes of Grain Boundary-related Phenomena” in Polycrystalline Material System.
6. Demand for Development of “A New Processing Technique for GBE”.
7. “The Importance of Grain Boundary Engineering (GBE)” increases with increasing “Density of Grain boundaries” and their Directionality” : “Nanocrystalline and Textured Materials”

Lecture on Grain Boundary & Interface Engineering

at Department of Materials Engineering, IISc, (No.2)

(18, November, 2015, Bangalore, India)

Grain Boundary and Interface Engineering for Structural and Functional Materials

Tadao Watanabe

Lab. of Materials Design and Interface Engineering, Dept. of Nanomechanics,
Graduate School of Engineering, Tohoku University, Sendai, Japan
Guest Scientist, Key Laboratory of Anisotropy and Texture of Materials,
Northeastern University (NEU) , Shenyang, China.

Acknowledgements

Coworkers at Tohoku Univ.:

H. Kokawa, S. Tsunekawa, T. Matsuzaki, K. Kawahara
S. Yamaura, S. Kobayashi, H. Fujii (S. V. R. Murthy+)

Coworkers : L. Zuo, X. Zhao, at NEU and Claude Esling at Univ. Metz

The Concept of Grain Boundary Design and Control: “Grain Boundary Engineering”

T. Watanabe : “An Approach to Grain Boundary Design for Strong and Ductile Polycrystals” Res Mechanica, 11 (1984), 47-84.

T. Watanabe: “Grain Boundary Engineering: Historical Perspective and Future Prospects” , J. Mater. Sci., 46 (2011), No.12, 4095-4115.

T. Watanabe: in “Microstructural Design of Advanced Eng. Mater.” Wiley (2013).

The Potential of Grain Boundary Engineering

- (1) Enhancement of “Beneficial Effects”
- (2) Control of “Detrimental Effects”
- (3) Generation of “A New Function” and “Desirable Bulk Property”
by Controlling “Grain Boundary Microstructure”
- (4) Properties are due to the Interaction of GB & Interfaces with Defects

Characterization of Grain Boundary Microstructure

- (1) Grain Boundary Character Distribution (GBCD)
- (2) Grain Boundary Connectivity, (3) Triple Junction Character Distribution,
- (4) GBCD vs Grain Size, (5) GBCD vs Texture (Grain Orientation Distribution)
- (6) Grain Boundary Inclination Distribution (Directional GBM)
- (7) Grain Boundary Chemistry Distribution

Grain Boundary & Interface Engineering for Advanced Materials

Intergranular Fracture Control



Superconducting Magnetic Field Heat Treatment System



Processing

- Application of . . .
- Magnetic field
 - Ultrasonic vibration

Mechanical Properties

- Intergranular fracture control
- Superplasticity
- Intergranular corrosion control

Interface Science and Engineering

Functional Properties

- Photovoltaic solar cell
- Shape memory effect
- Magnetism

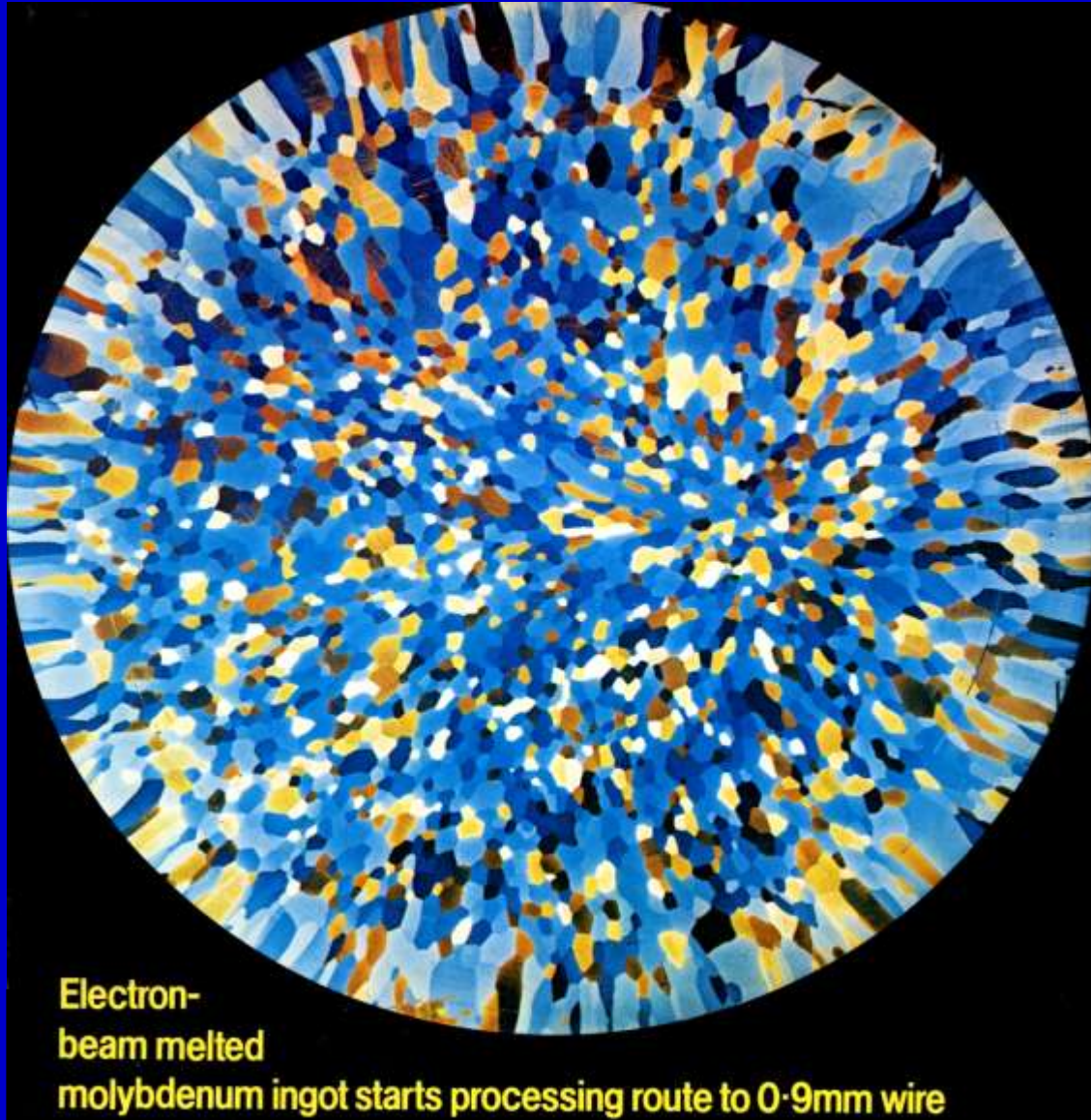
Grain Boundary Microstructures

- G.B. character
- G.B. structure
- G.B. chemistry



Evaluation of Electrical Property in Poly Silicon

A Polycrystal System of Grains and Grain Boundaries (Mo ingot solidified from the melt)

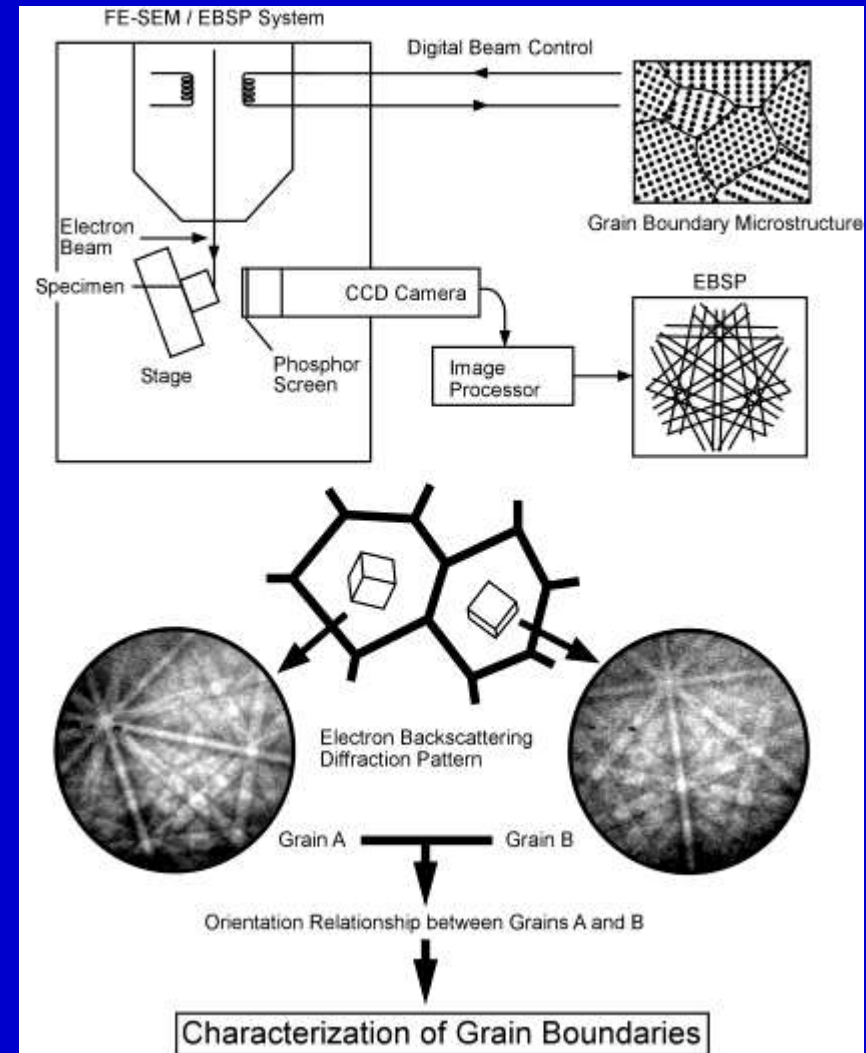


Recent Technique for Characterization of Grain Boundary Microstructures in Polycrystals

Orientation Imaging Microscopy (OIM)

B. Adams, S. I. Wright and K. Kunze:
Metal. Trans., 24A (1993), 819-831.

FE-SEM/EBSD/OIM
(Hitachi S-4200)



Characterization and Classification of Grain Boundaries

1. Low-angle Boundaries based on Dislocation Model.

---Pure Tilt-, Pure Twist-, Mixed-type Boundary.

2. High-angle Boundaries:

(a) High-angle Random/General Boundary

(b) High-angle Special Boundaries:

----**Symmetrical** and **Asymmetrical** Boundaries.

--- **Coincidence Site Lattice (CSL)** Boundaries.

--- **Plane-matching** Boundaries.

--- **Close-packed Plane Aligned** Boundaries.

Current Theories of Grain Boundary Structure.

“**The Structure-Unit Models**” of Periodic/Ordered GB Structures.

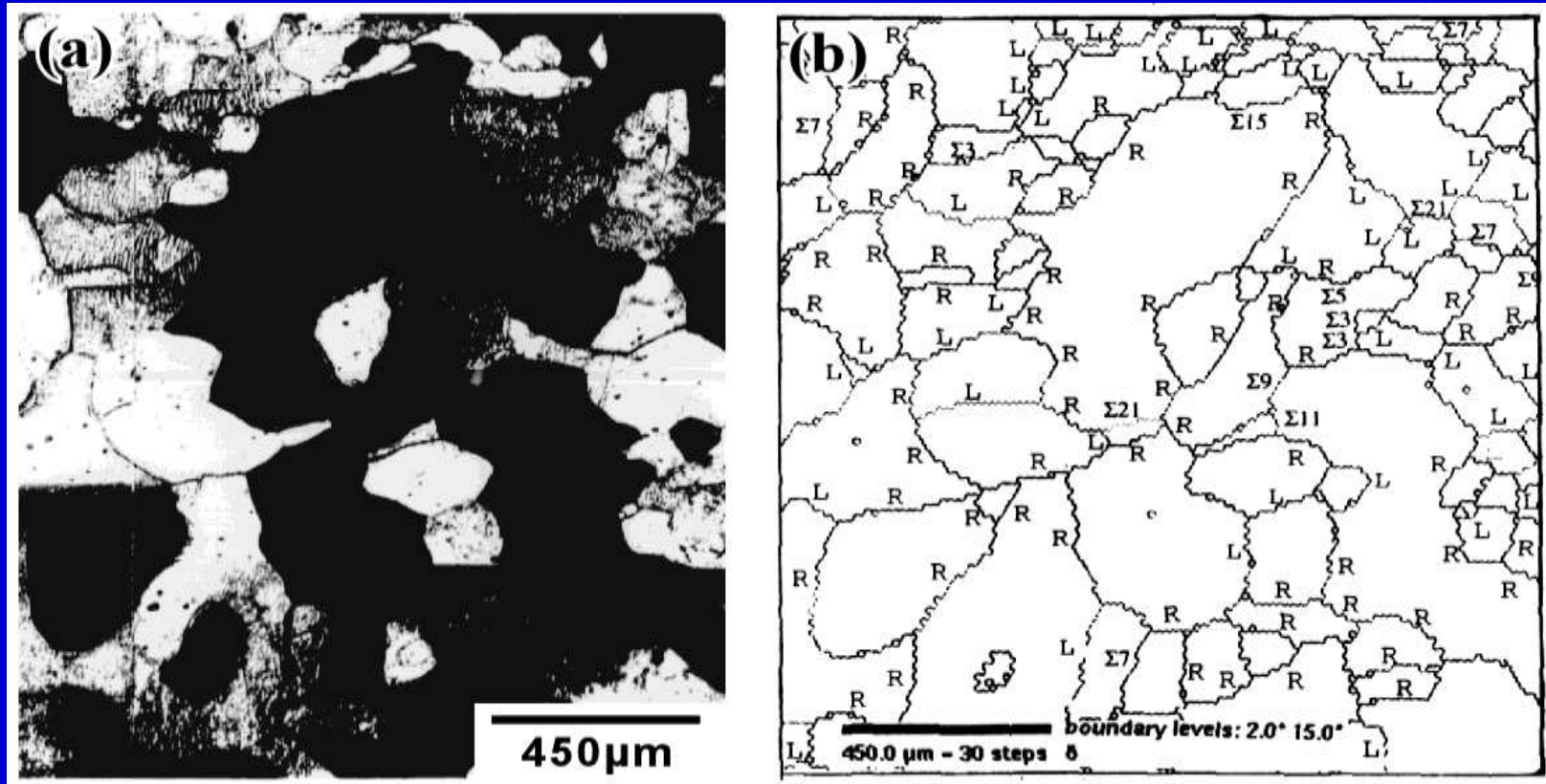
A. Sutton, V. Vitek: *Phi. Trans. Roy. Soc. Lond.*, A309 (**1983**), 1-36.

A. Sutton, R. W. Balluffi: *Interfaces in Crystalline Materials*,
Oxford Science Pubs., (**1995**), Chap.4, “Atomic Structure of Interfaces”

Characterization of Grain Boundary Microstructure in a Polycrystal by SEM-EBSP/OIM (Mo)

T. Watanabe, "Grain Boundary Architecture for High Performance Materials",
D. A. Smith Symp. on Grain Boundaries and Interfaces in Materials, TMS (1998), pp.19~28.

**Molybdenum Polycrystal (Produced by Thermomechanical Processing from Single
Crystal with {111} Initial Orientation 78% Deformed under Compression and then
Annealed at 1873K for 7.2ks).**

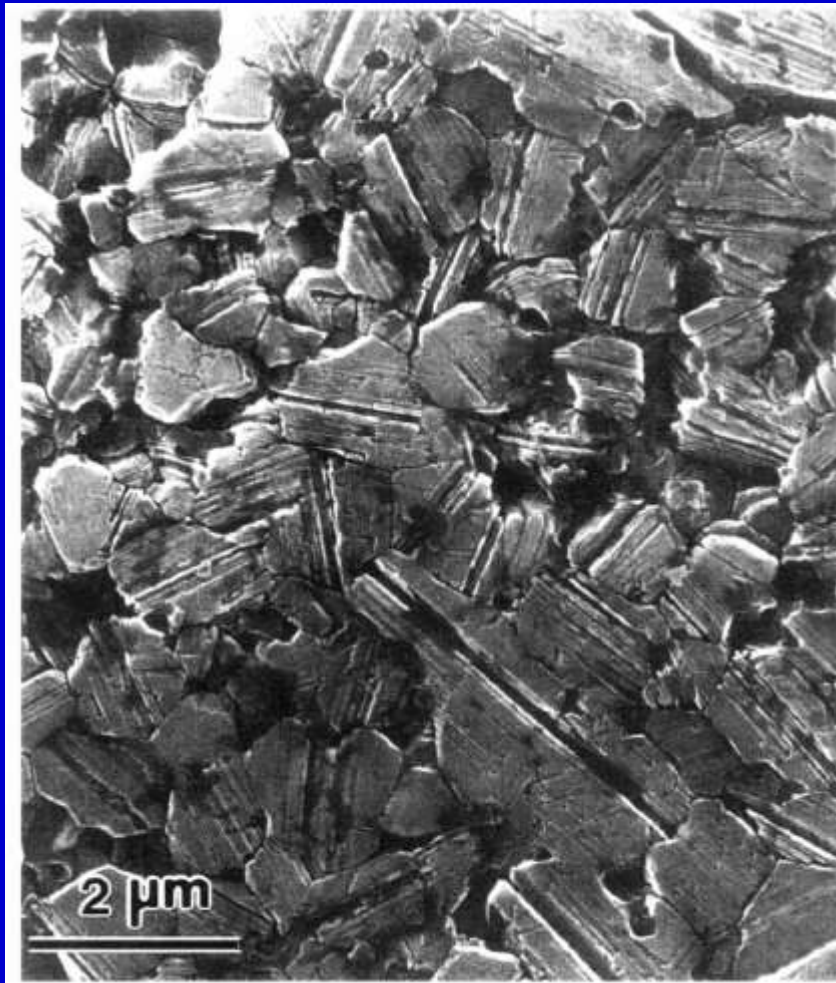


(a) Optical Micrograph.

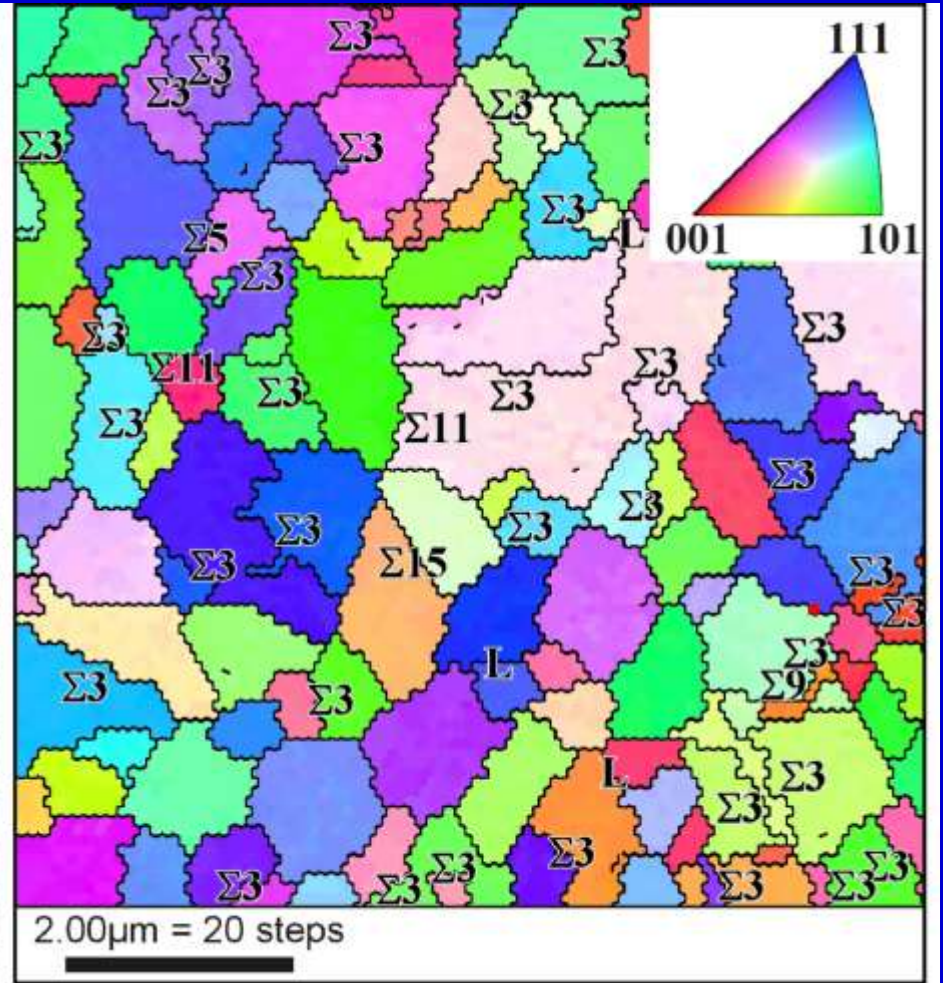
(b) GBCD and Boundary Connectivity.

OIM Analysis of Grain Boundary Microstructure β -SiC Polycrystal (Average grain size, $d \approx 1 \mu\text{m}$)

S. Tsurekawa, T. Watanabe, H. Watanabe, T. Tamari; Key Eng. Mater., Vol. 247 (2003), 327-330.



(a) SEM Observation

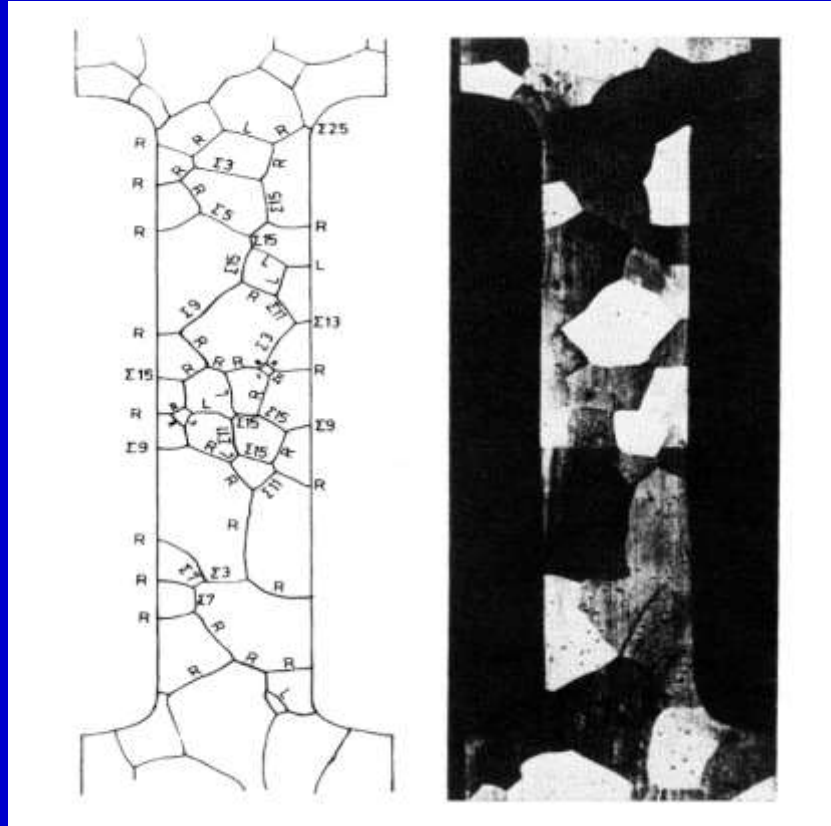


(b) Grain Orientation , Grain Boundary Character, GB Connectivity.

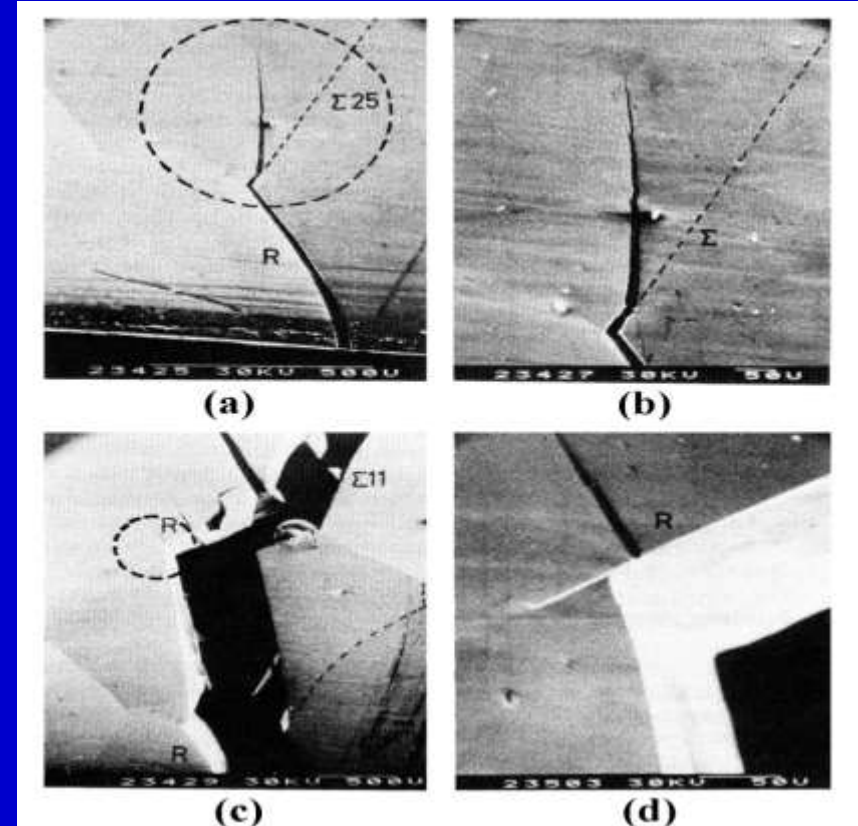
In-situ Observations of Fracture Processes in Polycrystals

-How to bridge between Property of Individual Boundaries and Bulk Property-

T. Watanabe; **Res Mechanica**, 11 (**1984**), No.1, 47-84.



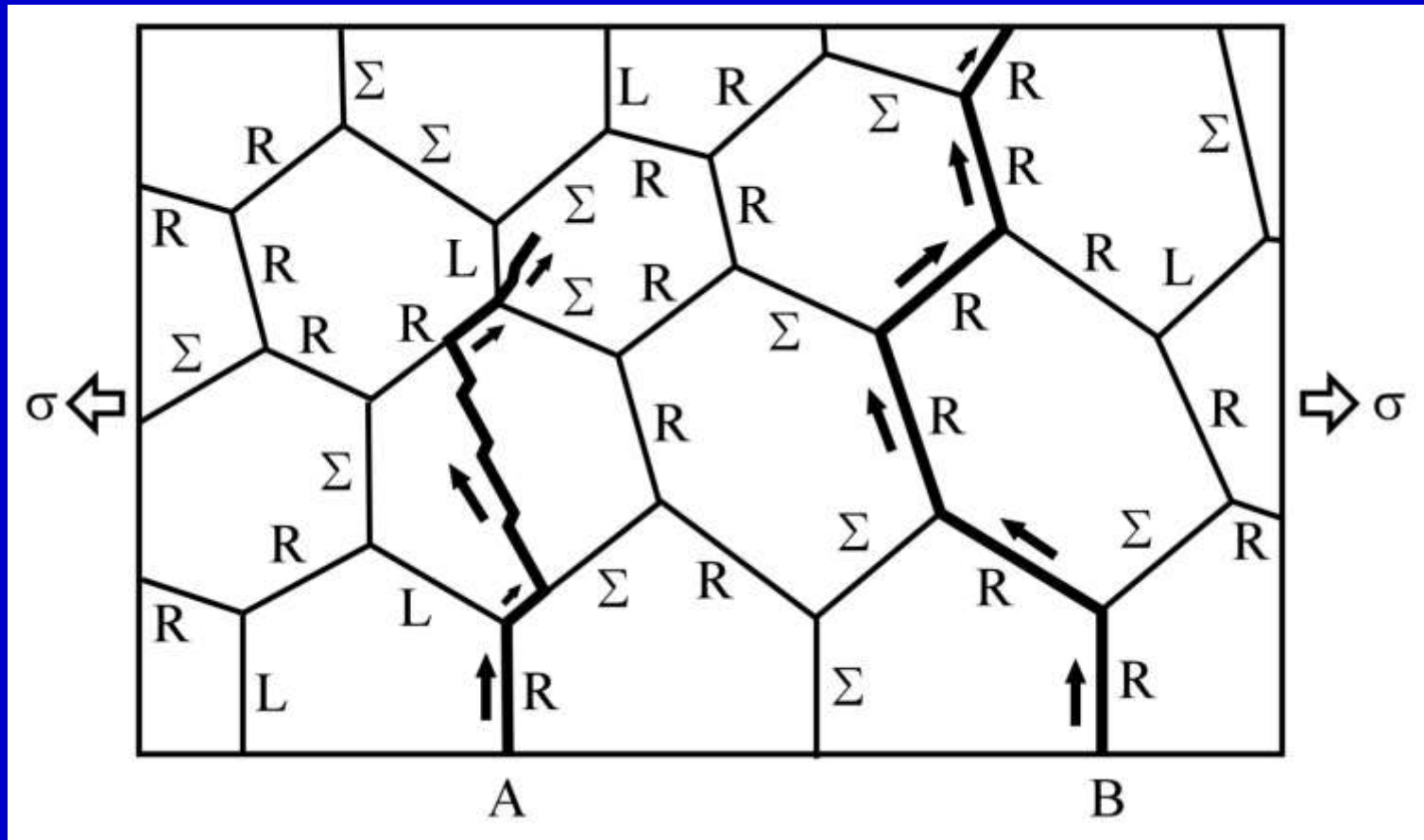
ECP Analysis and Characterization of Grain Boundaries in a Tensile Fracture Test Specimen. Beta-Brass Polycrystal with Grain Size from 1.4 to 4.0 mm. The Dimensions of the Gauge Part of the Specimen are 5 mm Wide, 20 mm Long and 1 or 2mm Thick.



In-situ Observation of Crack Propagation in Liquid-gallium-induced Fracture of Beta-Brass Polycrystal. Note the Change in Fracture Mode between Intergranular and Transgranular Fracture, depending on the Type of Grain Boundary in front of the Propagating Crack.

Grain Boundary Structure-dependent Fracture Processes in a Polycrystal

T. Watanabe: Res Mechanica, 11 (1984), 47-84.



Path A: Combined Process of Intergranular and Transgranular Fracture.

Path B: Typical Intergranular Fracture.

The First Systematic Study of GBCD in Metallic Polycrystals.

Al polycrystals produced by thermomechanical processing from single crystals with different initial orientations.

(SEM-ECP Analysis of GB Microstructure)

T. Watanabe, No. Yoshikawa, S. Karashima: Proc. ICOTOM-6, (1981), 609-618

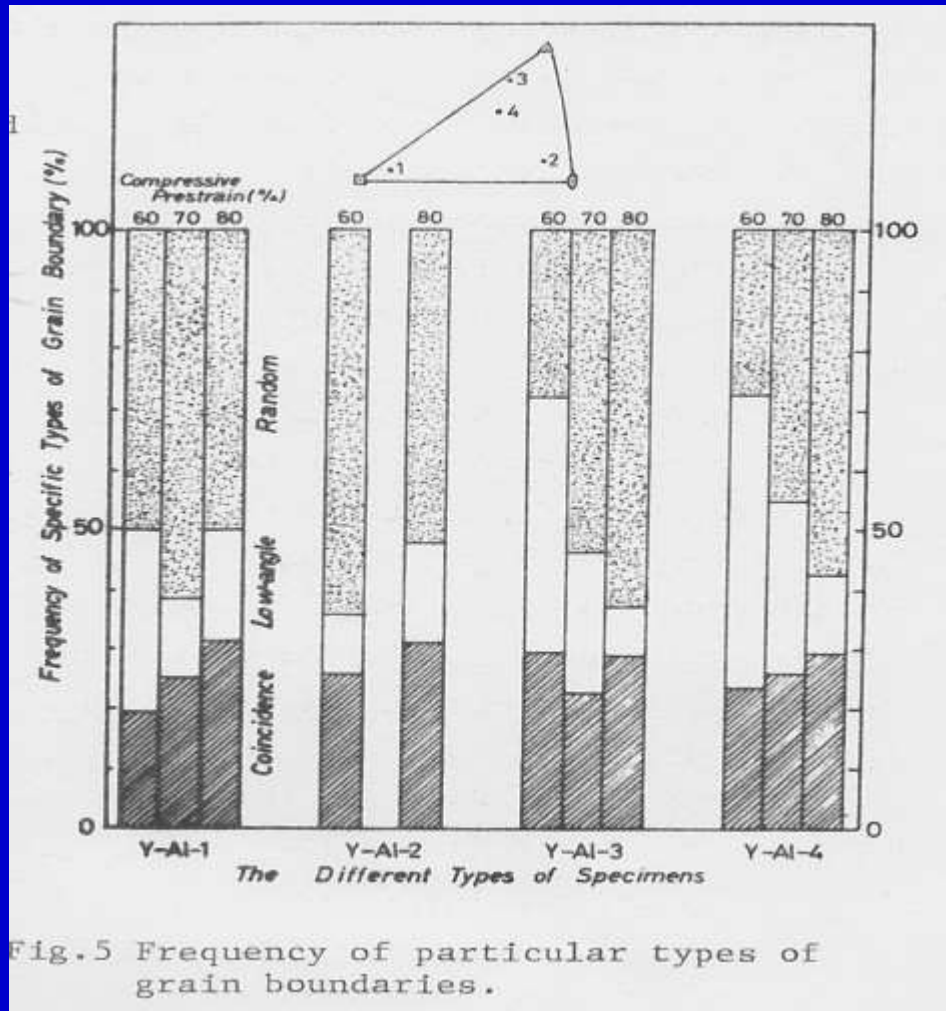


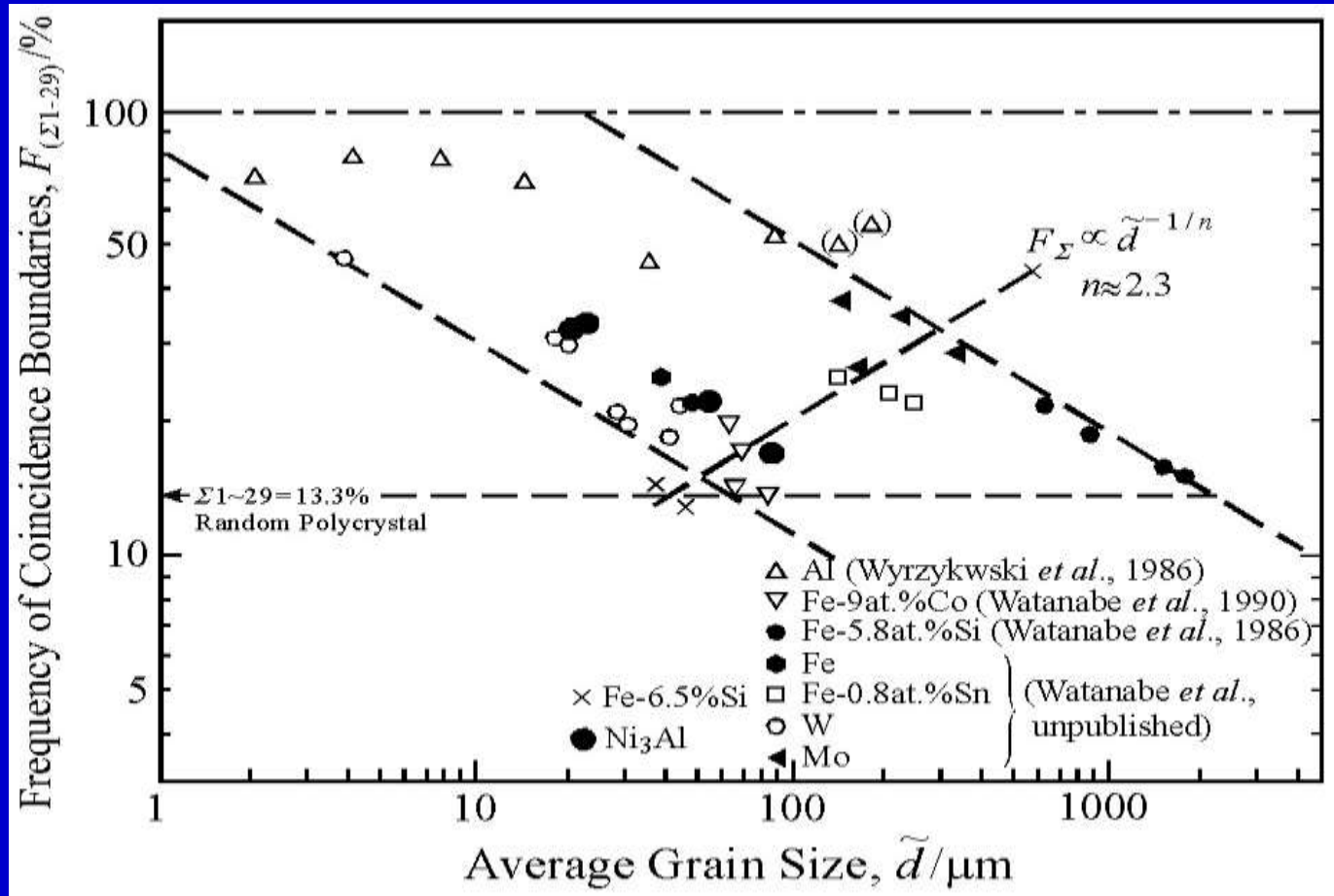
Fig.5 Frequency of particular types of grain boundaries.

“To what extent do we know about “GB. Microstructure” ?

Relation between Grain Size and Fraction of CSL Boundaries ?

Bulky Samples: Metals and Alloys produced by **Thermo-mechanical processing**

Thin Ribbon Sample: Fe-6.5%Si by **Rapid solidification and annealing.**



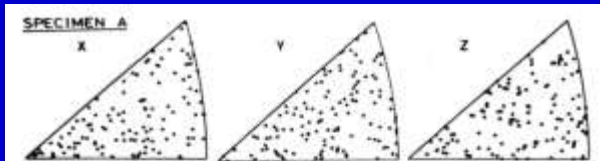
Grain Boundary Character Distribution (GBCD) vs Texture

T. Watanabe et al.: *Acta Met.*, 37(1989), 941, *Phil. Mag. Letters*, 59 (1989), 47, *Textures and Microstructures*, 20 (1993), 195-216.)

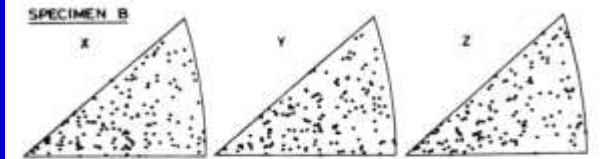
Grain Orientation Distributions for Fe-6.5 wt. % Si Ribbons Annealed Differently. **Specimen A**: 1173K, 3.6ks, **Specimen B**: 1363K, 600s, **Specimen C**: 1363K, 3.6 ks, **Specimen D**: 1473K, 3.6ks.

The Frequency of CSL Boundaries as a Function of Σ for Rapidly Solidified and Annealed Fe-6.5 wt.% Si Ribbons.

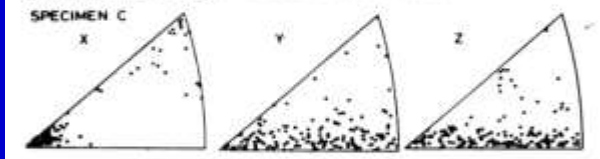
Spec. A



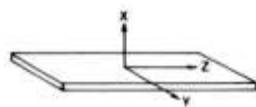
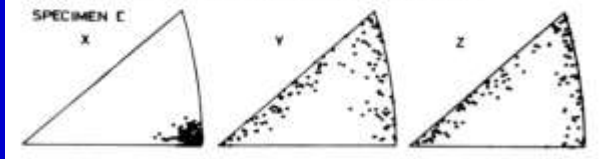
Spec. B



1100 TEXTURED RIBBON (Annealed at 1363K for 3.6ks.)

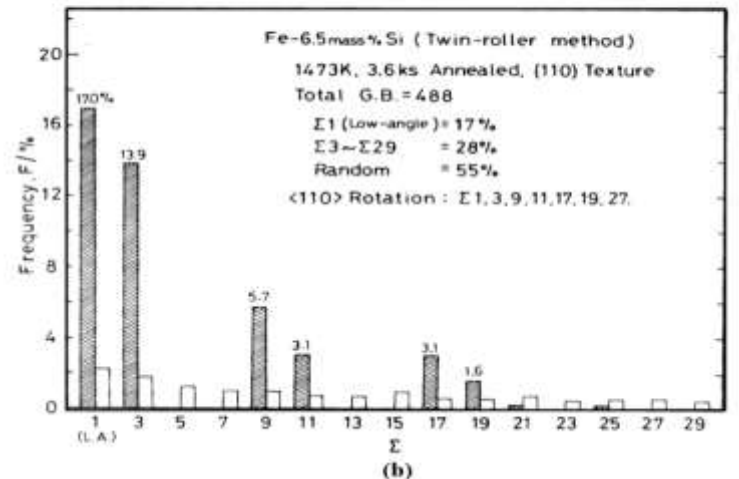
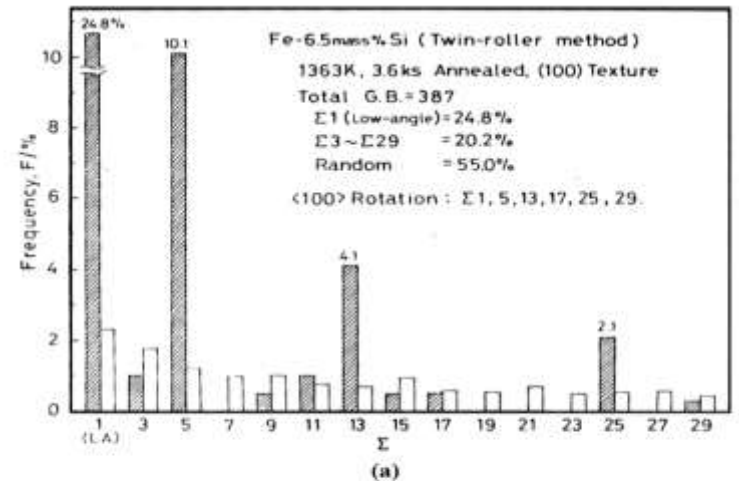


1110 TEXTURED RIBBON (Annealed at 1473K for 3.6ks.)



Spec. C

Spec. D



Spec. C

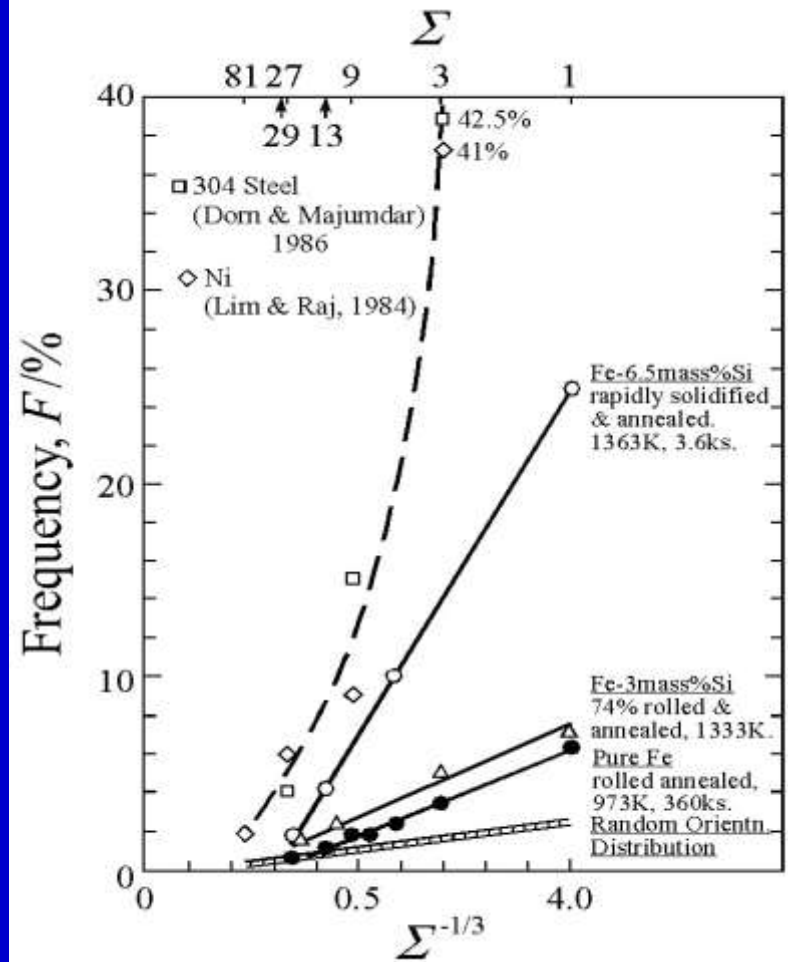
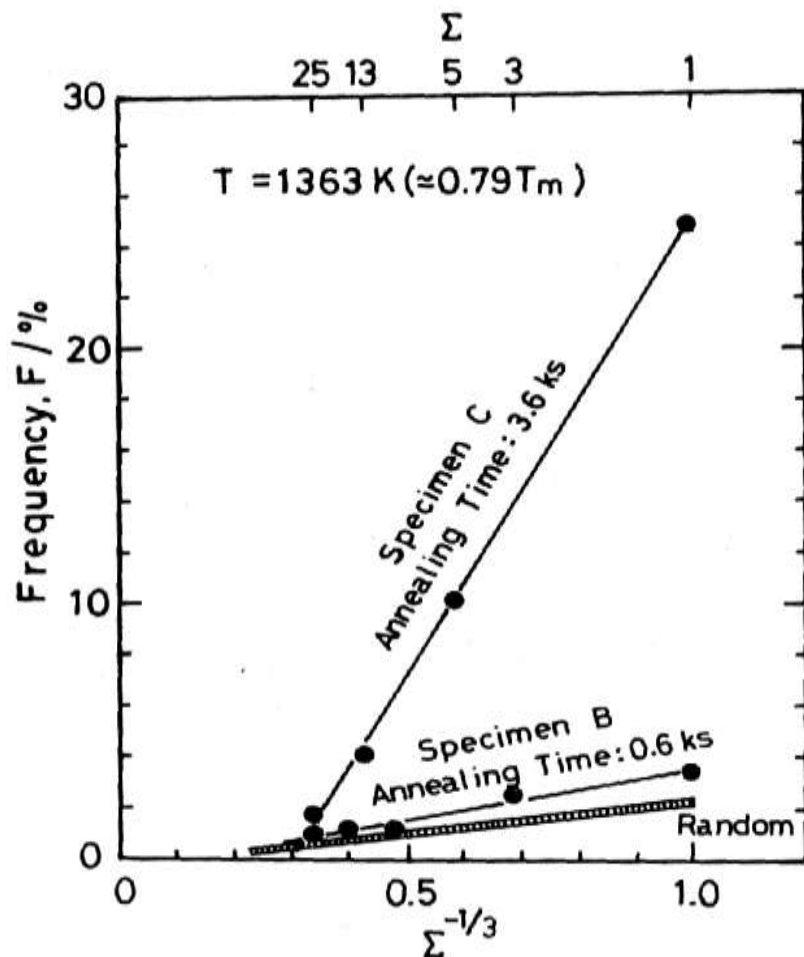
Spec. D

The Inverse Cubic Root Σ Plot of Coincidence Boundaries

T. Watanabe, H. Fujii, H. Oikawa, K. I. Arai: *Acta Metal*, Vol.37 (1989), 941~952

The Inverse Cubic Root Σ Dependence of Coincidence Boundaries in Rapidly Solidified and Annealed Fe-6.5 mass % Si Ribbons.

The Inverse Cubic Root Σ Dependence of the Frequency of Low Σ Coincidence Boundaries in Materials with BCC and FCC Structures.



Theoretical Work on Grain Boundary Character Distribution in Differently Textured Polycrystals in Cubic Crystal.

A. Garbacz, M. W, Grabski: Acta Met Mater., 41 (1993), 469-473

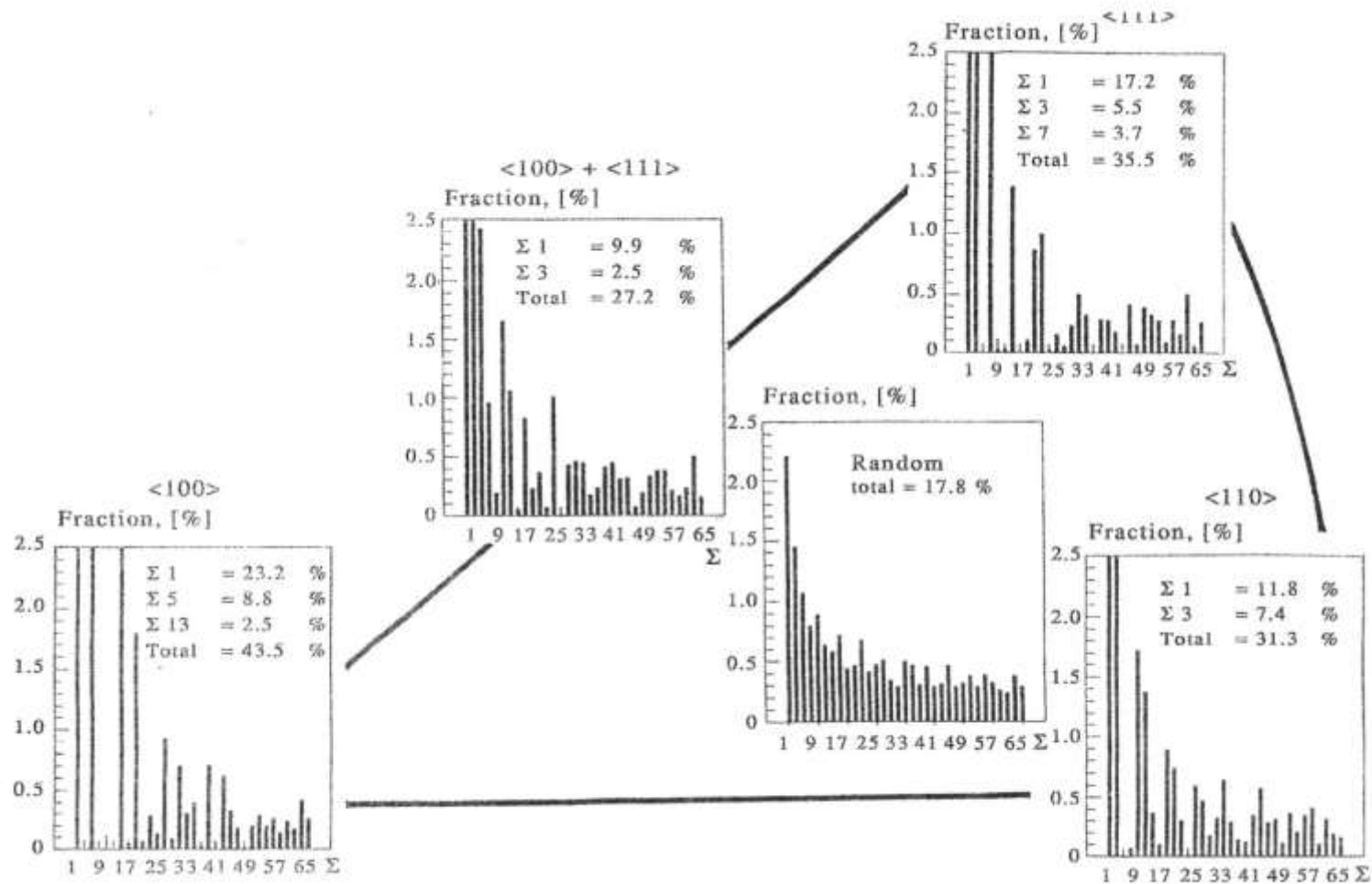
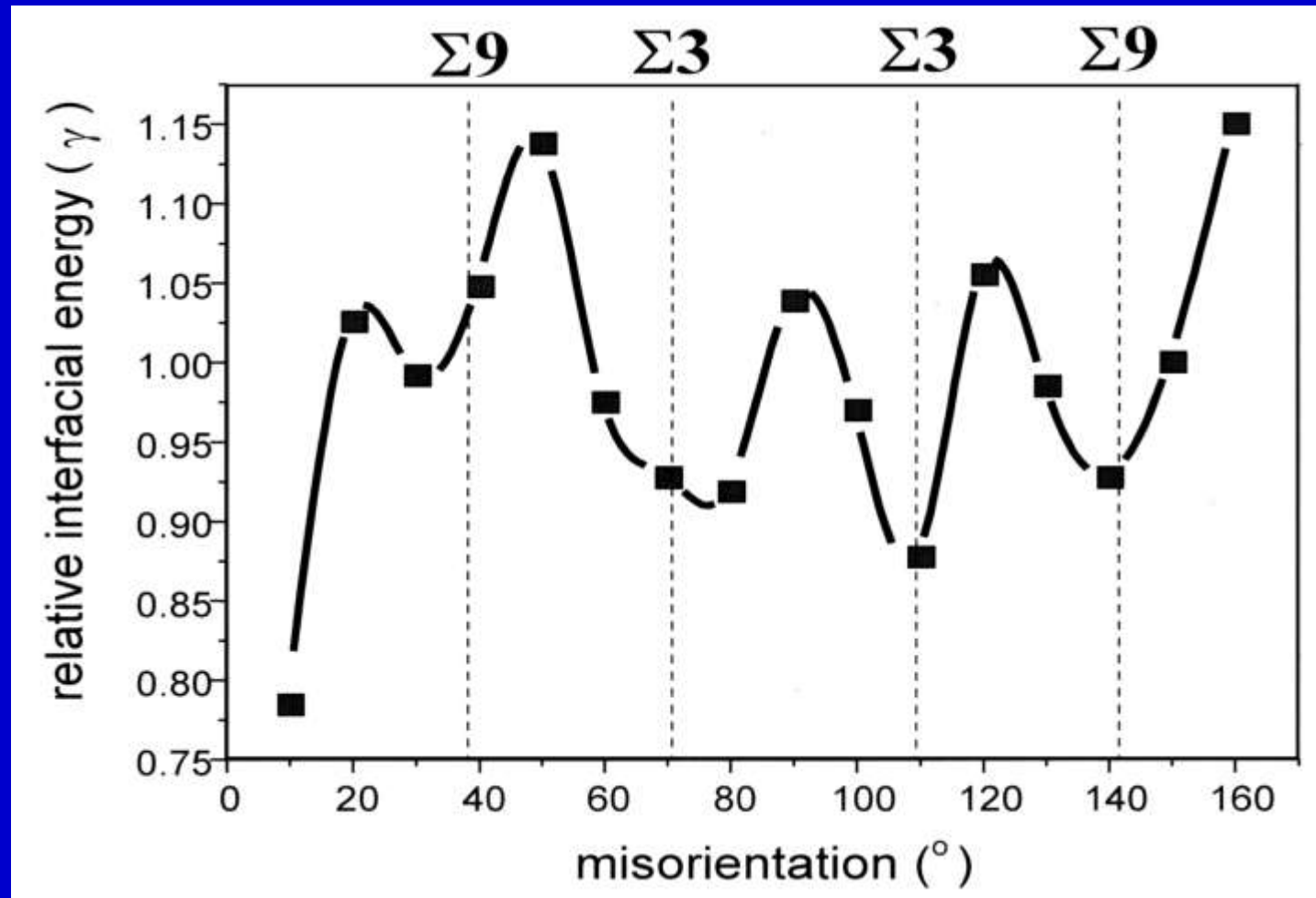


Fig. 7. The examples of distributions of CSL boundaries up to $\Sigma 65$ obtained for $\langle hkl \rangle$ textures described by model I for sharpness $N(0,5^\circ)$.

Grain Boundary Energy vs Misorientation Angle in {110} Textured Fe-6.5%Si Ribbon



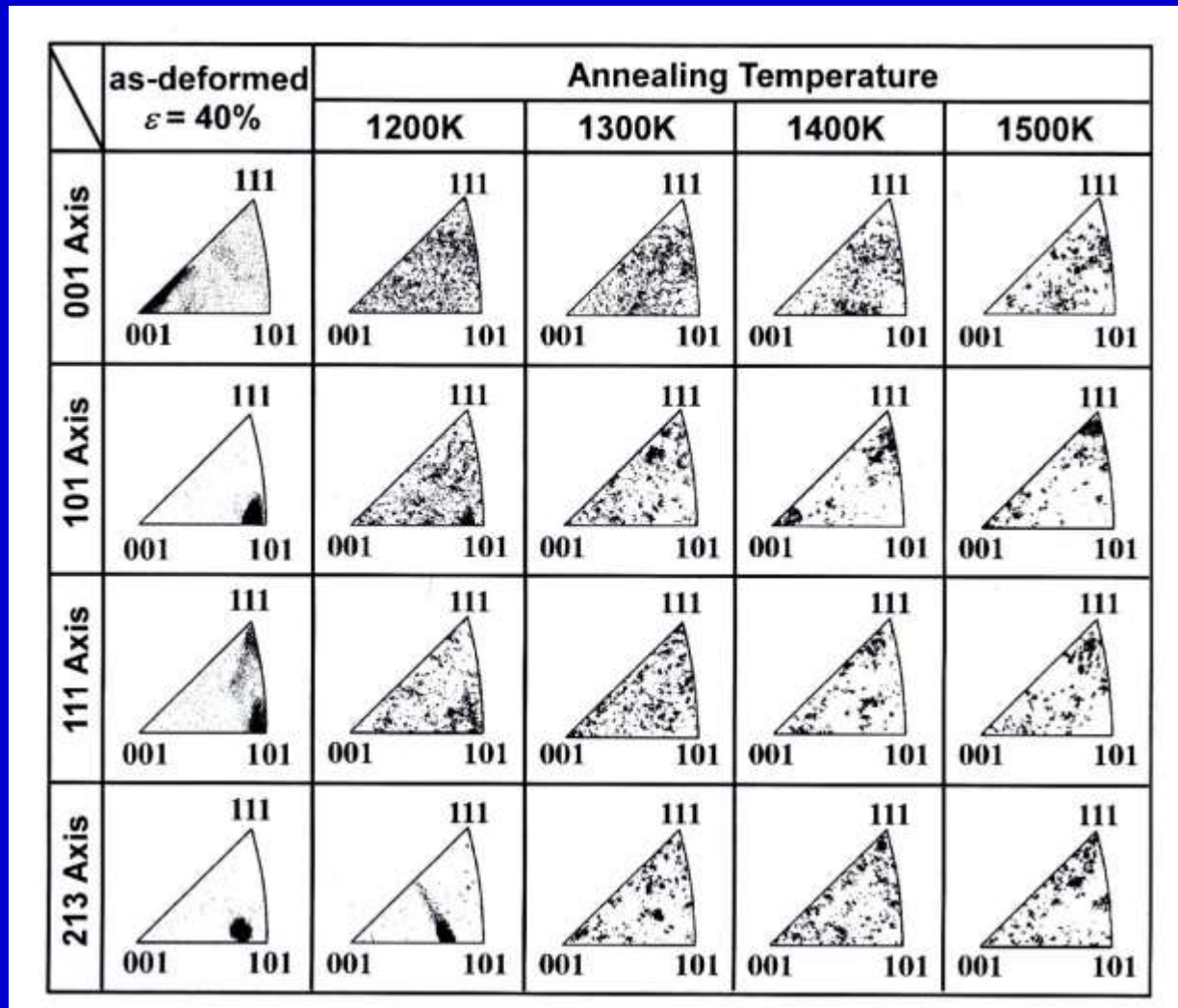
Misorientation Angles with Low Interfacial Energies Occur at Angles Known to Correspond to {110} CSL Symmetric Tilt Boundaries with small Sigma Values.

(A. Zimbouski, C. S. Kim, G. Rohrer, A. D. Rollett and T. Watanabe, (2003),

cited in T. Watanabe: J. Mater. Sci., 46 (2011), No.12, 4095-4115)

Annealing Textures in 304 L Stainless Steel produced by Thermomechanical Processing from Single Crystals with Different Initial Orientations

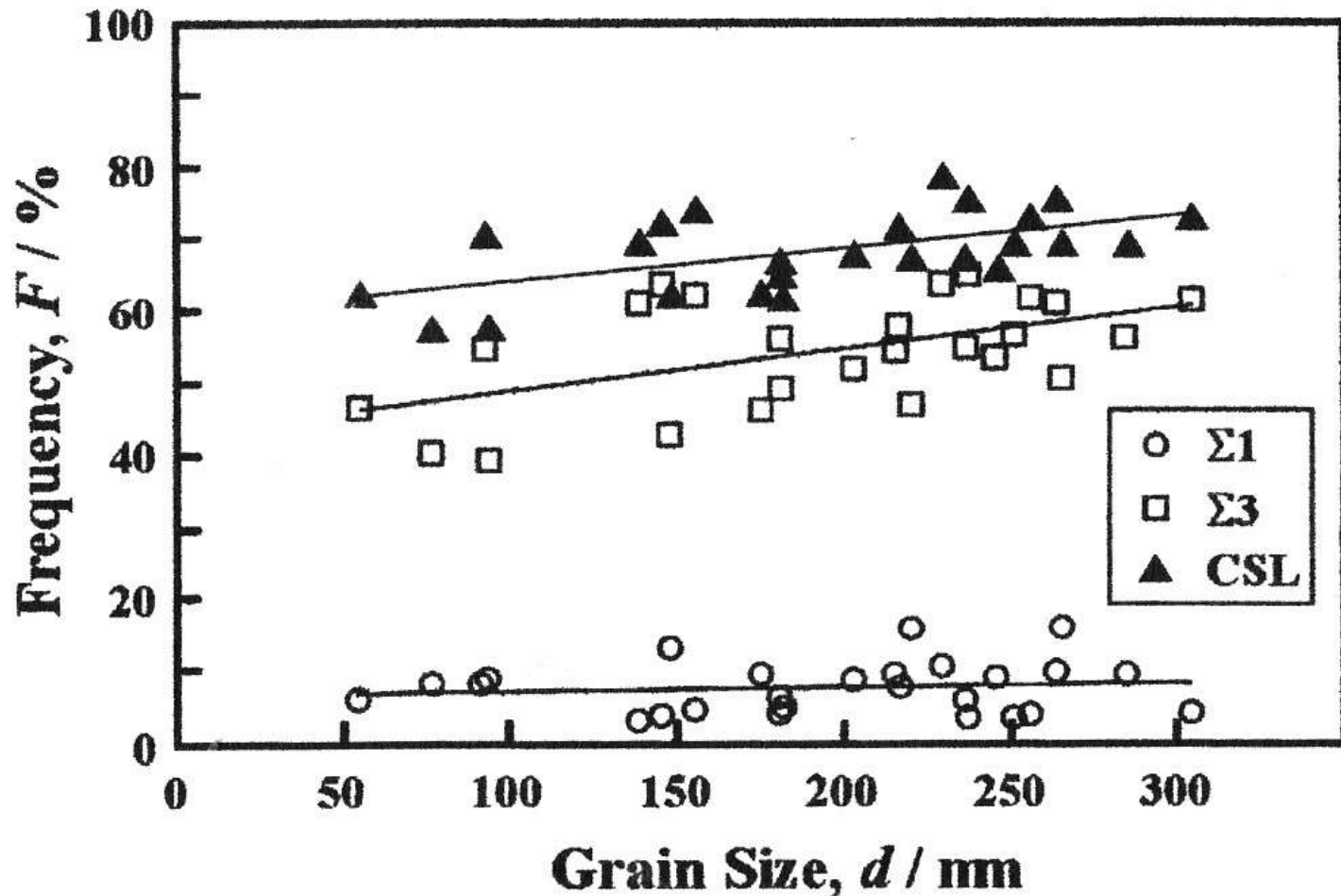
S. Tsurekawa, S. Nakamichi, T. Watanabe: Acta Mater., 54 (2006), 3617-3626



The Frequency of Low- Σ CSL Boundaries vs Grain Size

304L Austenitic Stainless Steel (with Low-Stacking Fault Energy)
produced by Thermomechanical Processing from Single Crystals

S. Tsurekawa, S. Nakamichi, T. Watanabe: *Acta Mater.*, 54 (2006), 3617-3626



Texture and GB Microstructure in Molybdenum

S. Kobayashi, S. Tsurekawa, T. Watanabe, A. Kobylanski:

“Control of grain boundary microstructures in molybdenum polycrystals by thermomechanical processing of single crystals”, *Phil. Mag.*, **88** (2008), 489-506.

Intergranular brittleness in bcc metals

499

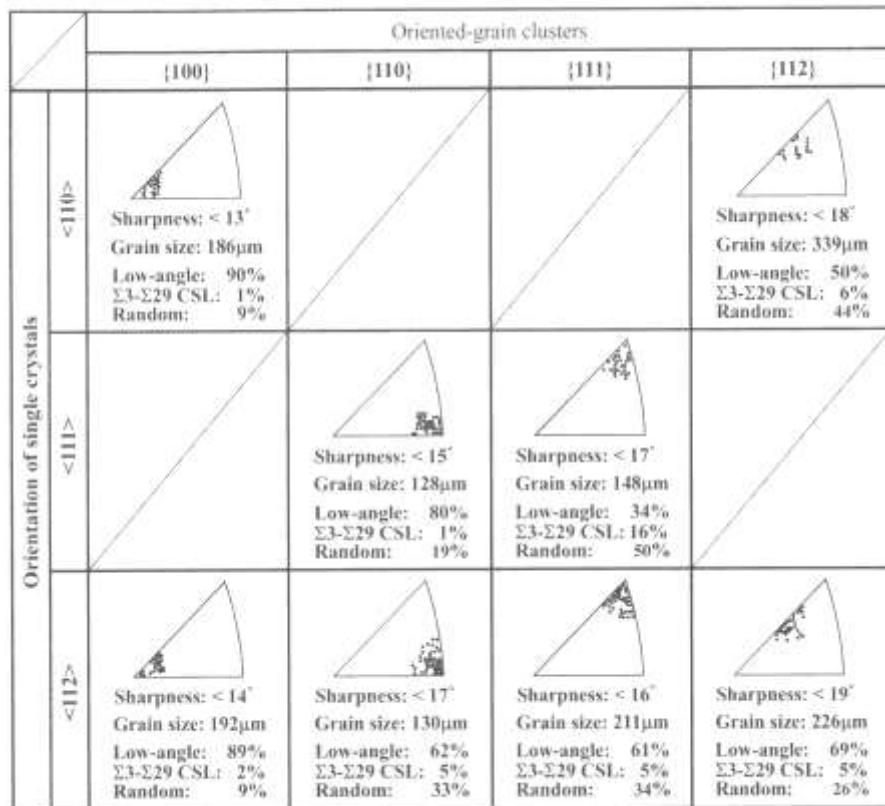
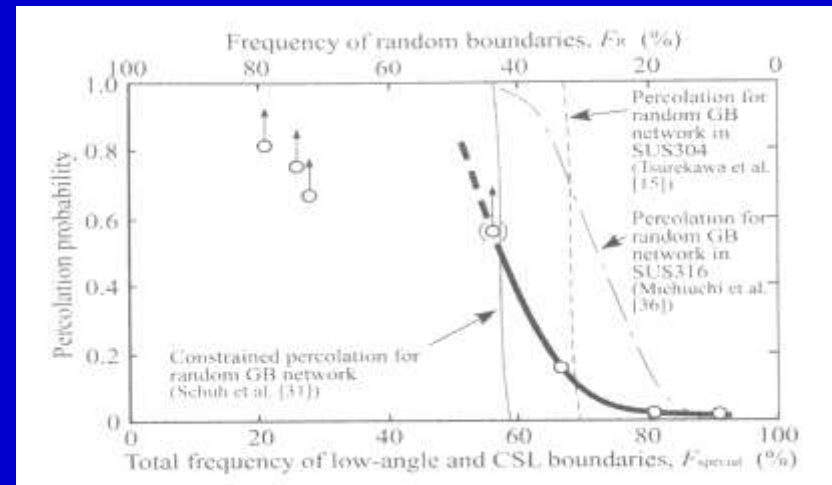
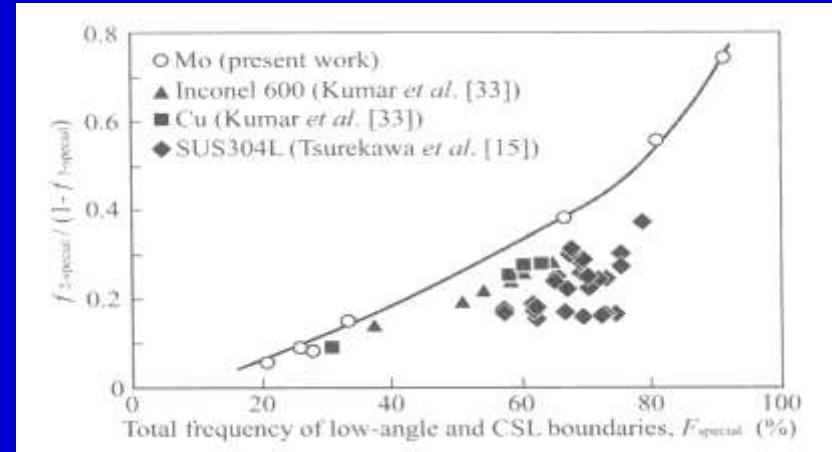


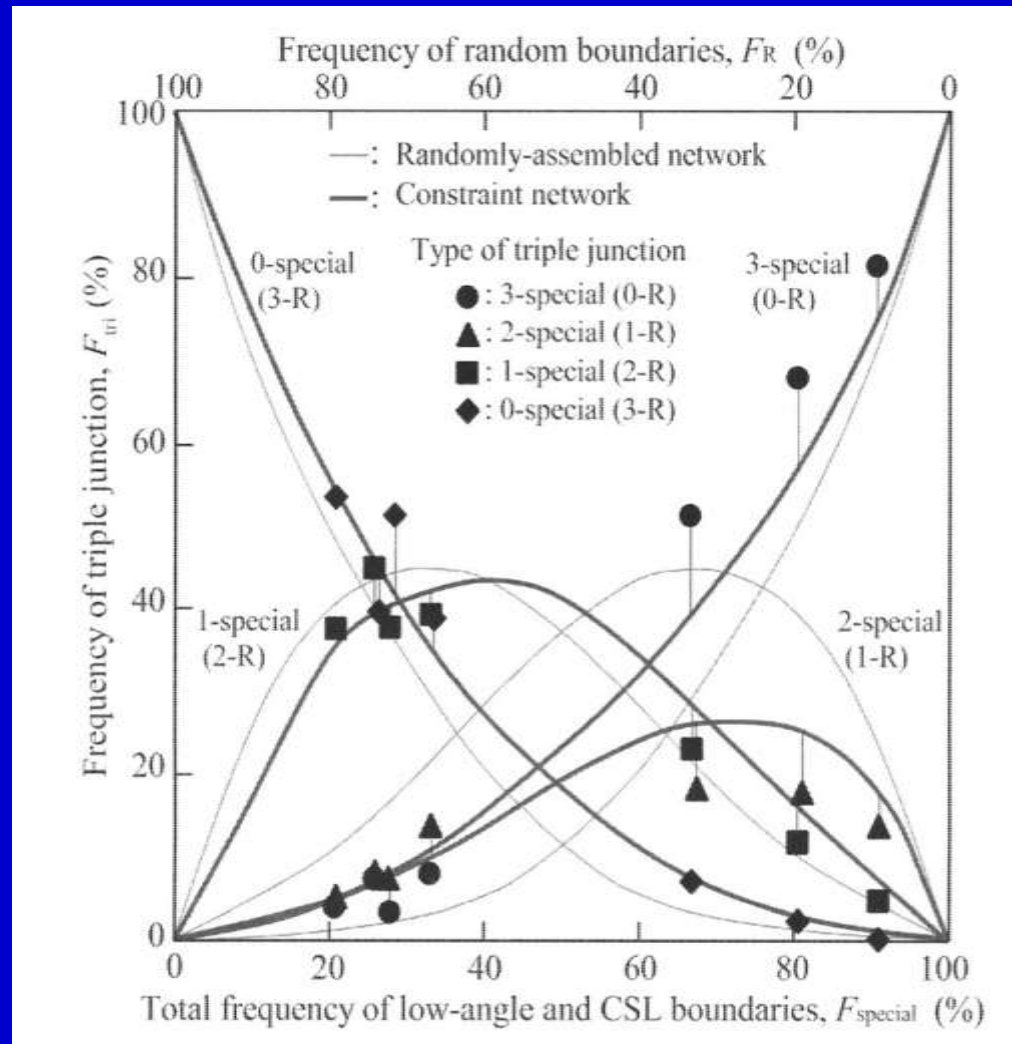
Figure 5. Inverse pole figure, average grain size and GBCD for distinct oriented grain clusters. In the pole figures, one data point shows the surface orientation of a single grain.



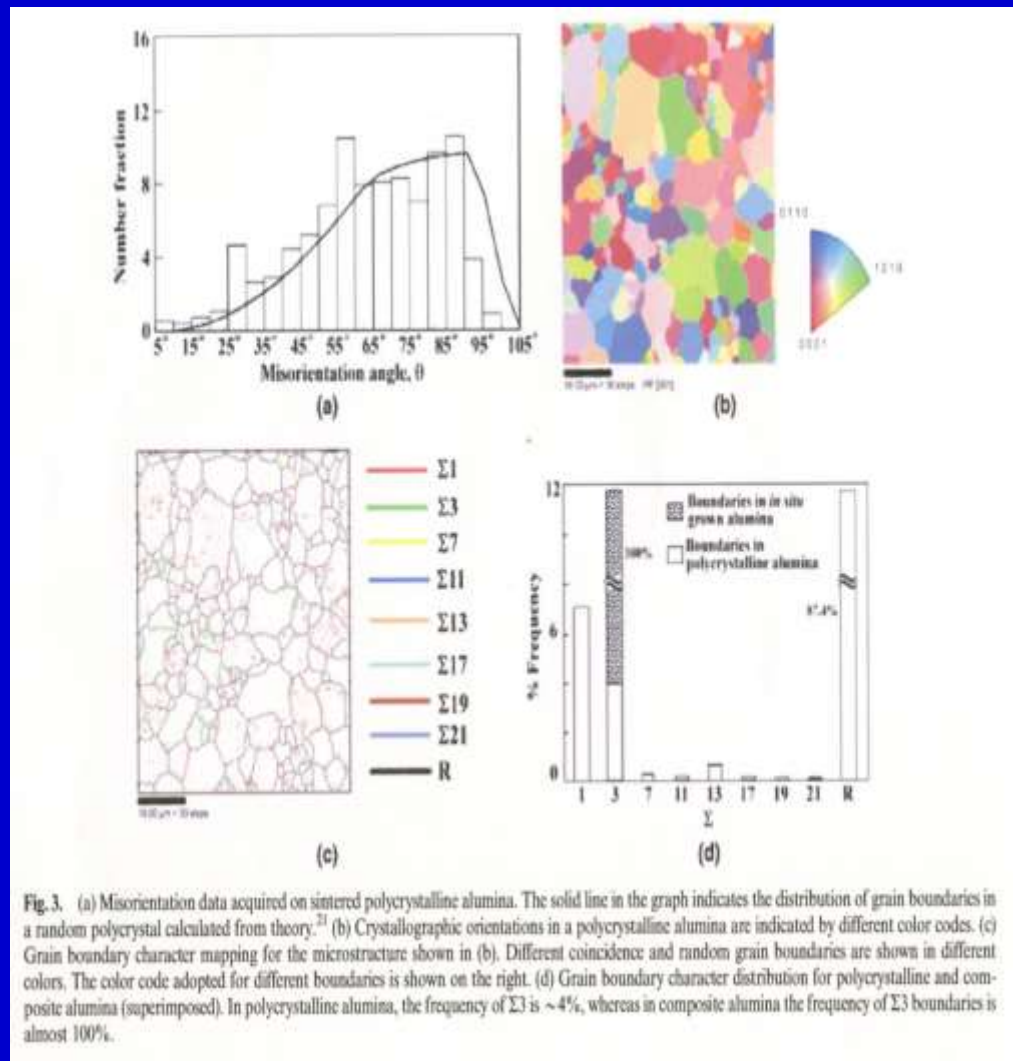
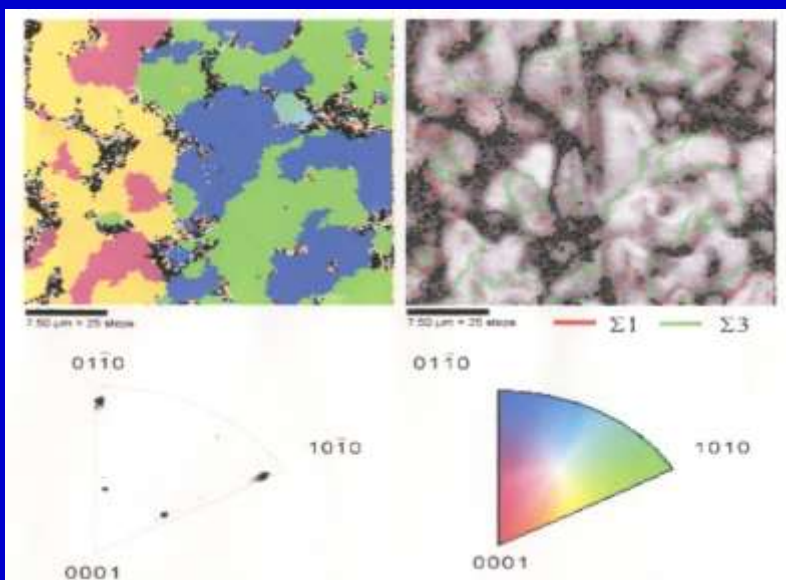
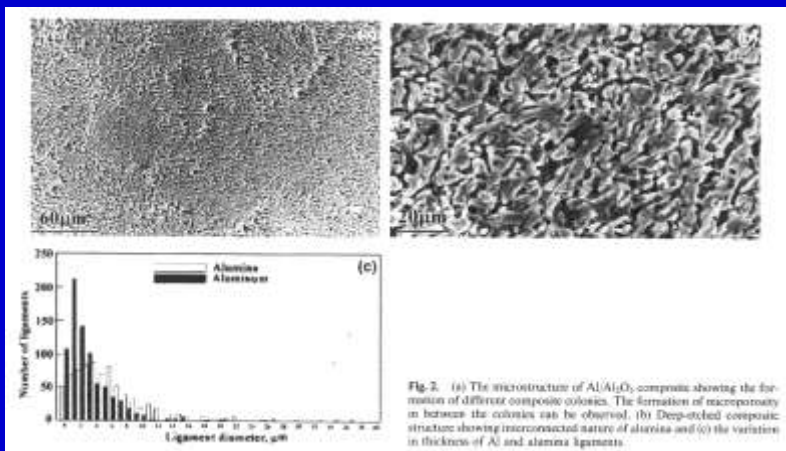
Texture and GB Microstructure in Molybdenum

S. Kobayashi, S. Tsurekawa, T. Watanabe, A. Kobylanski:

“Control of grain boundary microstructures in molybdenum polycrystals by thermomechanical processing of single crystals”, *Phil. Mag.*, 88 (2008), 489-506.



Grain Boundary Microstructure of Alumina produced by Reactive Metal Penetration (RME) ($F_{\Sigma 3} \approx 100\%$)



Our Long Pending Preproblem in Materials Development for Structural Materials.

- Enhanced strength tends to bring about Poor Ductility and Severe Brittleness in almost all kinds of Polycrystalline Materials:
 - Increasing grain size generally enhances GB Brittleness in metallic materials.
 - Severe GB Brittleness can also occur in Nano-crystalline materials.
 - The main source of Brittleness is GB fracture.
- Our Challenge: How to solve this dilemma ?

Long Pending Problem of Structural Materials:



How to Solve the Dilemma between Enhanced Strength and Brittleness in Structural Engineering Materials



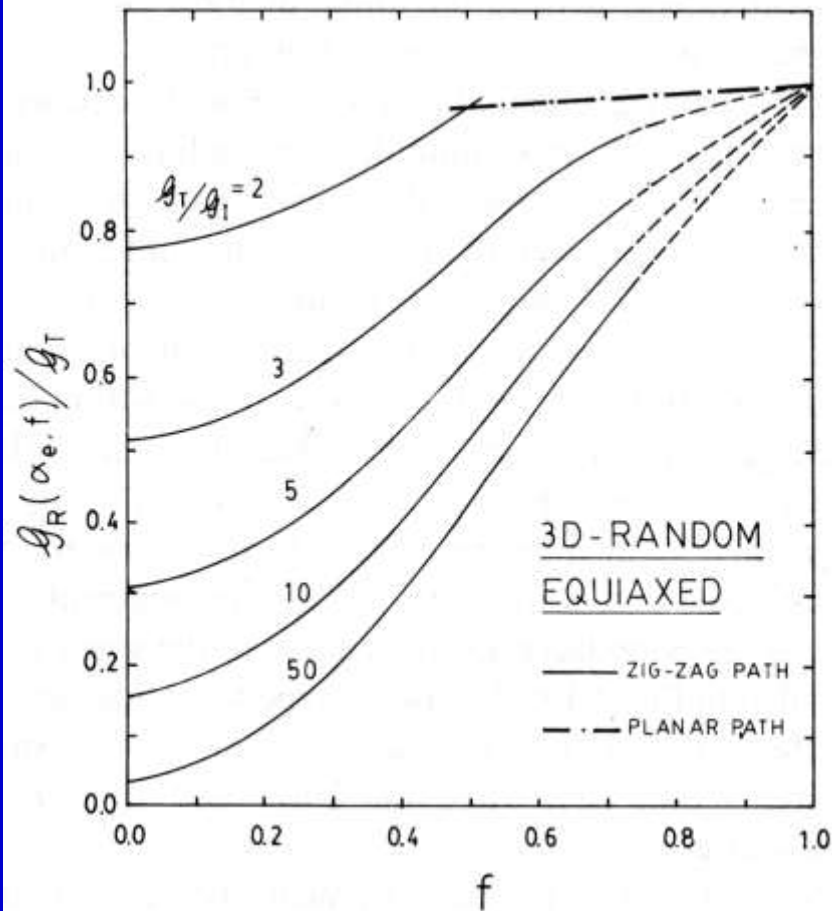
Our Challenge :

Toughening by Grain Boundary Engineering (GBE).

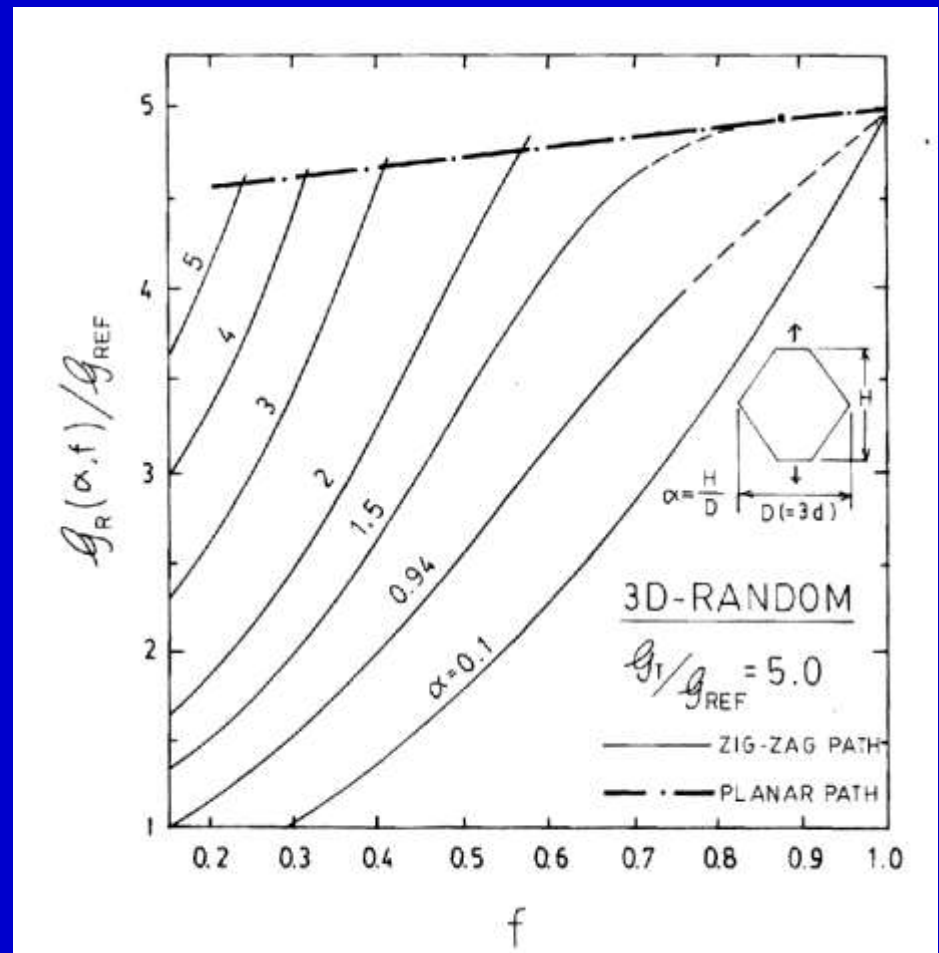
Modeling of GBCD-dependent Fracture Toughness of Polycrystals with Tetra-kaidecahedron-Shaped Grain Structure.

L.C. Lim and T. Watanabe: Acta Metall., 38 (1990), 2507-2616

Effect of the Overall Fraction of Low-Energy Boundaries, f , and G_T/G_I on Fracture Toughness of 3D Polycrystals

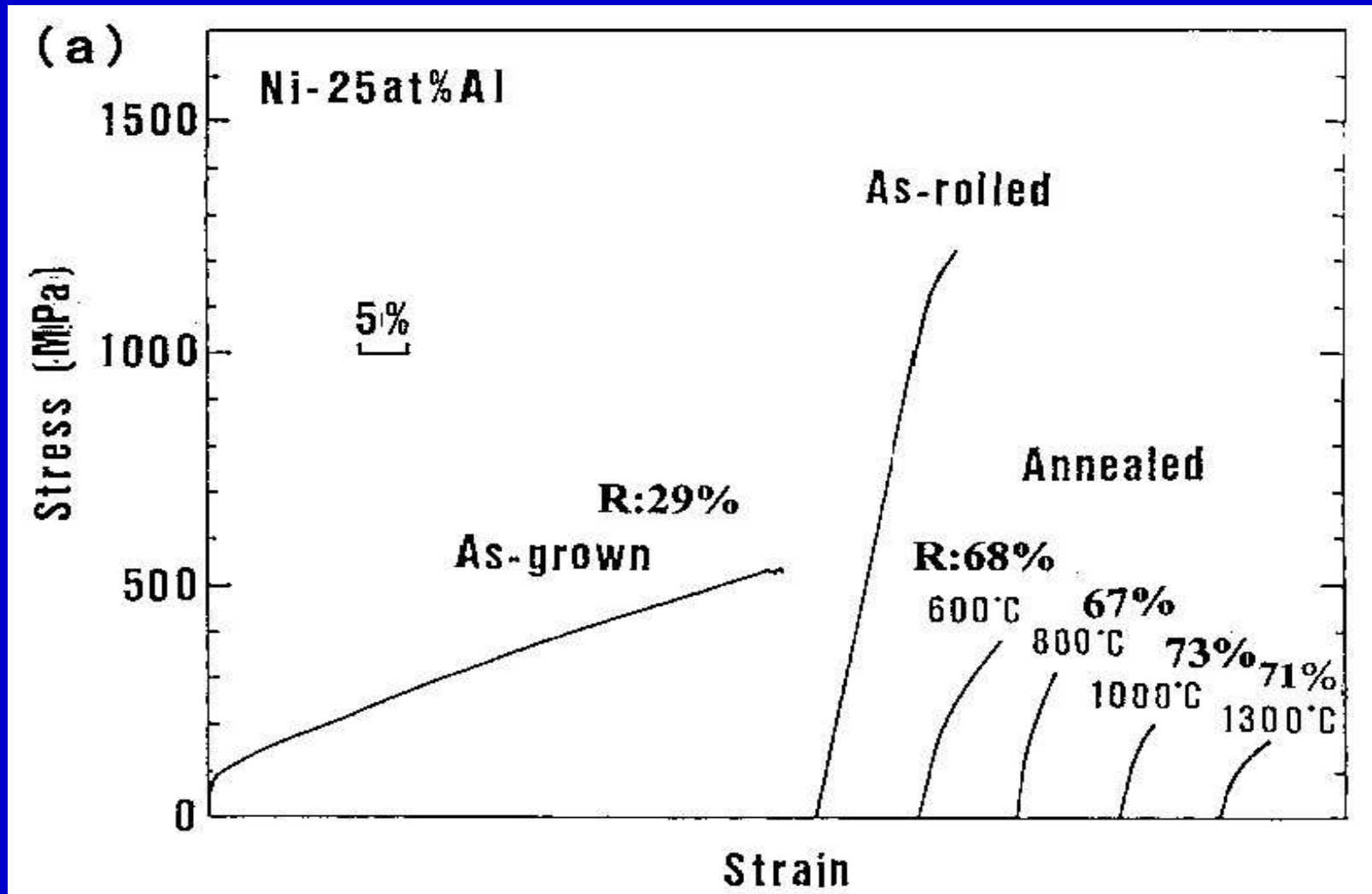


Effect of Grain Shape α and GB Inclination on Fracture Toughness of 3D Polycrystals.



Grain Boundary Engineering for Control of Intrinsic Brittleness of Ni₃Al Polycrystals without Boron

T. Watanabe, T. Hirano, T. Ochiai, H. Oikawa : Mater. Sic. Forum,157-162 (1994), 1103

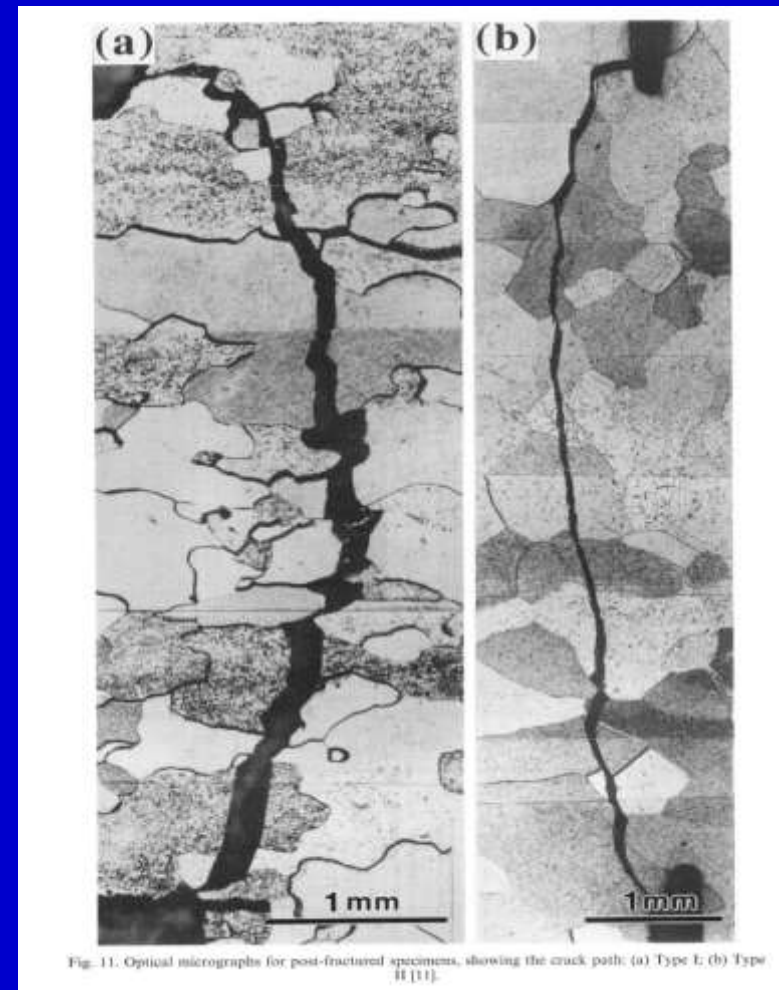
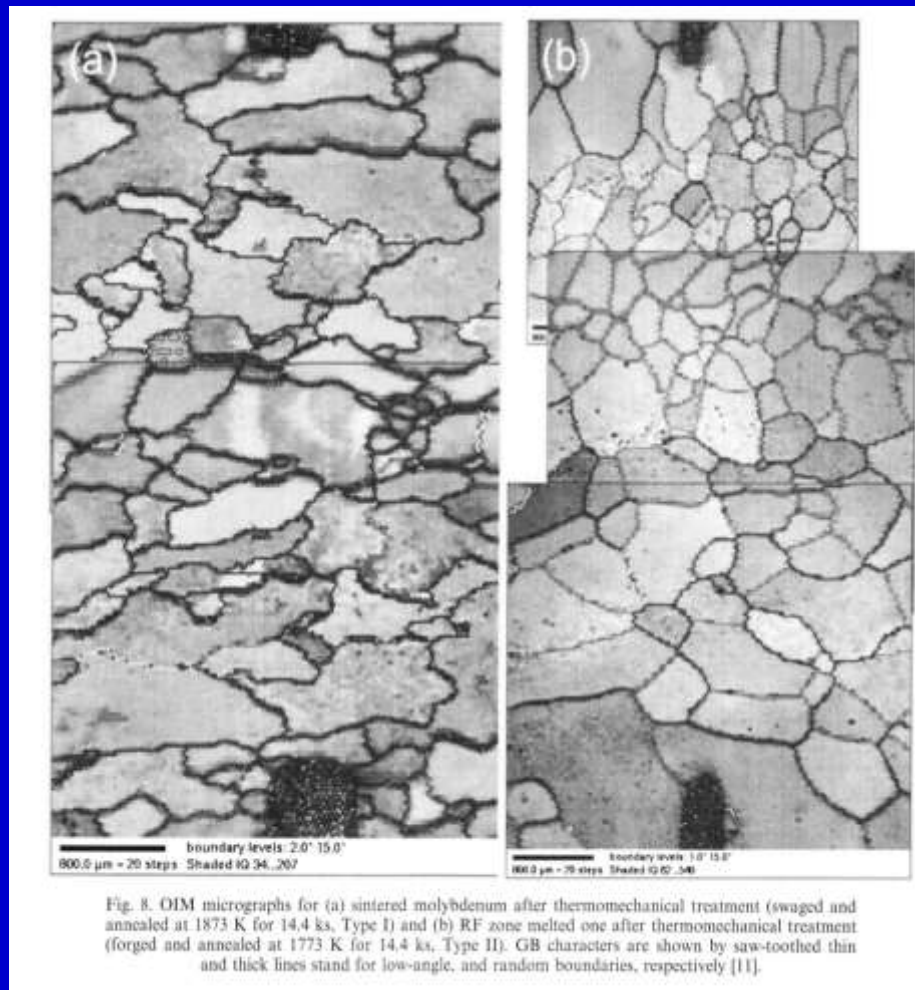


Fracture Behaviour in Molybdenum Polycrystals with Two Different Types of Grain Boundary Microstructures

T. Watanbe, S. Tsurekawa: Acta Mater., 47 (1999), 4171-4185

Before Fracture Test
Type I Type II

After Fracture Test
Type I Type II



Fracture Behaviour in Molybdenum Polycrystals with Two Different Types of Grain Boundary Microstructures

T. Watanabe, S. Tsurekawa: Acta Mater., 47 (1999), 4171-4185.

“The control of brittleness and development of desirable mechanical properties in Polycrystalline systems by grain boundary engineering”

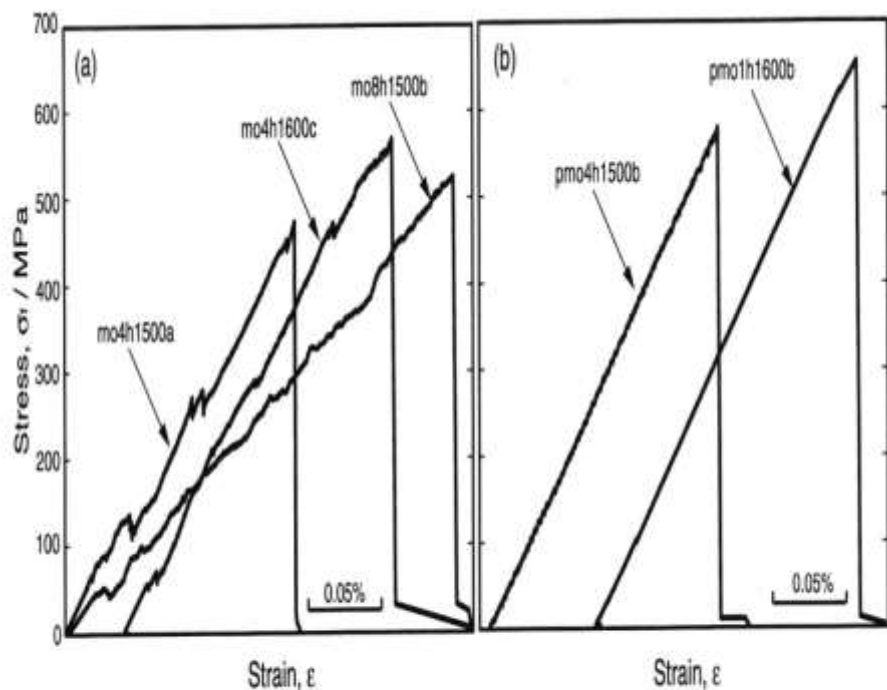


Fig. 10. Stress-strain curves for (a) Type I specimens with randomly oriented grains and (b) Type II specimens with textured grains [11].

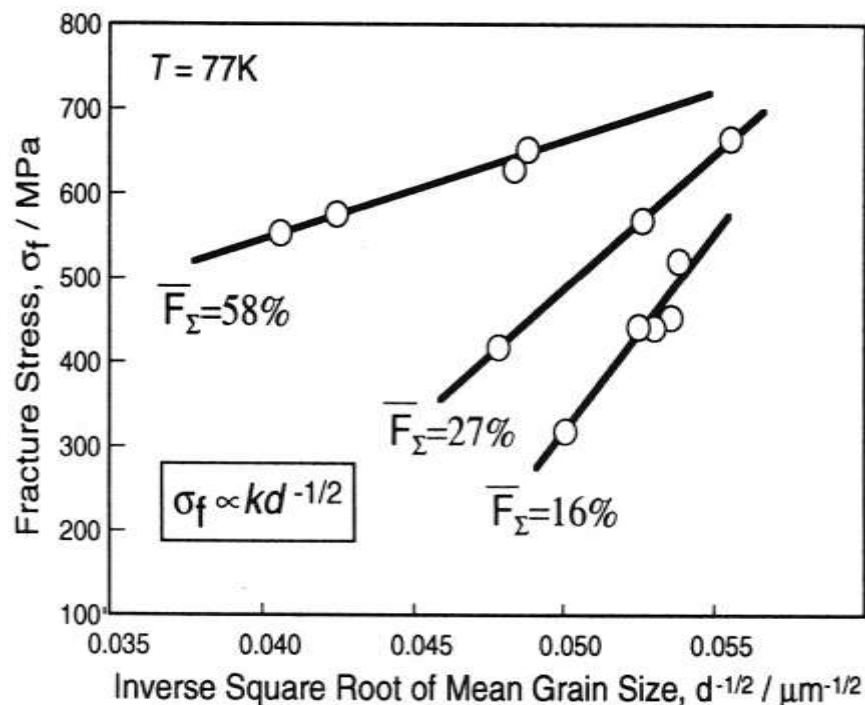


Fig.5 Fracture stress – grain size relationship. The mean fractions of the low Σ GBs are shown.

Grain Size Dependence of Fracture Stress controlled by GBCD in Polycrystalline Mo

Important Finding on The Hall-Petch:

The slope changes depending of GBCD.

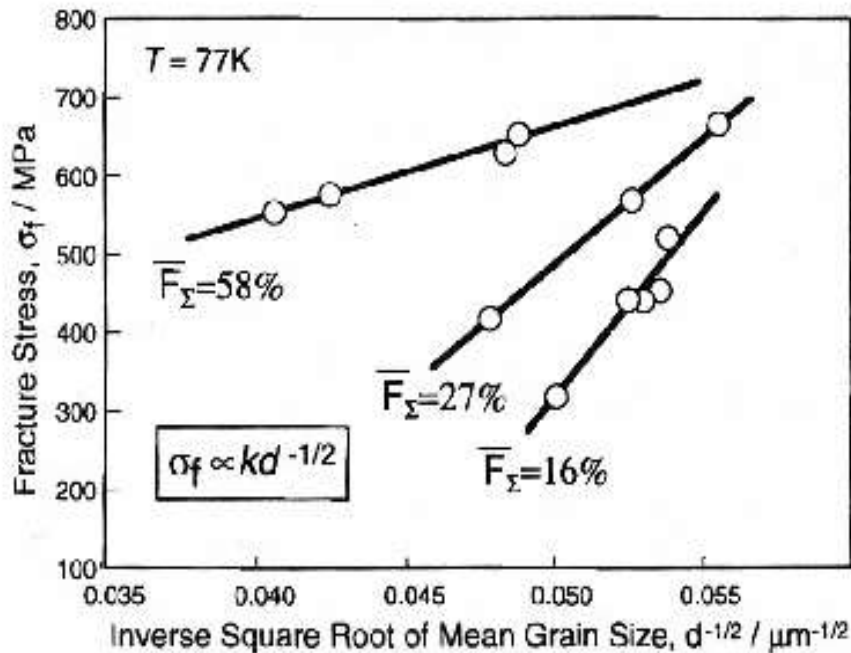


Fig.5 Fracture stress – grain size relationship. The mean fractions of the low Σ GBs are shown.

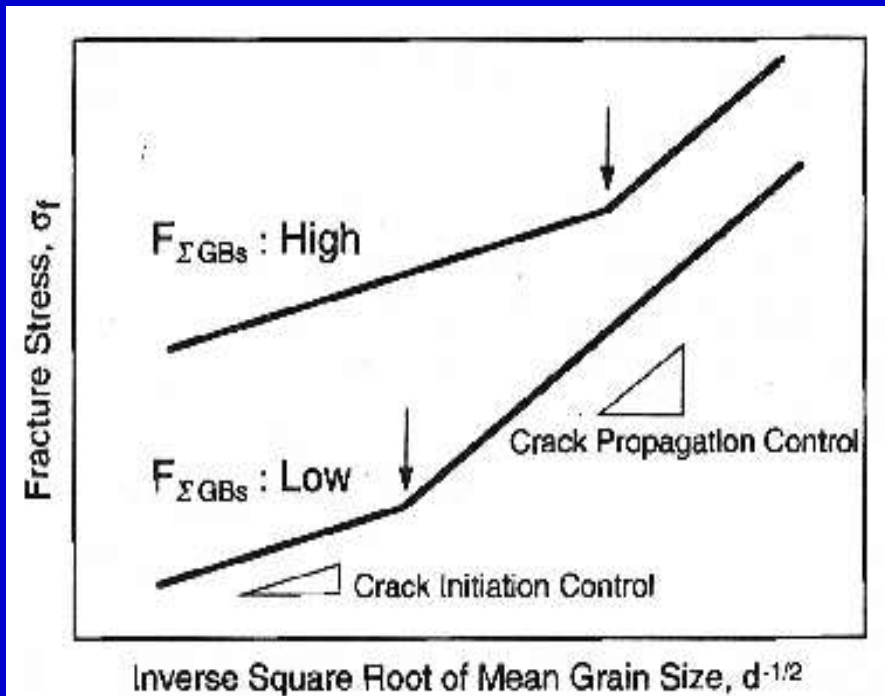
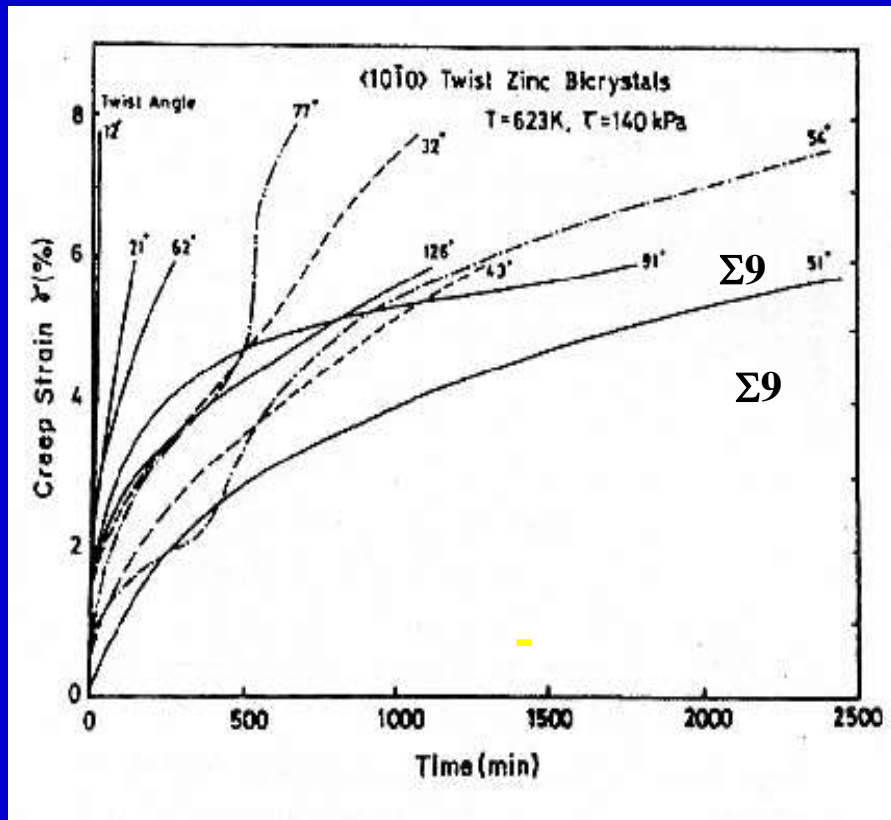


Fig. 6 Schematic explanation of grain size and GBCD dependence of fracture stress.

S. Tsurekawa, T. Watanabe; MRS. Proc. on Interfacial Engineering for Optimized Properties II, 586 (2000), 237~242

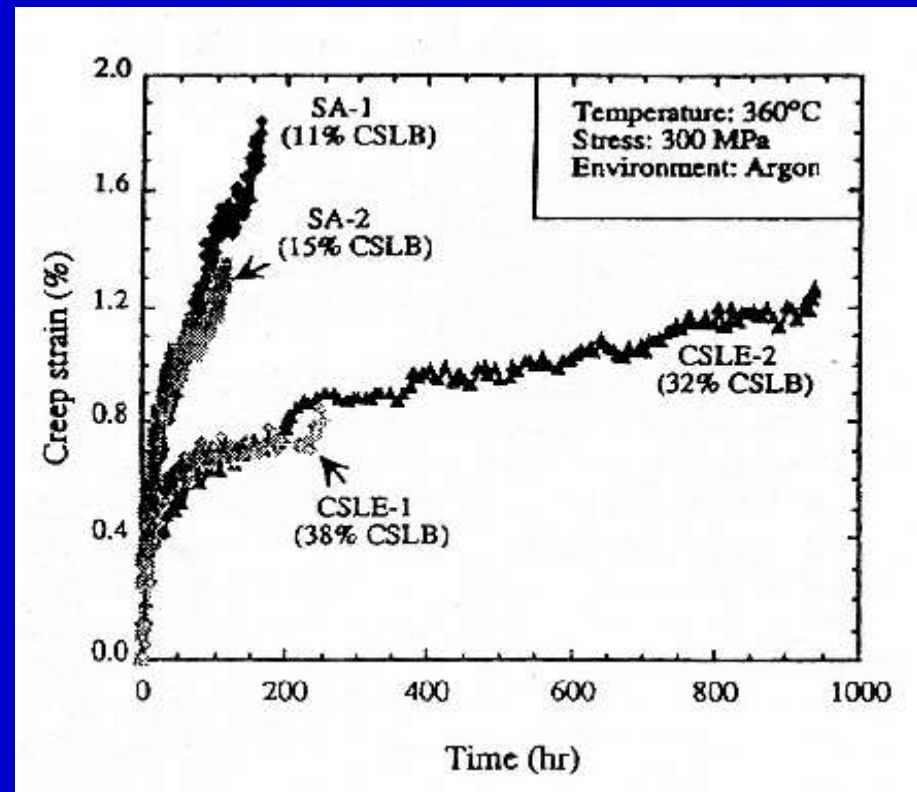
Grain Boundary Engineering for Improvement in Creep Strength of Zn Bicrystals and Ni-base Alloy Polycrystal.

Creep Curves for $\langle 10\bar{1}0 \rangle$ Twist Zinc Bicrystals with Different Boundaries under Constant Resolved Shear Stress.



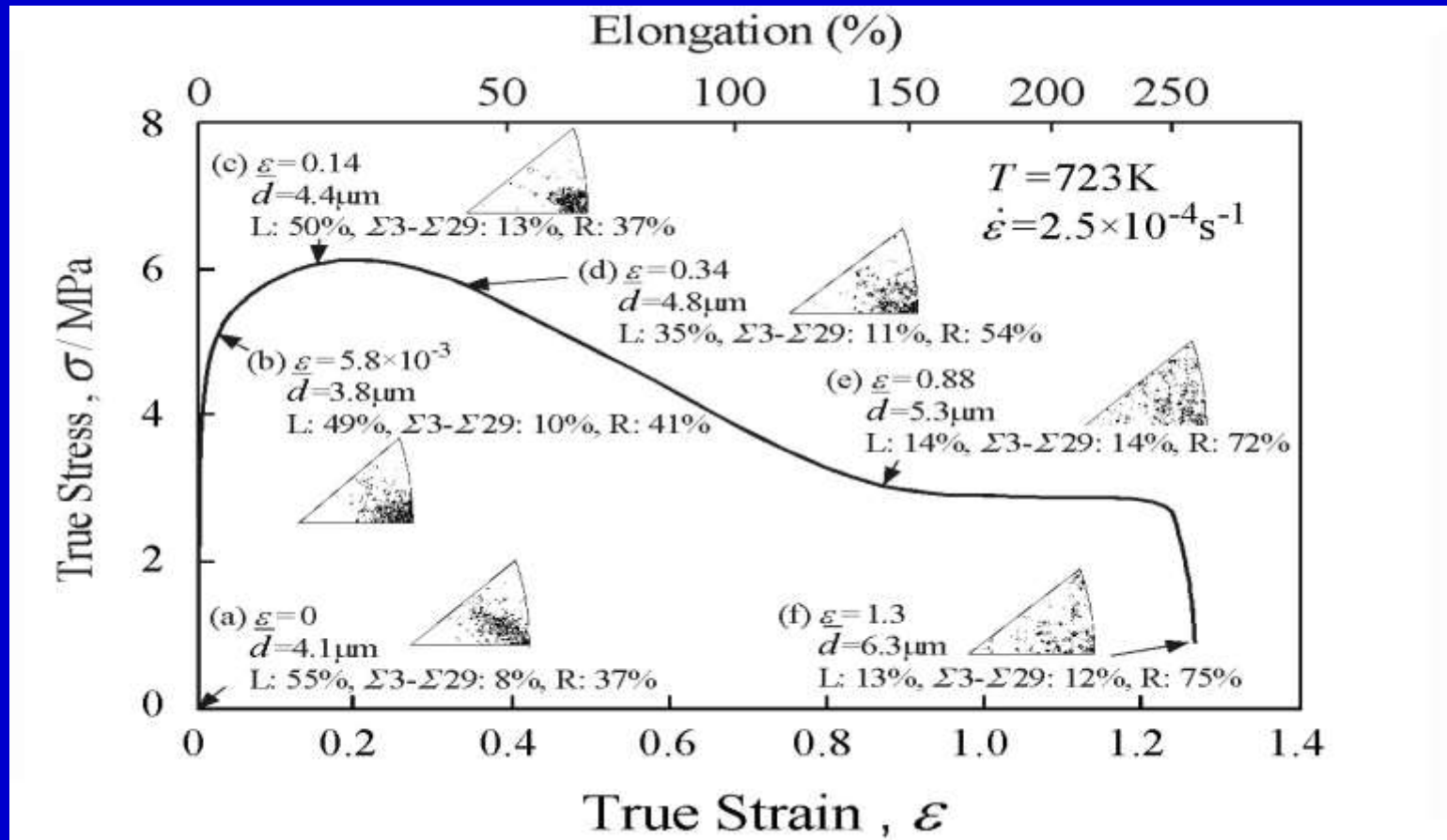
T. Watanabe, M. Yamada and S. Karashima;
Phil. Mag., A63 (1993), 1013.

Effect of the Frequency of Low Σ (CSL) Boundaries on Creep Deformation in Ni-16Cr-9Fe Alloy at 360°C, $\sigma = 300$ MPa.



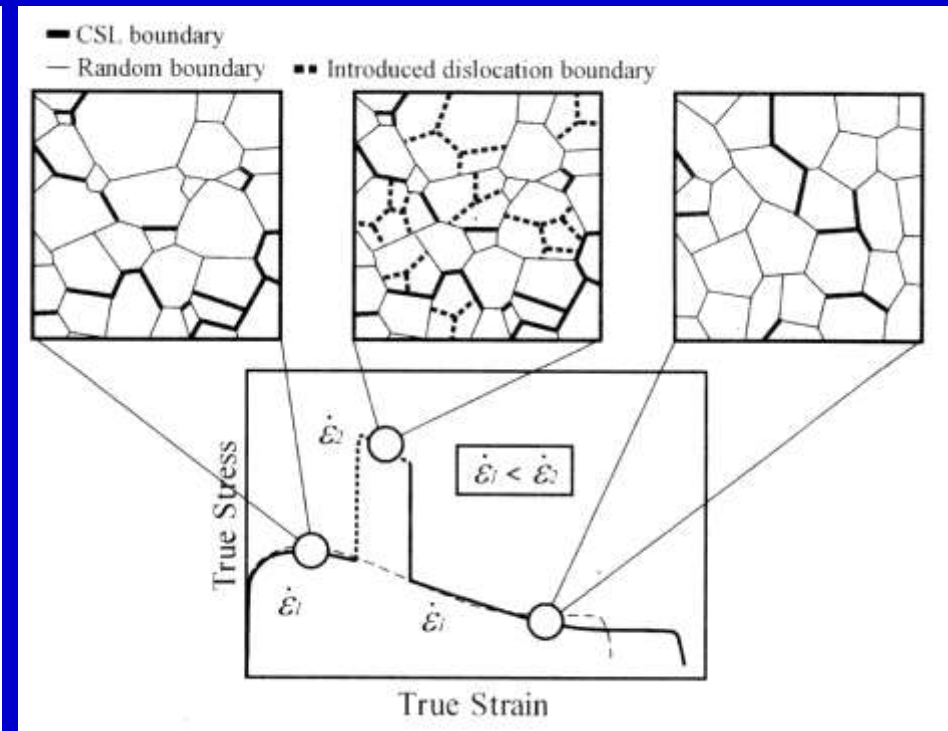
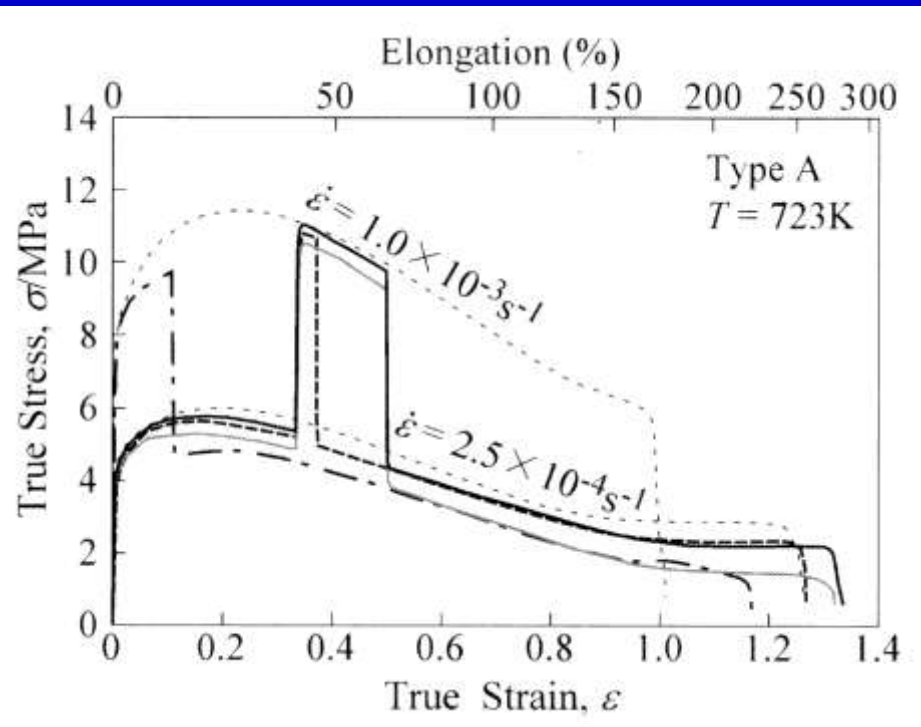
T. Thaveprungsriporn and G. S. Was;
Scripta Mater., 35 (1996), 1, B. Alexandreanu
& G. S. Was: Scripta Mater. 54 (2006), 1047.

Change in Grain Boundary Microstructure during Super-plastic Deformation in Al-Li Alloy.



Note: Evolution of an optimum grain boundary microstructure, particularly the fraction of random boundaries during super-plastic deformation.

Evolution of Optimal Grain Boundary Microstructure for Enhancement of Super-plasticity in Al-Li Alloy.



Demonstration of Improvement in Super-Plasticity by a Strain Rate Change Test at 723K.

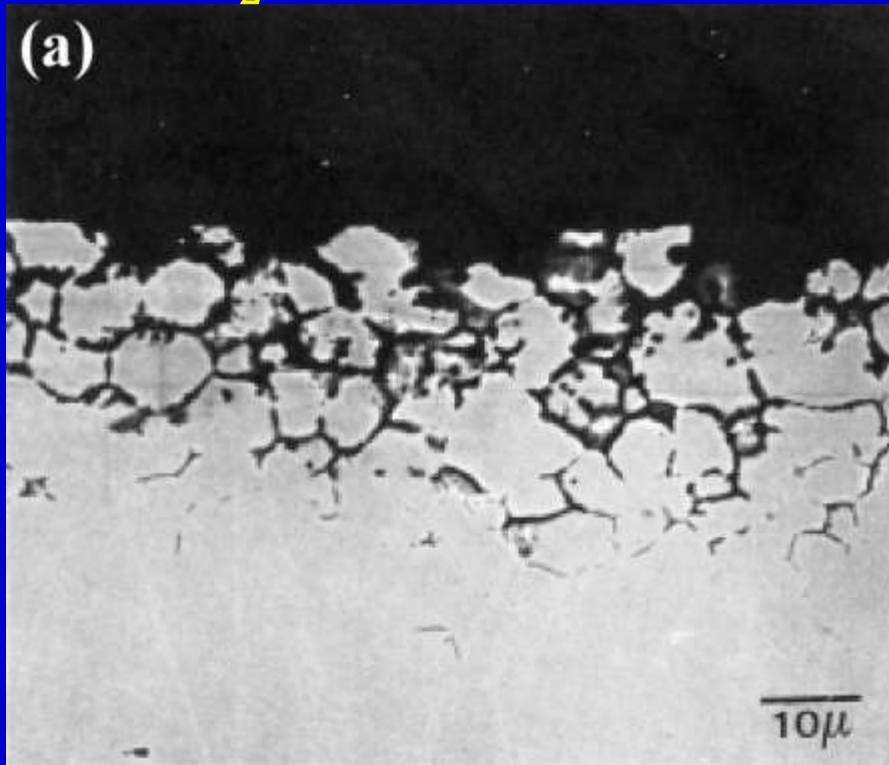
Schematic Illustration for Evolution of a new Grain Boundary Microstructure for Improvement in Superplasticity.

Grain Boundary Engineering for Control of Intergranular Corrosion in Alloy 600 (75Ni-16Cr-9Fe Alloy)

P. Lin, G. Palumbo, U. Erb, K. T. Aust: Scripta Met. Mater., 33 (1995), 1387-1392.

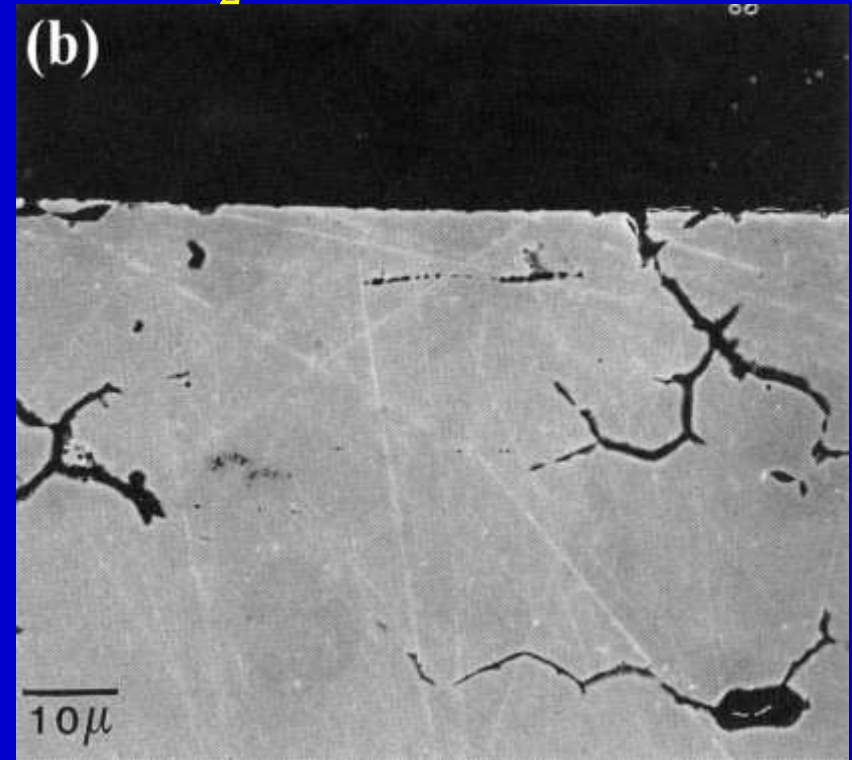
(a) Conventional Material

$F_{\Sigma} = 37\%$ ($\Sigma 1 \sim \Sigma 29$)



(b) GBE Processed Materials

$F_{\Sigma} = 70\%$ ($\Sigma 1 \sim \Sigma 29$)



1. G. Palumbo, E. M. Lehockey and P. Lin: “Applications for Grain Boundary Engineered Materials”, J. Metals, 50 (1998), No.2, 40-43.

Grain Boundary Engineering (Pb-based Battery Grid Alloy)

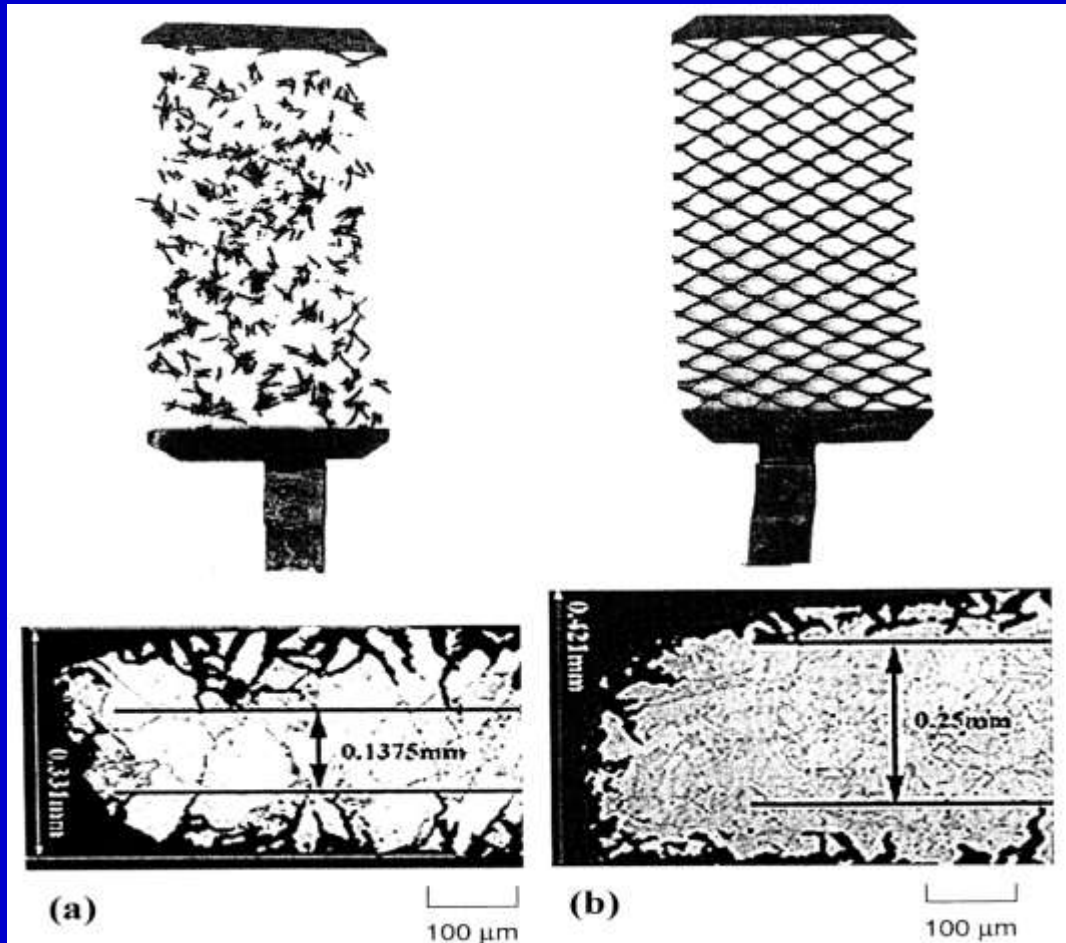
Pb-Ca-Sn-Ag Lead-Acid Positive Battery Grids Following 40 Charge-Discharge cycles in H_2SO_4 at $70^\circ C$ (1-1.781V Direct Current).

(a)

Conventional

(Cast and Wrought)

$F_\Sigma = 15\%$



(b)

GBE-Processed

$F_\Sigma = 50\%$

1. E. M. Lehockey, G. Palumbo, P. Lin and A. Brennenstuhl: Metal. Mater. Trans., 29A (1998), 387-396.
2. G. Palumbo, U. Erb: “Enhancing the operating life and performance of lead-acid batteries via grain boundary engineering”, MRS Bulletin, 24 (1999), No.11, 27-32.

Grain Boundary Engineering for GB Corrosion Control in 304 Stainless Steel

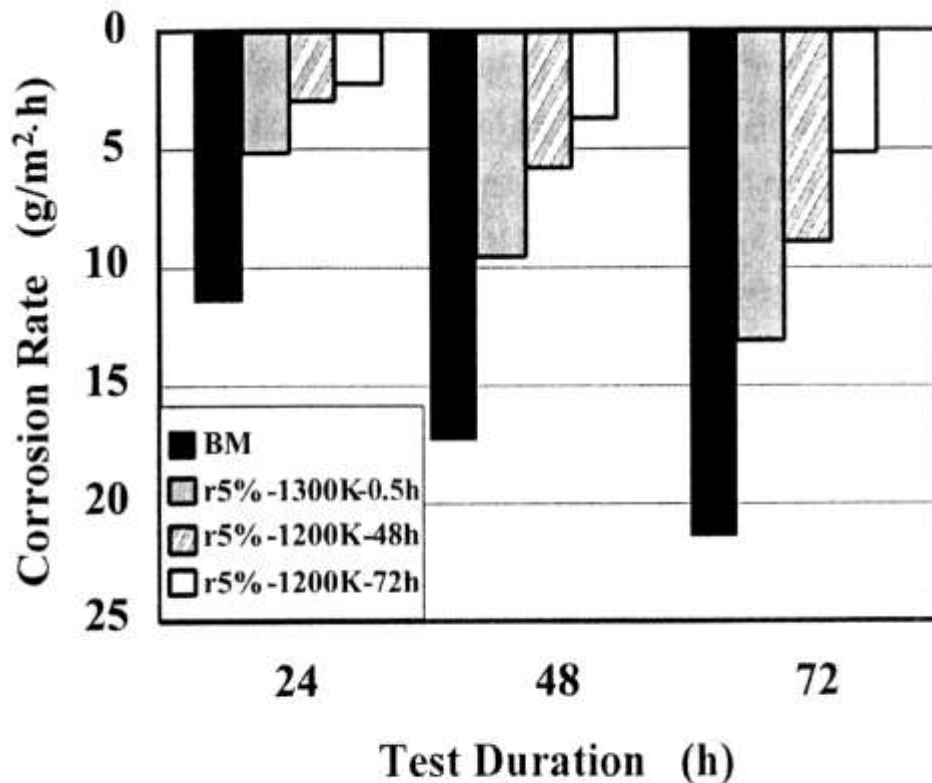
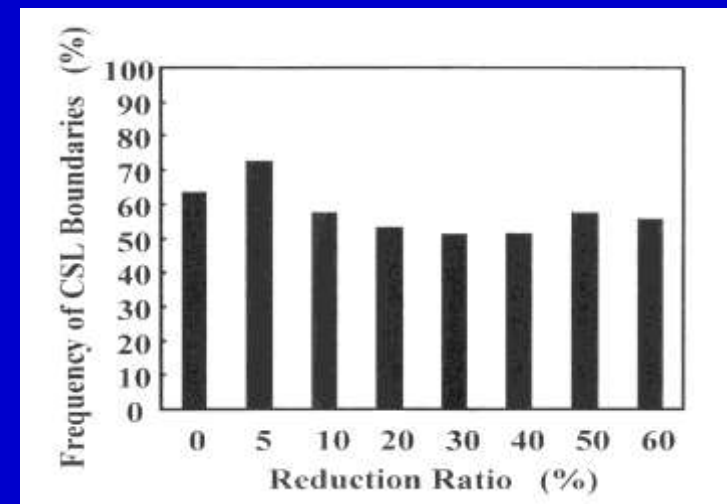
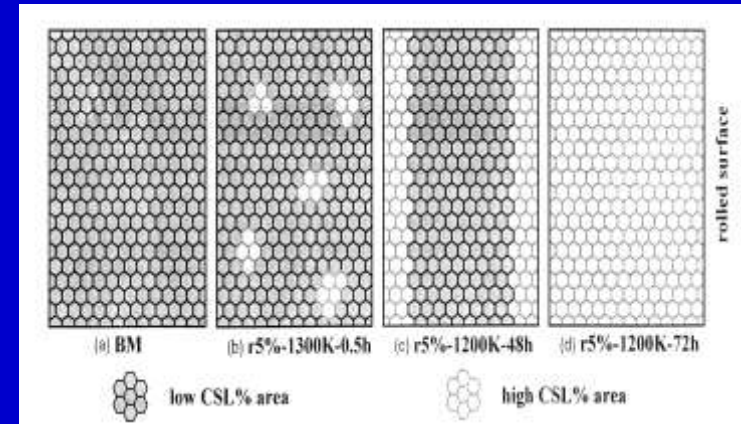


Fig. 9. The corrosion mass-loss of the BM and the strain-annealed specimens during the ferric sulfate-sulfuric acid test.

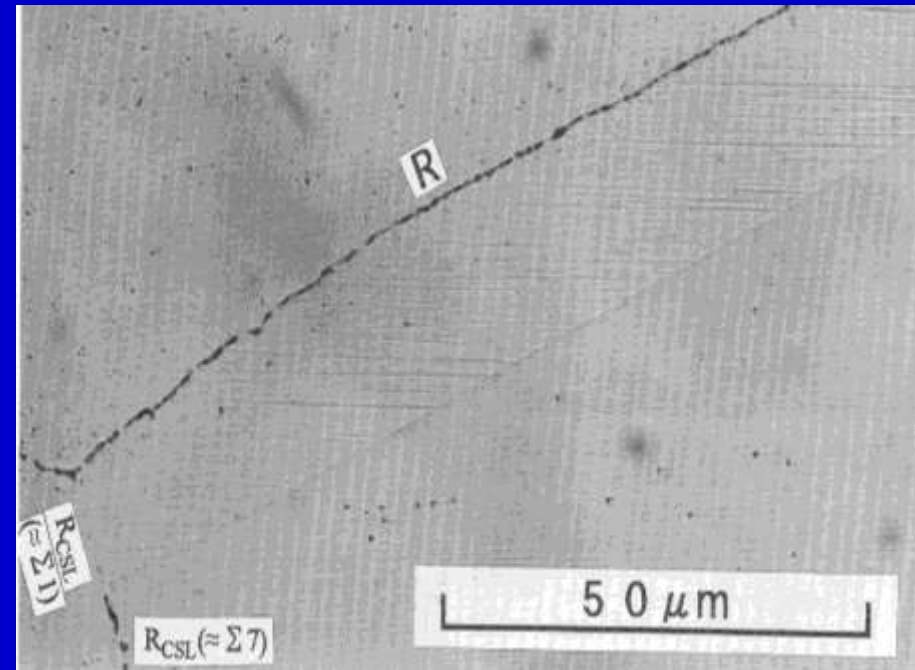
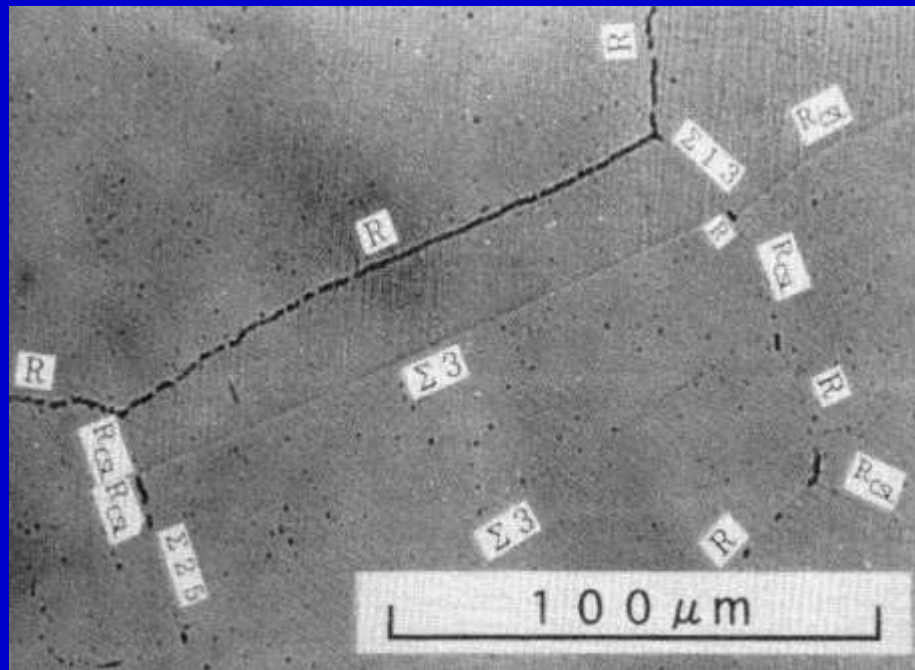


M. Shimada, H. Kokawa, Z.J. Wang, Y.S. Sato, I. Karibe: Acta Mater., 50 (2002), 2331.

“Optimization of GBCD for intergranular corrosion resistant 304 stainless steel by GBE”

Improvement in Oxidation Resistance and Control of Oxidation-induced Brittleness by Grain Boundary Engineering

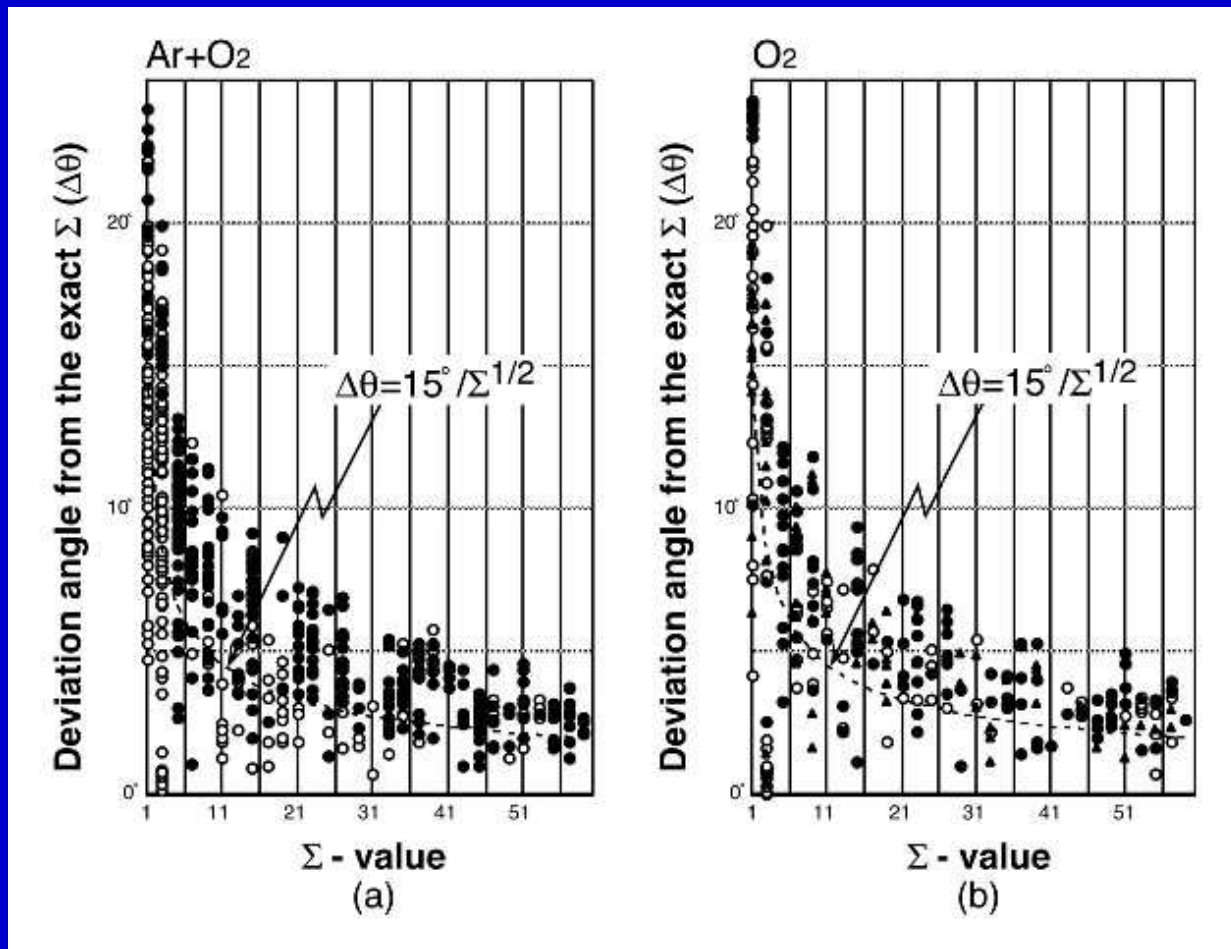
Observations of Structure-Dependent Intergranular Oxidation in Ni-40at%Fe Alloy



Note: Random boundaries are preferential sites for oxidation, but low- Σ not.

S. Yamaura, Y. Igarashi, S. Tsurekawa, and T. Watanabe:
Acta mater. Vol.47,(1999), 1163-1174.

Grain Boundary Engineering for The Control of Intergranular Oxidation Brittleness



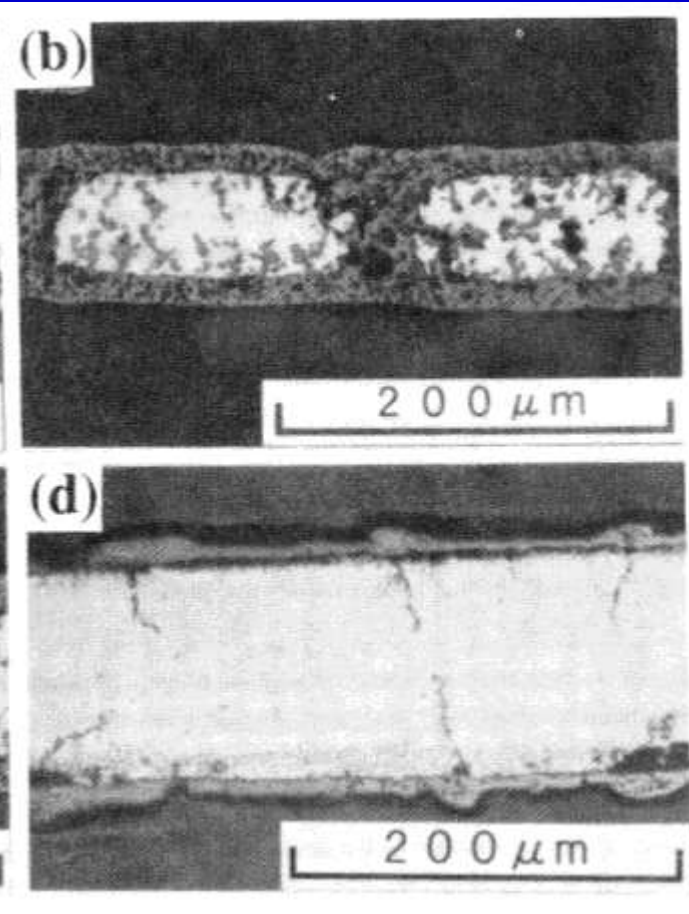
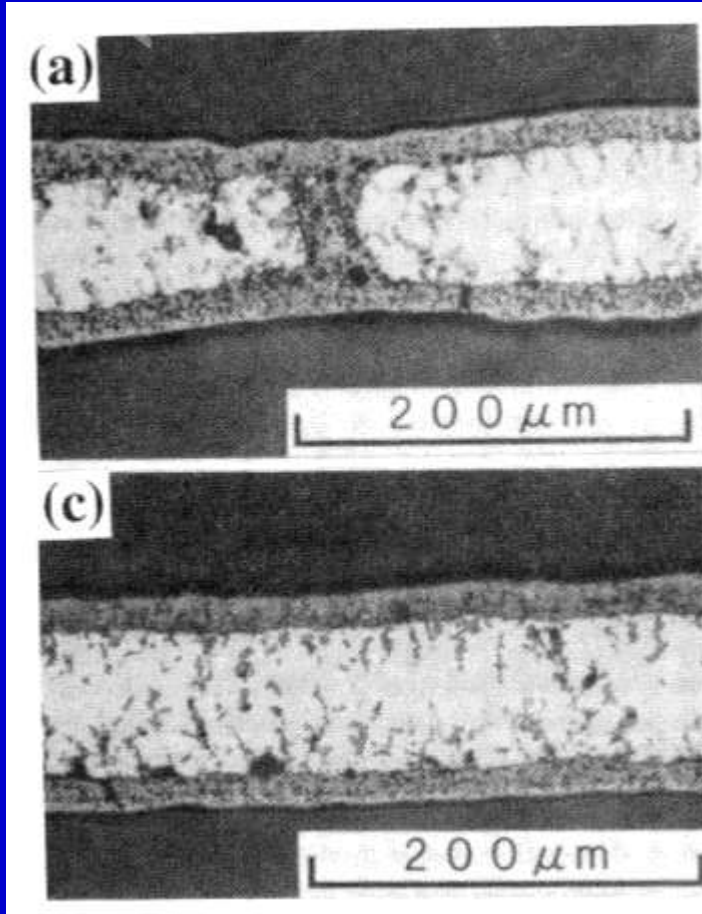
Dependence of Intergranular Oxidation Morphology on Σ Value and Deviation Angle $\Delta\theta$. ● : Heavily Oxidized Boundary, ▲ : Slightly Oxidized Boundary, ○ : Non-Oxidized Boundary.

(S. Yamaura, Y. Igarashi, S. Tsurekawa, and T. Watanabe, Acta mater. Vol.47,(1999), 1163-1174.)

Grain Boundary Engineering for Improvement in Oxidation Resistance by controlling GBCD

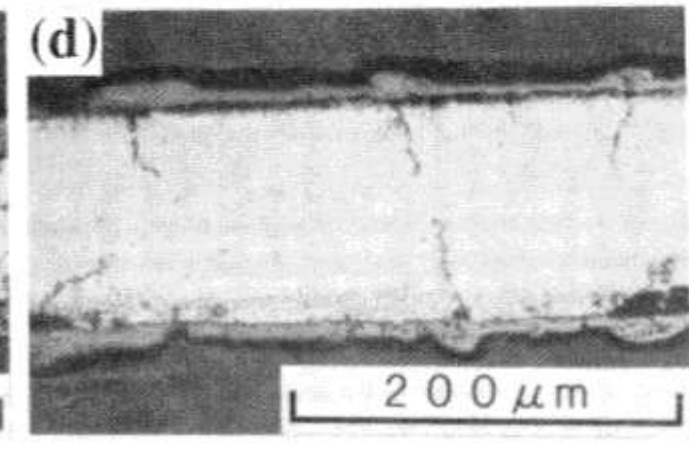
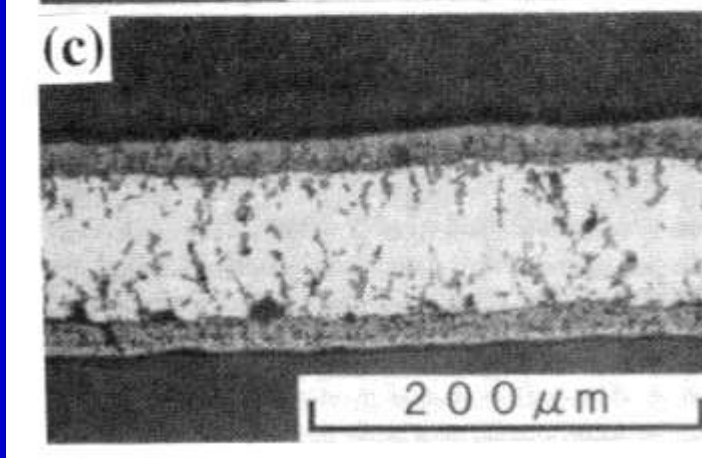
(Ni-39wt.%Fe Alloy: S. Yamaura et. al: Acta Mater., 47 (1999), 1163.)

$F_R=62.8\%$



$F_R=61\%$

$F_R=33\%$



$F_R=28.5\%$

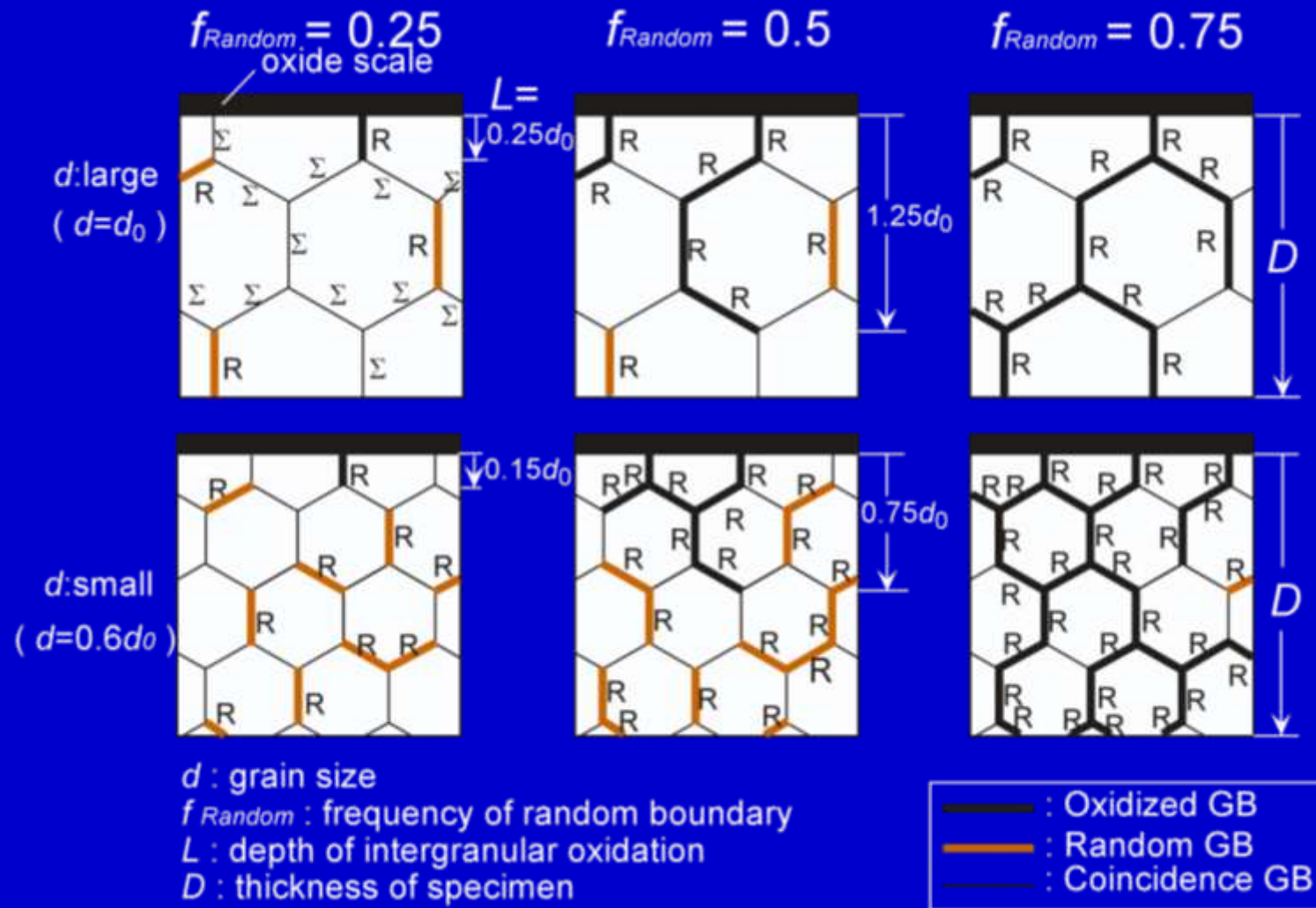
(a) As-Solidified at 28.3m/s, $d=2\mu\text{m}$

(b) As-Solidified at 14.1m/s, $d=3.7\mu\text{m}$

(c) Solidified-Annealed at 1073K, 1h,
 $d=3.5\text{mm}$

(d) Solidified-Annealed at 1473K, 1h,
 $d=50\mu\text{m}$

Principle of Control of Oxidation-Induced Intergranular Brittleness by Grain Boundary Engineering



S. Yamaura, Y. Igarashi, S. Tsurekawa, T. Watanabe: *Properties of Complex Inorganic Solids 2*, ed. by A. Meike et al, Kluwer Acad. Plenum Pub., 2006, pp.27-37.

Effect of Triple Junction Character on Crack Propagation in Polycrystals

S. Kobayashi, S. Tsunekawa, T. Watanabe: Phil. Mag. 86 (2006), 5419-5429,
“Structure-dependent triple junction hardening and intergranular fracture in Mo”

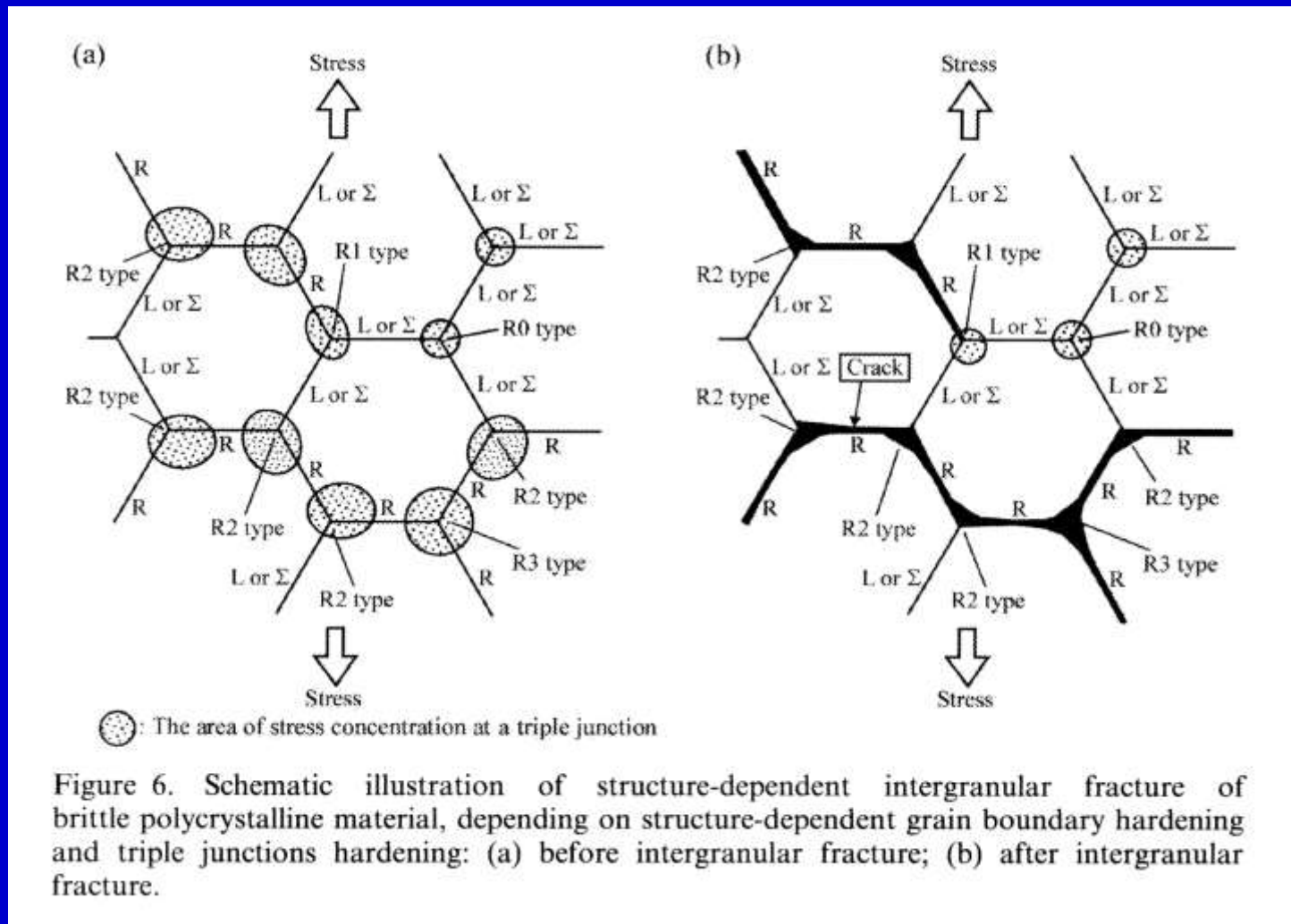
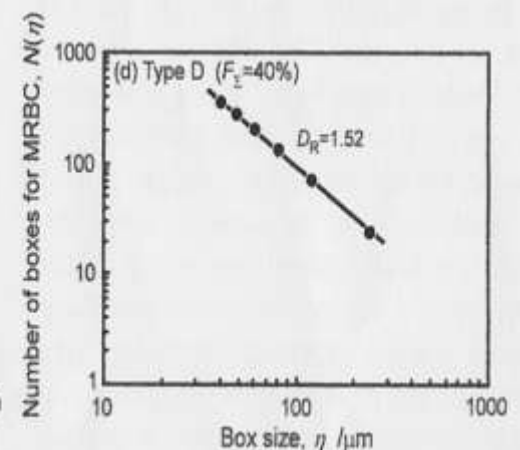
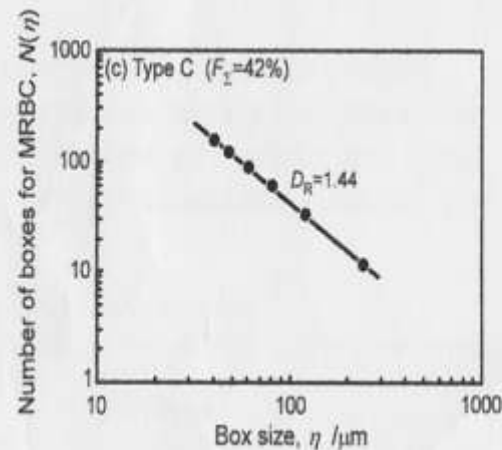
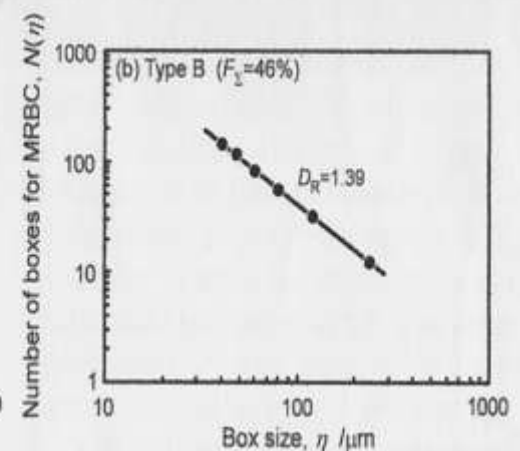
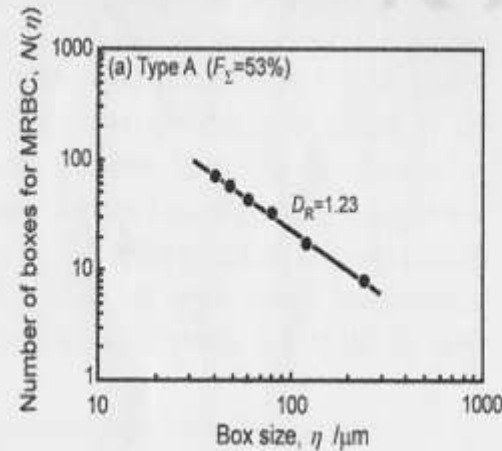
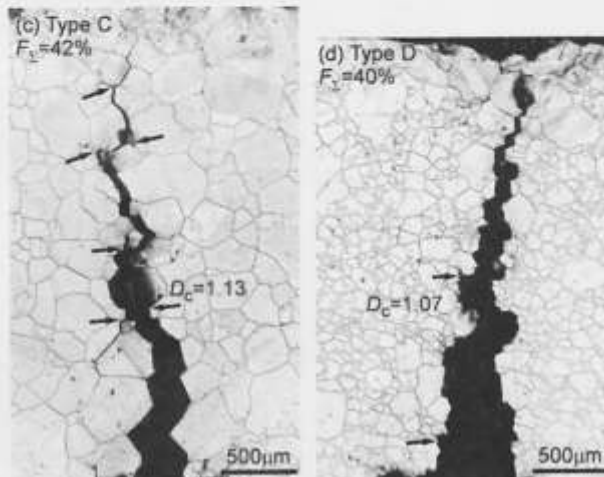
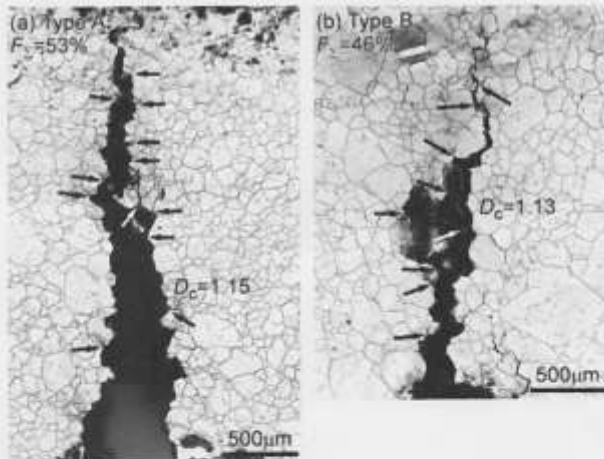


Figure 6. Schematic illustration of structure-dependent intergranular fracture of brittle polycrystalline material, depending on structure-dependent grain boundary hardening and triple junctions hardening: (a) before intergranular fracture; (b) after intergranular fracture.

The First Attempt of Fractal Analysis for Control of Brittle Fracture based on GBs in Polycrystalline Nickel.

S. Kobayashi, T. Maruyama, S. Tsurekawa, T. Watanabe: Acta Mater., 60 (2012), 6200.

“Grain boundary engineering based on fractal analysis for control of segregation-induced intergranular brittle fracture in polycrystalline nickel”.

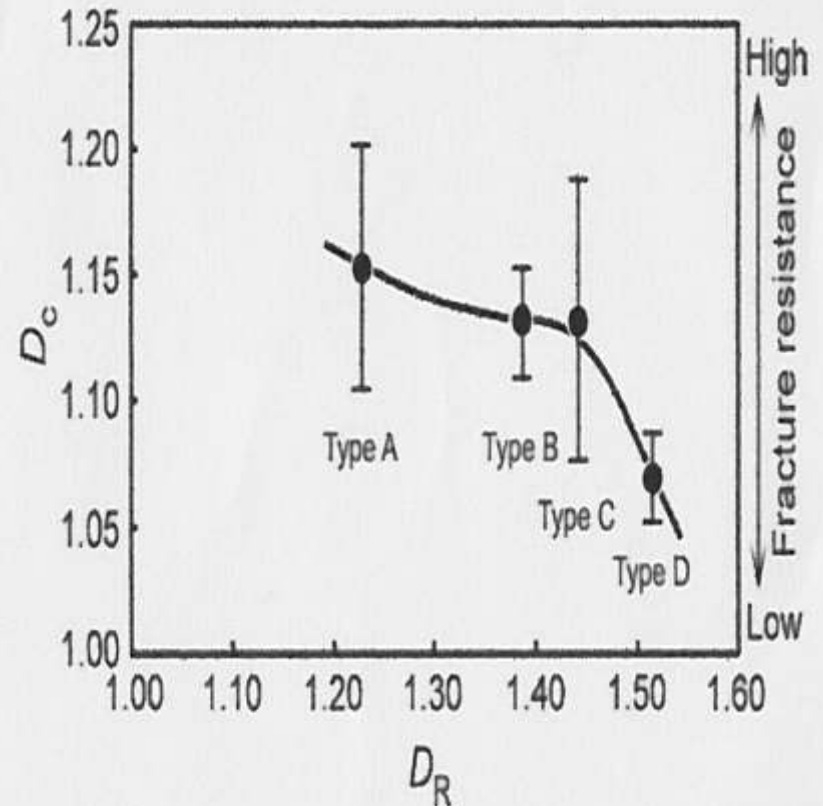
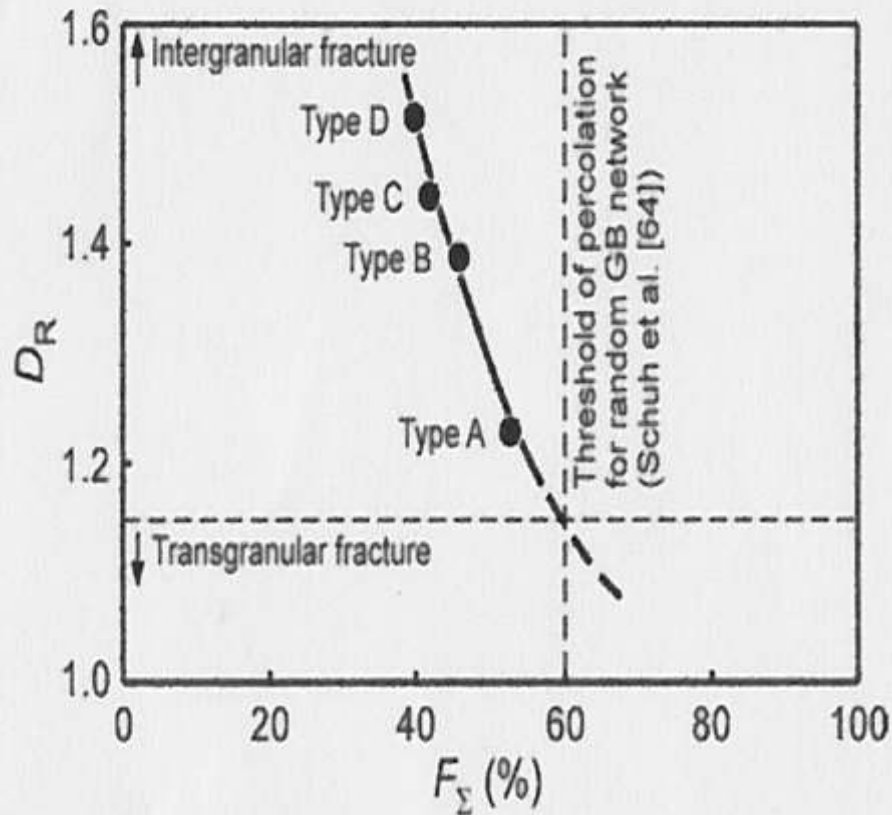


Fractal Approach to Control of Intergranular Brittleness:

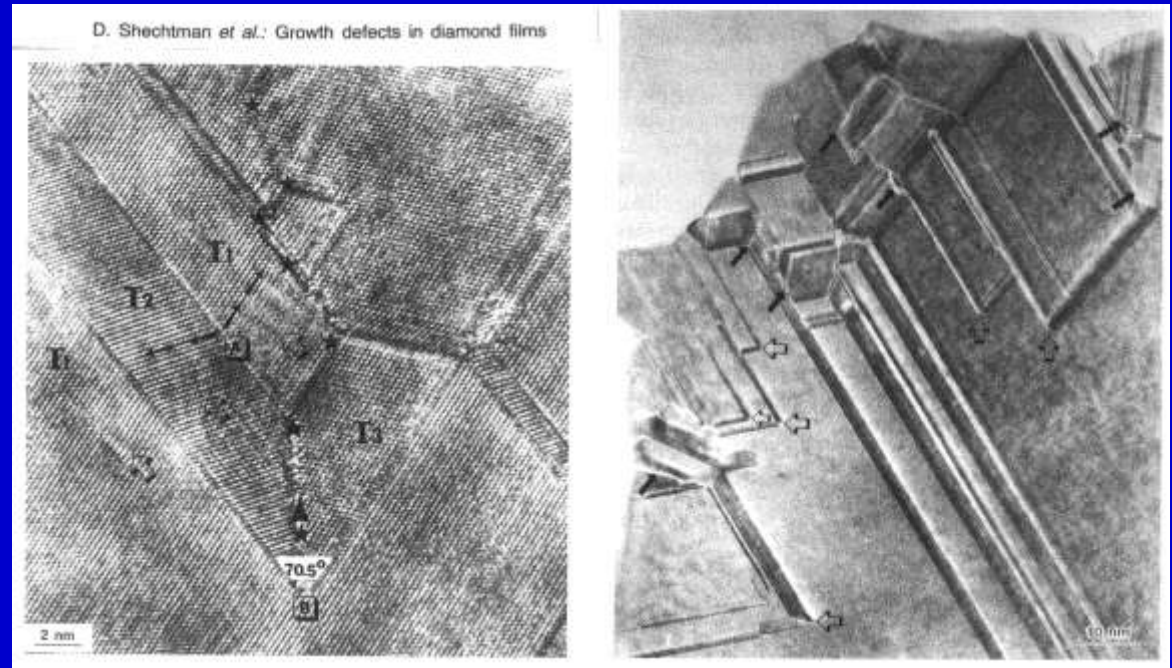
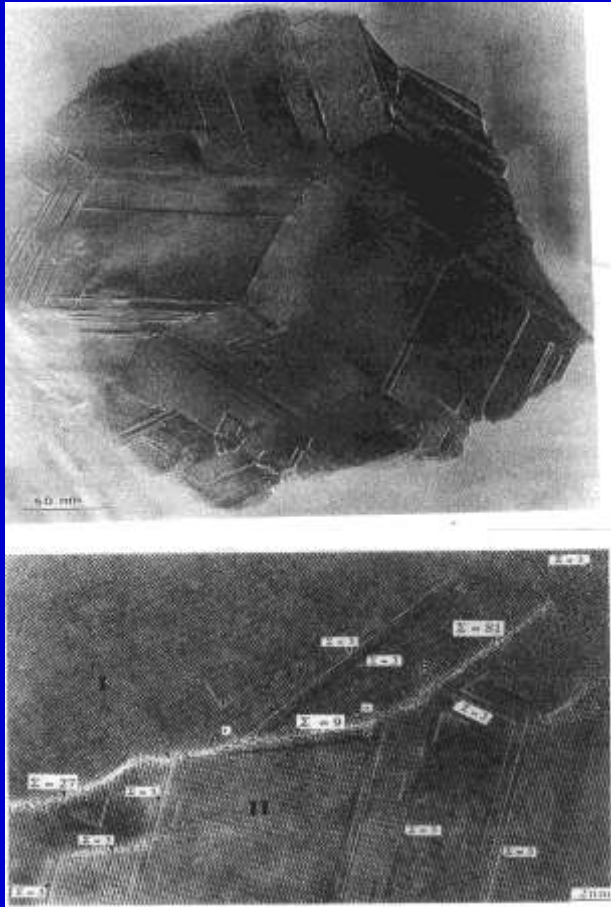
→ Random Boundary Cluster Size, D_R as a Function of the Frequency of Fracture-resistant Boundaries.

S. Kobayashi, T. Maruyama, S. Tsunekawa, T. Watanabe: *Acta Mater.*, 60 (2012), 6200

“Grain boundary engineering based on fractal analysis for control of segregation-induced intergranular brittle fracture in polycrystalline nickel”.



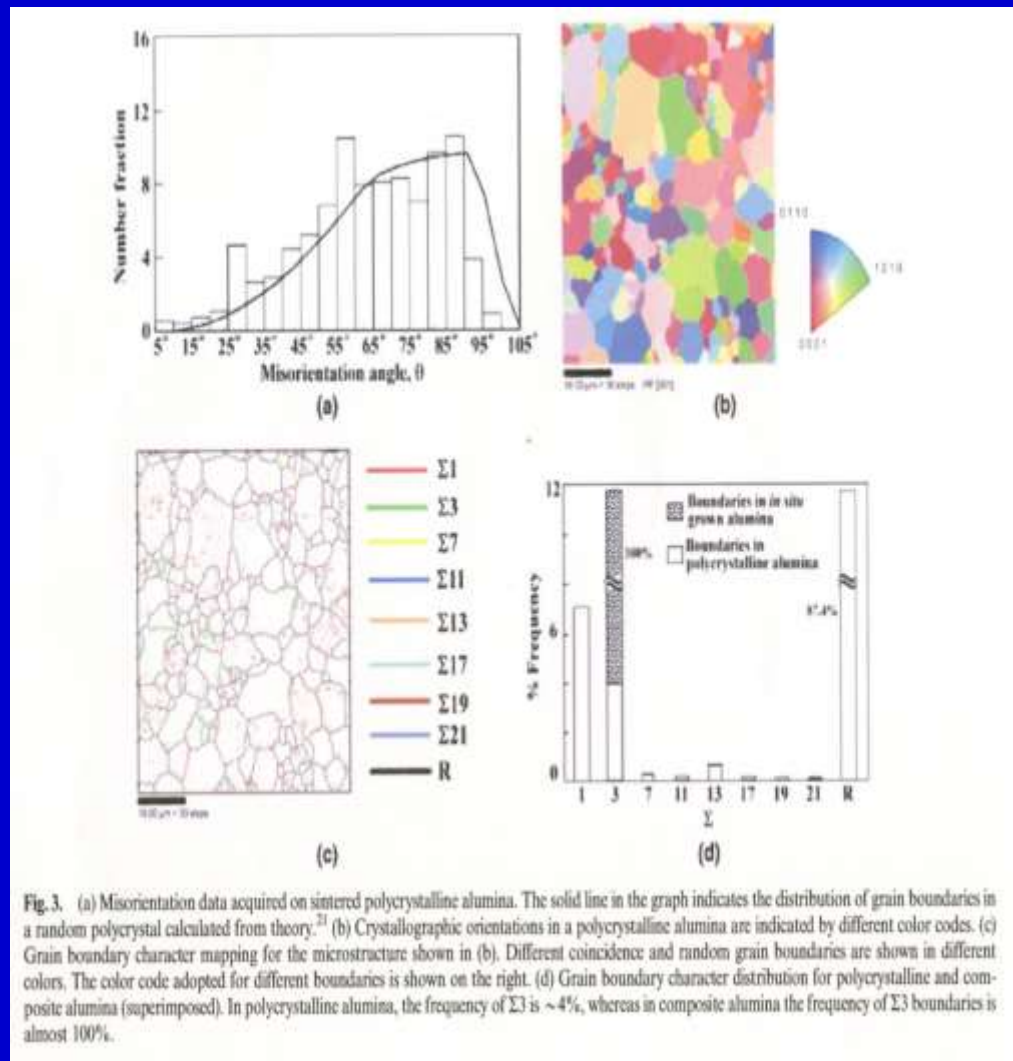
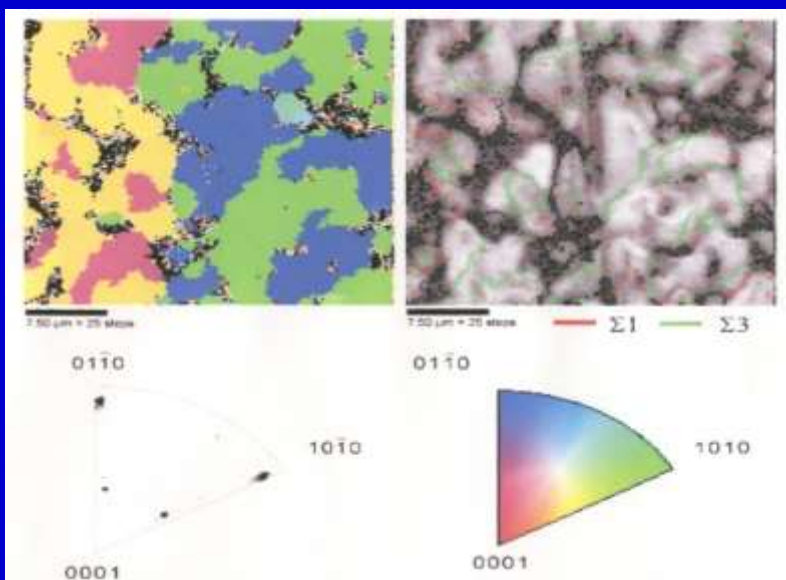
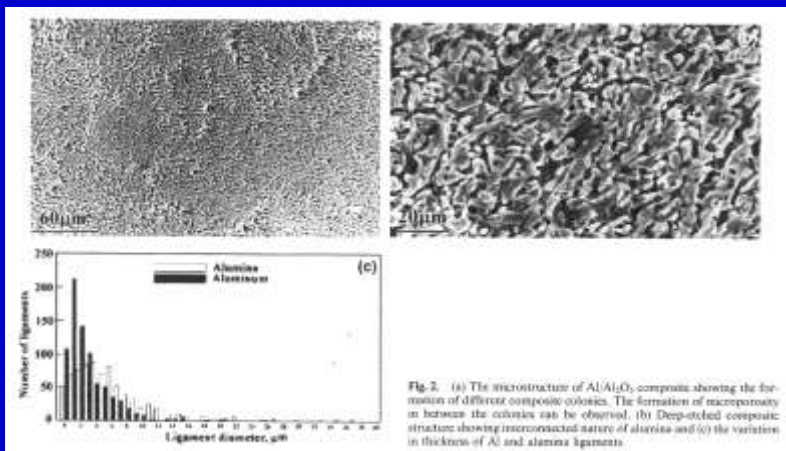
Twin Boundaries as Growth Defects in Diamond Films



Dominant occurrence of Twin boundaries
at edge of diamond film.

D. Shechtman, J. L. Hutchinson, L. H. Robins, E. N. Farabaugh, A. Feldman:
J. Mater. Res., 8 (1993), No.3, 473-479.

Grain Boundary Microstructure of Alumina produced by Reactive Metal Penetration (RME) ($F_{\Sigma 3} \approx 100\%$)



Mandelbrot et al's Statement on Fracture Control
by using Fractal Dimension D, based on Fractal
Analysis of Fracture Surfaces in Maraging Steel.

Mandelbrot, BB, Passoja DE, Paullay ME: Nature, 308 (1984), 721.

- **“The fractal dimension D is a measure of toughness**
in metals and the value of D decreases smoothly
with an increase of the impact energy measured by
- **a standard Charpy impact test. This relationship**
must reflect the change in the microstructure that
occur during aging”

On the basis of their fractal analysis of fracture
surfaces in **maraging steel.**

Grain Boundary Engineering for Advanced Materials through New Material Processing Methods

1. Thermomechanical Processing

- (1) Conventional TM Processing
- (2) ECAP Processing, & others.

2. Directional Processing under Gradient Temp.

Solidification, Annealing/Cryst.-Phase Transf.

3. External Field –Applied Processing

(1) Magnetic Field Application

Annealing, Crystallization, Solidification,
Phase transformation, Rejuvenation,

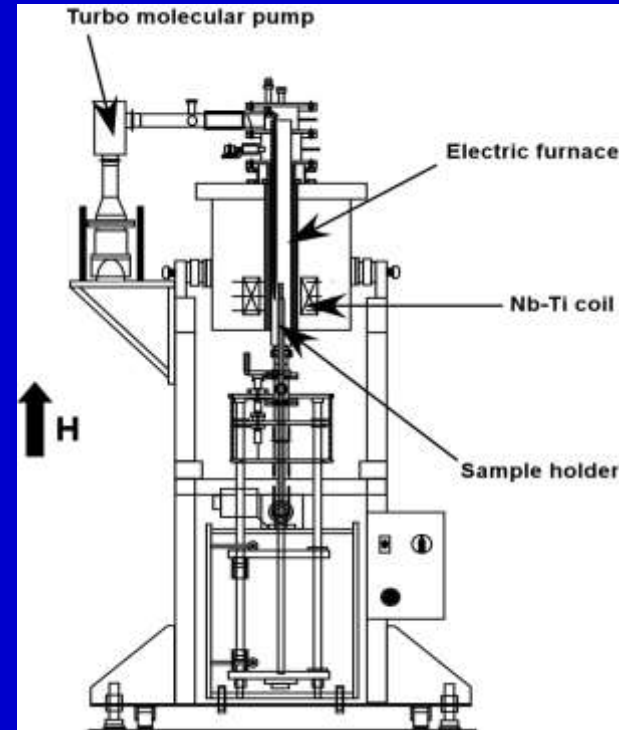
(2) Electric Field Application

4. Environment-Controlled Processing

- (1) Deposition Processing (PVD, CVD, etc)
- (2) Vacuum/Gass (Low, High, Surface energy-driven)

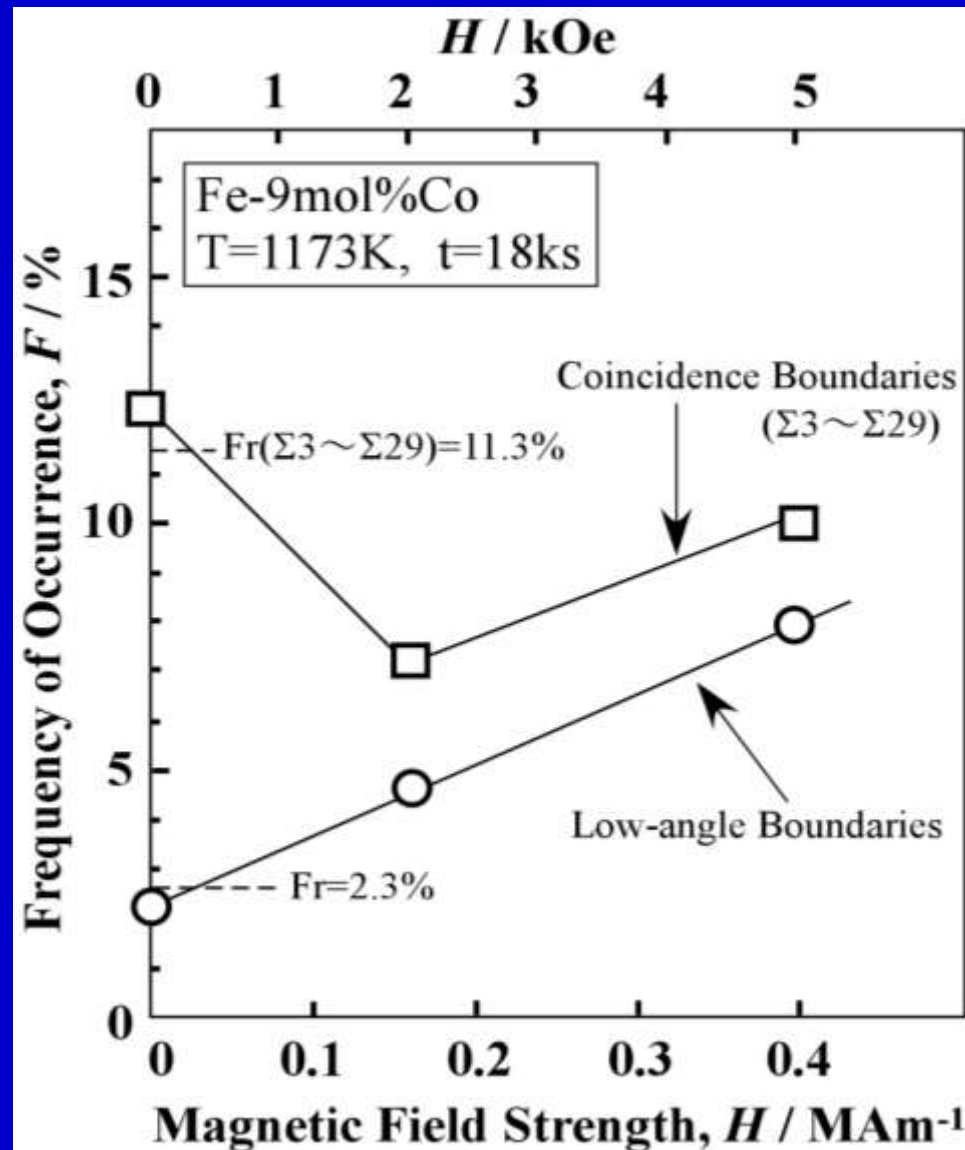
Grain Boundary Engineering by Mag. Field Application.

1. Magnetic Annealing (Control of Abnormal Growth, Segregation Brittleness)
2. Magnetic Sintering, 3. Magnetic Crystallization from Amorphous-state
4. Magnetic Solidification, 5. Magnetic Rejuvenation of Damaged Materials.



1. T. Watanabe, S. Tsunekawa, X. Zhao, L. Zuo: “**Grain Boundary Engineering by Magnetic Field Application**”, *Scripta Mater.*, 54 (2006), 969-975, Viewpoint Set on Grain Boundary Engineering.
2. T. Watanabe, S. Tsunekawa, X. Zhao, L. Zuo and C. Esling: “**A New Challenge : GBE for Advanced Materials by Magnetic Field Application**”, *J. Mater. Sci.*, 41 (2006), 7747-7799.

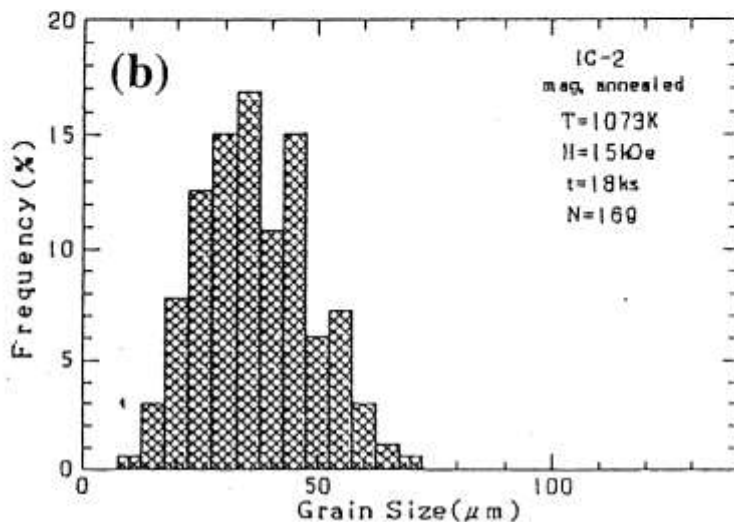
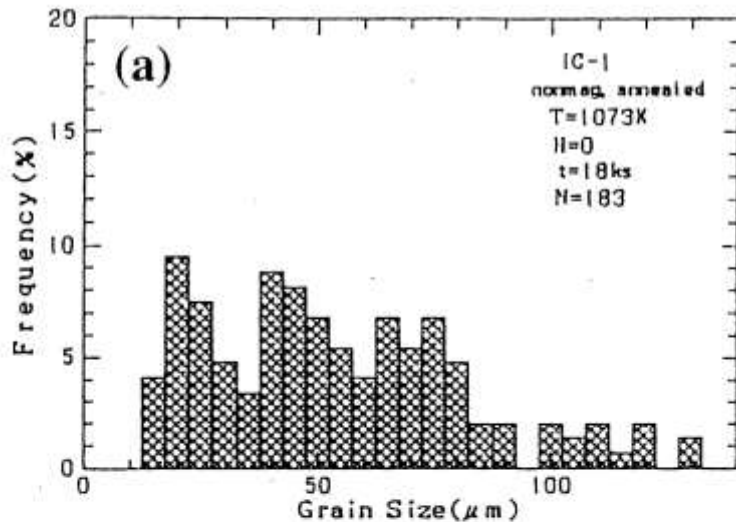
The Effect of Magnetic Annealing on GBCD in Fe-9mass%Co Alloy Polycrystals.



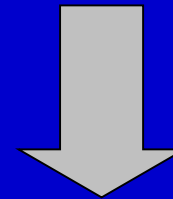
Effect of Magnetic Annealing on Grain Growth

Fe-50mol%Co ribbons.

N. Ono, K. Kimura and T. Watanabe : Proc. Inter n. Conf. Thermomechanical Processing of Steel and other Materials, (1997), 2125-2131.



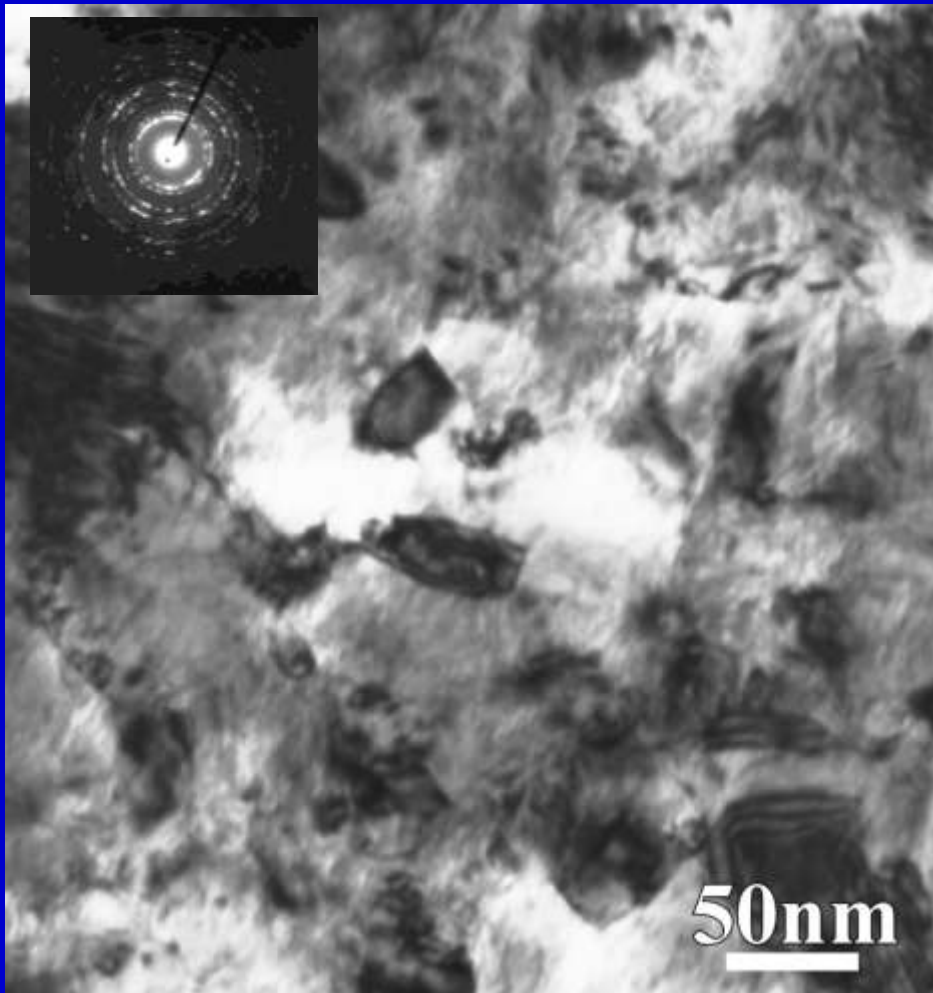
Control of Abnormal Grain Growth and Evolution of Homogeneous Grain Microstructure.



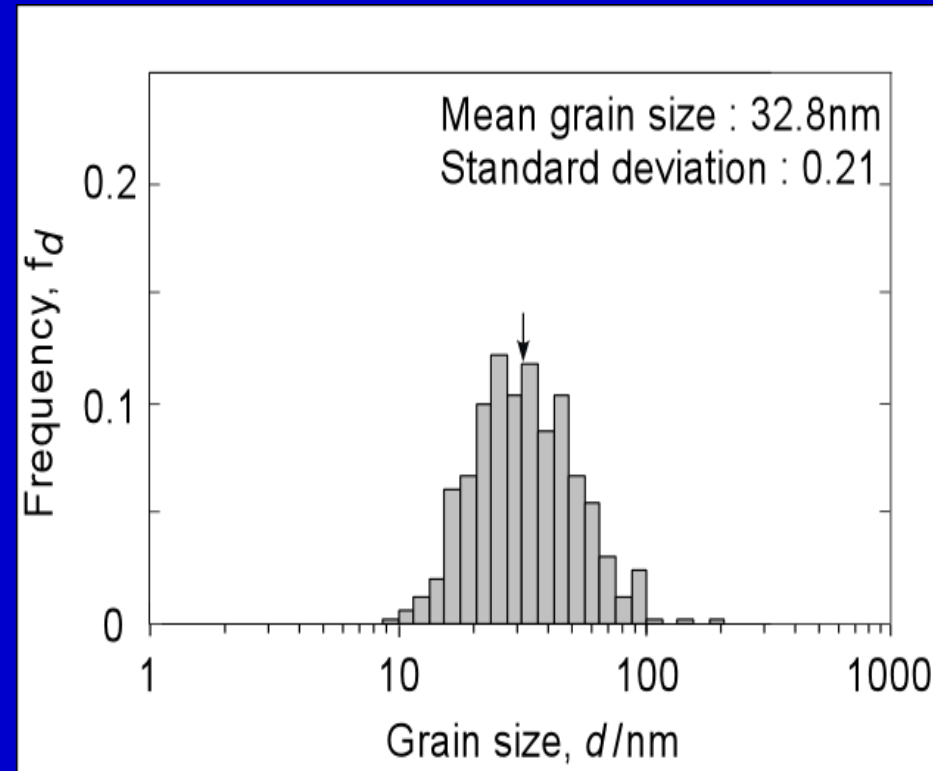
Improvement of Thermal Stability in Nanocrystalline Materials

Initial State of Electrodeposited Nanocrystalline Ni

K. Harada, S. Tsurekawa, T. Watanabe, G. Pslumbo, *Scripta. Met.*, 49 (2003), 367-372.



Grain Size Distribution

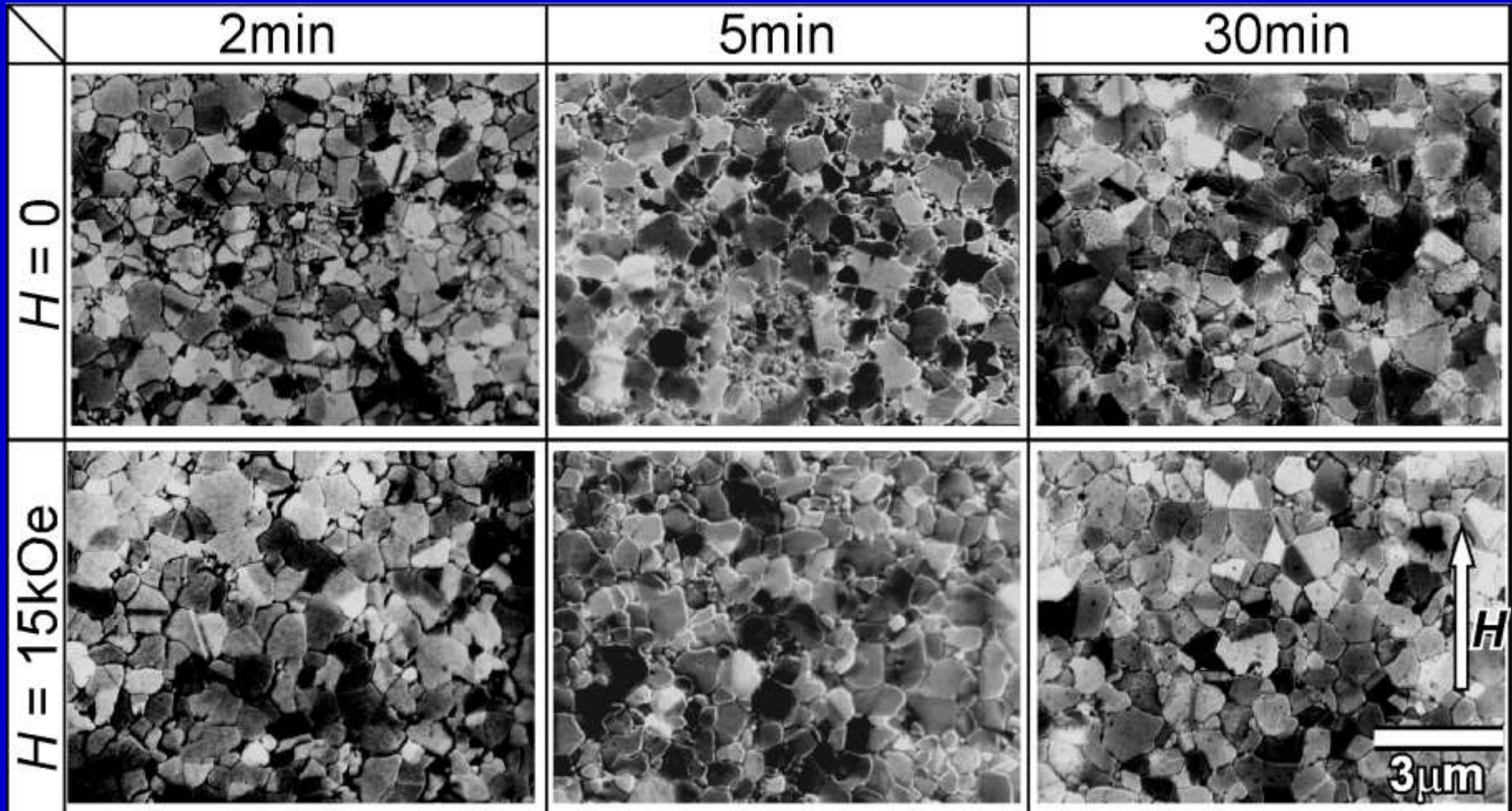


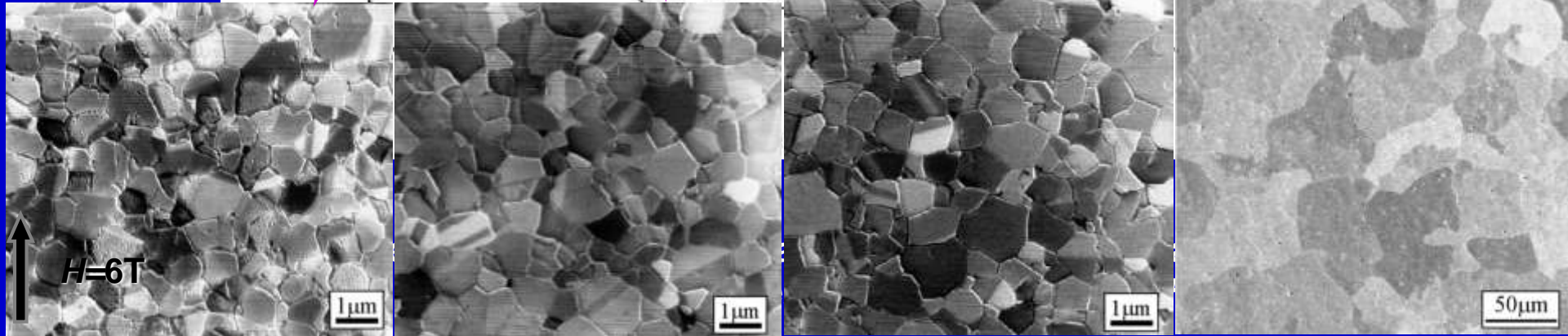
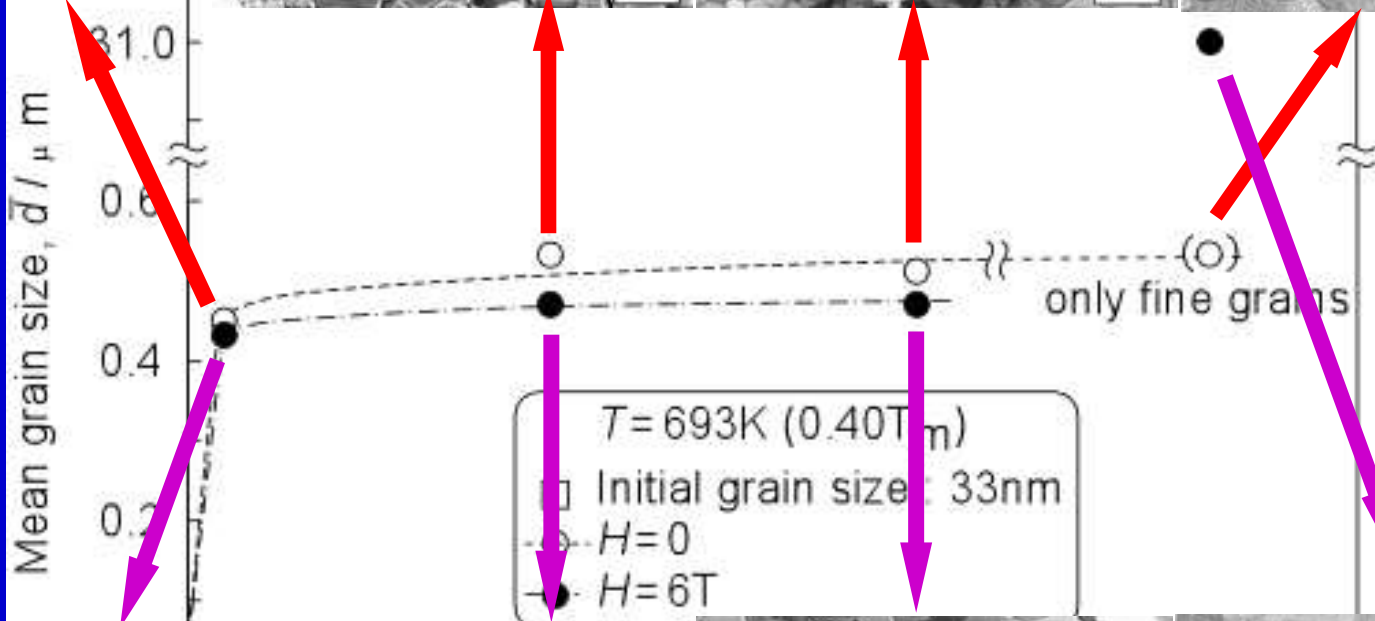
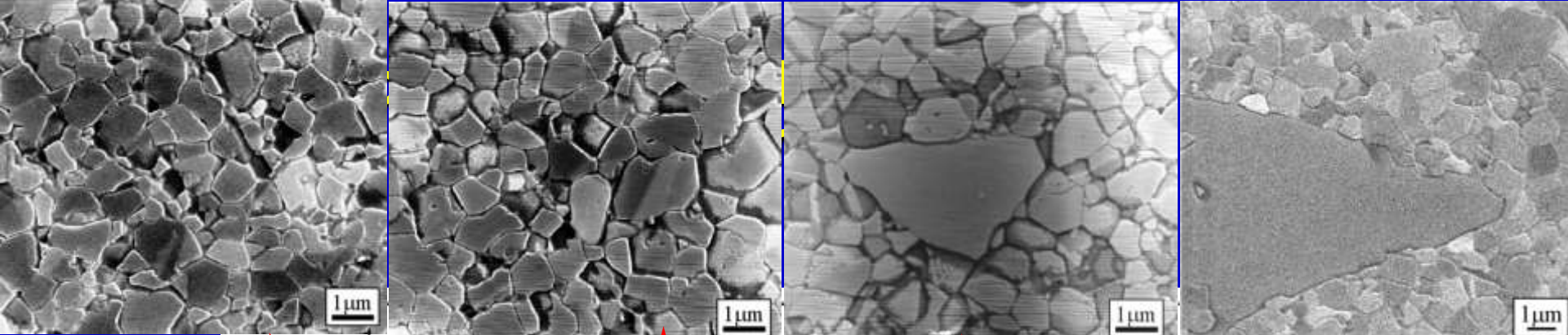
TEM Image and Diffraction Pattern for Nanocrystalline Ni.

Enhanced Homogeneity of Grain Size and GB Microstructure by Magnetic Annealing in Nanocrystalline Nickel

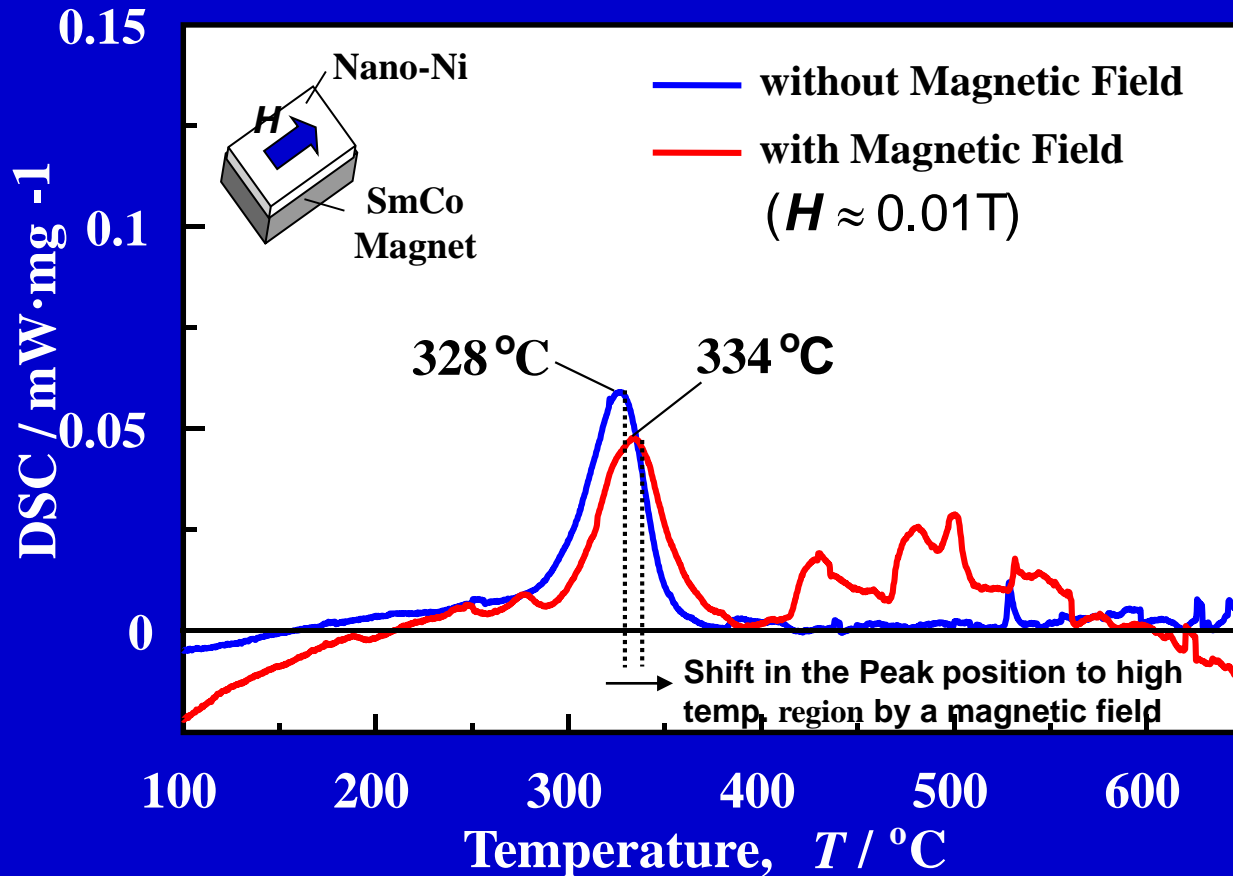
K. Harada, S. Tsurekawa, T. Watanabe, G. Palumbo, Scripta. Met., 49 (2003), 367-372.

SEM Micrographs of Nanocrystalline Nickel Annealed at 573K without and with an Applied Magnetic Field of 1.2MA/m.





Effect of a Magnetic Field on DSC Profiles Associated with Annealing in Nanocrystalline Nickel



$Q_{\text{exo}} = 6.4 \text{ J/g}$
(without a Magnetic Field)

$Q_{\text{exo}} = 5.4 \text{ J/g}$
(with a Magnetic Field)

Av. Grain Size
(After Exothermal Peak)

$\tilde{d} = 565 \text{ nm}$

$\tilde{d} = 680 \text{ nm}$

Initial Av. Grain Size: 40nm



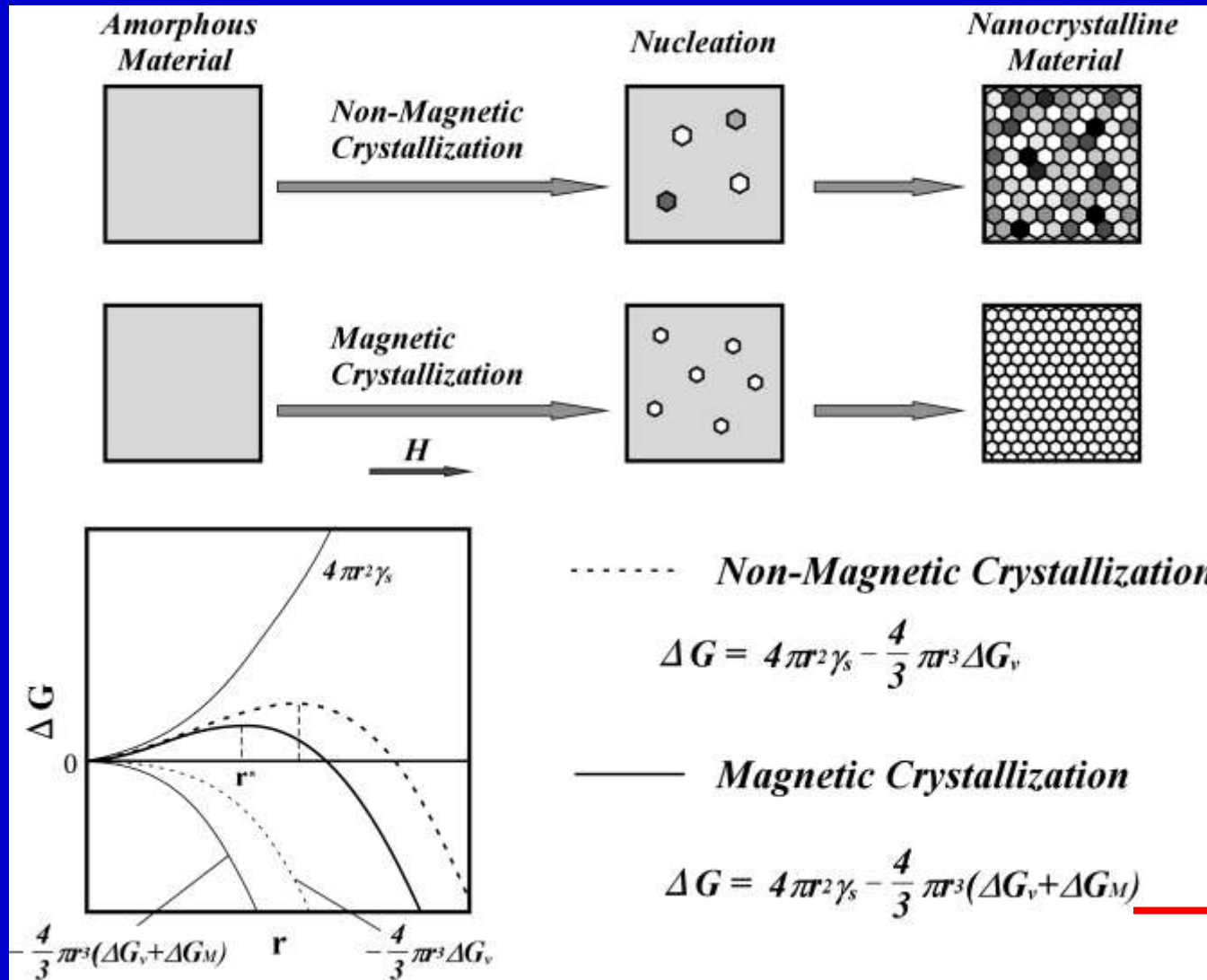
Decrease of GB Energy
in a Magnetic Field

Note: Thermal Stability in Nanocrystalline Nickel can be enhanced by Application of a Magnetic Field.

(Y.Ando, S.Tsurekekawa and T.Watanabe, Fall Meeting of JIM 11 ~ 13, (2003), Sapporo Japan.)

The Concept of Magnetic Crystallization in Amorphous Alloys for Ferromagnetic Nanocrystalline Material

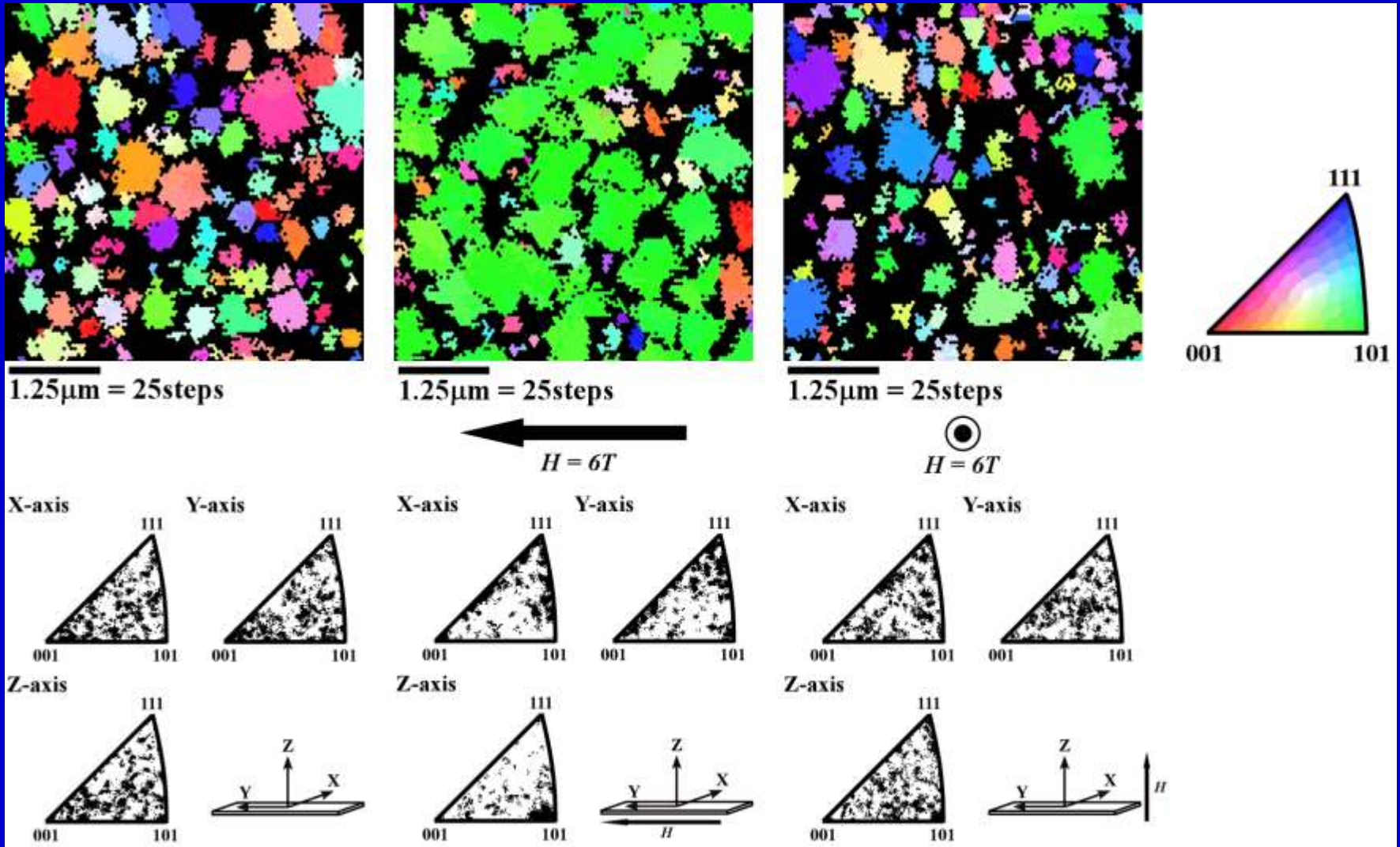
H. Fujii, S. Tsurekawa, T. Matsuzaki, T. Watanabe: Phil. Mag. Letters, 86 (2006),113-122.



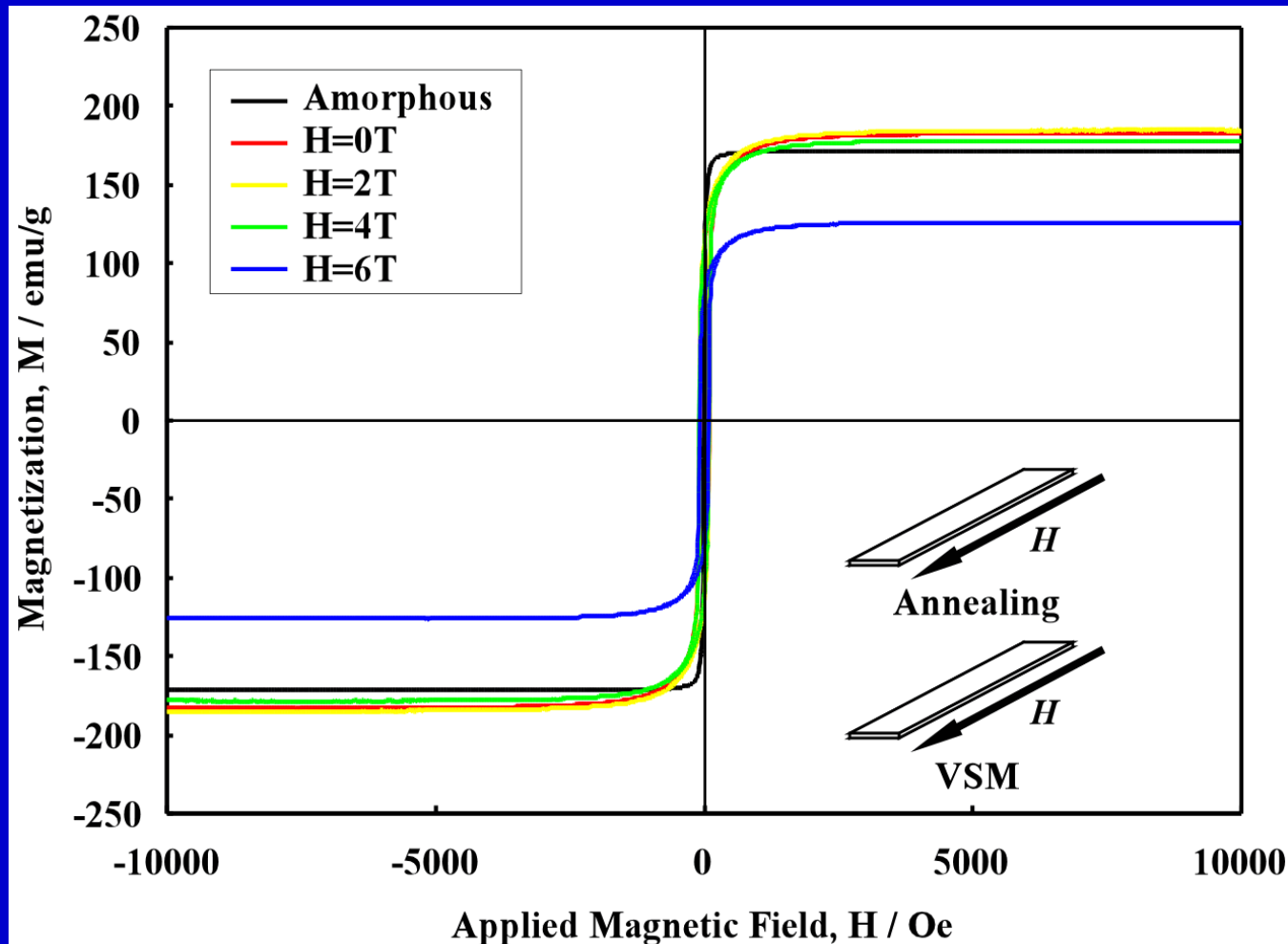
Magnetic Crystallization from Amorphous-state :

Fe₇₈Si₉B₁₃ Alloy Ribbons crystallized in Magnetic Field at 853 K for 1.8ks.

H. Fujii, S. Tsurekawa, T. Matsuzaki, T. Watanabe; Phil. Mag. Letters, 86 (2006),113-122.



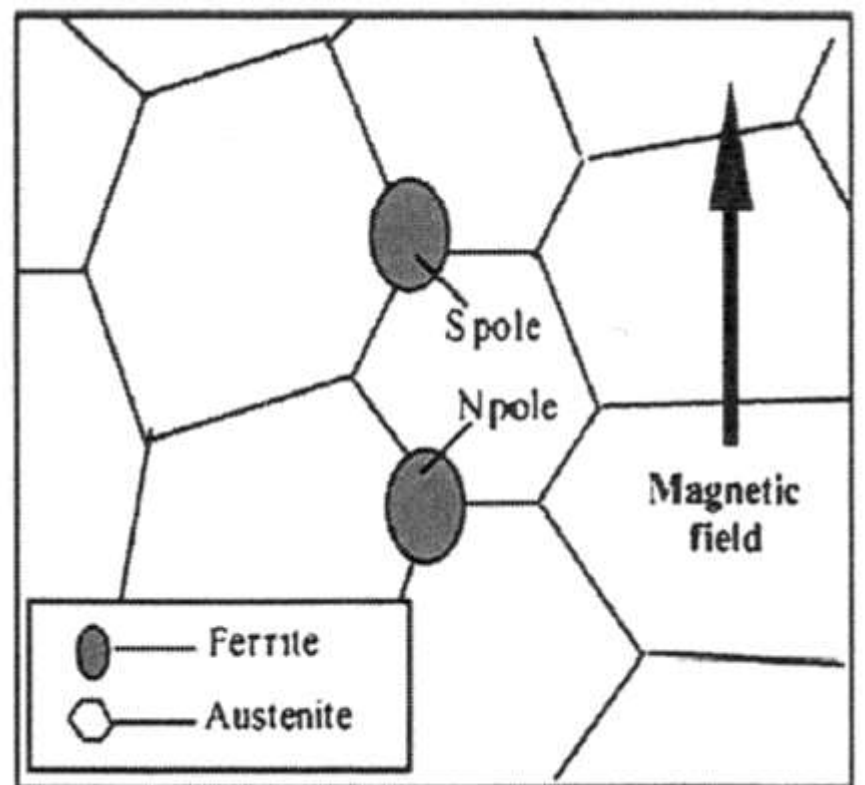
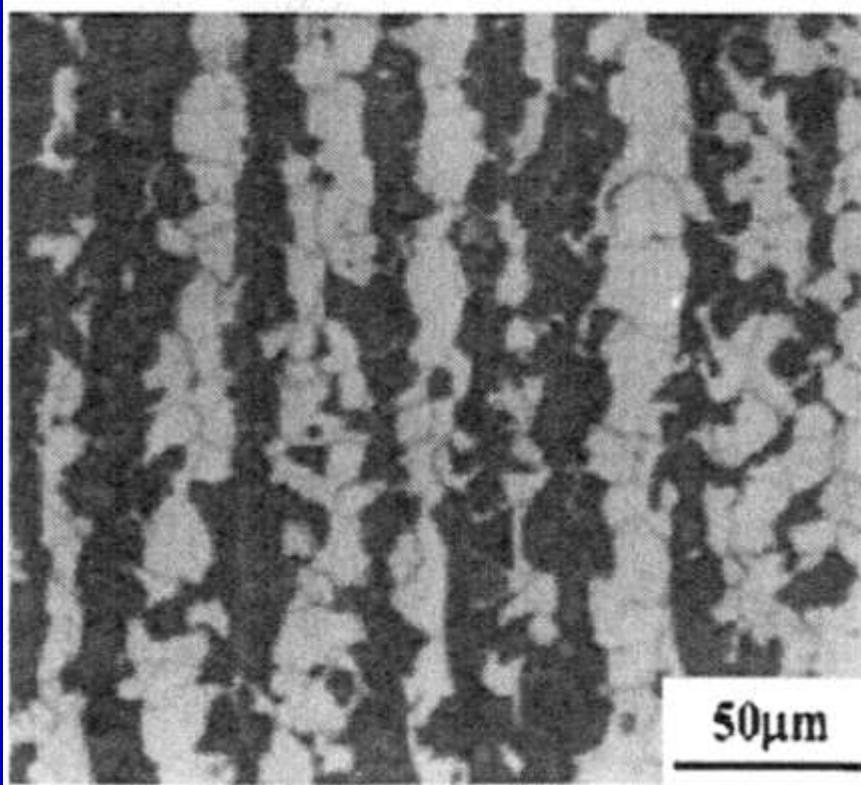
Magnetic Properties of Fe₇₈Si₉B₁₃ Ribbons produced by Magnetic Crystallization at 853 K.



H. Fujii, S. Tsunekawa, T. Matsuzaki, T. Watanabe; **Phil. Mag. Letters**, 86 (2006), 113-122, "Evolution of a sharp {110} texture in microcrystalline Fe₇₈Si₉B₁₃ during magnetic crystallization from the amorphous phase"

Directional Growth of Ferrite Grains nucleated at Triple Junctions during Cooling under a Magnetic Field.

Y. Zhang, C. He, X. Zhao, L. Zuo, C. Esling, J. He; *J. Mag. Mag. Mater.*, 284 (2004), 287.



(a)

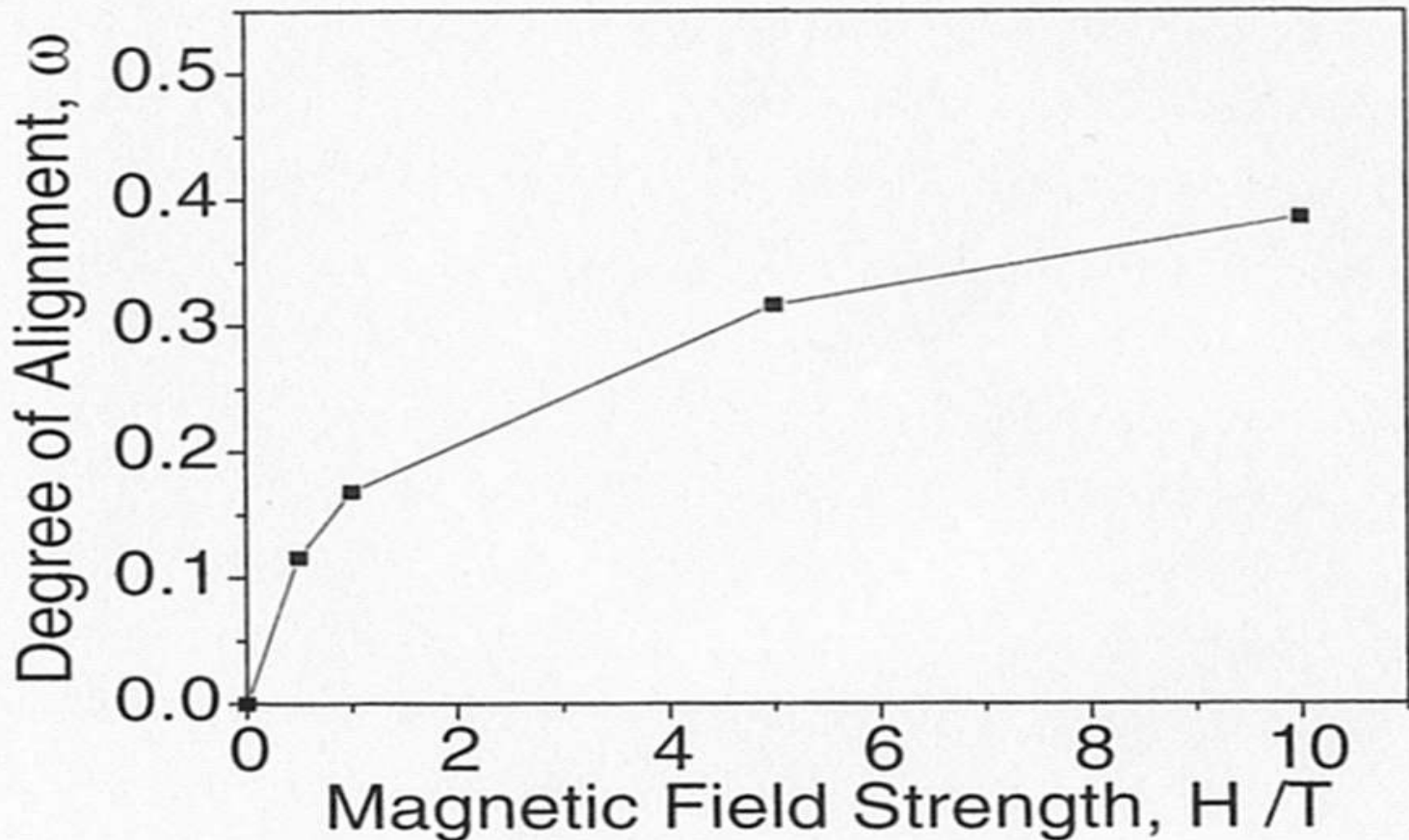
(b)

(a) Microstructure after Heating at $T=1153\text{K}$ for 33 min and Cooling at $10\text{ }^\circ\text{C}/\text{min}$ under $H=14\text{T}$, Bright area: Ferrite, Dark Area: Pearlite Colonies.

(b) Schematic Illustration of Nucleation of Ferrite Grains at Austenite Triple Junctions along the Magnetic Field Direction

Effect of Magnetic Field Strength, H, on Ferrite Elongation in Fe-0.4mass%C Alloy

After :H.J. Hao, H. Ohtsuka, P. de Rango, H. Wada; *Mater. Trans.*, 44(2003), 211-213,
“Quantitative Characterization of the Structural Alignment in Fe-0.4C Alloy Transformed in High Magn. Fields.”



Suppression Mechanism of Tin Segregation by External D.C. Magnetic Field

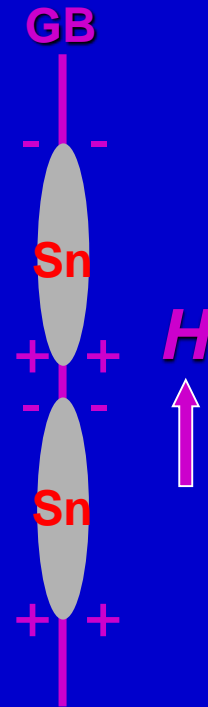
Magnetic Free Energy

For **Ferromagnetic** Material, U_f

$$U_f = -\mu_0 \left(H - \frac{NM_s}{2} \right) M_s$$

For **Paramagnetic** Material, U_p

$$U_p = -\frac{1}{2} \mu_0 \chi (1 - \chi N) H^2$$



M_s : Saturation Magnetization

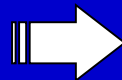
N : Demagnetizing Factor

H : Magnetic Field Strength

χ : Susceptibility

$|\chi| \ll 1$ for **paramagnetic** materials (Sn: 2.7×10^{-8})

$$U_p \gg U_f$$

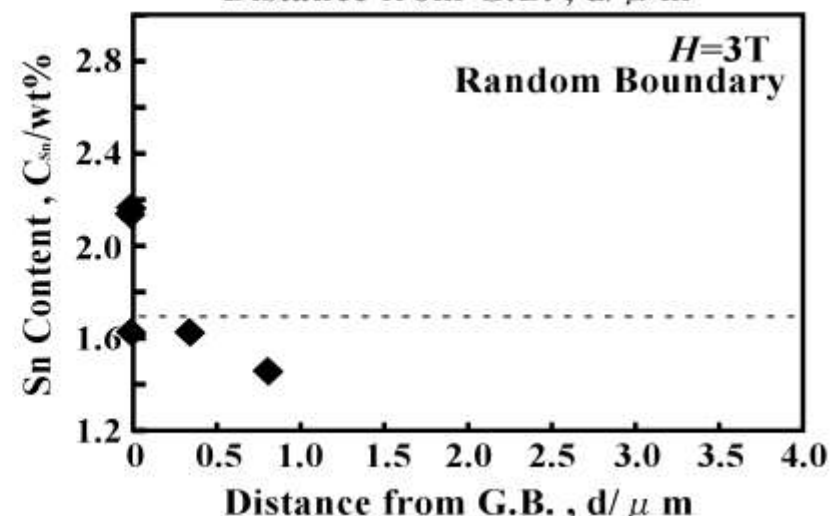
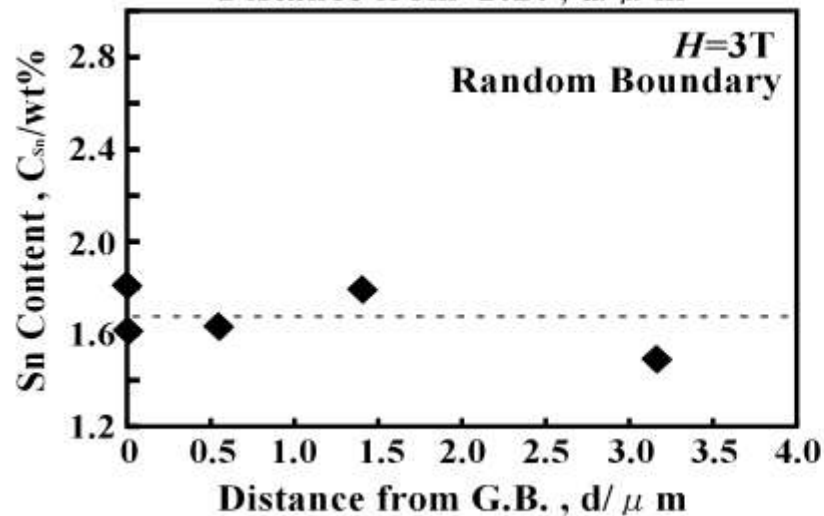
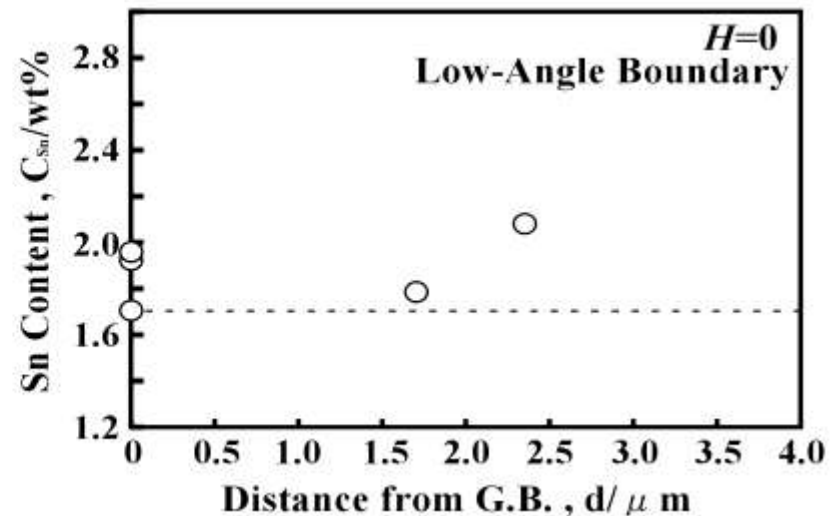
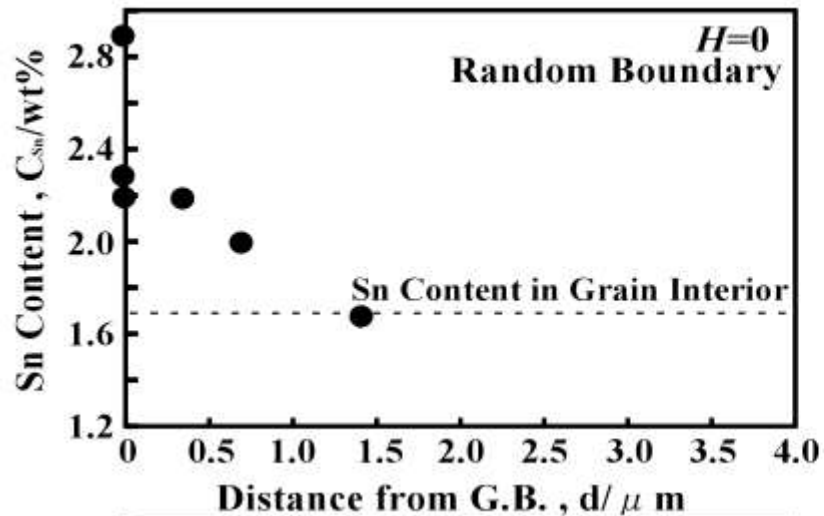


Sn atoms can be rejected from GBs to reduce magnetic free energy

Control of Segregation-induced Grain Boundary Brittleness in Fe-Sn Alloy by Magnetic Annealing

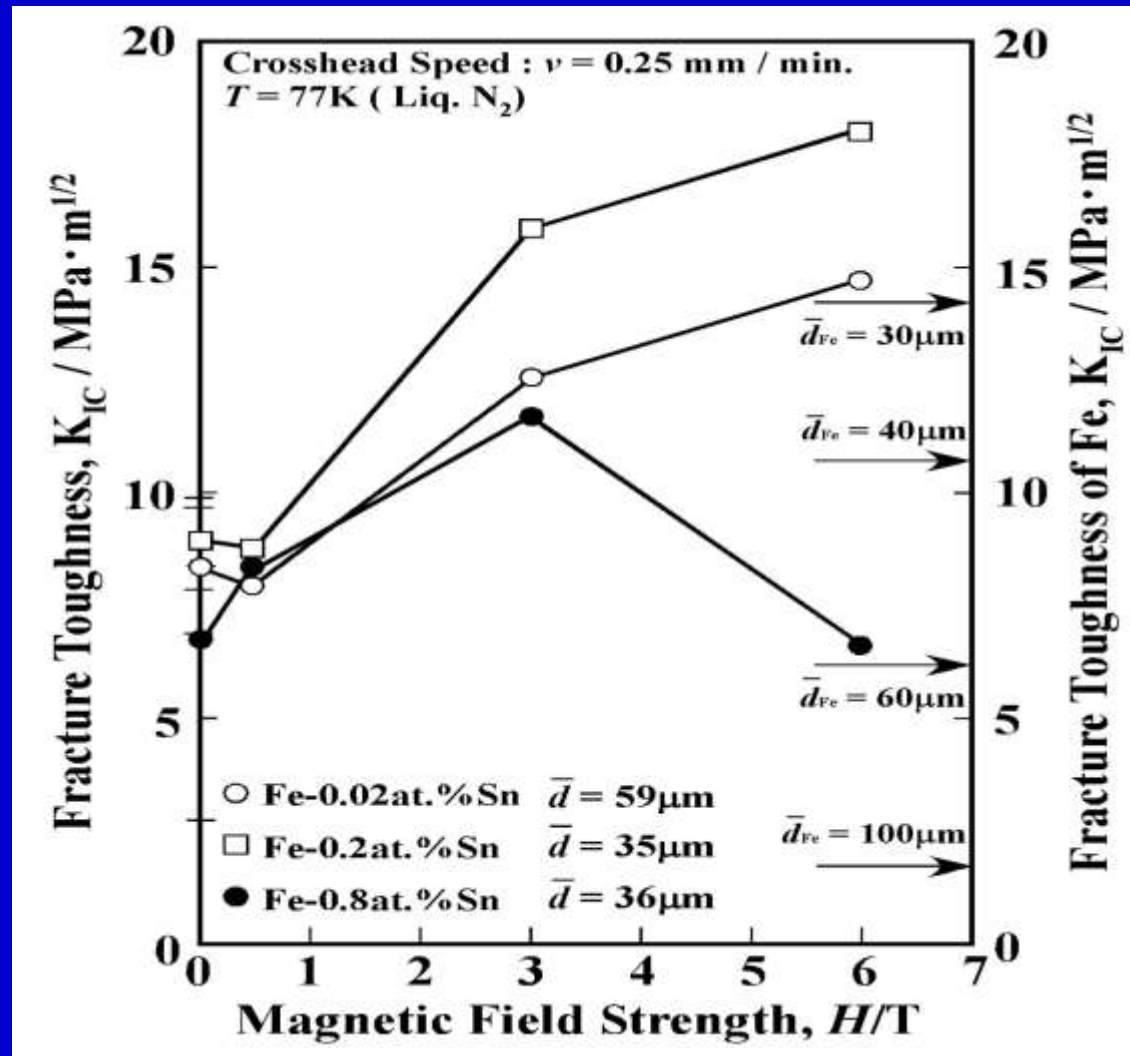
S. Tsunekawa, K. Kawahara, K. Okamoto, T. Watanabe, R. Faulkner;

Mater. Sci. Eng., A387-389 (2004), 442.



Grain Boundary Engineering for Control of Sn-induced Brittleness by Magnetic Field Application in Fe-Sn Alloys.

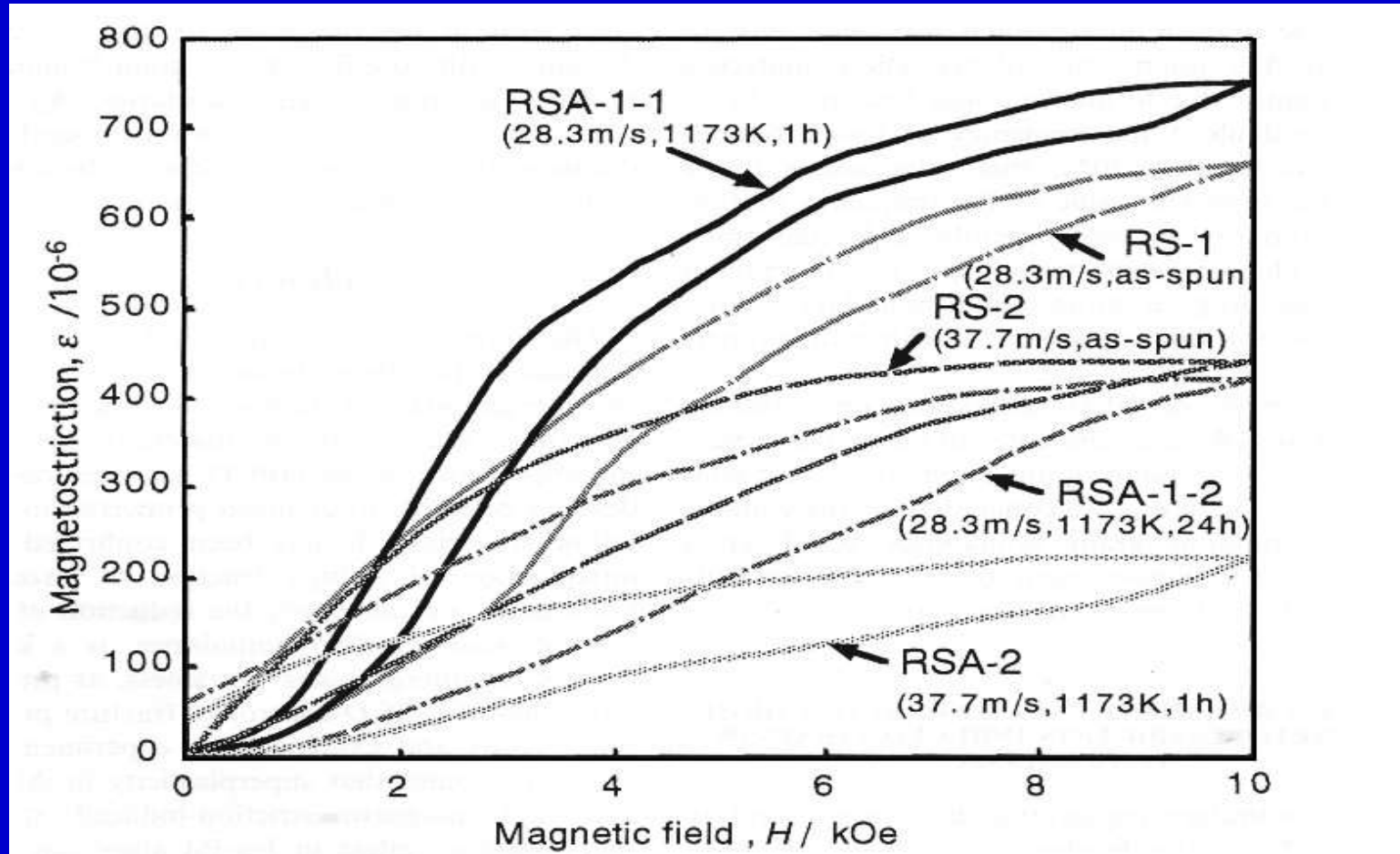
S. Tsurekawa, K. Okamoto, K. Kawahara, T. Watanabe; *J. Mater. Sci.*, 40 (2005), 895-901.



Grain Boundary Engineering for High Performance

“Ferromagnetic Fe-Pd Shape Memory Alloy”

“Magnetostriction vs Magnetic Field Strength Characteristics”



Fe-29.6 at.% Pd Ribbons rapidly Solidified and Annealed at 1173 K.

(Y. Huruya, N.W. Hagood, H.Kimura and T.Watanabe; Mat. Trans. JIM, 39 (1998), 1248-1254.)

Grain Boundary Character Distribution (GBCD) Controlled

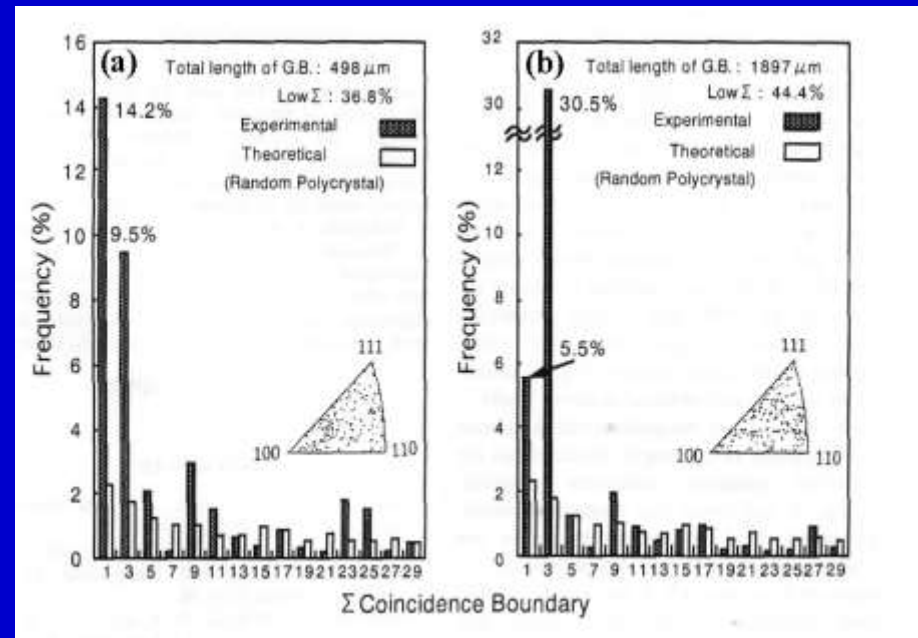
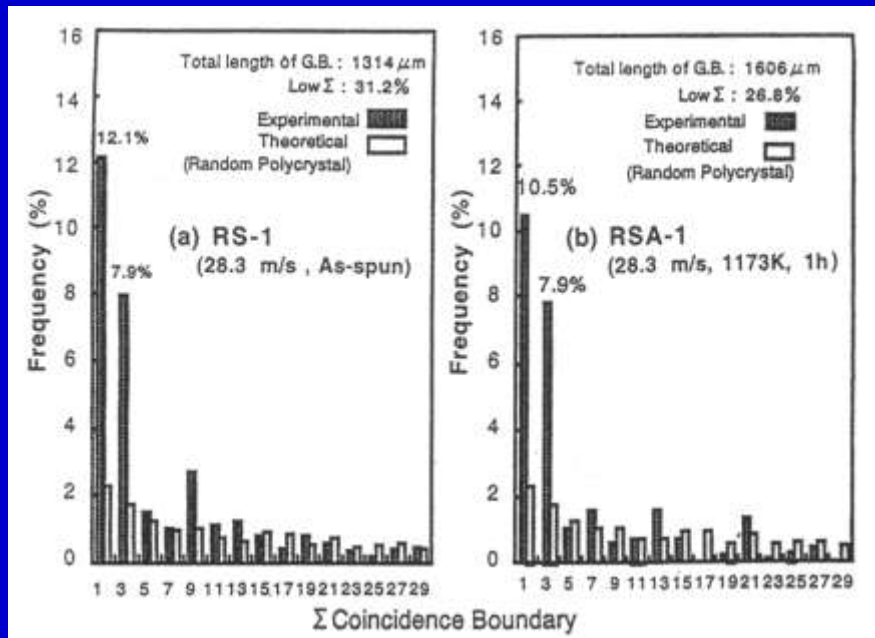
Magnetostriction in Fe-29.6 at.%Pd Shape Memory Alloy

As Solidified (RS-1), Annealed (RSA-1)

(Rapidly Solidified at 28.3m/s)

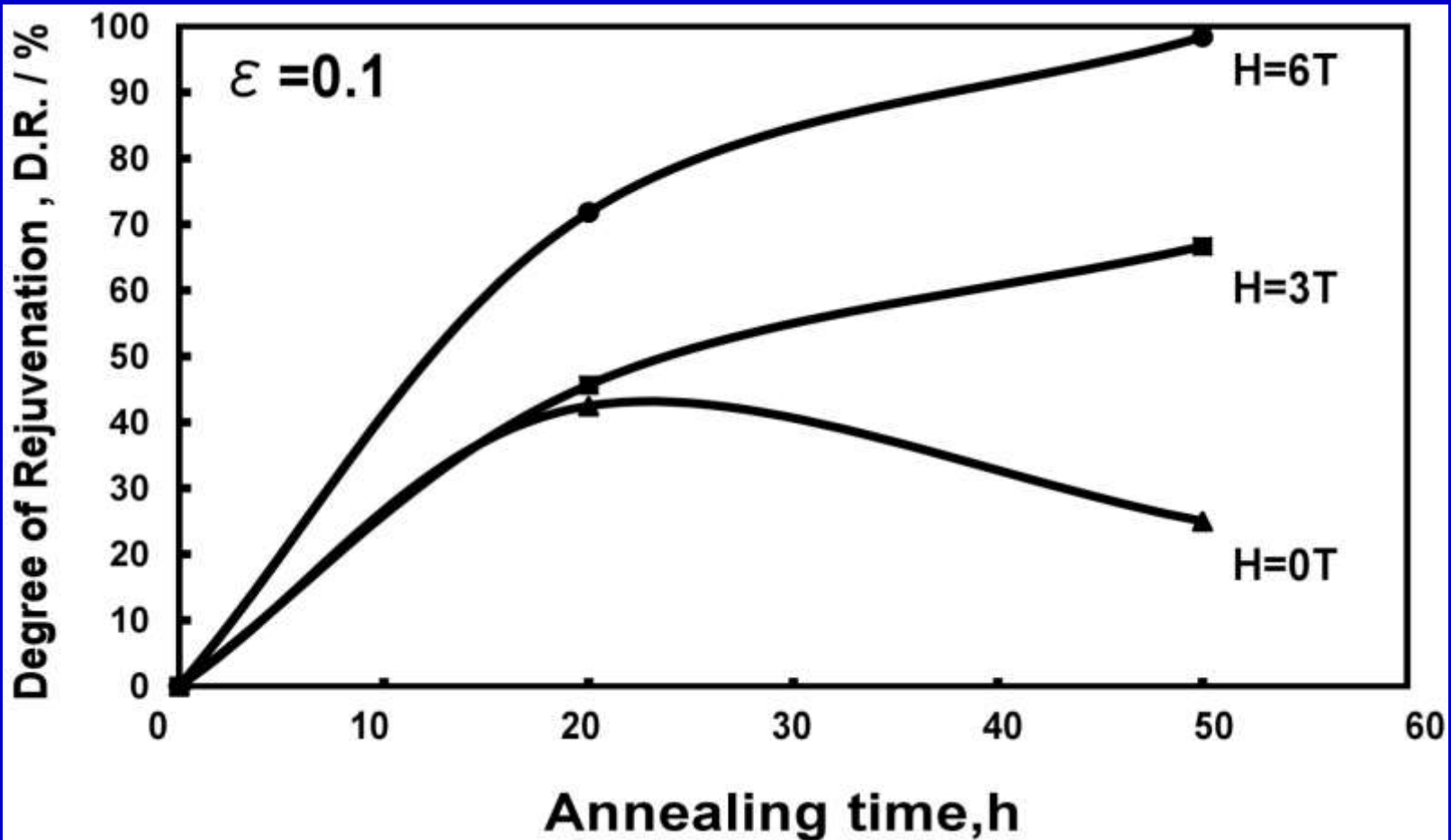
As solidified (RS-2), Annealed (RSA-2)

(Rapidly solidified at 37.3m/s)



Note: The presence of a high density of Σ 3 boundaries degrades the level magnetostriction in ribbon-shaped specimens of Fe-29.6 at.% Pd ferromagnetic shape memory alloy.

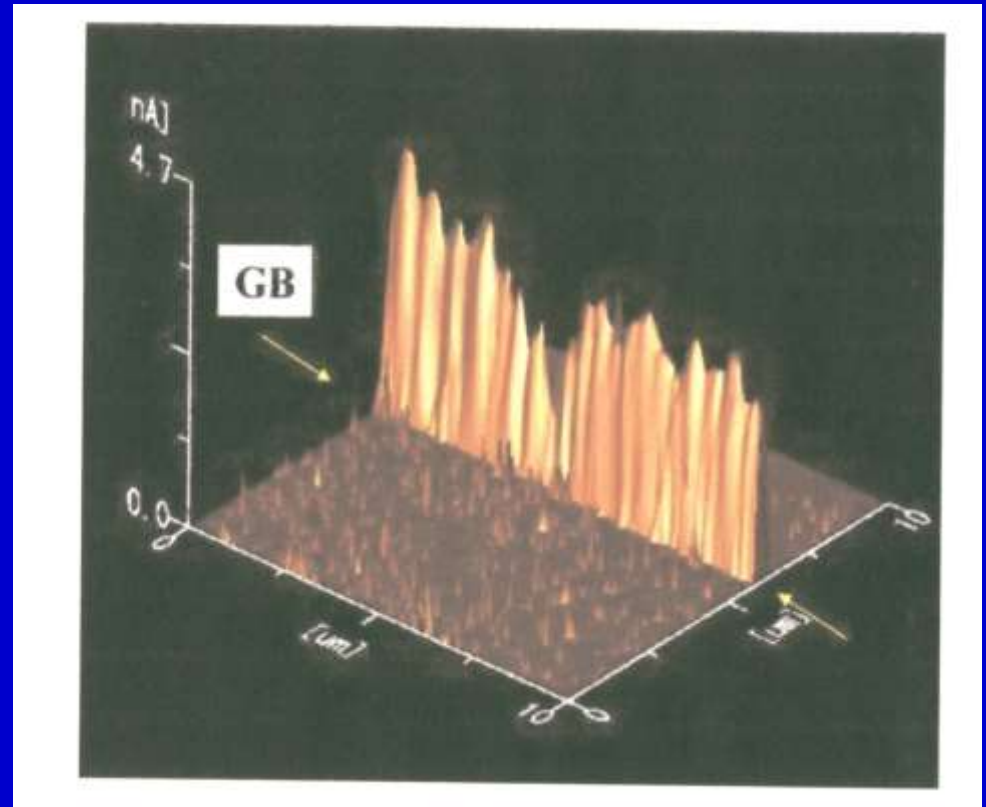
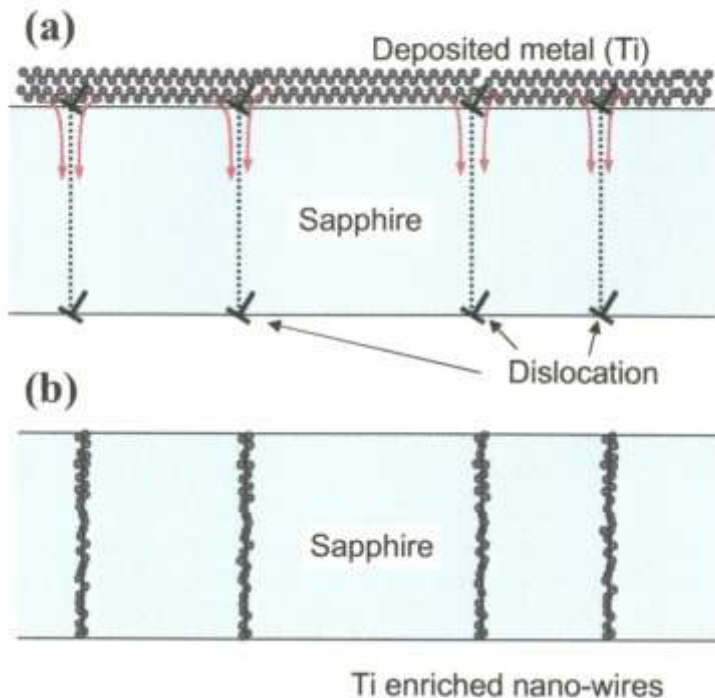
Rejuvenation of Deformation-Induced Cavities by Magnetic Annealing in Fe-Co Alloy (T=1023K)



**T. Watanabe, S. Nishizawa, S. Tsurekawa: *Complex Inorganic Solids*,
Proc. 3rd Intern. Alloy Conf. (IAC-3), Springer (2005), 327-336.**

Generation of A New Function attempted by “Dislocation and GB-Interface Engineering

Y. Ikuhara / *Progress in Materials Science* 54 (2009) 770–791



Y. Ikuhara: “Nanowire Design by Dislocation Technology”,
Progress in Materials Science, 54 (2009), 770-791.

Interface Engineering based on the Electronic Space Charge at Interphase Boundaries in Nanocomposite.

2009 Institute of Metals Lecture
The Minerals, Metals & Materials Society

Are There Ways to Synthesize Materials Beyond the Limits of Today?*



HERBERT GLEITER

A growing number of studies in recent years indicate that the preparation methods or the diagnostic tools developed in nanoscience and nanotechnology (NS/NT) may be used to synthesize materials beyond the limits of today. In this article, the following three kinds of materials synthesized by means of this approach are discussed. (1) Materials with tuneable atomic structures and densities. They are synthesized by introducing a high density of interfaces (*i.e.*, interfaces spaced a few nanometers) into glasses and by subsequently delocalizing the enhanced free volume associated with these interfaces. (2) The alloying of conventionally immiscible components in the form of solid solutions. The alloying process is achieved by generating nanocomposites of these immiscible components. Due to the electronic space charge associated with the resulting interphase boundaries, the electronic structure of the nanocomposites is modified in the vicinity of the interphase boundaries. This modification changes the mutual solubility of the components so that even components that are completely immiscible in the electrically neutral state (such as Ag and Fe) form solid solutions in the space charge regions.

Herbert Gleiter : Met. Mater. Trans., 40A (2009), 1499-1509

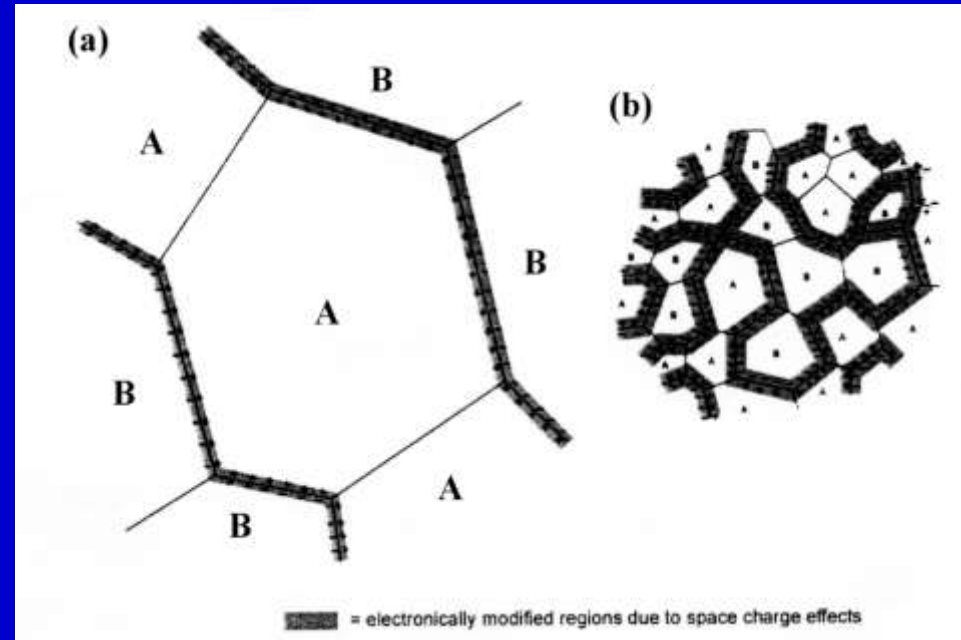
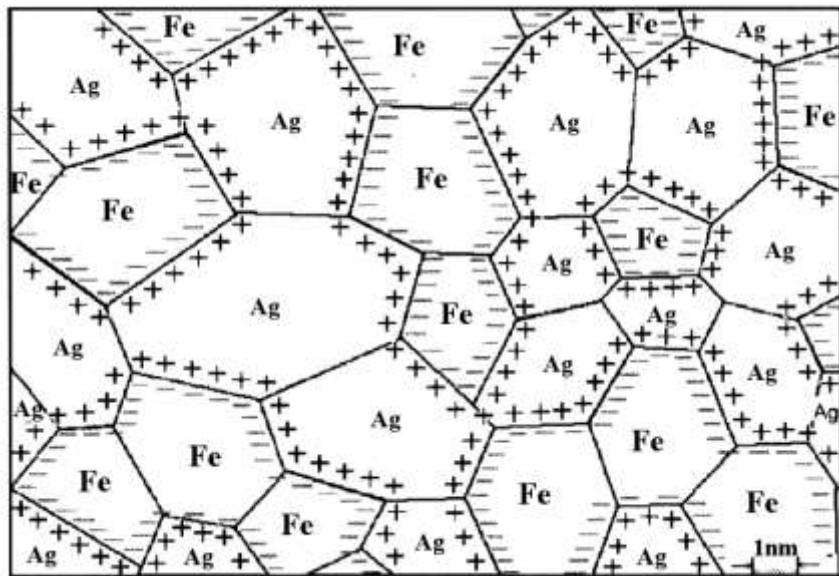
Possible Application of Grain Boundary Engineering to Functional Materials

“Is there a Hidden World of New Materials and Effects between the Elements of the Periodic Table ?”

Herbert Gleiter

Materials Transactions JIM, Vol.44 (2003), Mo.6 1057-1067

Nanostructured Functional Materials



Space Charge Distribution in a Nanocomposite consisting of nm-sized Ag and Fe Crystals. At the Heterophase Boundaries between Ag/Fe-Crystals Space Charge Regions are Formed.

(a) Space Charge Regions (Gray Areas) in a Metallic Polycrystal of A and B, the Crystal Size being Large in comparison to the width of the Space Charge Regions. (b) Space Charge Regions in a Metallic Nanocomposite of A and B.

Lecture on Grain Boundary & Interface Engineering
at Department of Materials Engineering, IISc, (No.3)
(on 20th November, 2015, Bangalore, India)

Part One: Grain Boundary & Interface Engineering
for Thin Film Materials.

Part Two: Nature-inspired Interface Engineering
for Living Biological Materials

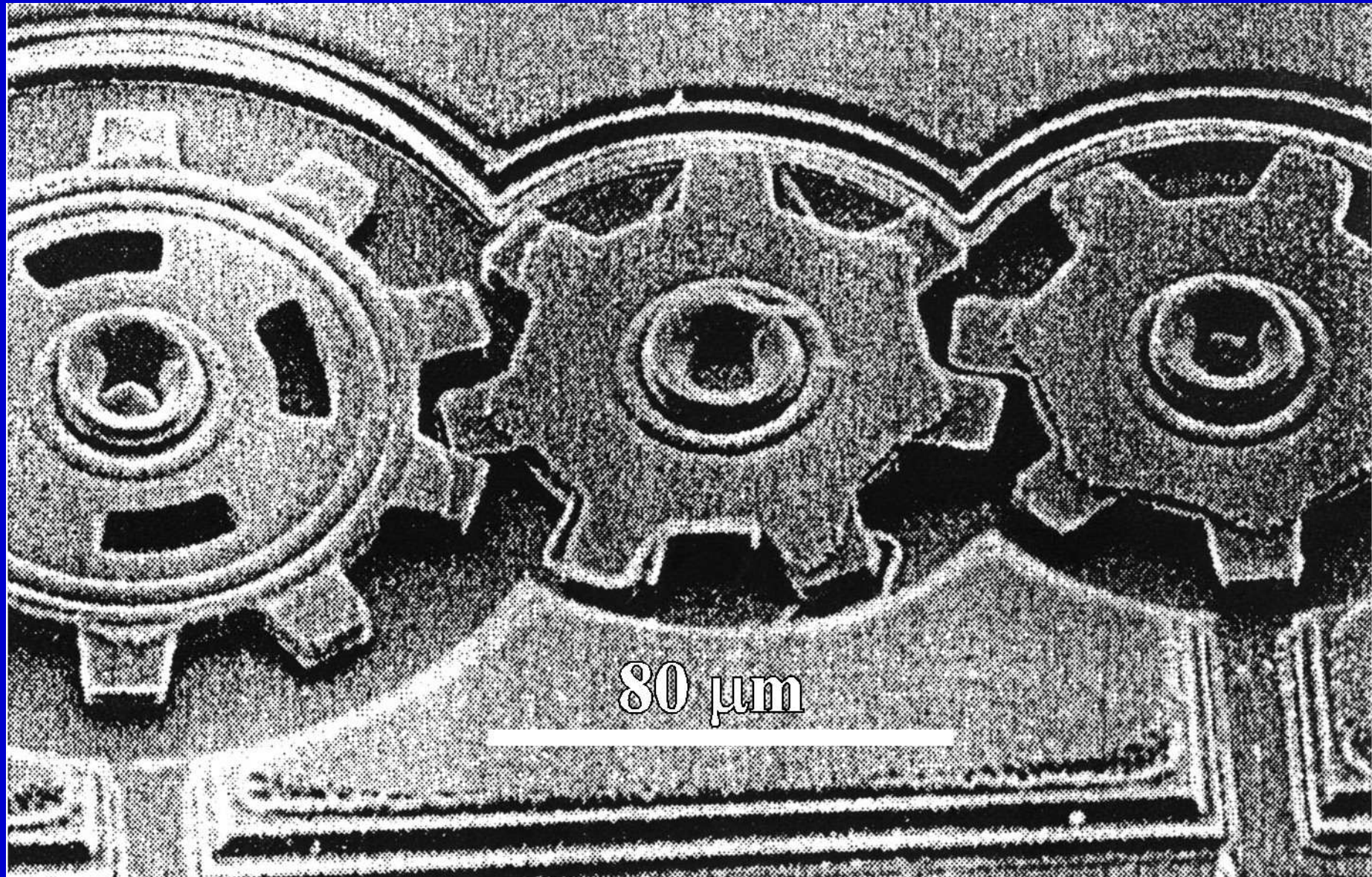
Tadao Watanabe

Lab. of Materials Design and Interface Engineering, Dept. of Nanomechanics,
Graduate School of Engineering, Tohoku University, Sendai, Japan
Guest Scientist, Key Laboratory of Anisotropy and Texture of Materials,
Northeastern University (NEU) , Shenyang, China.

.

Part One:
Grain Boundary & Interface Engineering
for Thin Film Materials.

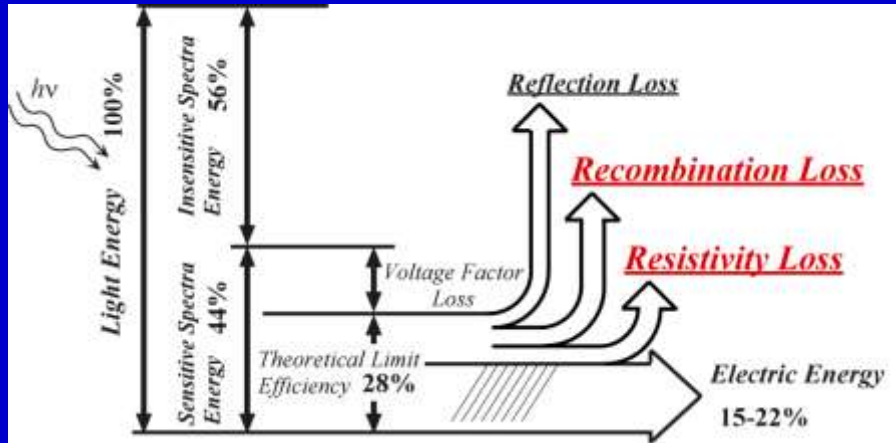
How to control the Microstructure in Polycrystals for a Micromechine ?



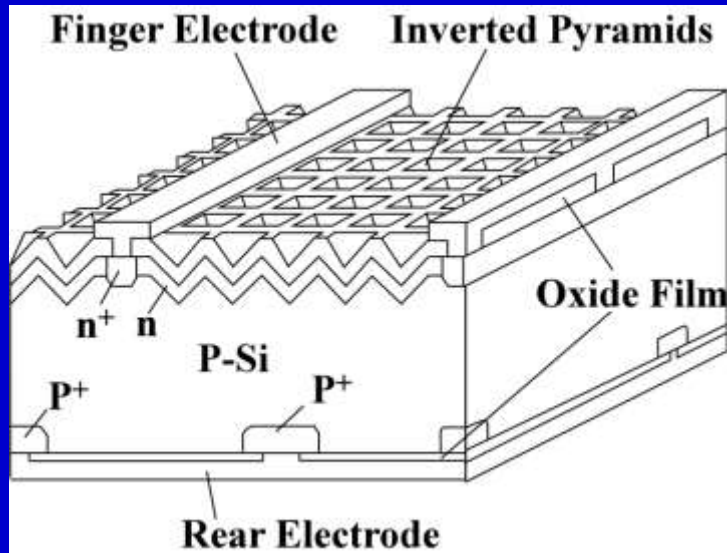
Polysilicon Gear Train with the Diameter from 128 ~ 185μm.

Si-based Solar Cell Energy Development

The Origin of Loss during Conversion

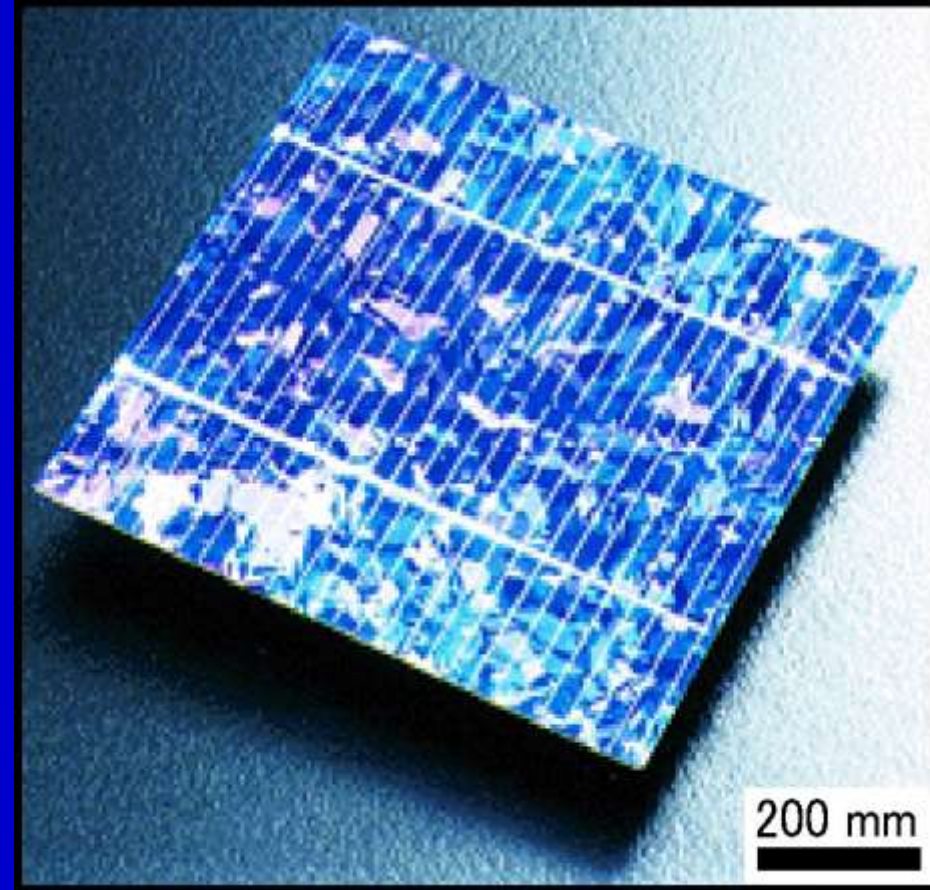


Solar Energy Conversion and Loss Factors.



Grain Boundaries act as ...

- Electron-Hole Recombination Sites
- Electrical Potential Barriers



Schematic Illustration of Silicon Solar Cell. Polycrystalline Silicon Solar Cell.

(A.Wang, *et al.* Appl. Phys. Lett., 57 (1990), 602.)

(Refer to SHARP company HP, 2001)

Possible Applications of GBE to Thin Films with Desirable Properties and High Performance

(Requirements for Thin Films and MEMS materials)

1. Grain Boundary Engineering for Thin Films & Ribbons.

- (1) Precise Microstructure Control for High Performance and Reliability.
- (2) Enhancement in Fracture Toughness. --- **W, Mo, Ceramics (Al_2O_3 , SiC, etc.)**
- (3) Improvement in Wear Resistance. --- **Diamond and Ceramic Coatings**
- (4) Enhancement in Corrosion Resistance.
- (5) Development of High Performance --- **Ferromagnetic Shape-memory Alloys**
- (6) High Performance Mechanical Flexibility for Polysilicon Solar Cells.

2. Grain Boundary & Interface Engineering for Electro-Magnetic Ceramics.

- (1) Generation of a New function & Multi-functionality.
- (2) Improvement of Performance of existing function and properties.
- (3) Control of Intrinsic Intergranular Brittleness.

Important Pending Issue of Processing Thin Films

“How to control “Abnormal Grain Growth” in Thin Films”

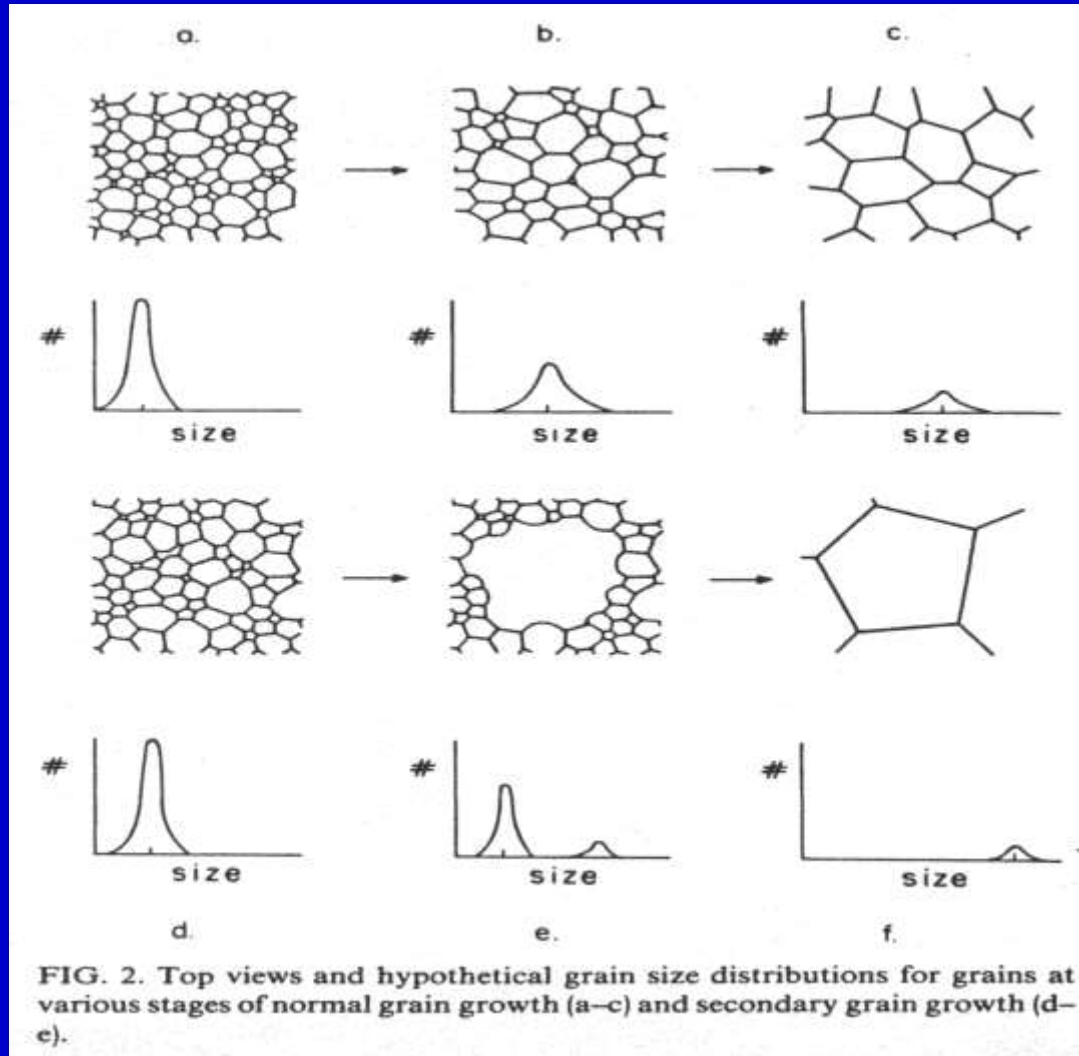
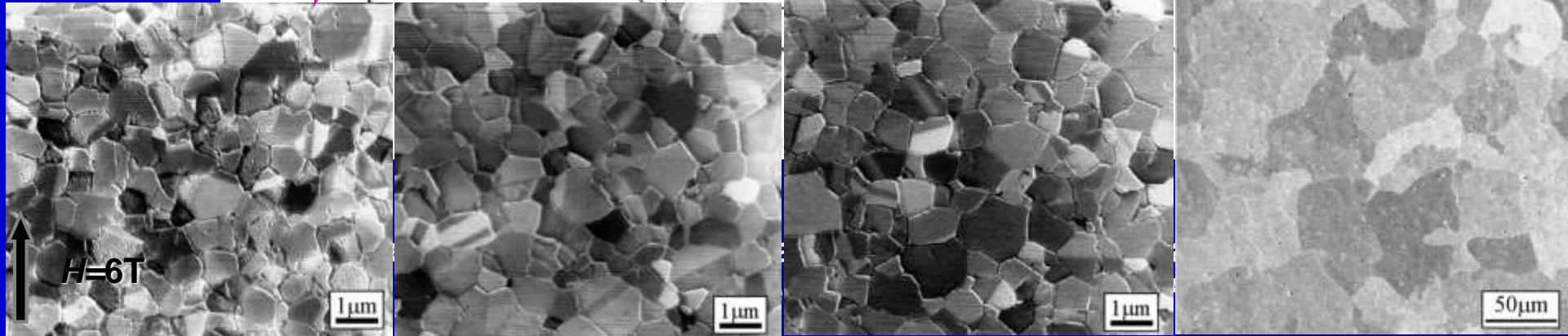
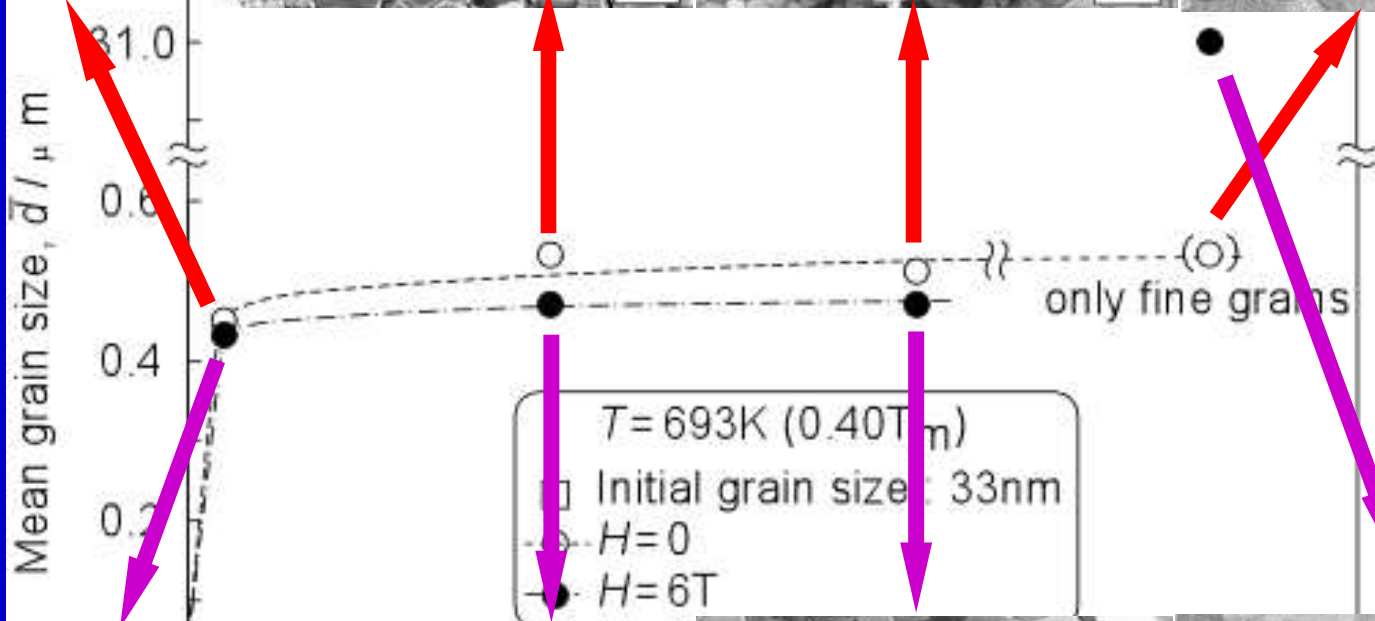
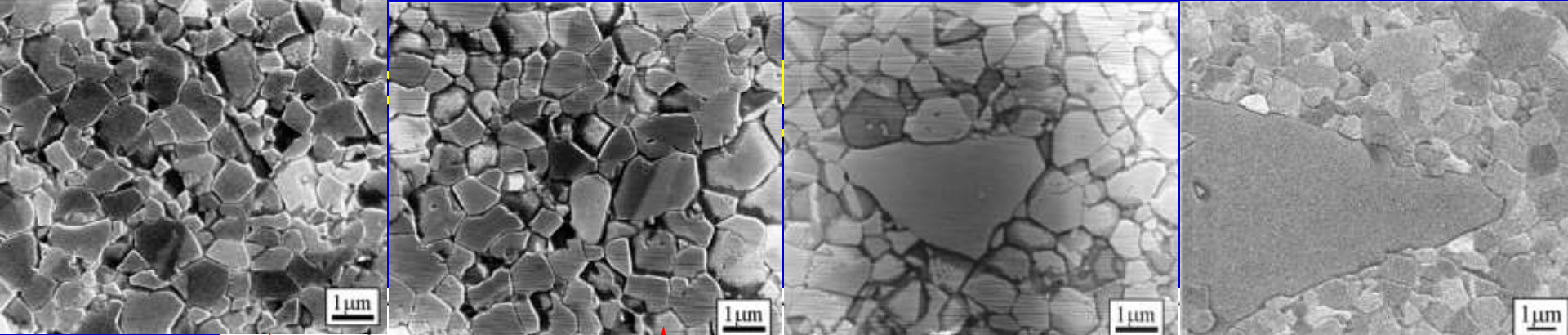


FIG. 2. Top views and hypothetical grain size distributions for grains at various stages of normal grain growth (a-c) and secondary grain growth (d-e).

C. V. Thompson; J. Appl. Phys., 58 (1985), 763-772.

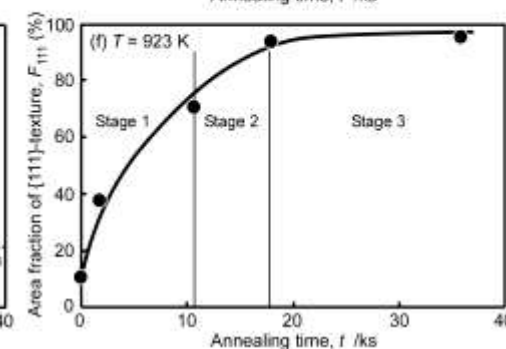
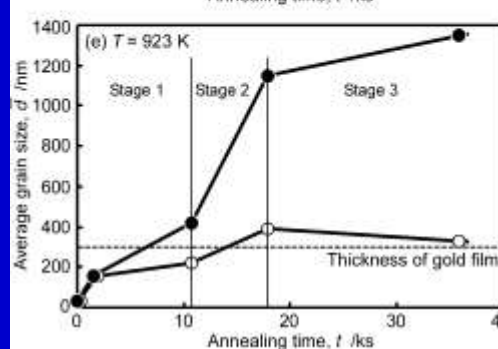
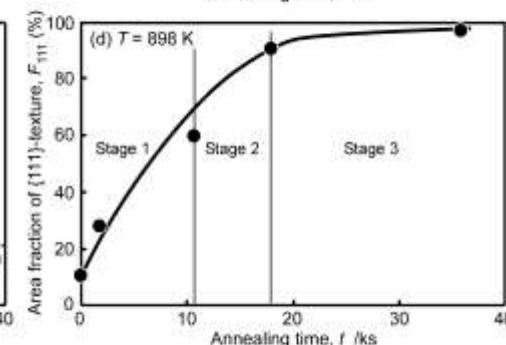
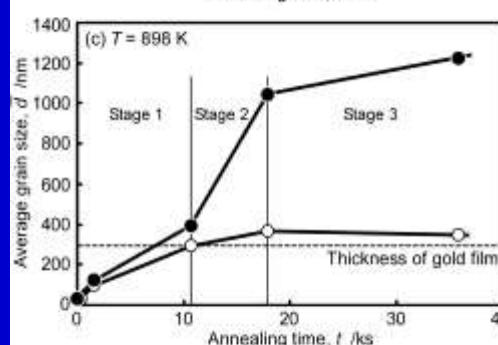
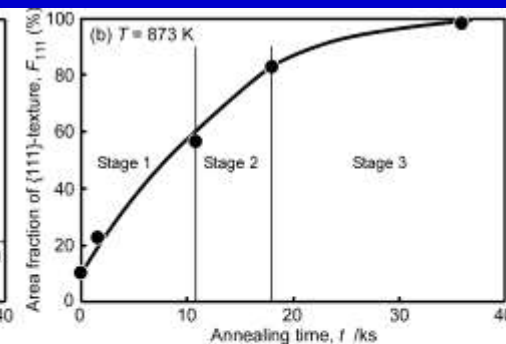
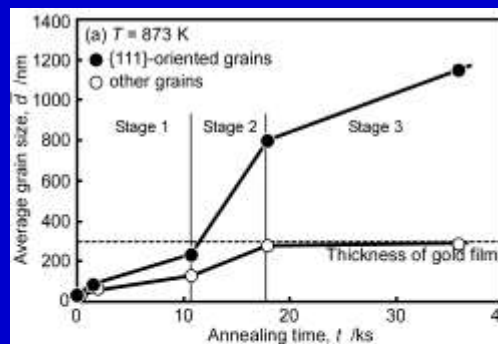
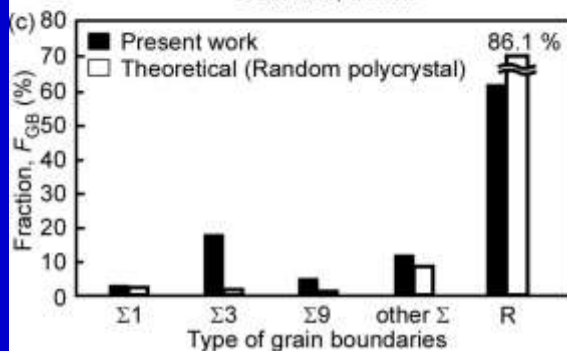
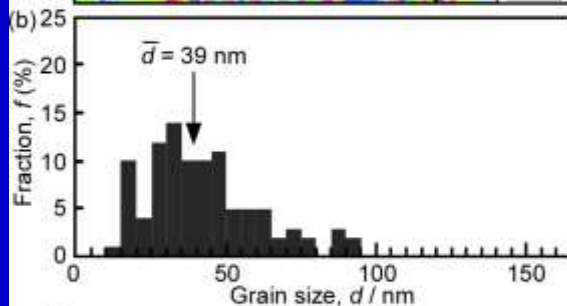
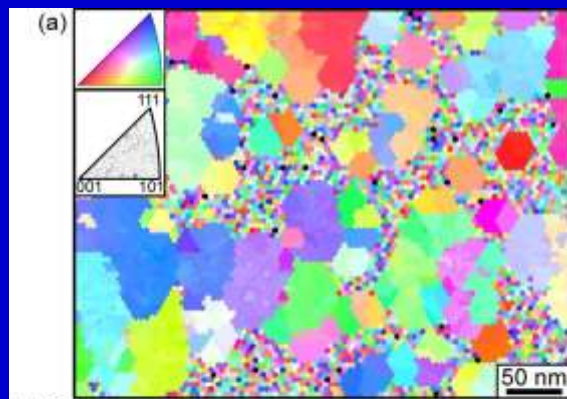


Grain Boundary Engineering through Texturing in Au Thin Films:

- Surface Energy-Driven Grain Growth and Texture Evolution -

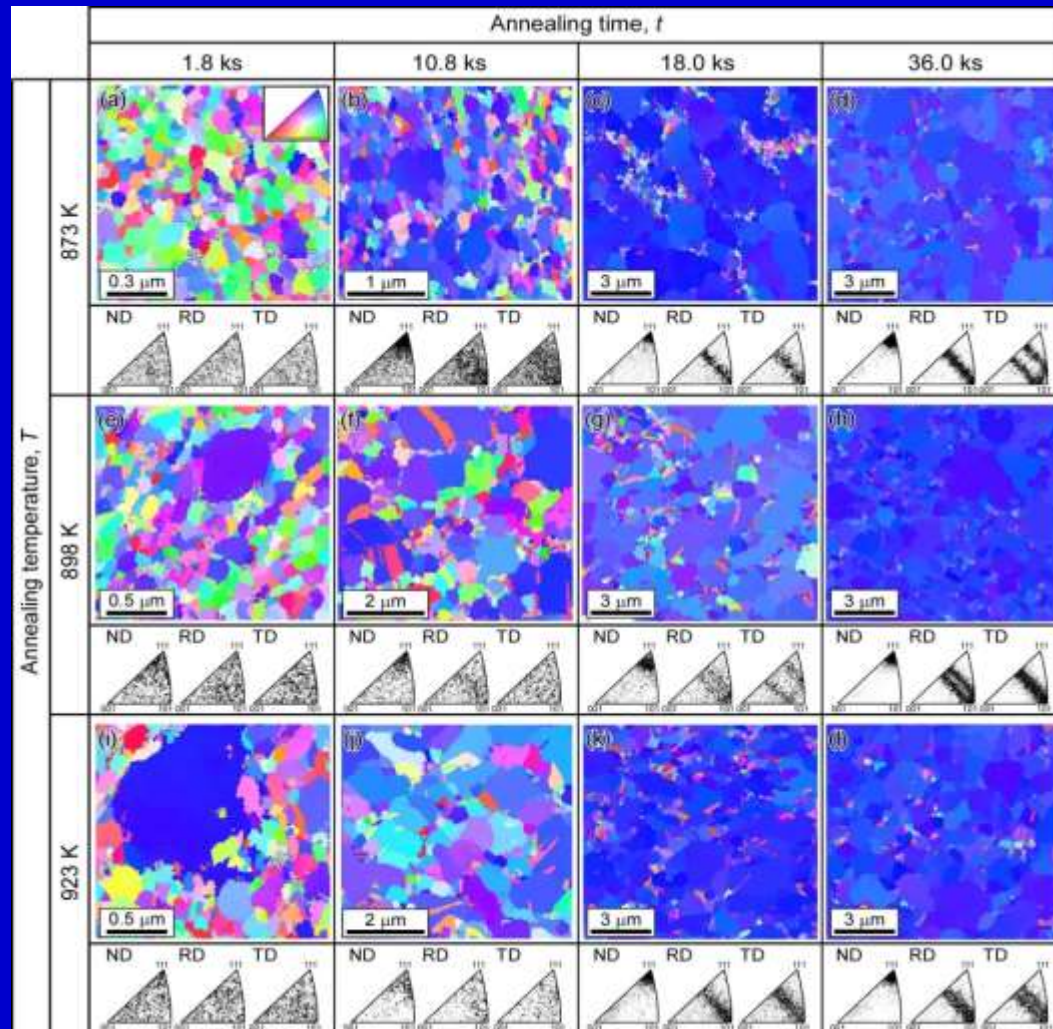
S. Kobayashi, H. Takagi, T. Watanabe: *Phil. Mag.*, (2013)

“Grain boundary character distribution and texture evolution during surface energy-driven grain growth in nanocrystalline gold thin films”



Grain Boundary Engineering through Texturing in Au Thin Films:

- Surface Energy-Driven Grain Growth and Texture Evolution-



S. Kobayashi, H. Takagi, T. Watanabe: Phil. Mag., (2013)

“Grain boundary character distribution and texture evolution during surface energy-driven grain growth in nanocrystalline gold thin films”

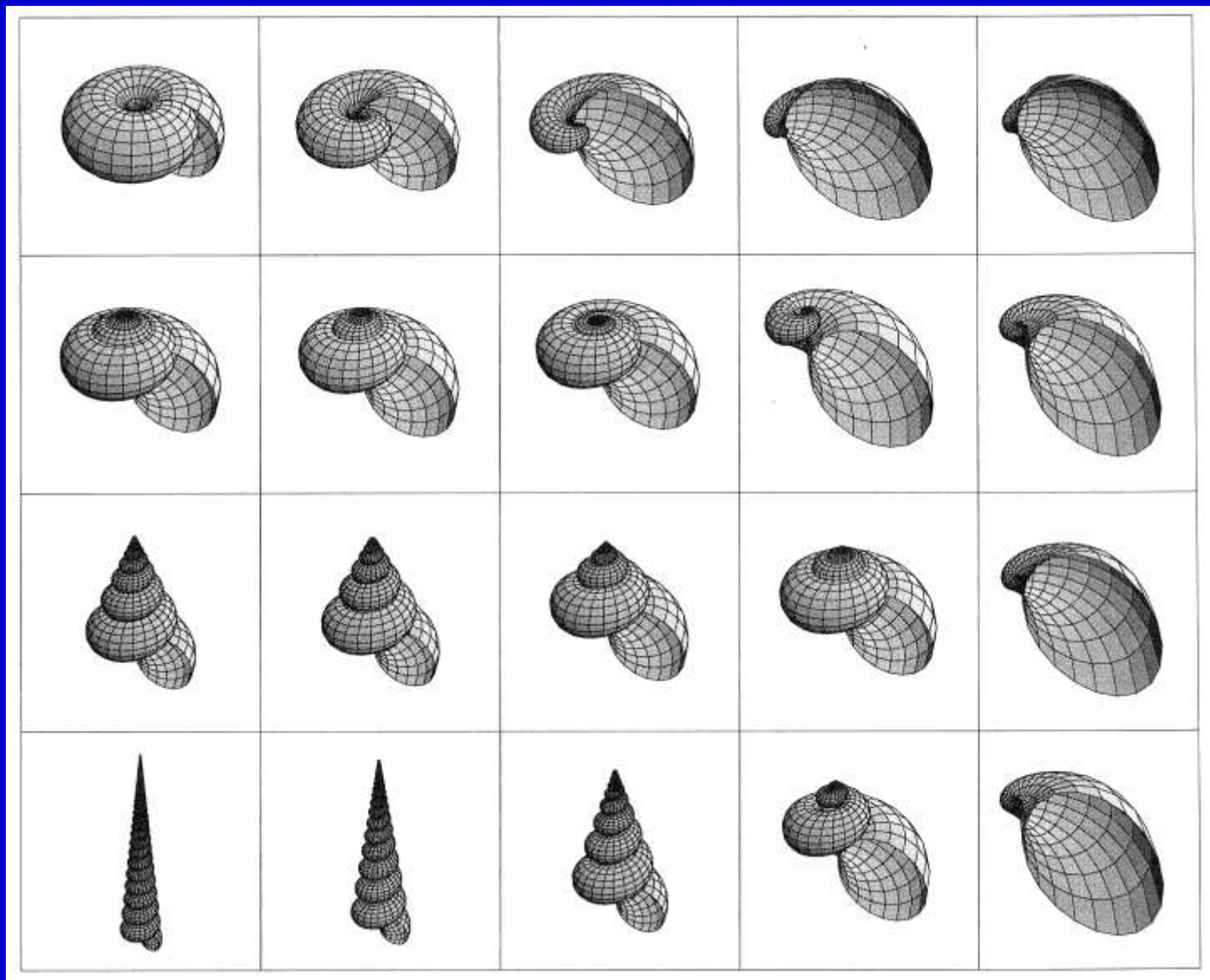
Pending Materials Problems to be solved by GBE in the 21st Century

1. Control of Brittle Fracture which inevitably brings a serious disaster to human society.
2. Highly reliable and long life Nuclear Reactor Material to be used for Safe Power Reactor.
3. High performance Photovoltaic Materials to convert clean Solar Energy to electricity.
4. Establishment of Interface Engineering for Recyclability of Used or Damaged Materials.
5. Development of a New Multi-functional Material.
6. Interface Engineering for Biological Materials.

Part Two:

Nature-inspired Interface Engineering for Living Biological Materials

- 1. Generation of Strong & Tough Materials from Soft & Weak Components.**
- 2. Generation of A New Function to be applied to Medical Field.**
- 3. Learning of Versatility of Shapes & Functions applicable to Interface Engineering.**



**Different Types of Shell Shape Found in Nature ; Folding and Coiled Structure.
(S.WOLFRAM, “A NEW KIND of SCIENCE”, Wolfram media Inc., 2002.)**

Literature Survey about a microstructure in shells

1. O. B.Boggild, **“The shell structure of the mollusks”**, K. Danske Vidensk. Selsk. Skr. Copenhagen, 2 (1930), 232.
2. J.D.CURREY and A.J.KOHN, **“Fracture in the crossed-lamellar structure of *Conus* shell”**, J. Mater. Sci. 11 (1976), 1615.
3. V. J. Laraia and A.H. Heuer, **“Novel Composite Microstructure and Mechanical Behavior of Mollusk Shell”**, J. Am. Ceram. Soc., 11 (1989), 2177.
4. N.V.WILMOT, D.J.BARBER, J.D.TAYLOR and A.L.GRANHAM, **“Electron microcopy of molluscan crossed-lamellar microstructure”**, Phil. Trans. R. Soc. Lond. B, 337 (1992), 21.
5. L.T.KUHN-SPEARING, H.KESSLER, E.CHATEAU, R.BALLARINI, A.H.HEUER and S.M.SPEAEING, **“Fracture mechanisms of the *Strombus gigas* conch shell: implications for the design of brittle laminates”**, J. Mater. Sci., 31 (1996), 6583.
6. S.WEINER and L.ADDADI, **“Design strategies in mineralized biological materials”**, J. Mater. Chem., 7(5) (1997), 689.
7. D.CHATEIGNER, C.HEDEGAARD and H.-R.WENK, **“Mollusc shell microstructure and crystallographic textures”**, J. Structural Geology, 22 (2000), 1723.
8. Q.L.FENG, F.Z.CUI, G.PU, R.Z.WANG and H.D.LI, **“Crystal orientation, toughening mechanisms and a mimic of nacre”**, Mater. Sci. Eng., C11 (2000), 19.
9. R.Z.WANG, Z.SUO, A.G.EVANS, N.YAO and I.A.AKASY, **“Deformation mechanisms in nacre”**, J. Mater. Res., 16 (2001), 2485.
10. A.G.EVANS, Z.SUO, R.Z.WANG, I.A.AKASY, M.Y.HE and J.W.HUTCHISON, **“Model for the robust mechanical behavior of nacre”**, J. Mater. Sci., 16 (2001), 2475.
11. H.TONG, J.HU, W.MA, G.ZHONG, S.YAO and N.CAO, **“In situ analysis of the organic framework in the prismatic layer of mollusc shell”**, Biomaterials, 23 (2002), 2593.
12. F.SONG, X.H.ZHNG and Y.L.BAI, **“Microstructure and characteristics in the organic matrix layers of nacre”**, J. Mater. Res., 17 (2002), 1567.

Fracture in the crossed-lamellar structure of *Conus* shells

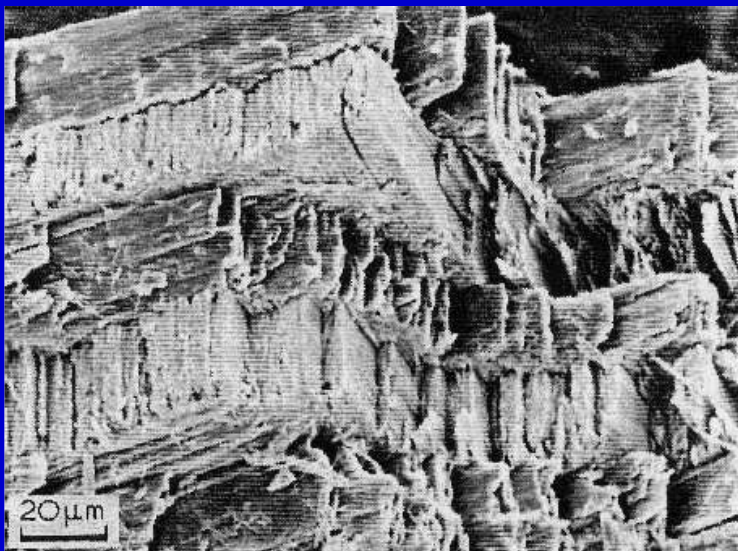
J.D.CURREY

Department of Biology, University of York, York, UK

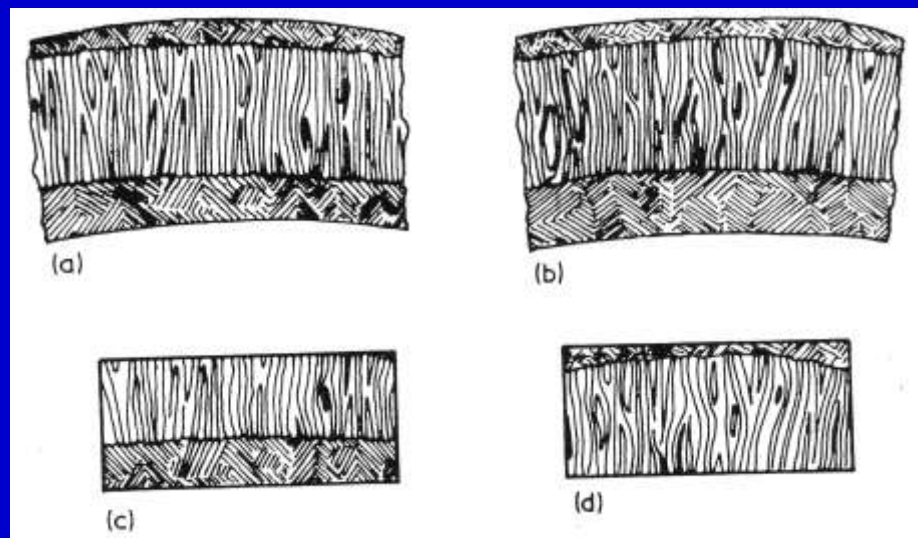
A.J.KOHN

Department of Zoology, University of Washington, Seattle, Washington USA

Crossed-lamellar crystal architecture is the characteristic textural pattern of the calcium carbonate shell in many kinds of molluscs. By loading specimens from shells of the genus *Conus* in various orientations in bending tests it is shown that crossed-lamellar structure is highly anisotropic. This anisotropy is to be expected from the microscopic and submicroscopic structure, particularly the substructure of the primary lamellae and their orientation to one another, and from the paths taken by cracks travelling through layers of different orientation.



Fracture surface of crossed-lamellar structure.



Schematic of the **three layers structure** of the *Conus* shell.

Our Microstructural and Mechanical Study on Japanese hard Clam (“Hamaguri”)

Motivation and Questions

- 1. Why many types of shells can be robust and tough to fracture, while they are composed of intrinsically weak aragonite (calcium carbonate) ?**
- 2. How can we toughen brittle materials like ceramics through control of interfacial microstructure in biological materials, nature-inspired Interfacial Engineering ?**

Well-Assembled and Crossed-lamellar Microstructure **for Robust Mechanical Properties** **of Bioceramic Shell Structure**

Tadao WATANABE, Kota KIDO and Sadahiro TSUREKAWA

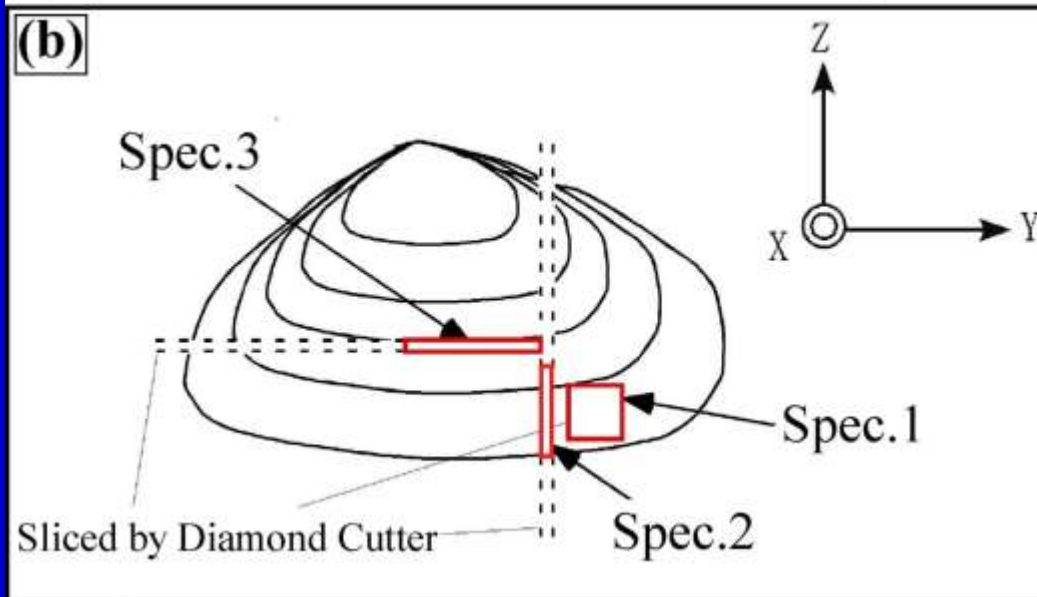
Laboratory of Materials Design and Interface Engineering

Department of Machine Intelligence and Systems Engineering

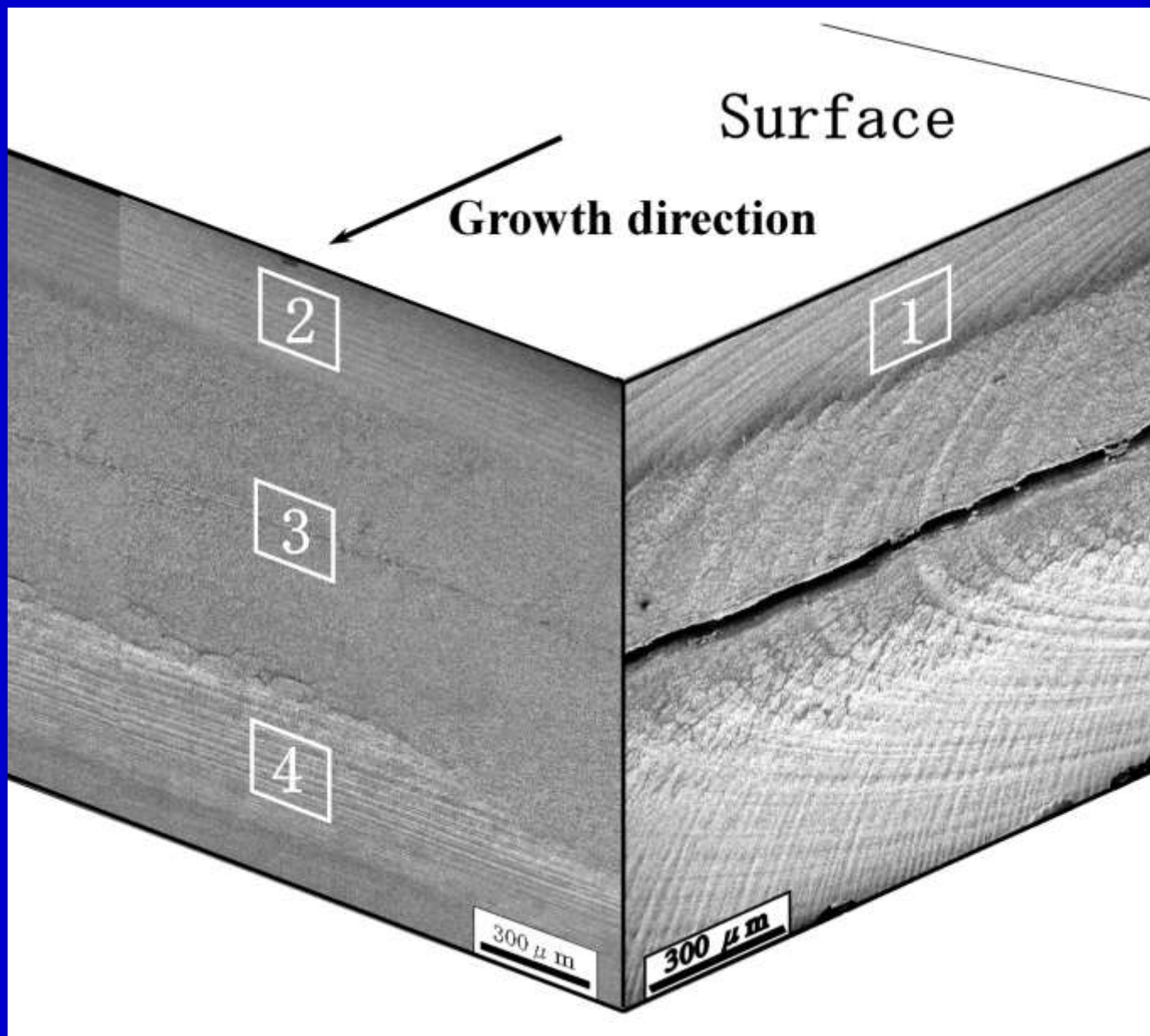
Graduate School of Engineering, Tohoku University, Japan

Outline

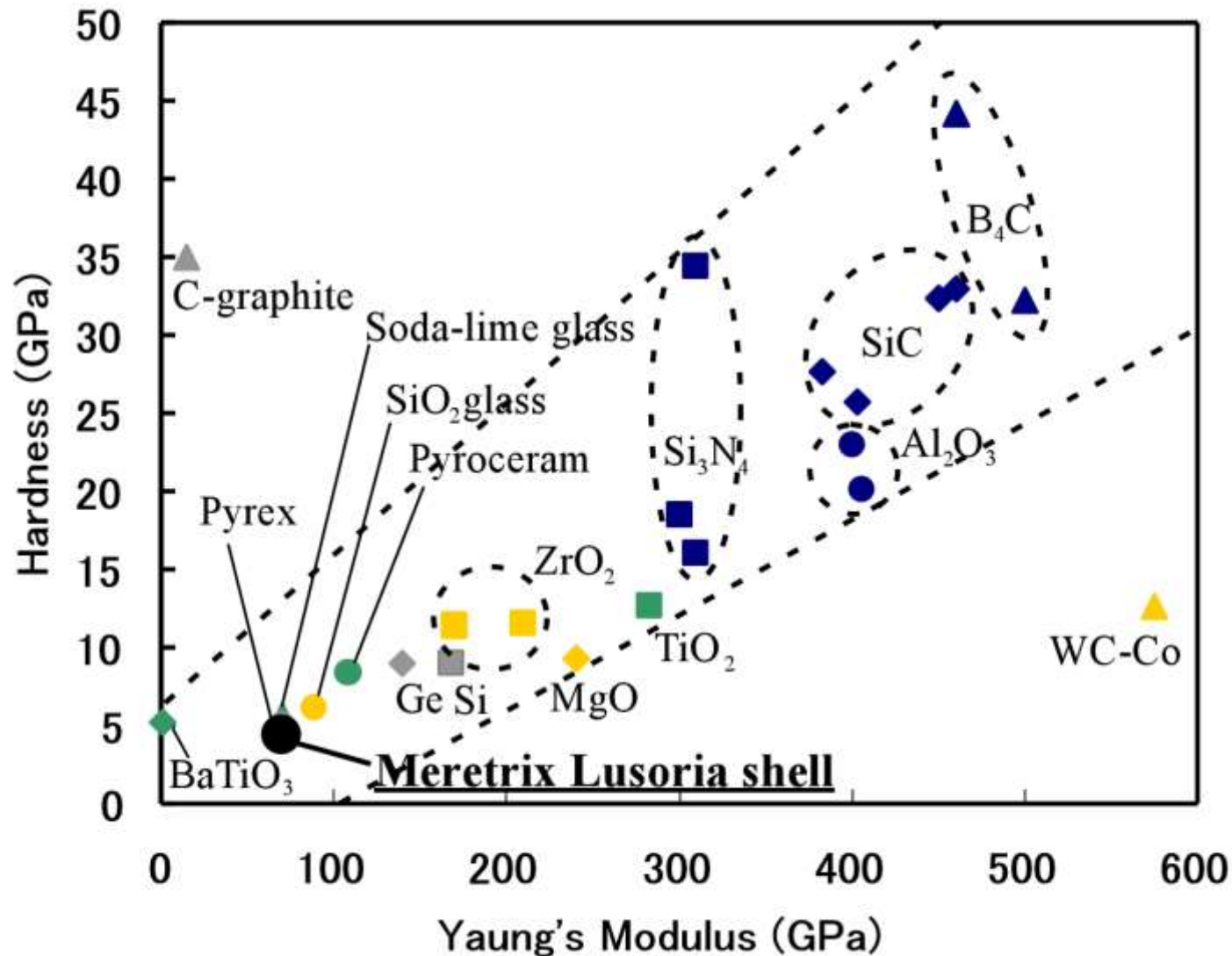
- 1. Importance of the Control of Interfacial Fracture in Brittle Materials.**
- 2. Learning Optimum Microstructure from Natural Bioceramic Structures.**
- 3. SEM Observation of Microstructure in Japanese Clam (*Meretrix Lusoria*).**
- 4. Hardness and Fracture Toughness Measurements of the Shells with Crossed-lamellar Microstructure.**
- 5. Conclusion**



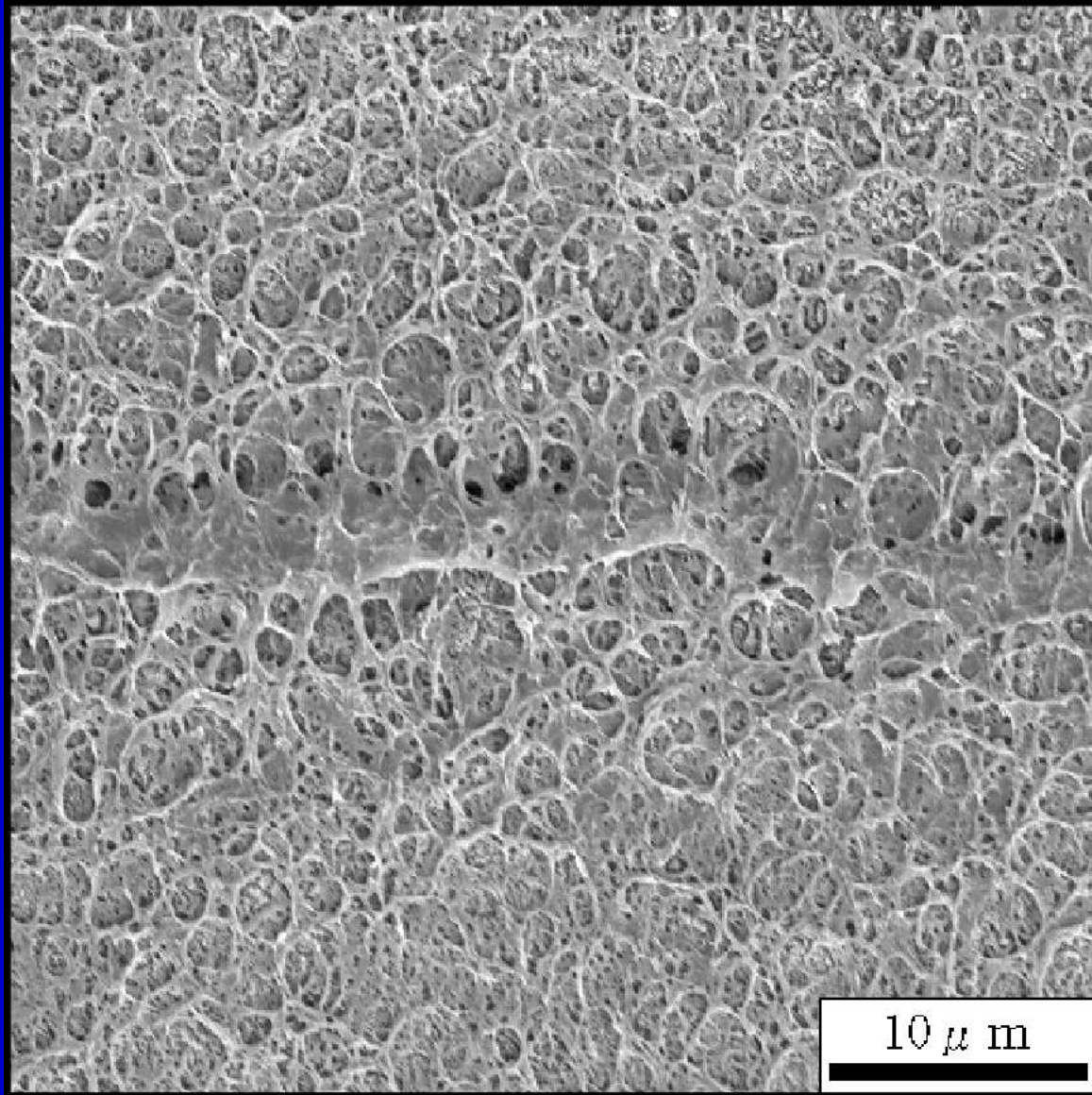
Photograph of *Meretrix Lusoria* (Japanese hard clam) (a). Schematic Illustration of Sampling Positions in *Meretrix Lusoria* shell (b).



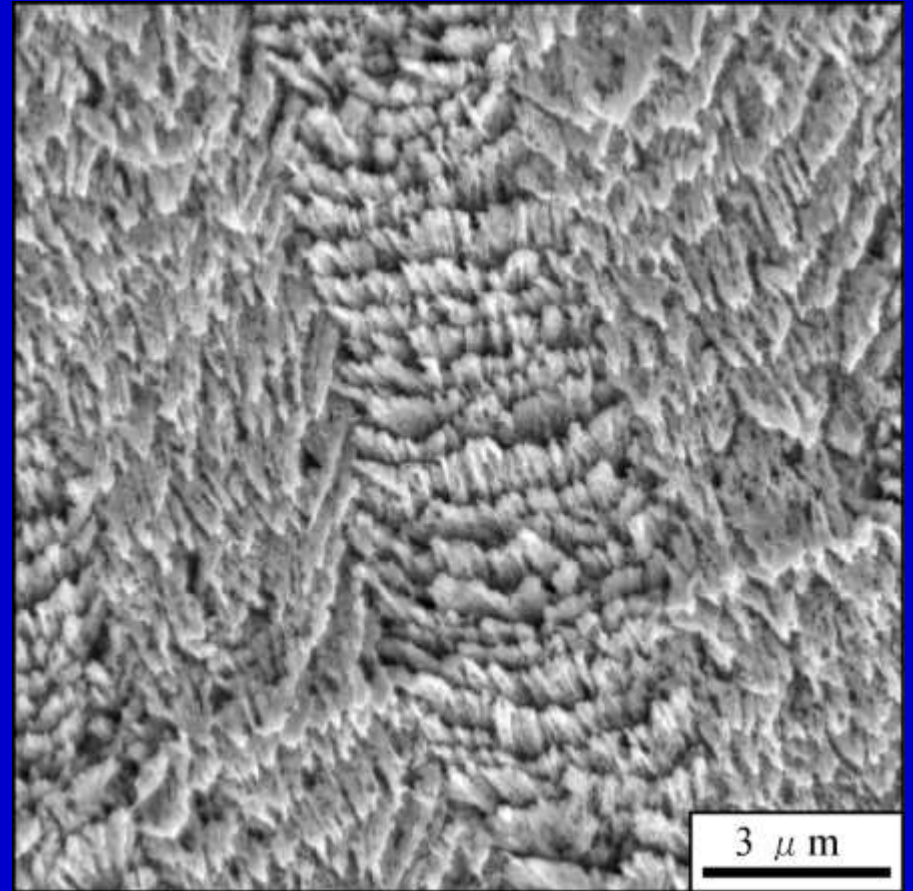
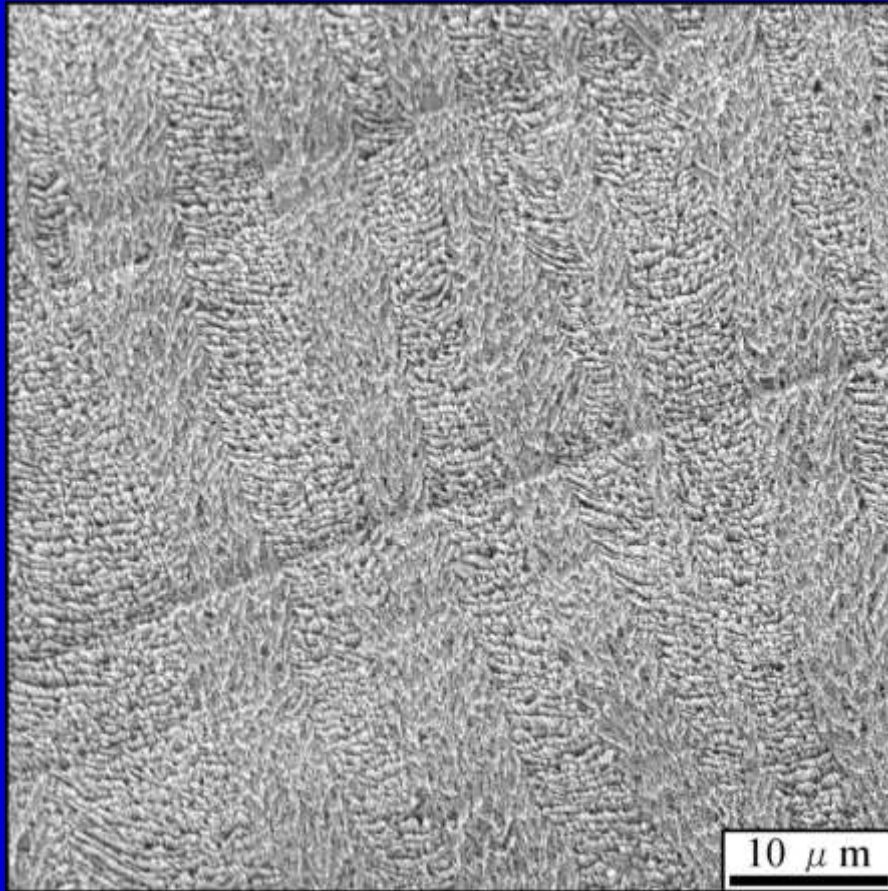
High Magnification Observation of Layered Structure in Japanese Hard Clam (*Meretrix Lusoria*).



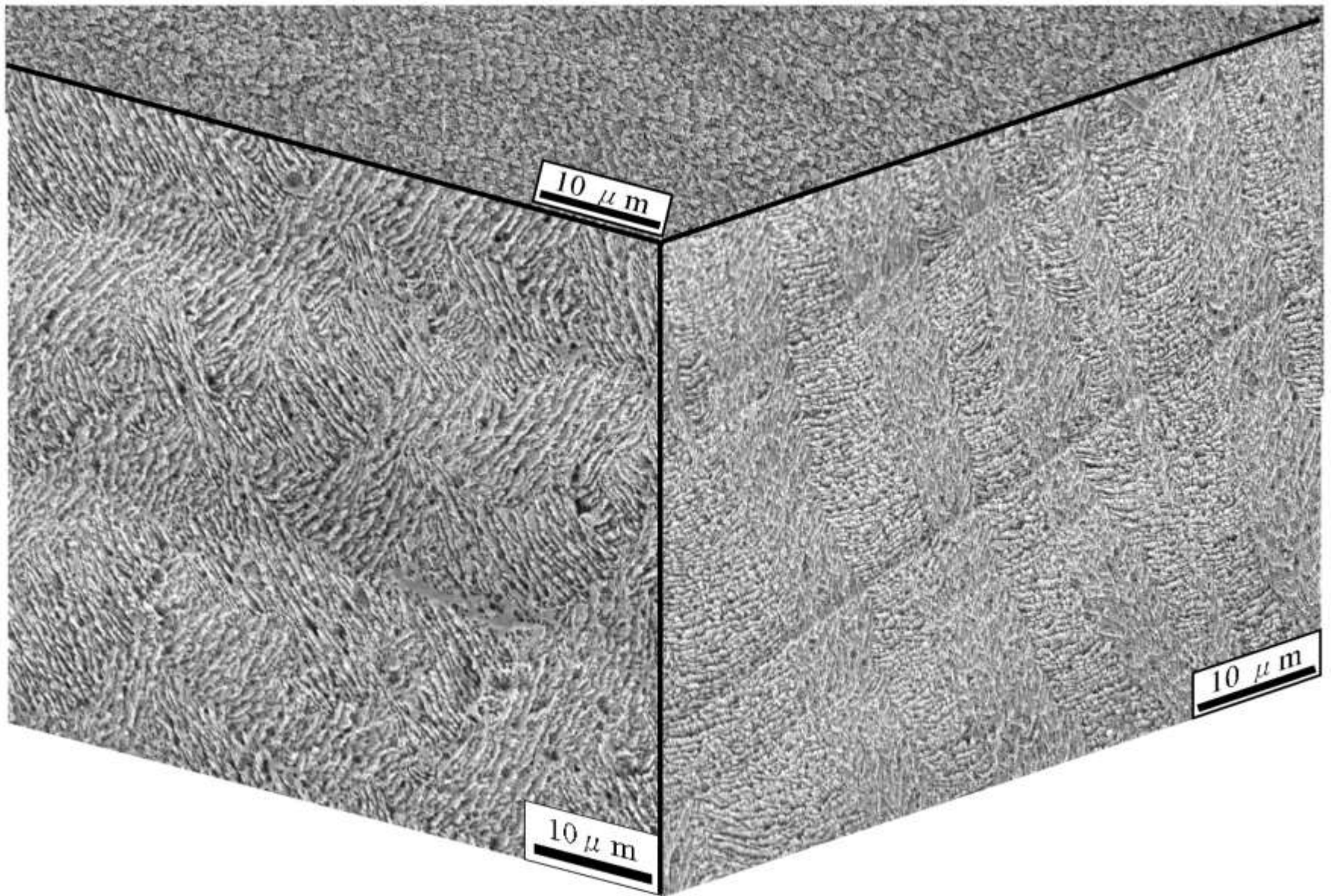
Vickers Hardness as a Function of Young's Modulus for Various Types of Brittle Materials. (I. J. McCollm, "Ceramic Hardness", (1990).)



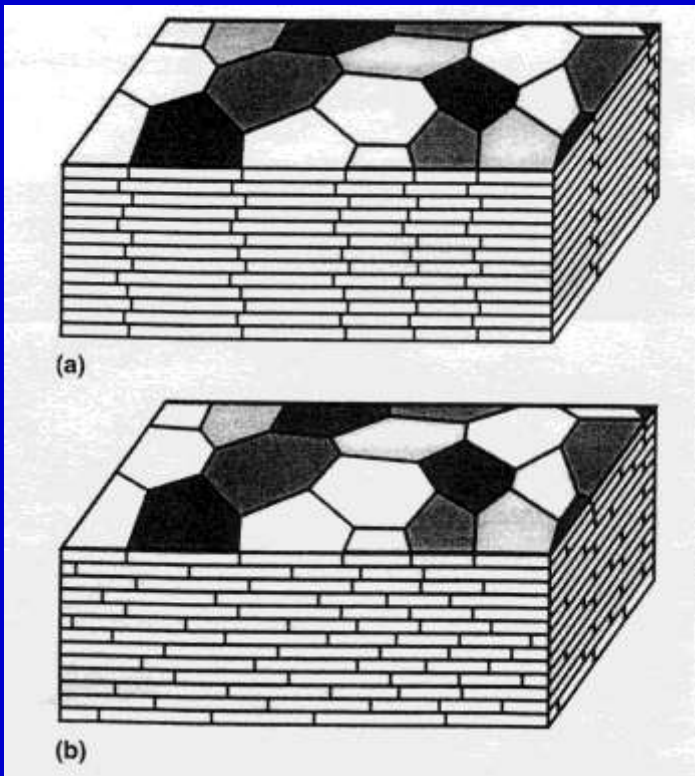
SEM Micrograph of the middle layer in Japanese Hard Clam (*Meretrix Lusoria*) in Spec.2. Three dimensionally network structure and complicated channel structure in the middle layer .



SEM Micrographs of Japanese Hard Clam (*Meretrix Lusoria*) in Spec.2. Enlargement view from the outer layer in Spec.2. Right hand side is higher magnification micrograph.



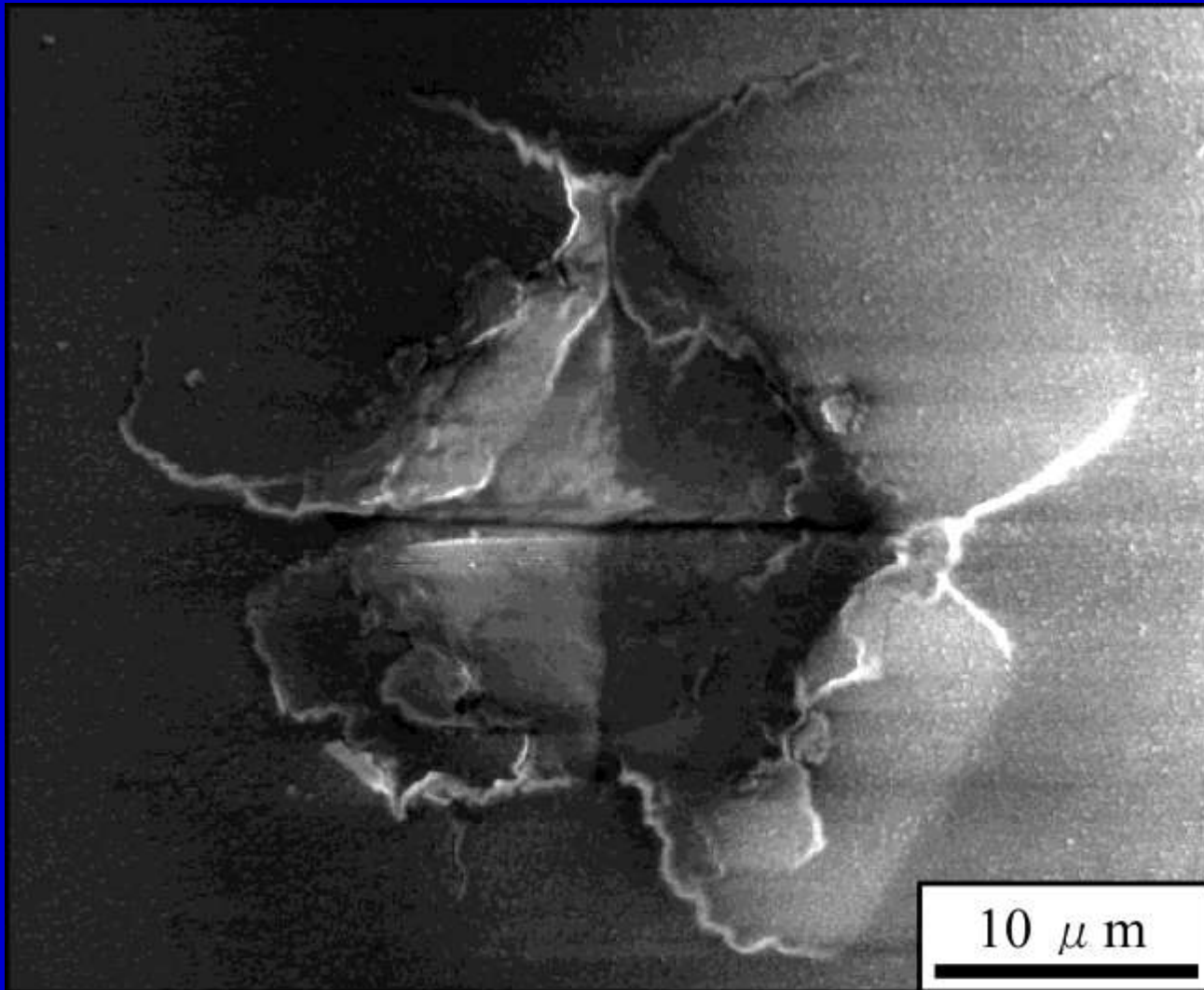
Crossed-lamellar Microstructure in the Outer Layer Observed in Japanese Hard Clam (*Meretrix Lusoria*).



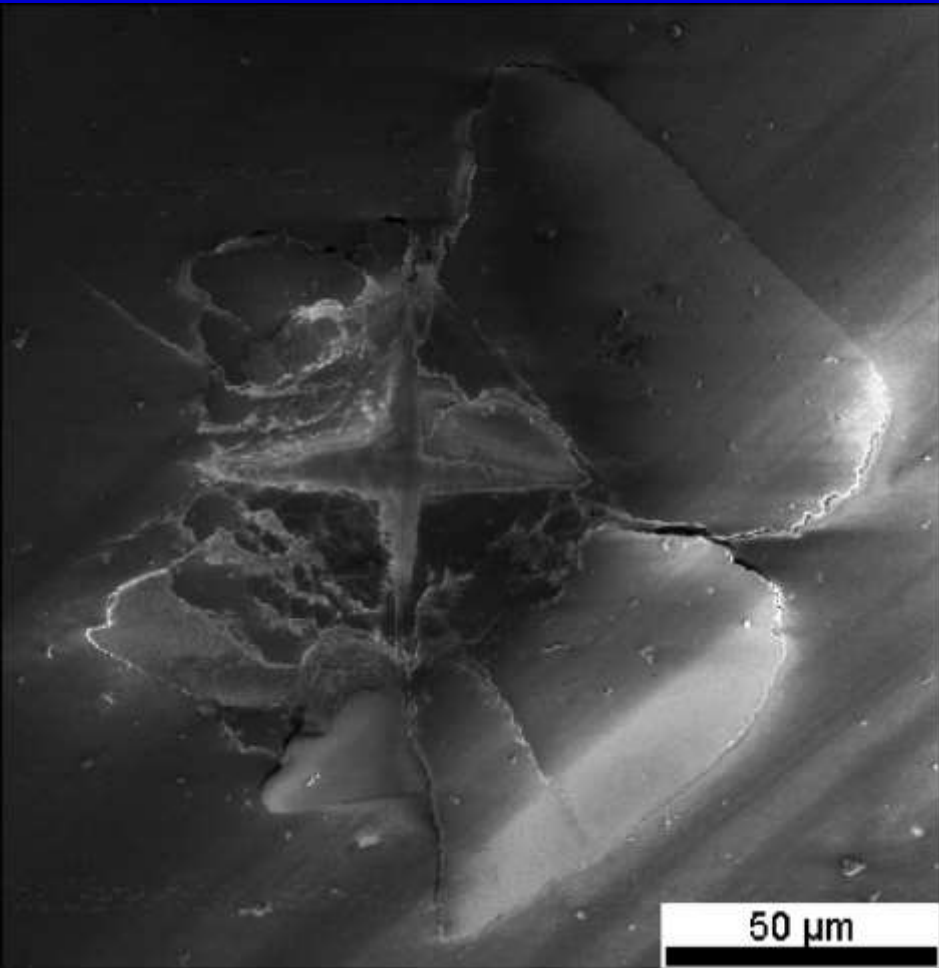
Schematic Illustrations of (a) Columnar Nacre/abalone Shell and (b) Sheet Nacre/pearl Oyster. Polygonal Aragonite Tablets are adhered into a Lamellar Structure by a thin Organic Interlayer. In Columnar Nacre, the Intertablet Boundaries are correlated into a tessellated Arrangement. (R.Z.Wang *et al.* J. Mater. Sci., 16 (2001), 2485, Deformation mechanisms in nacre.)



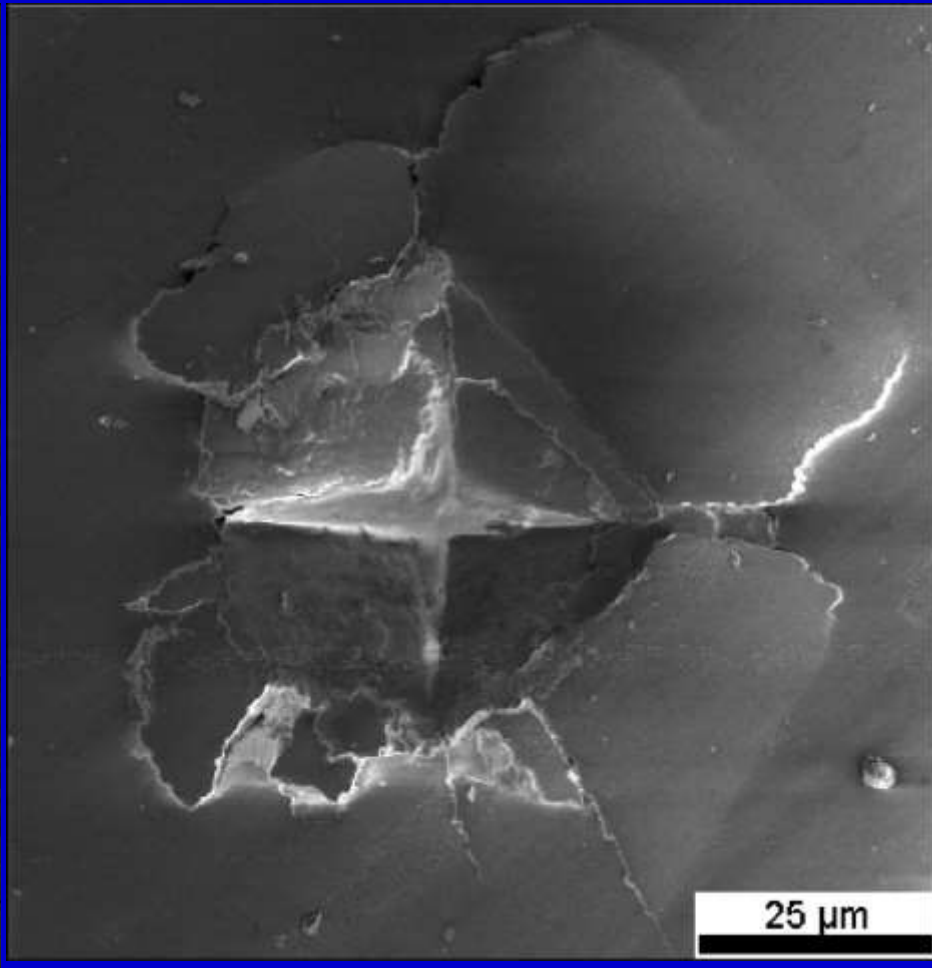
TEM Micrograph of the Platelets in Nacre. (Q.L.Feng *et al.* Mater. Sci. Eng., C11 (2000), 19.)



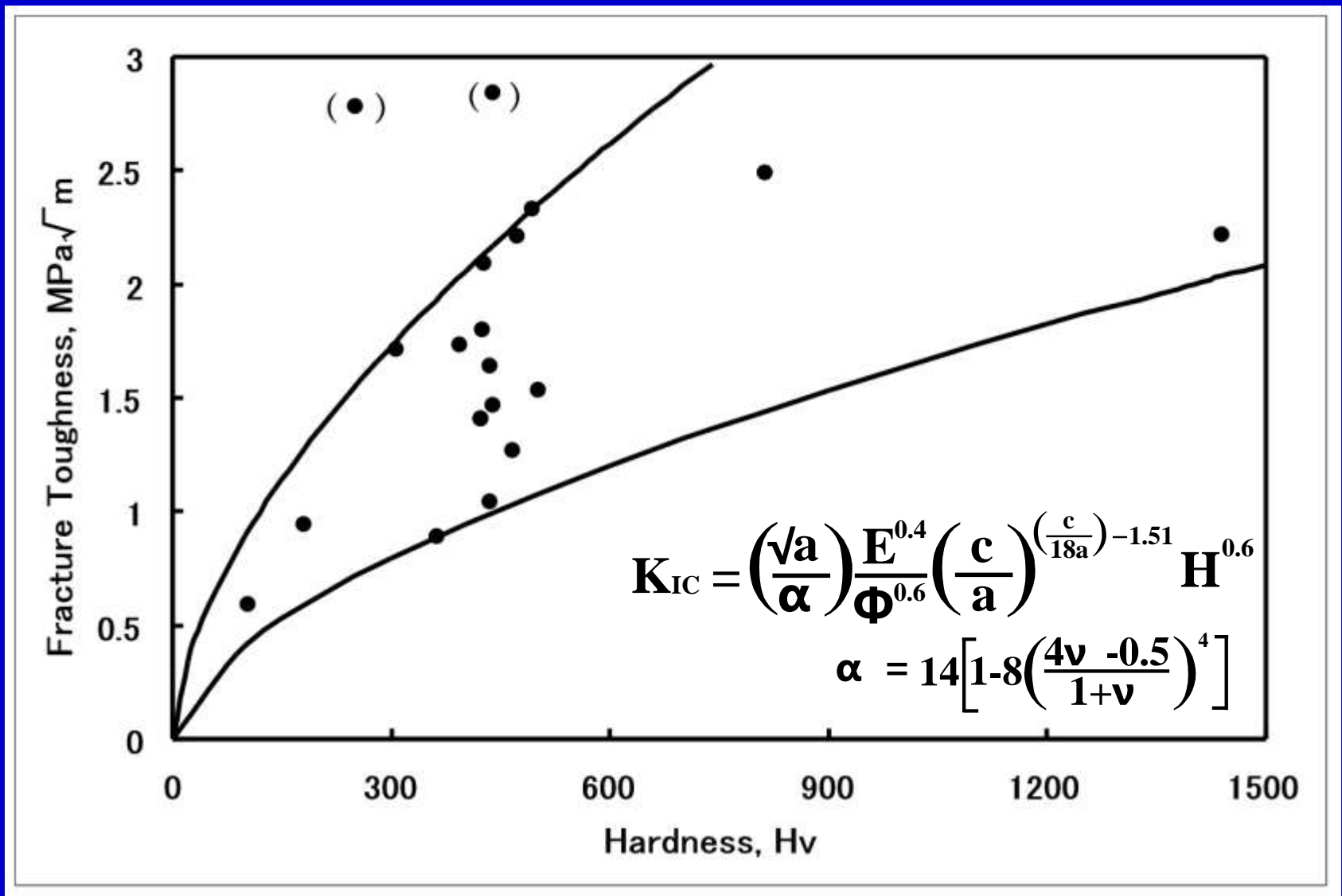
SEM Micrograph of Vickers Indentation in Japanese Hard Clam (*Meretrix Lusoria*). Note the Deflection of Crack from the Tip of Indentation.



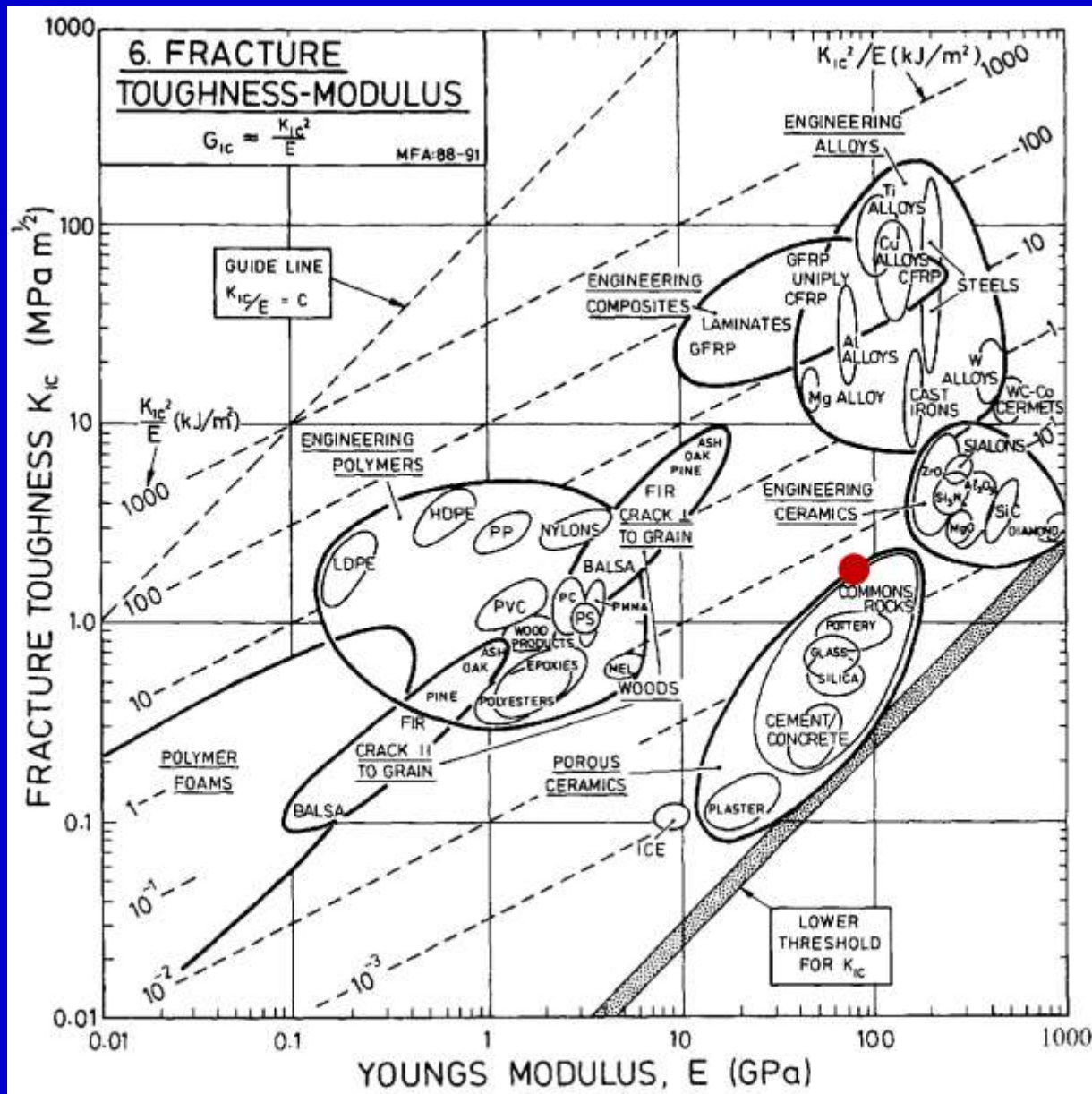
(a) Load = 0.5 kgf
Hardness, Hv = 181
 $K_{IC} = 0.94 \text{ MPa} \cdot \text{m}^{1/2}$



(b) Load = 1.0 kgf
Hardness, Hv = 813
 $K_{IC} = 2.49 \text{ MPa} \cdot \text{m}^{1/2}$



Fracture Toughness vs. Hardness Relationship for Japanese Hard Clam (*Meretrix Lusoria*).

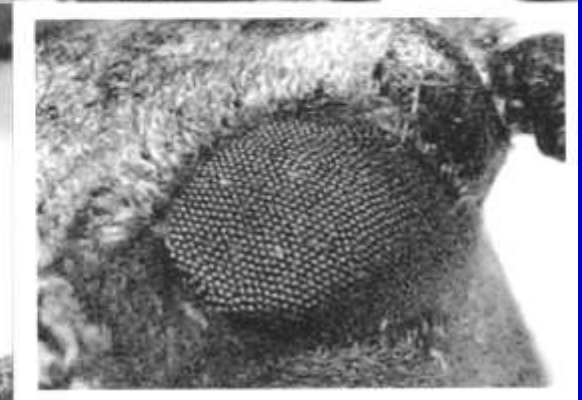


Fracture Toughness, K_{Ic} , plotted against Young's Modulus, E . (M.F.Ashby, "Materials Selection in Mechanical Design" (1992).)

Note: The Data obtained from this work locate at the top level in porous ceramic group.

- 1. Multi-layered and Crossed-lamellar microstructures were observed.**
- 2. Fracture Toughness, K_{IC} , determined by Indentation Technique shows almost top value among those for Porous Ceramics.**
- 3. Presence of Interfaces between Lamellae plays important roles in Toughening of Brittle Ceramic Structure with Crossed-lamellar Microstructure.**
- 4. Crossed-lamellar Microstructure confers Optimal and Robust Mechanical Property on Natural Bioceramic Structure.**

昆虫の複眼に見られる微細構造と光学機能 (Corneal Microstructure of Insects and Optical Performance)





Grain boundaries and coincidence site lattices in the corneal nanonipple structure of the Mourning Cloak butterfly

Ken C. Lee and Uwe Erb*

Full Research Paper

Open Access

Address:
Department of Materials Science and Engineering, University of
Toronto, Toronto, Ontario, M5S 3E4, Canada

Email:
Ken C. Lee - kenc.lee@mail.utoronto.ca; Uwe Erb* -
erb@ecf.utoronto.ca

* Corresponding author

Keywords:
butterfly-eye structure; coordination defects; sigma grain boundaries

Beilstein J. Nanotechnol. **2013**, *4*, 292–299.
doi:10.3762/bjnano.4.32

Received: 30 January 2013
Accepted: 18 April 2013
Published: 02 May 2013

This article is part of the Thematic Series "Advances in nanomaterials".

Guest Editors: H. D. Gleiter and T. Schimmel

© 2013 Lee and Erb; licensee Beilstein-Institut.
License and terms: see end of document.

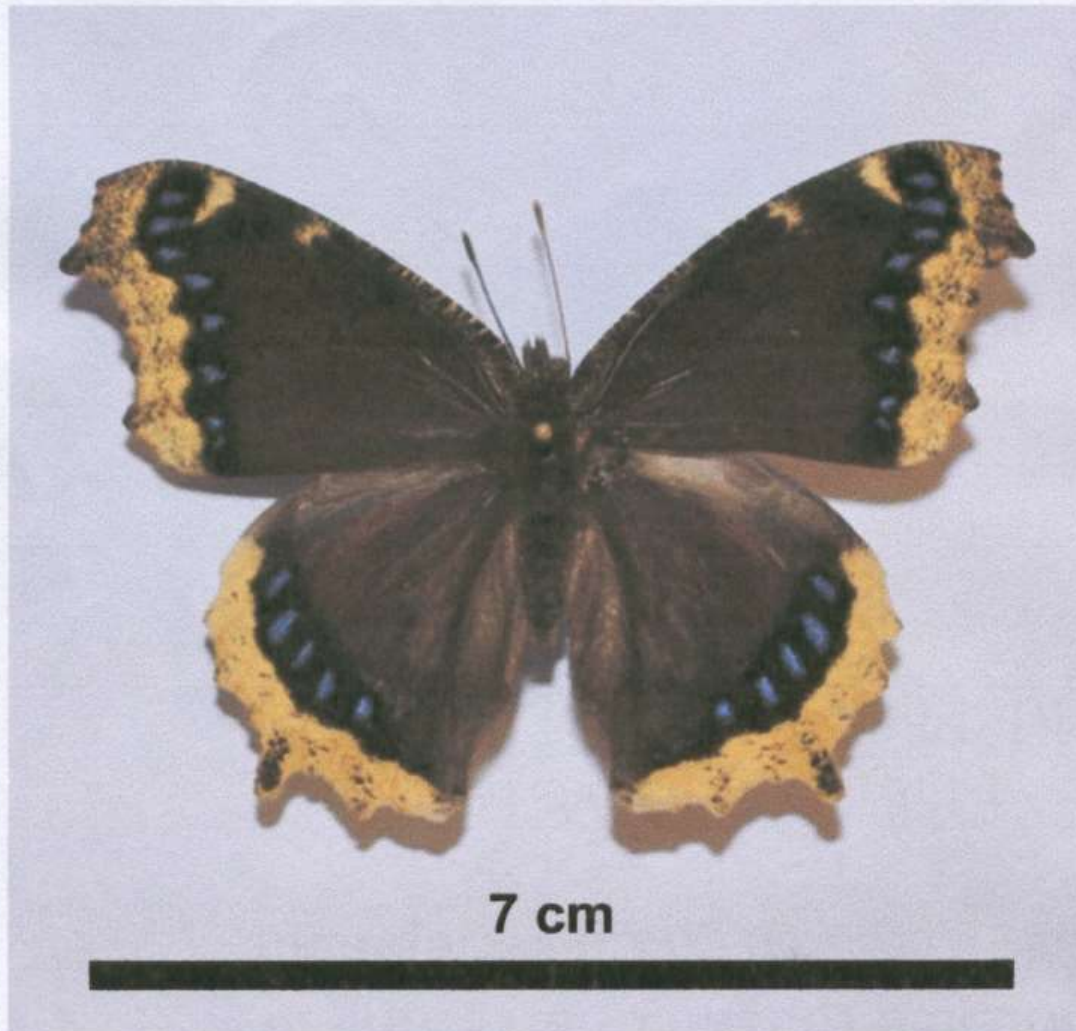


Figure 1: Mourning Cloak Butterfly

The Corneal Nipple Nanostructure of Eye of Mourning Cloak Butterfly

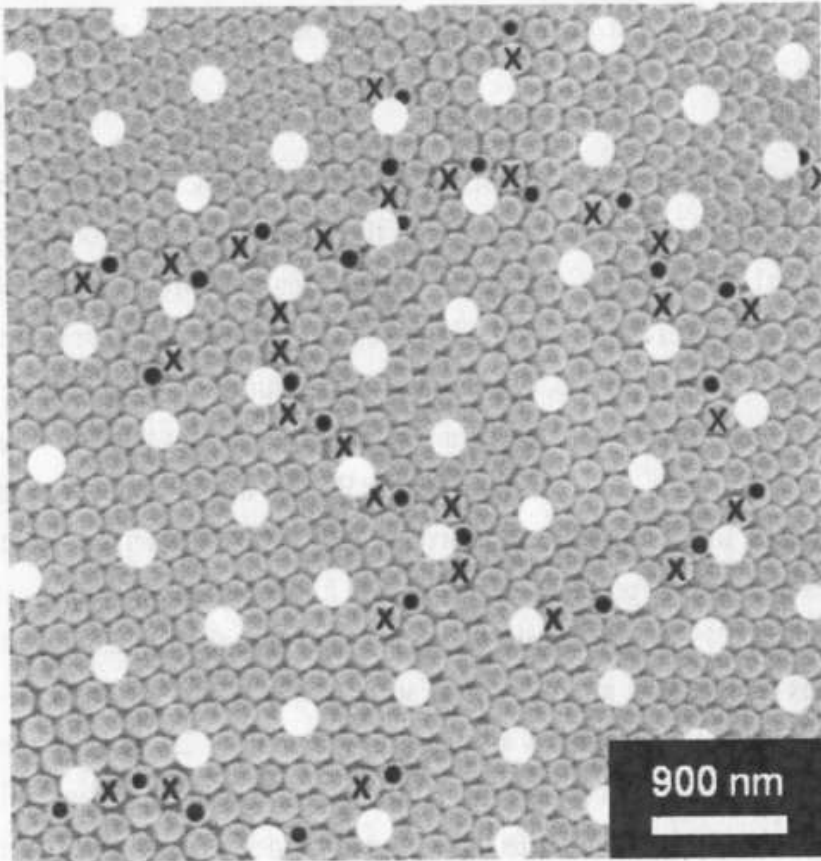


Figure 7: Extended $\Sigma 13$ coincidence site lattice covering several crystals (magnification: 13,000 \times).

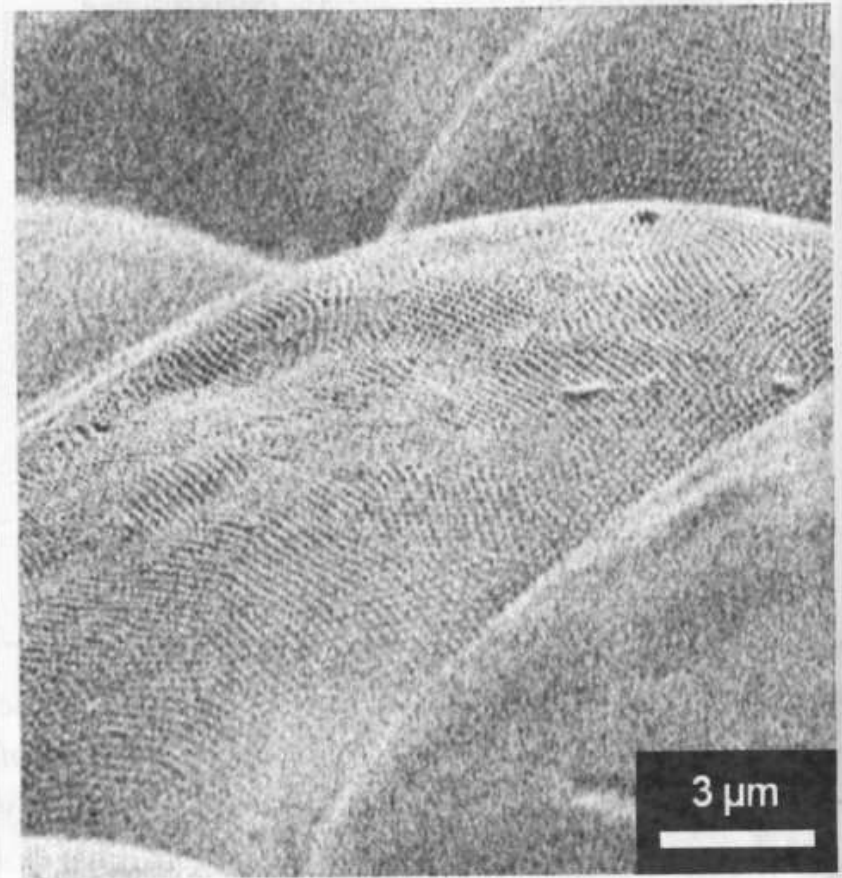


Figure 8: Several facets at very high tilt angle showing the curvature on each facet surface (magnification: 4,000 \times).

Nipple structure consisting of rows of 5-7 coordination-defects, with a CSL Superlattice indicated by white circles.

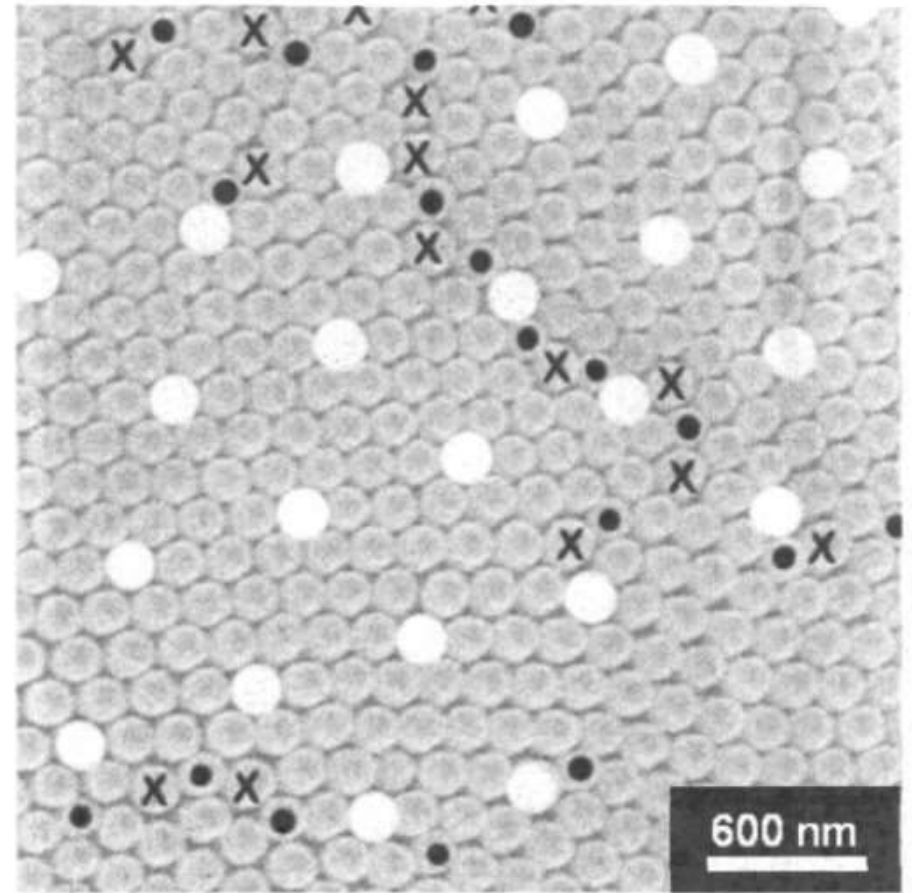
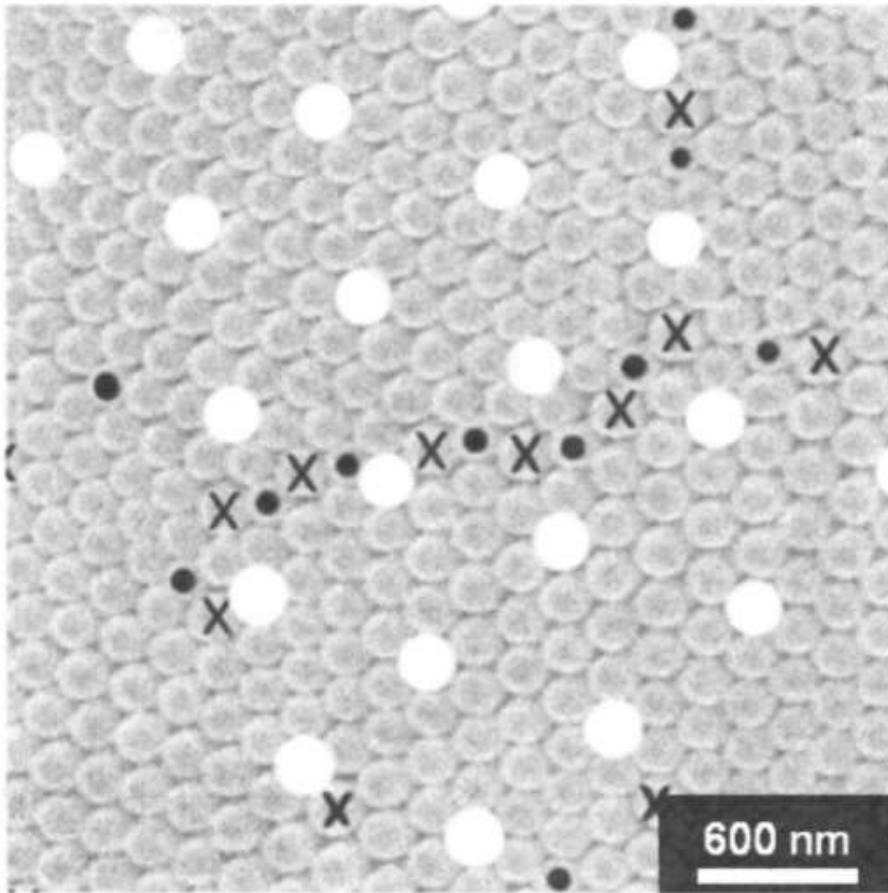


Figure 4: Examples of $\Sigma 13$ grain boundaries between crystals (domains) in the nipple structure consisting of rows of 5–7 coordination-defects. White circles indicate nipple positions belonging to a coincidence site lattice (CSL) superlattice (magnification: 20,000 \times).

Grain Boundary Character Distribution (GBCD) in Corneal Nanonipple Structure of Mourning Cloak Butterfly (Total Number of GBs=73)

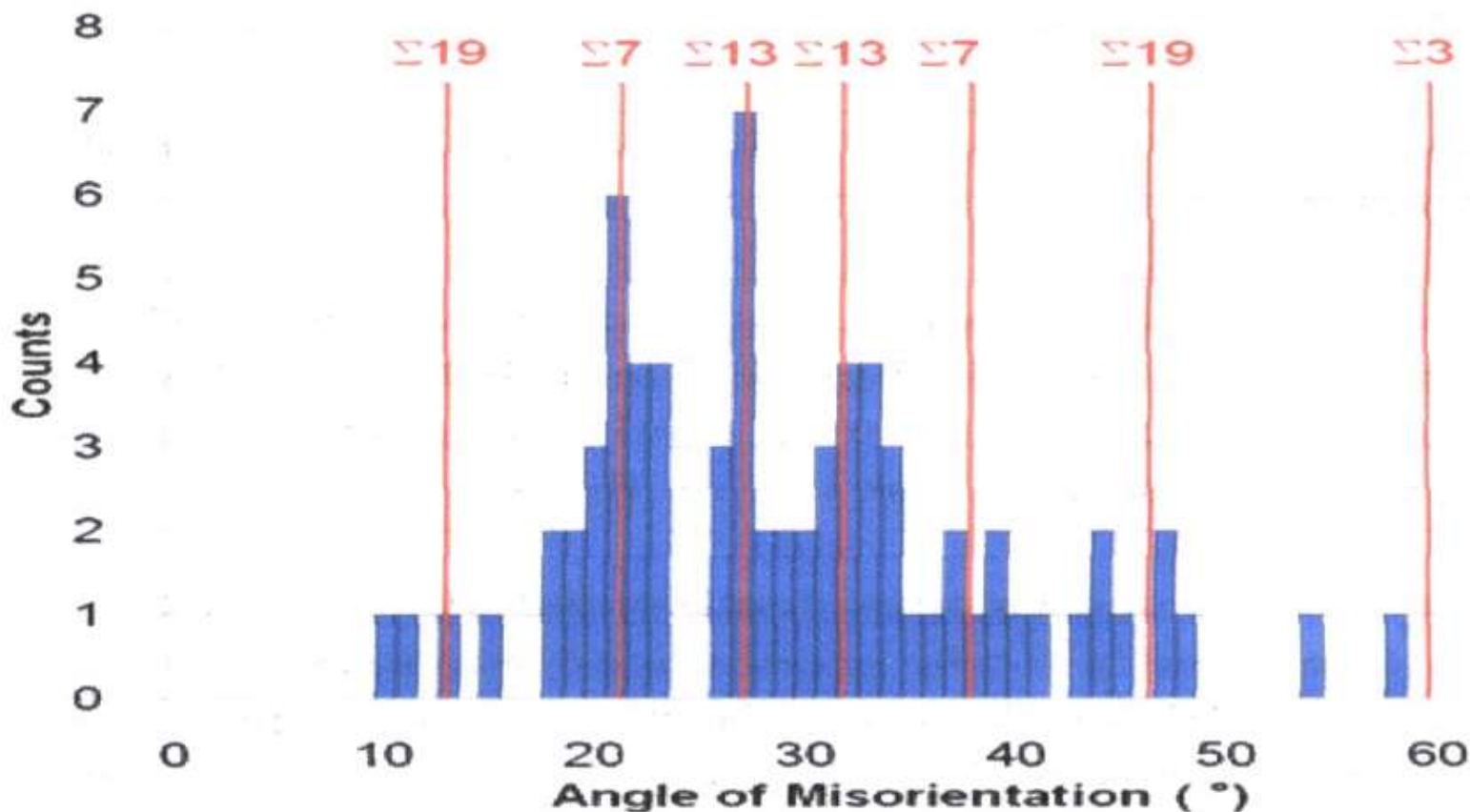


Figure 6: Histogram showing the misorientations around the common $\langle 111 \rangle$ direction between adjacent crystals in the Mourning Cloak nanonipple structure.

Coincidence Site Lattices for $\Sigma=7$, $\Sigma=13$ and $\Sigma=19$

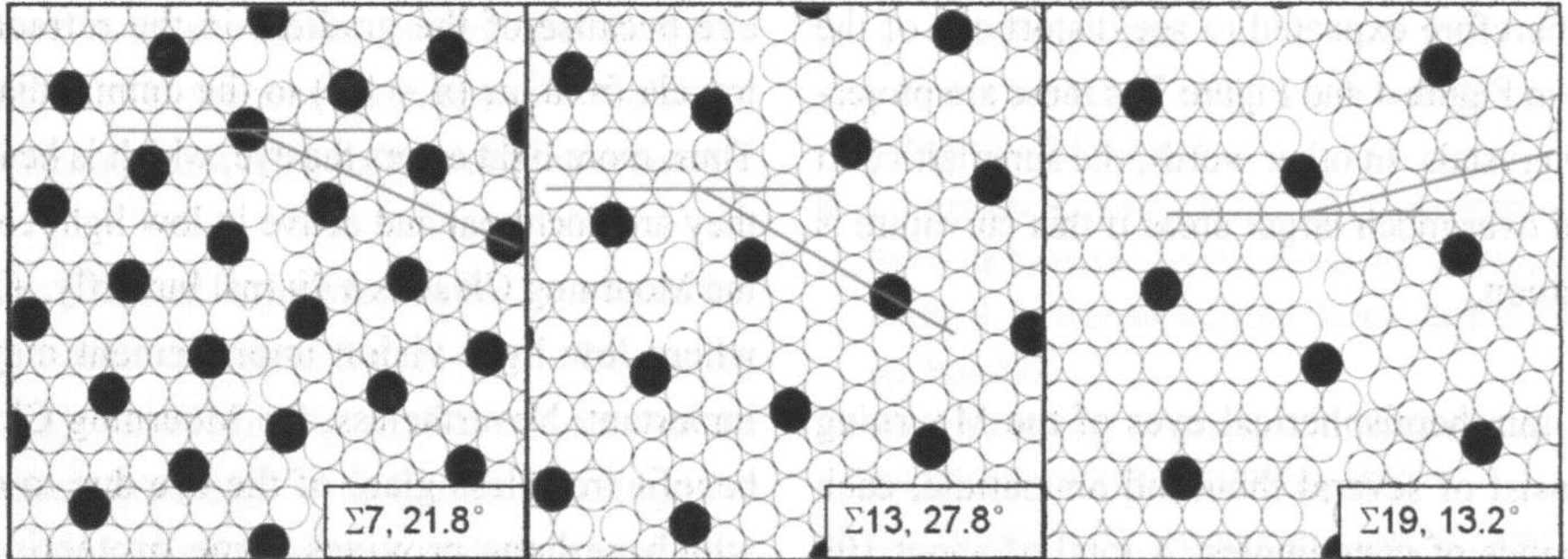
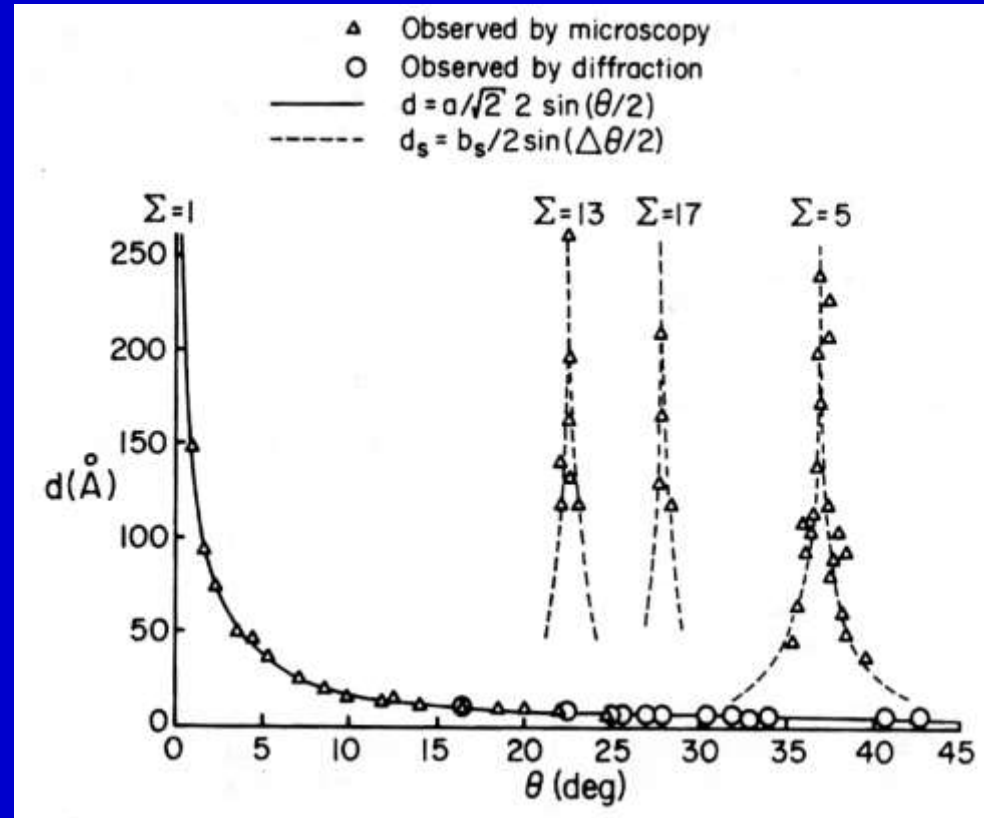
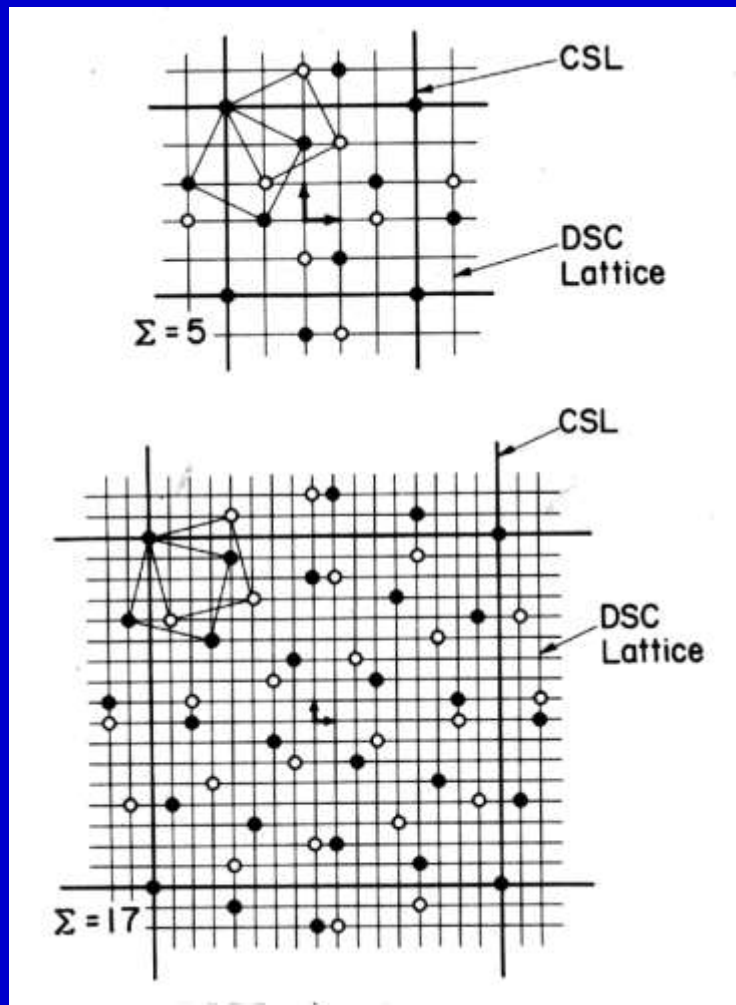


Table 1: Σ -values for CSL lattices generated by misorientations θ about the common $\langle 111 \rangle$ rotation axis together with $\Delta\theta$ values according to Equation 4.

Σ	θ ($^\circ$)	$\Delta\theta$ ($^\circ$)
19	13.2	3.4
7	21.8	5.7
13	27.8	4.2
13	32.2	4.2
7	38.2	5.7
19	46.8	3.4
3	60.0	8.7

Displacement Shift Complete (DSC) Lattice Model



DSC-Lattices formed by interpenetrating (001) planes of simple Cubic Lattices rotated with respect to one another by Angle θ around [001]. Top: $\theta = 36.9$ ($\Sigma = 5$). Bottom: $\theta = 28.1$ ($\Sigma = 17$). The Burgers vectors of the DSC-intrinsic dislocations are shown at the center of each diagram.

Observed Primary Relaxation Spacing, d , and Secondary Relaxation Spacing, d_s , in [001] Twist Boundaries in Gold as a Function of Twist Angle θ .

R. W. Balluffi: "Grain Boundary Structure and Segregation", Interfacial Segregation, ASM., (1979), 193-237.

Table 2: Distances between coincident sites on the eye of the Mourning Cloak butterfly.

Σ	grating distance (nm)
7	$d_1 = 529$ $d_2 = 917$
13	$d_1 = 721$ $d_2 = 1249$
19	$d_1 = 872$ $d_2 = 1509$



Artful interfaces within biological materials

Biological materials have a wide range of mechanical properties matching their biological function. This is achieved via complex structural hierarchies, spanning many length scales, arising from the assembly of different sized building blocks during growth. The interfaces between these building blocks can increase resistance to fracture, join materials of different character, make them deform more easily and provide motility. While they represent only a tiny fraction of the overall volume, interfaces are essential for the integrity and function of the overall tissue. Understanding their construction principles, often based on specialized molecular assemblies, may change our current thinking about composite materials.

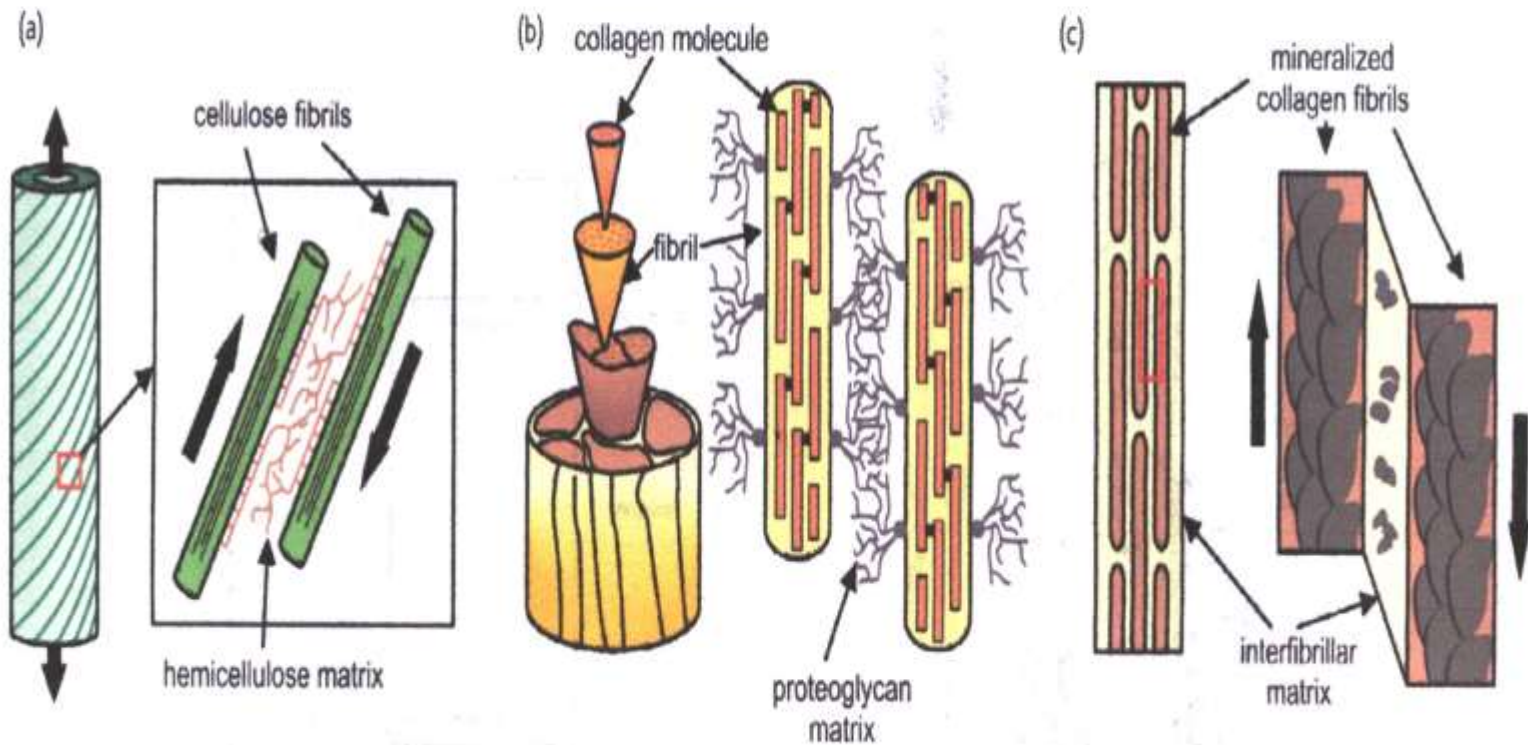
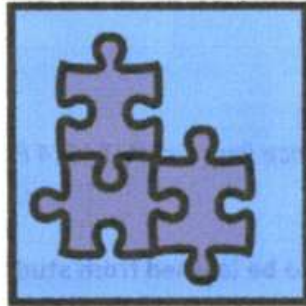


Fig. 5 Interfaces providing plastic or viscoelastic deformation between (a) cellulose fibrils in the wood cell wall (figure based on⁸⁴), (b) collagen fibrils in the tendon (figure based on⁸⁹), and (c) mineralized collagen fibrils in bone (figure based on⁹⁰).

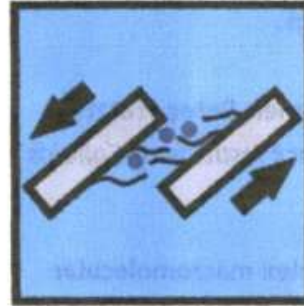
Interfaces Improving Material Toughness

(a)



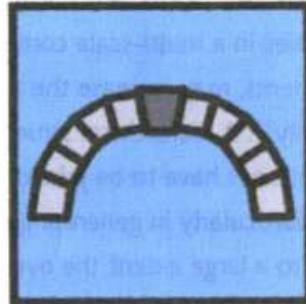
Interfaces Allowing Materials to Deform

(c)



Interfaces Bridging Different Materials

(b)



Interfaces Allowing Materials to Move

(d)

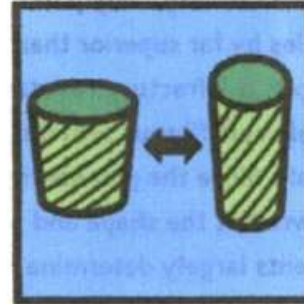


Fig. 1 Four different examples of how interfacial design can influence the mechanical behavior of biomaterials are addressed: (a) interfaces which improve the fracture resistance of a material by introducing soft interfaces (e.g. nacre), (b) interfaces that act as bridges between materials of highly different mechanical properties (e.g. mussel byssus), (c) interfaces that allow materials to deform plastically (e.g. bone and wood), and (d) interfaces that allow materials to act as actuators of motion/stress (e.g. the scales of the pine cone).

Important Literature & Reviews on Interface Engineering of Biological Materials.

- (1). J.W.C. Dunlop, R. Weikamer, P. Fratzl:
Materials Today, 14 (2011), No.3, 70-78
“Artful Interfaces within Biological Materials”
- (2). P. Fratzl, R. Weinkamer:
Progress in Materials Science, 52 (2007), 1263-1334,
“Nature’s Hierarchical Materials”
- (3). J.W.C. Dunlop, P. Fratzl: Ann. Rev. Mater. Res.,
40 (2010), 1-24,
“Biological Composites”

Interfacial Engineering – a Perspective

E. D. Hondros; *Materials Science and Engineering*, A 166 (1993), 1-10.

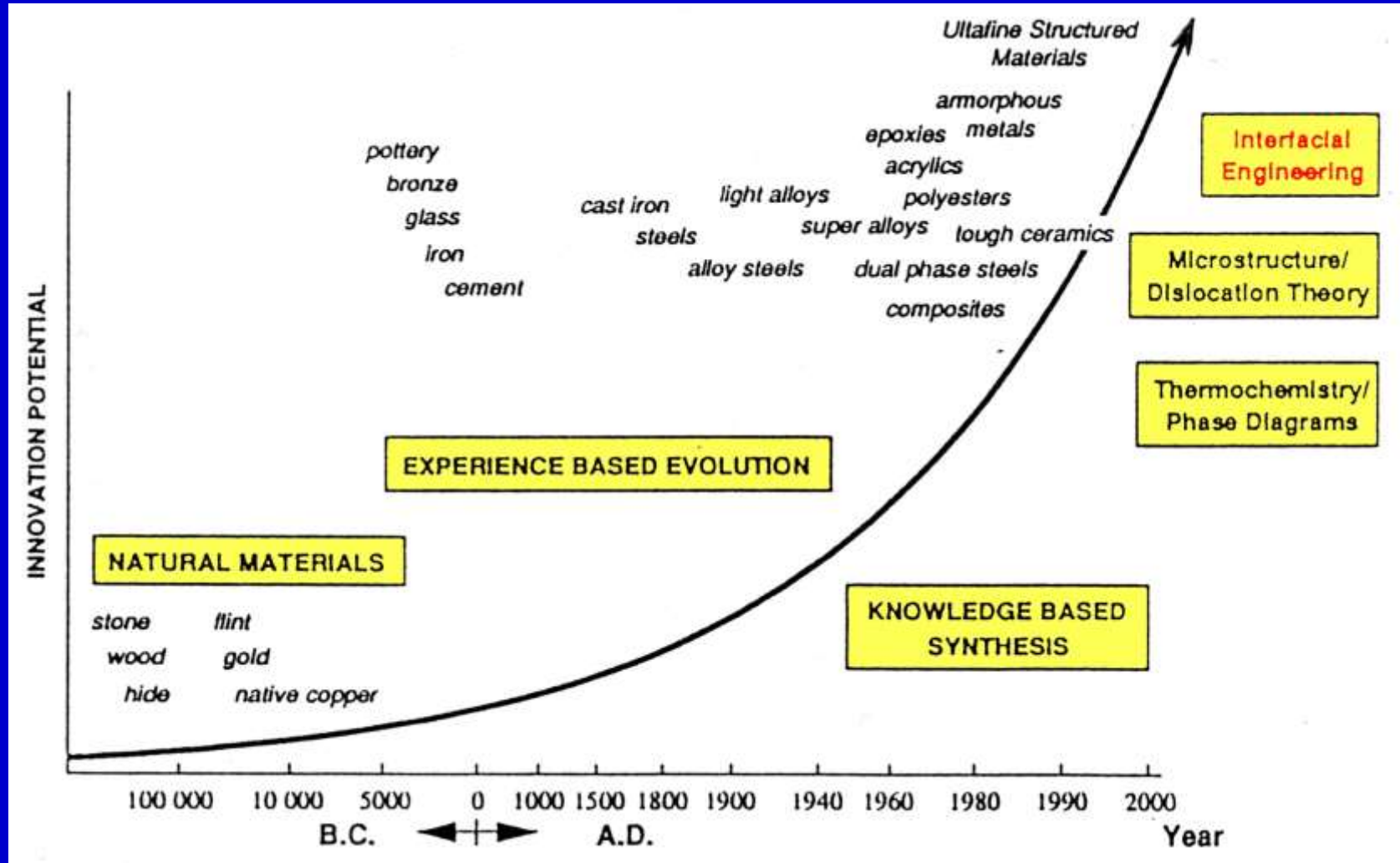


Fig. 1. Description on an Imaginary Scale of the Evolution of the Innovation Content of Materials.

Summary

1. **Structure-dependent properties** of grain boundaries are the source of function and performance in polycrystalline materials. **Some grain boundaries can be active, but others are inactive in function-generating metallurgical phenomena.** It has been well evidenced at the end of last century that **Grain Boundary and Interface Engineering** can confer desirable mechanical properties and high performance to a “**Polycrystal System**” by designing and controlling of the **grain boundary microstructure.**
2. Now we are facing **the Second stage of Grain Boundary and Interface Engineering** to produce a New type of “**Structural or Functional Material**” not replaceable by any existing ones. **Nanostructured materials** and **Thin Films** with an extremely high density of Interfaces are on one side, but there is a strong demand for “**Low-dimension GBE**” which may be also one of the targets of **MEMS**, together with “**Further Improvement in Performance of Conventional materials**”, in the 21st century.

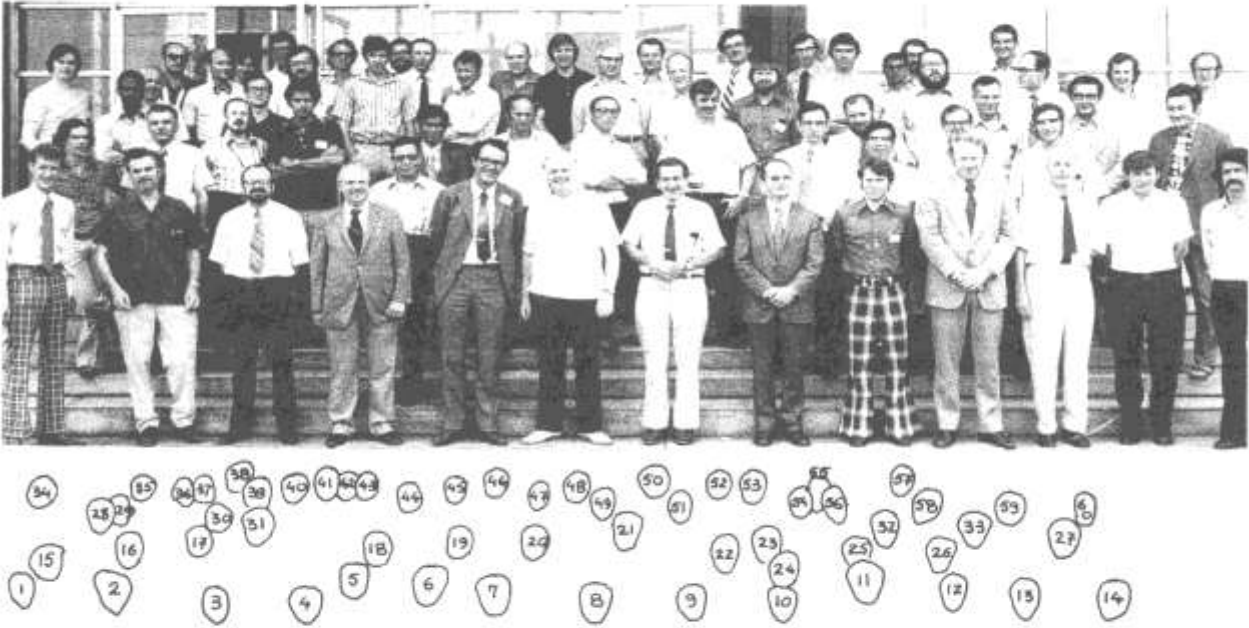
3. In near future, **the third stage of Grain Boundary and Interface Engineering** will be coming which may bring about a such New types of **“Structural or Functional Material”** only those **living creatures like plants, animals and living cells** can exhibit their function and performance those are never produced and demonstrated by **presently existing Materials Science and Engineering**. For this purpose, a new challenge awaits those who are given their original insight into a possibility to create a new function and excellent performance unpredictable from our current scientific knowledge. **Multi-disciplinary knowledge of Materials Science and Engineering, including Living Organic Materials** may open a **New Era of Interface-controlled Materials with a amazing function and performance.**

Thank you for kind Attention
and
Interest in Grain Boundary
Engineering

Why were Peoples so much attracted by Studies of GBs and Interfaces and involved in them ?

CANADIAN METALLURGICAL QUARTERLY Volume 13 Number 1 (1974)

International school on grain boundaries (in 1973, Montreal, Canada)



Pictured above are those who took part in the Summer School. On reconnaît ceux qui participèrent à notre école-été.

(1) J.S. Daniel (2) R.W. Cahn (3) R.W. Armstrong (4) P. Lacombe (5) Hsun Hu (6) D.A. Smith (7) K. Lücke (8) K.T. Aust (9) C. Goux (10) L. Swanger (11) D.F. Stein (12) D. McLean (13) G.H. Bishop (14) J.P. Bailon (15) J.M. Dorlot (16) I. Szkrumelak (17) N. Packan (18) Han Nyo (19) F.B. Thomson (20) C. Roques-Carmes (21) J.W. Provan (22) J.L. Scardina (23) J.I. Dickson (24) K.Y. Chen (25) W.W. Lindstrom (26) C.M. Maucione (27) G. Martin (28) O.A. Bamiro (29) P.A. Thrower (30) R. Coladas-Calvo (31) R. G. Pinheiro (32) P.R. Morris (33) A. Zaoui (34) W.A.T. Clark (35) M. Braunovic (36) M.E. Glicksman (37) P. Hastings (38) W.R. Bitler (39) R.A. Masumura (40) M. Galopin (41) G.T. Higgins (42) G. Guerin (43) T.G. Langdon (44) G. Barò (45) P.E. Evans (46) B.F. Dyson (47) J.H. Westbrook (48) M. Biscondi (49) H.A. Damian (50) N. Bassim (51) J.E. Doherty (52) A. Galibois (53) R.L. Edgar (54) S.N. Tiwari (55) J. Masouave (56) R.D. Zordan (57) C. Lemaignan (58) J.H. Peretzko (59) R.C. Pond (60) G.J.C. Carpenter.

December, 2002



I notice that Grain Boundary Design features increasingly, especially in Japanese journals, and has spread from usual grain sizes down to nano-sizer.

I am still lucky with health and this year have spent short holidays in Germany (Berlin mainly), Iceland, Ireland (2 countries I have never visited before) and Spain.

W. L.

To celebrate our great Pioneer in GB research field !!
Dr. Donald McLean who had 100th Birthday on July 25, 2015





T. Watanabe

D. A. Smith

Y. Ishida

(1996)

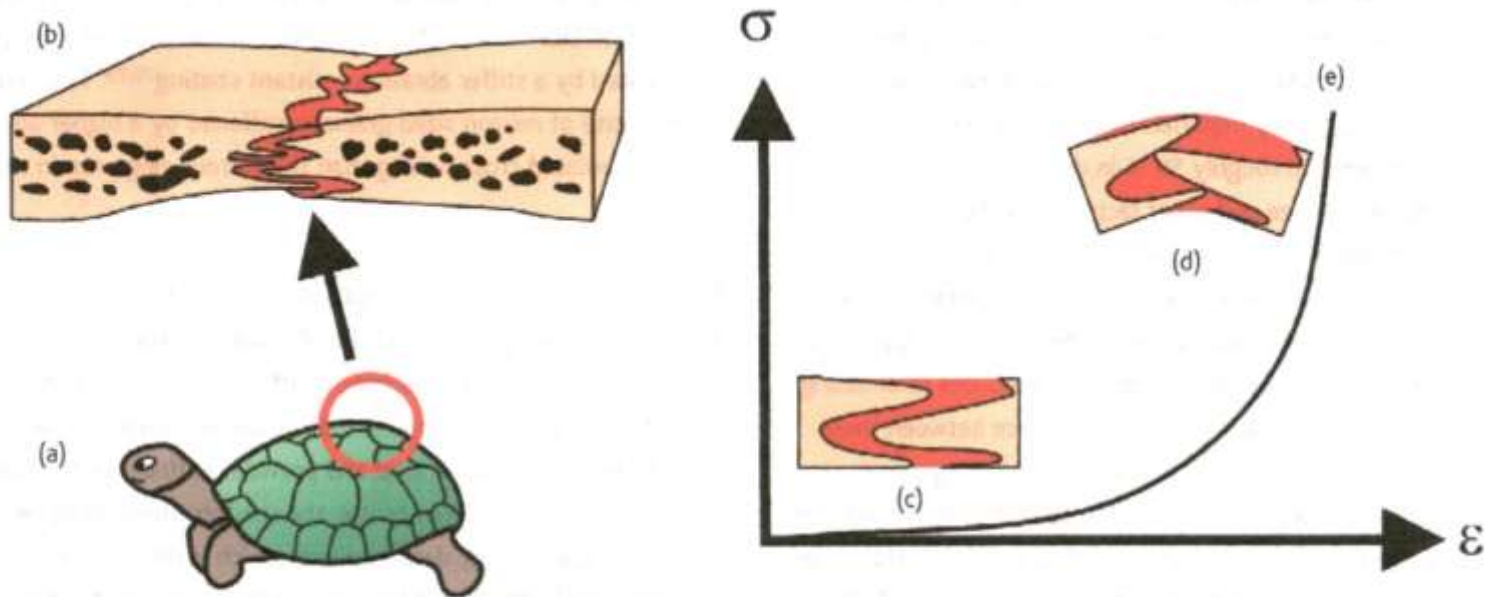


Fig. 6 (a) The shell of the red slider turtle is made up of (b) modified ribs which are linked together by a suture consisting of interdigitating protrusions of bone separated by a soft collagenous layer. For small amounts of bending (c), deformation is concentrated in the soft layer, however upon large deformations (d) the interdigitations of bone interlock resulting in a significant stiffening of the composite, as illustrated by a schematic stress-strain curve (e) (figure based on¹⁶).

Relation between Toughness and Modulus for Natural Materials

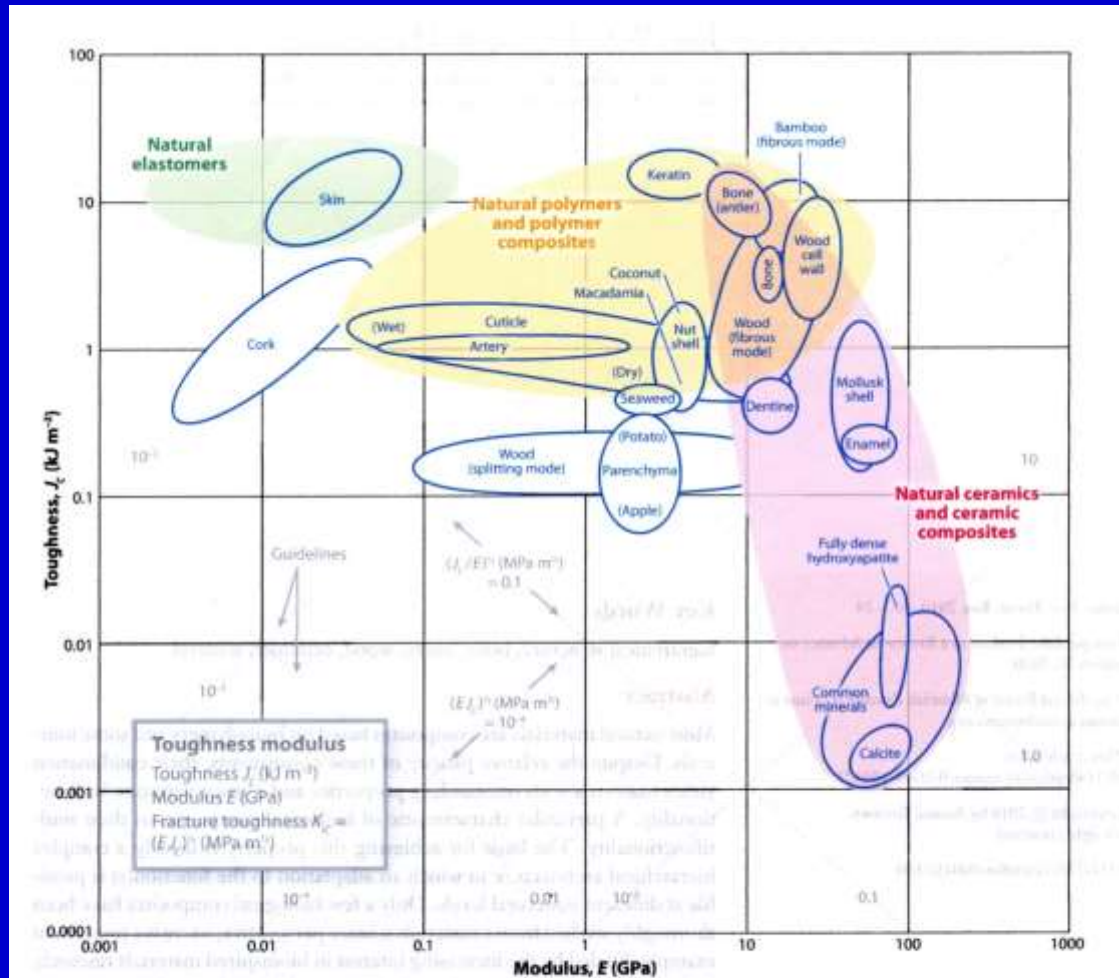


Figure 1

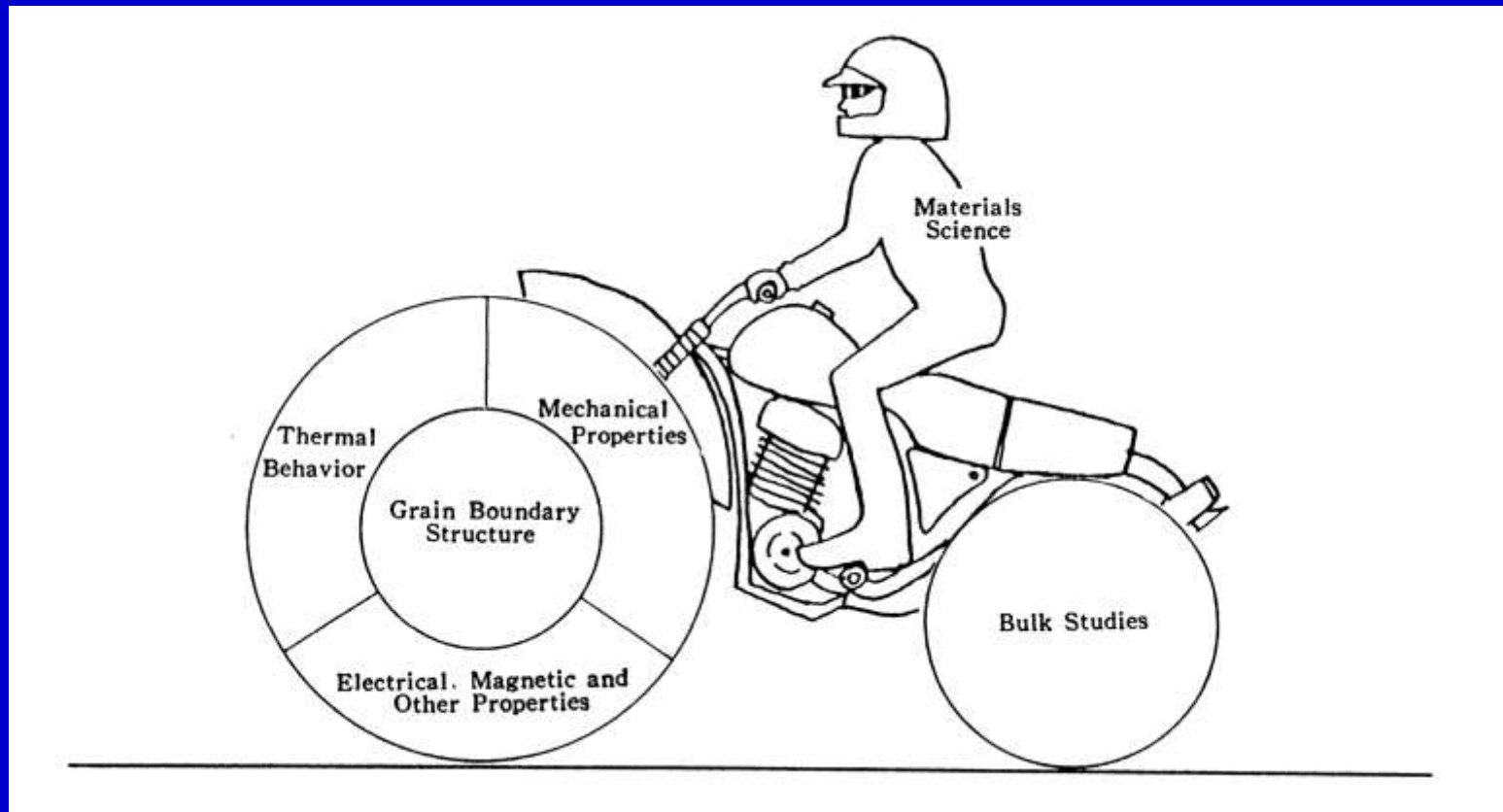
Materials property chart showing the relation between toughness and modulus for natural materials. Materials vary widely for both parameters, but many mechanically important materials populate the upper right corner, where both stiffness and toughness are large. Drawn from Reference 4 with permission from Taylor and Francis (<http://www.informaworld.com>).

Memorium
Yoichi Ishida (1935 – 1996)



Central Roles of Grain Boundary Structure in Studies of Grain Boundary Properties and Bulk Properties.

Prof. Yoichi Ishida emphasized “**Importance of Grain Boundary Structure**”:
in his Closing Remarks for the Intern. Conf. on **Grain Boundary Structure and Related Phenomena**, Trans. JIM., Vol.27 (**1986**),1101.



Thickness Effect on the Flow Stress in Polycrystalline Materials with Various Grain Sizes

(S. Miyazaki, K. Shibata & H. Fujita: Acta Met., 27(1979), 855-862)

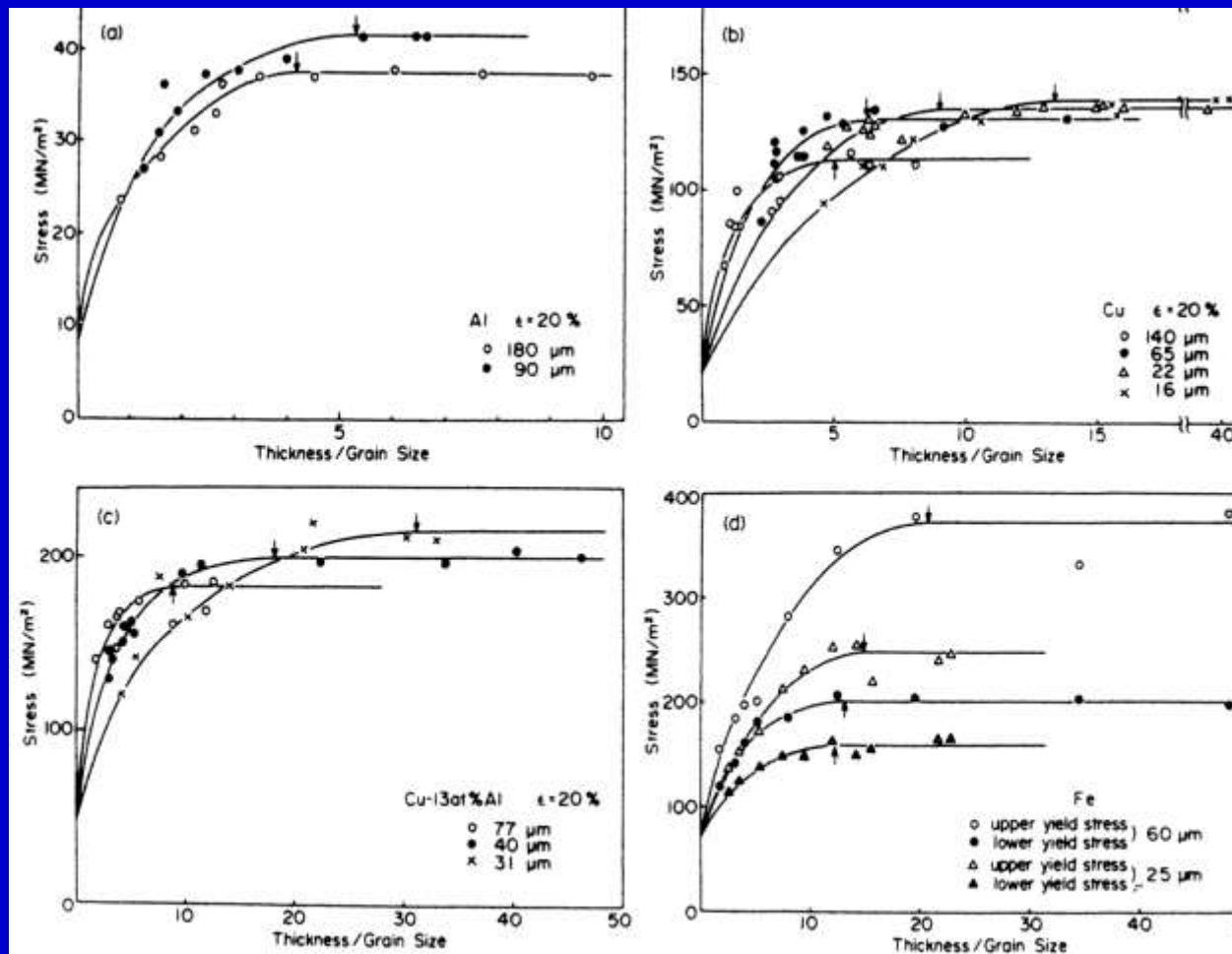
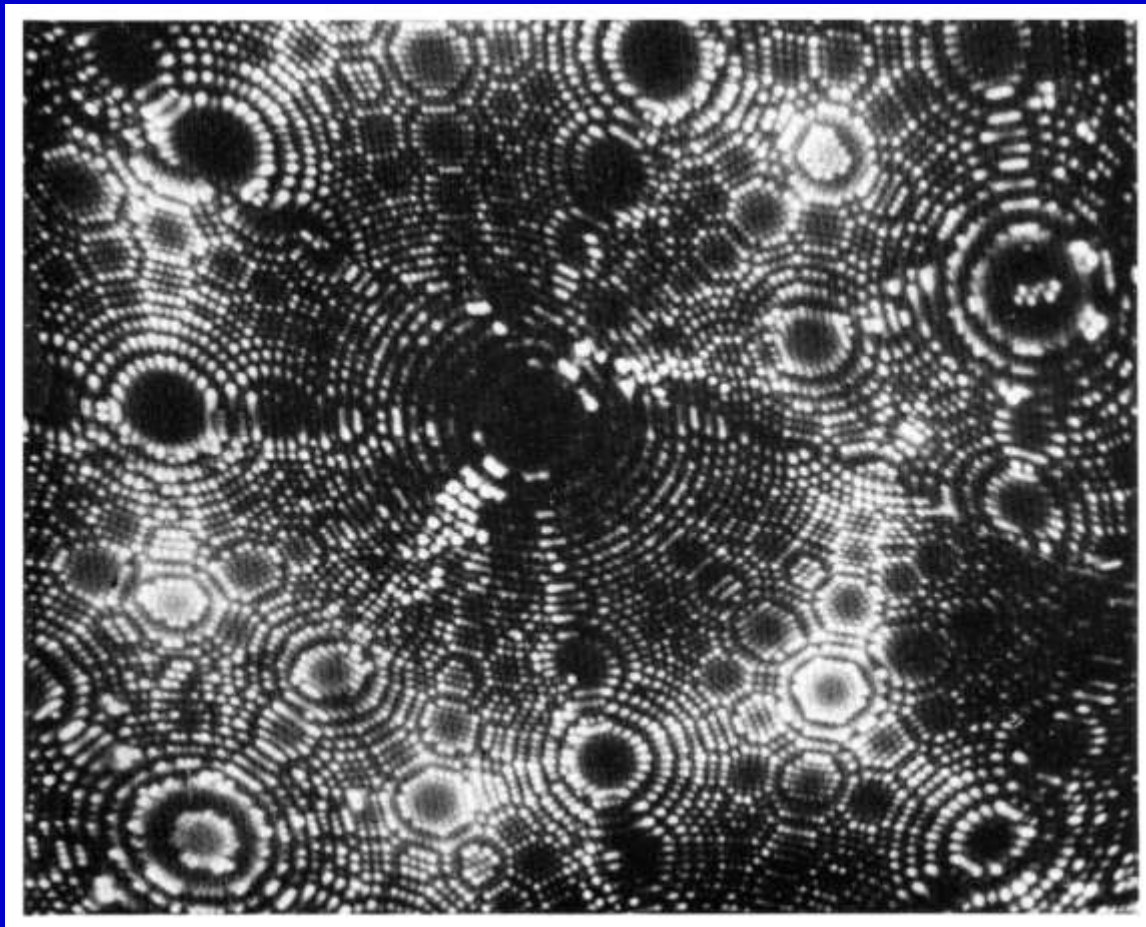


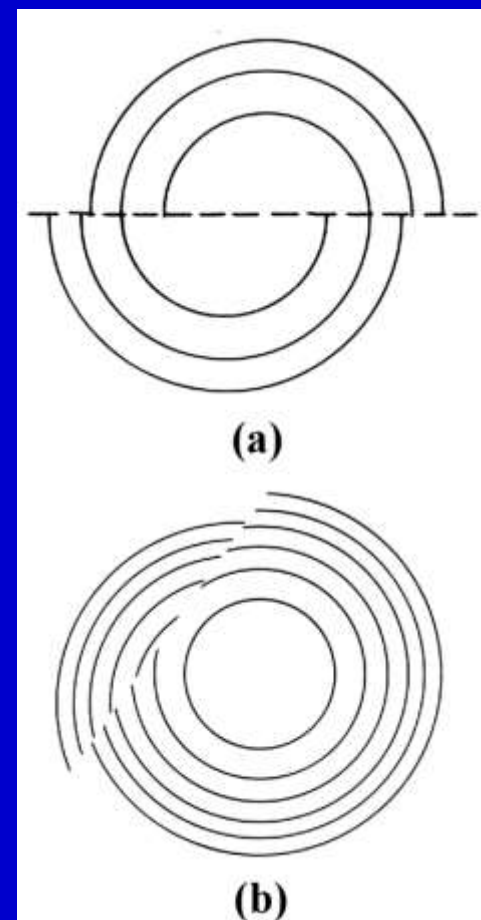
Fig. 3. Thickness effect on the flow stresses in polycrystalline (a) Al, (b) Cu, (c) Cu-13at% Al and (d) Fe with various grain sizes.

Observations on Atomistic Structure of Grain Boundaries by Field-Ion Microscopy (FIM)

K. M. Bowkett and D. A. Smith : *Field Ion Microscopy*, North-Holland (1970)



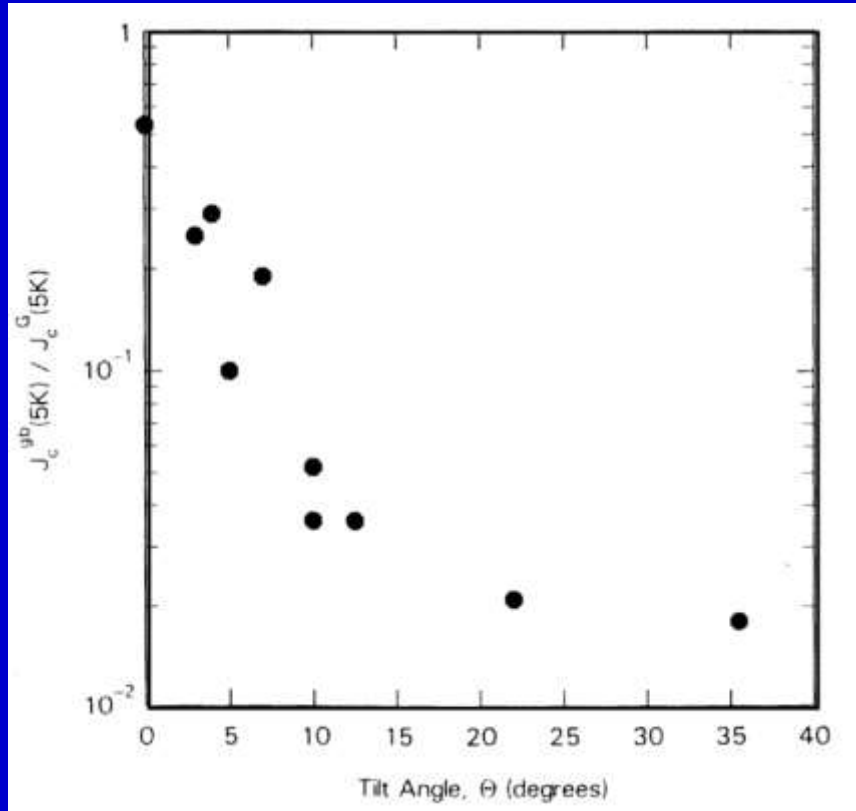
Grain Boundary Intersecting a Tungsten Specimen. (J. Hren)



Diagrams of Structure of Twist Type Boundary in Field Ion Emission. (M. A. Fortes)

Electrical Properties of Grain Boundaries

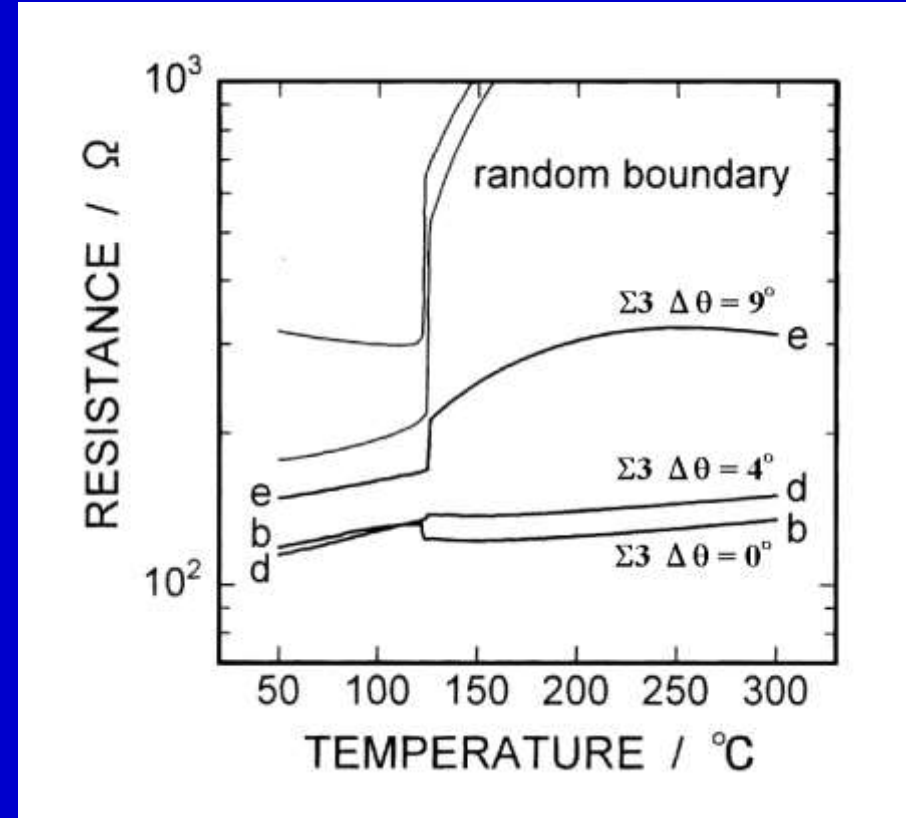
Critical Current Density J_c of YBCO



The grain-boundary critical current density J_c normalized by the average value for two grains at 4.2-5K as a function of the misorientation angle in the basal plane in YBCO.

D. Dimos, *et al.* Phys. Rev. Lett., 61 (1988), 219.

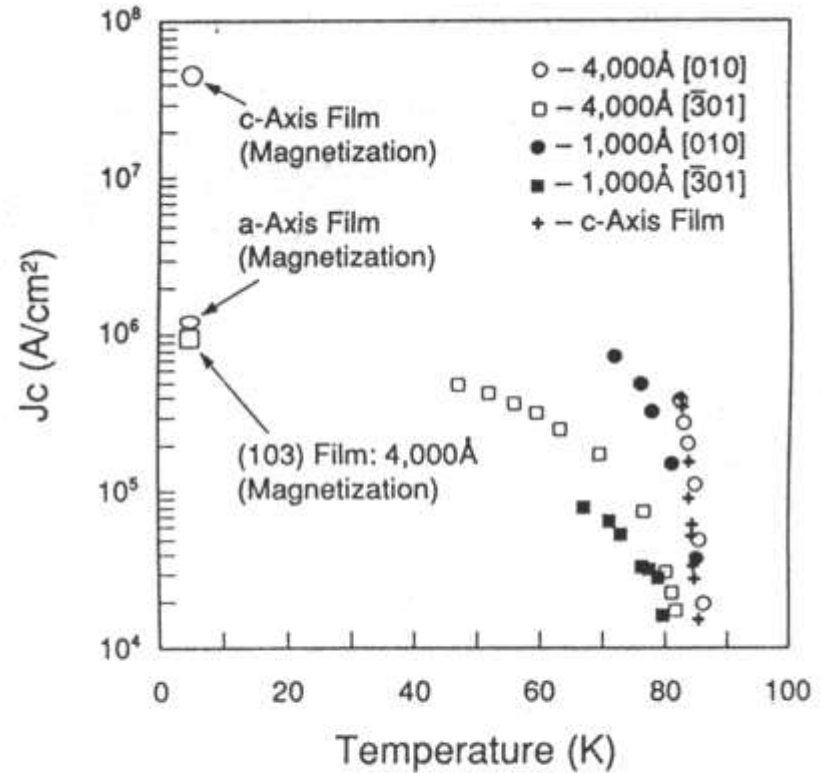
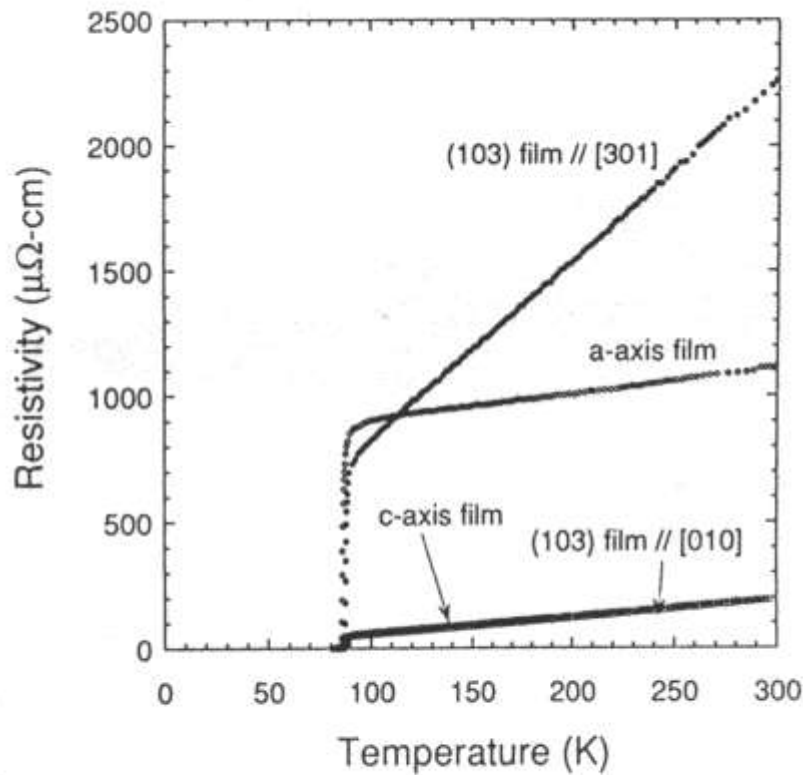
PTCR Characteristic of $SrTiO_3$



Misfit angle $\Delta\theta$ dependence of Resistance-Temperature Characteristic of $\Sigma = 3$ Boundary with and without misfit angle.

K. Hayashi, T. Yamamoto and T. Sakuma, J. Am. Ceram. Soc., 79 (1996), 1669.

Transport Properties controlled by Grain Boundary Microstructure of YBCO



a

b

Figure 3. Resistivity (a) and critical current (b) vs. temperature data for c-axis, a-axis, and (103) films.

Microstructure and Transport Properties of Various 90° Grain Boundaries in YBa₂Cu₃O₇ Thin Films.

C. E. Eom, J. M. Phillips, A.E. Marshall, T.H. Geballe;
Interface Science, 1 (1993), 267-286.
(Special Issue on Interfaces in High T_c Superconductors)
ed. By S. E.Bacock and K.L. Merkle

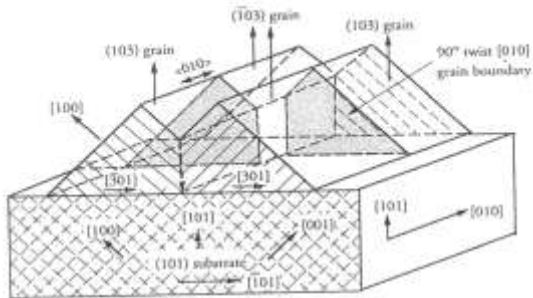


Figure 9. Three-dimensional schematic diagram of a (103)/(103) YBCO film showing a 90° [010] twist boundary. The twins are not shown here.

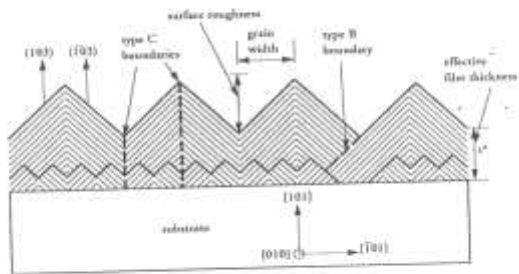


Figure 10. Schematic cross-section diagram of a (103) film looking into the YBCO [010] directions showing growth kinetics and various boundaries.

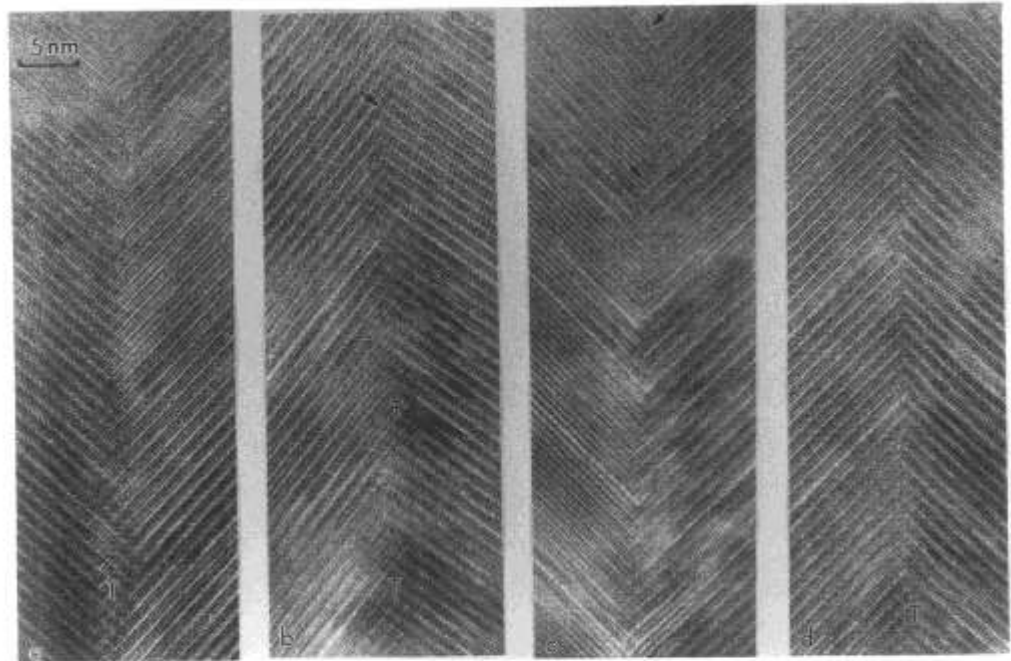


Figure 11. A series of four approximately symmetrical adjacent grain boundaries in a (103) film. The TEM specimen increases in thickness from top to bottom. Basal-plane-faced (BPF) faceting can be observed, especially in the thinner region (e.g., arrows in (b) and (c)). However, the precise boundary plane is very difficult to identify in these regions. In the thicker regions of (a) and (b), the twist overlap (*T*) is readily apparent.

Conclusions

In order to study optimal Microstructure and Mechanical properties in Brittle Bioceramic Structure, Japanese Hard Clam consisted of Aragonite was studied.

- 1. Multi-layered and Crossed-lamellar microstructures were observed.**
- 2. Fracture Toughness, K_{IC} , determined by Indentation Technique shows almost top value among those for Porous Ceramics.**
- 3. Presence of Interfaces between Lamellae plays important roles in Toughening of Brittle Ceramic Structure with Crossed-lamellar Microstructure.**
- 4. Crossed-lamellar Microstructure confers Optimal and Robust Mechanical Property on Natural Bioceramic Structure.**